1990

Barrier Island Evolution, Delta Plain Development, and Chenier Plain Formation in Louisiana.

Patrick Shea Penland
Louisiana State University and Agricultural & Mechanical College

INFORMATION TO USERS

The most advanced technology has been used to photograph and reproduce this manuscript from the microfilm master. UMI films the text directly from the original or copy submitted. Thus, some thesis and dissertation copies are in typewriter face, while others may be from any type of computer printer.

The quality of this reproduction is dependent upon the quality of the copy submitted. Broken or indistinct print, colored or poor quality illustrations and photographs, print bleedthrough, substandard margins, and improper alignment can adversely affect reproduction.

In the unlikely event that the author did not send UMI a complete manuscript and there are missing pages, these will be noted. Also, if unauthorized copyright material had to be removed, a note will indicate the deletion.

Oversize materials (e.g., maps, drawings, charts) are reproduced by sectioning the original, beginning at the upper left-hand corner and continuing from left to right in equal sections with small overlaps. Each original is also photographed in one exposure and is included in reduced form at the back of the book.

Photographs included in the original manuscript have been reproduced xerographically in this copy. Higher quality 6" x 9" black and white photographic prints are available for any photographs or illustrations appearing in this copy for an additional charge. Contact UMI directly to order.

U·M·I

University Microfilms International
A Bell & Howell Information Company
300 North Zeeb Road, Ann Arbor, MI 48106-1346 USA
313/761-4700 800/521-0600

Order Number 9112261

Barrier island evolution delta plain development, and chenier plain formation in Louisiana

Penland, Patrick Shea, Ph.D.

The Louisiana State University and Agricultural and Mechanical Col., 1990

U·M·I
300 N. Zeeb Rd.
Ann Arbor, MI 48106

BARRIER ISLAND EVOLUTION, DELTA PLAIN DEVELOPMENT, AND CHENIER PLAIN FORMATION IN LOUISIANA

A Dissertation

Submitted to the Graduate Faculty of the
Louisiana State University and
Agricultural and Mechanical College
in partial fulfillment of the
requirements for the degree of
Doctor of Philosophy

in

The Department of Geography and Anthropology

by

Patrick Shea Penland
B.A., Jacksonville University, 1976
M.S., Louisiana State University, 1979

August 2, 1990

ACKNOWLEDGEMENTS

The author would like to express great appreciation to the persistent and continuous support of my parents, S. Perry Penland, Sr., and Sybil C. Penland in the pursuit of the Ph.D. degree. Great appreciation is also extended to my wife, Carol, and the children, Sasha and Kelsey, who experienced the Ph.D. program with me. The valuable assistance of Karen Ramsey, Karen Westphal, and Tangular Williams in preparing the dissertation document is greatly appreciated.

The research results presented in this manuscript was conducted while at the LSU Department of Geography and Anthropology (1977-1979), LSU Department of Geology (1980), LSU Laboratory for Wetland Soils and Sediments (1980-1982), and the Louisiana Geological Survey (1982-present). The principal coastal research theme in Louisiana focused on the geomorphic development of the Mississippi River delta and chenier plains and the processes of change. During this period the author benefitted from the association with R. H. Kesel, A. J. Lewis, D. E. Vermeer, and H. J. Walker in the LSU Department of Geography and Anthropology; D. Nummedal in the LSU Department of Geology and Geophysics; J. M. Coleman, S. A. Hsu, S. P. Murray, and H. H. Roberts at the LSU Coastal Studies Institute; I. A. Mendelssohn and W. H. Patrick at the LSU Laboratory for Wetland Soils and Sediments; C. G. Groat and G. F. Hart in the Louisiana Geological Survey and D. W. Davis at Nicholls State University. A special mention must be made to my close colleagues, Ron Boyd (Dalhousie University), Duncan M. FitzGerald (Boston University), William Ritchie (University of Aberdeen), and John R. Suter (Louisiana Geological Survey, today Exxon).

The "Barrier Island Evolution" chapter is derived from a series of four papers in the Journal of Sedimentary Petrology (Penland et al., 1988a), Marine Geology (Penland et al., 1985), IEEE Oceans (Penland and Boyd, 1981), and the Transactions of the Gulf Coast Association of Geological Societies (Penland et al., 1981). John Barwis (Shell), Michael E. Field (USGS), and Donald J. P. Swift (Old Dominion) were reviewers and discussions with Rufus J. LeBlanc, Ron Boyd, Randolph A. McBride, Dag Nummedal, William Ritchie, H. H. Roberts, and J. R. Suter helped to improve the development of concepts presented. In 1987, the SEPM awarded the "Excellence of Poster Presentation Award" to the poster entitled, "Inner Shelf Shoal Formation through Transgressive Barrier Submergence" (Penland et la., 1987).

The "Delta Plain Development" chapter is derived from a series of four papers in ASCE - Coastal Sediments '87 (Penland et al., 1987b), SEPM (Penland et al., 1987), CSPC - Sequences, Stratigraphy and Sedimentology (Penland and Suter, 1987), and the Louisiana Geological Survey-Coastal Geology Publication Series (Penland et al., 1988b). Discussions with Rufus LeBlanc, Ron Boyd, Randolph A. McBride, Edward McFarlan, Dag Nummedal, William Ritchie, Harry H. Roberts, and John R. Suter improved the concepts presented in Chapter 2. In 1987, the SEPM and Mineralogist awarded the "Excellence of Poster Presentation Award" to a poster entitled "New Depositional Model for the Mississippi River Delta Plain" (Penland et al., 1987c).

The "Chenier Plain Formation" chapter is derived from a series of papers in Marine Geology (Penland and Suter, 1989), SEPM (Penland and Suter, 1989), and SEPM (Penland et al., 1988a). Brian Greenwood (Toronto) and Bill Carter (Ulster) were reviewers and discussions with Rufus LeBlanc, Ron Boyd, Randolph A. McBride, Edward McFarlan, Dag Nummedal, William Ritchie, H. H. Roberts, and J. R. Suter helped to improve the concepts presented.

Appendix A contains the letters of permission from the publishers to use the material presented in this dissertation. Appendices B, C, D, E, and F contain the data bases described in the text.

TABLE OF CONTENTS

LIST OF FIGURES

ABSTRACT

Coastal Louisiana has long served as a laboratory for delta and chenier plain research due to the presence of North America's largest river, the Mississippi. The development and preservation of transgressive depositional systems in abandoned delta complexes follows the process of *transgressive submergence* in which the horizontal component of reworking occurs during shoreface retreat, combined with a vertical component of submergence acting to preserve the sequence. The evolution of transgressive depositional systems in each of the abandoned Holocene Mississippi River delta complexes can be summarized in a three-stage model beginning with stage 1, an *erosional headland and flanking barriers;* stage 2, a *transgressive barrier island arc*; and stage 3, an *inner shelf shoal*. The current Mississippi River delta model depicts a single Holocene delta plain consisting of six delta complexes sequentially deposited over the last 7000 years by the delta switching process. The delta plain is now viewed as consisting of two separate delta plains deposited at different sea level positions. Termed the Modern and Late Holocene, these two delta plains are separated by a regional ravinement surface several hundred kilometers along strike in extent and bounded updip by a relict shoreline of maximum transgression, the Teche shoreline. The Late Holocene delta plain consists of a set of delta complexes deposited during a sea level stillstand some 6 m below the present, 7000-4000 yBP. A relative sea level rise between 4000-3000 yBP to about present sea level led to the transgressive submergence of the Late Holocene delta plain, generating Trinity Shoal, Ship Shoal, and the Teche shoreline. The Modern delta plain began building seaward of the Teche shoreline about 3000 yBP. The St. Bernard and Lafourche delta complexes and associated transgressive shorelines represent the abandoned portions of the Modern delta plain, separated from the underlying Late Holocene delta plain by the regional Teche ravinement surface.

INTRODUCTION

Coastal Louisiana has long served as a laboratory for delta and chenier plain research due to the presence of North America's largest river, the Mississippi River (Figure 1). The first significant study of the modern Mississippi River delta was by A. C. Trowbridge (1930). His research recognized the basic concept of distributary development and abandonment by examining the landscape surrounding New Orleans. Later research in the 1930's by R. J. Russell and H. V. Howe described the regional geology of the Mississippi River delta plain in Plaquemines and St. Bernard parishes as well as the chenier plain in Vermilion and Cameron parishes (Russell and Howe, 1935; Howe et al., 1935; Russell, 1936; Russell and Russell, 1939). H. N. Fisk (1944, 1947, 1948, 1952, 1960, 1961; Fisk et al., 1954) is responsible for producing a classic series of reports and papers on the alluvial valley, delta plain, and chenier plain of the Mississippi River documenting the geologic framework, coastal processes, and sediment facies architecture. McIntire (1958) produced the first chronology for distributary shifting using archeological evidence. Kolb and Van Lopik (1958) produced the first chronostratigraphic model for the Mississippi River depicting the "delta switching" concept. Scruton (1960) built on this delta switching model and defined the concept of the constructional phase and destructional phase within the framework of a "delta cycle" for the Mississippi River delta plain. Concurrently to the west in the chenier plain, Gould and McFarlan (1959) completed the most detailed geologic assessment focusing on the chronological development, particularly how the delta cycle process relates to mudflat and chenier ridge formation. Since 1953, the Coastal Studies Institute at Louisiana State University has produced a prolific volume of literature on regional deltaic variability, quantitative coastal processes, detailed stratigraphy, and evolution of coastal Louisiana (Coleman et al., 1964; Coleman and Gagliano, 1964; Coleman and Wright, 1975; Coleman, 1966; Morgan and Shaver, 1970; Coleman et al., 1974; Coleman and Prior, 1980; Van Heerden and Roberts, 1980; Wells and Kemp, 1981; Wells and Roberts, 1981; Van Heerden and Roberts, 1988; Coleman, 1988; Coleman and Roberts, 1988a,b). The most recent chronostratigraphic model presented for the Mississippi River delta plain is by Frazier (1967, 1974). He recognized five major delta complexes comprised of more than 16 individual delta lobes.

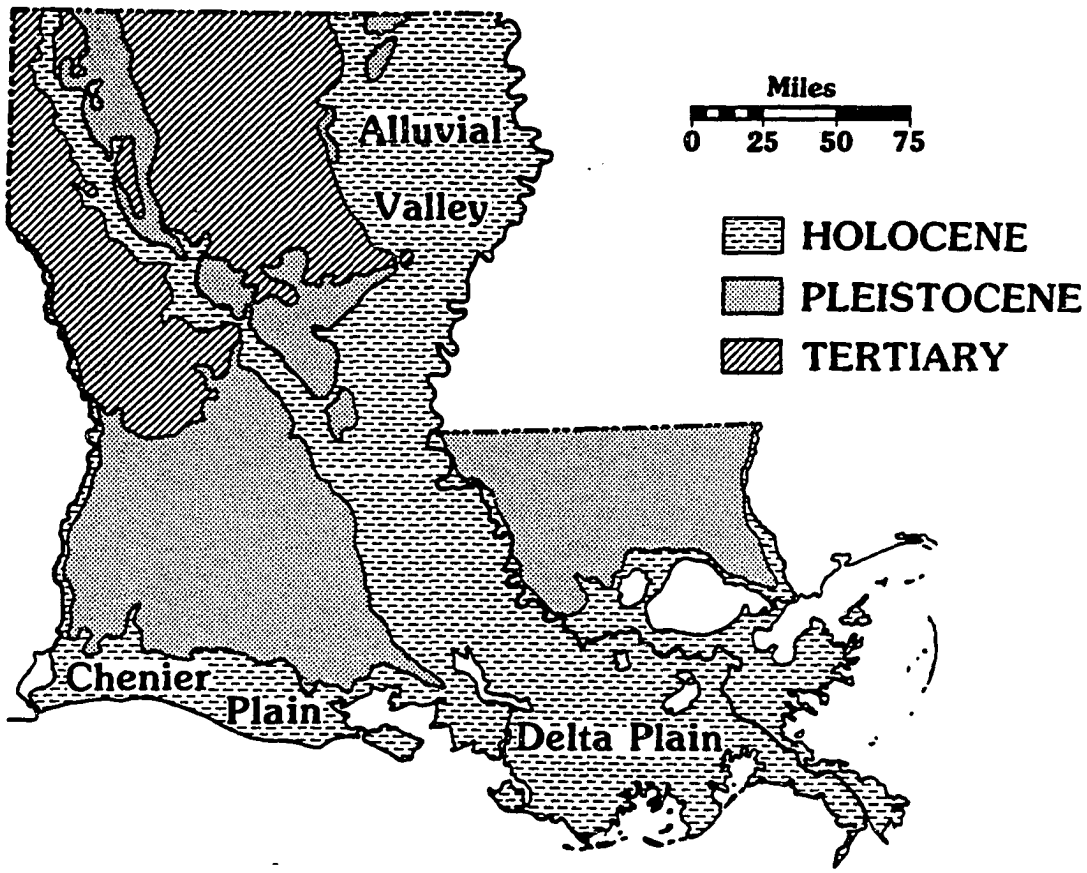

Figure 1. Physiography of Louisiana depicting the location of the Mississippi River delta and chenier plains.

The work presented here builds on the more than half-a-century of Mississippi River delta and chenier plain research by incorporating new high-resolution seismic, vibracore, and radiometric data from extensive areas onshore and offshore which, previously, were never surveyed in detail (Appendix B, C, D, E, and F). Interpreting these new research results required tying the offshore and onshore data together using improved marine geophysical survey techniques (Figure 2). This data base is in contrast to earlier research results based primarily on land-based controls. The research which produced the results presented here, was conducted between 1979 and 1989 and is ongoing. Initial research efforts were focused on understanding the abandoned part of the delta cycle, barrier island evolution, estuary development, and geomorphic change. In the course of this research, new seismic and vibracore data was used to re-evaluate the earlier single Holocene delta plain models. The "Methodology" chapter presents the data used in this study, describes the facies types, and explains how the cross sections were built.

In the "Barrier Island Evolution" chapter, the geomorphic evolution, geologic history, and stratigraphy of Louisiana's barrier island and shelf shoal systems are organized within the framework of a three-stage evolutionary model. These coastal features represent the transgressive depositional systems of the abandoned Mississippi River delta complexes. Previous researchers recognized concepts that focused on delta abandonment (Russell, 1936), formation of delta margin shoreline sands (Fisk, 1955) and the delta cycle (Scruton, 1960), however the transgressive depositional systems had never been organized into a model expanding the evolutionary process, stratigraphy, and geologic history of these barrier shoreline and shelf shoal systems. In the "Delta Plain Development" chapter, the geologic history of the Mississippi River delta plain is re-evaluated. The depositional models of the Mississippi River delta plain by Fisk (1944), Kolb and Van Lopik (1966), and Frazier (1967) depict a single Holocene delta plain 5000-7000 years old. New offshore seismic and vibracore data indicate the single Holocene delta plain model can be refined and divided into three individual delta plains separated by regional ravinement surfaces generated by brief, rapid eustatic events. In the "Chenier Plain Formation" chapter, the geomorphology and geologic history of the chenier plain is re-evaluated in light of new data from the Mississippi River delta plain. Emphasis is placed on refining the timing and features of the maximum flooding surface and shoreline as well as cross-correlating with delta switching events to the east.

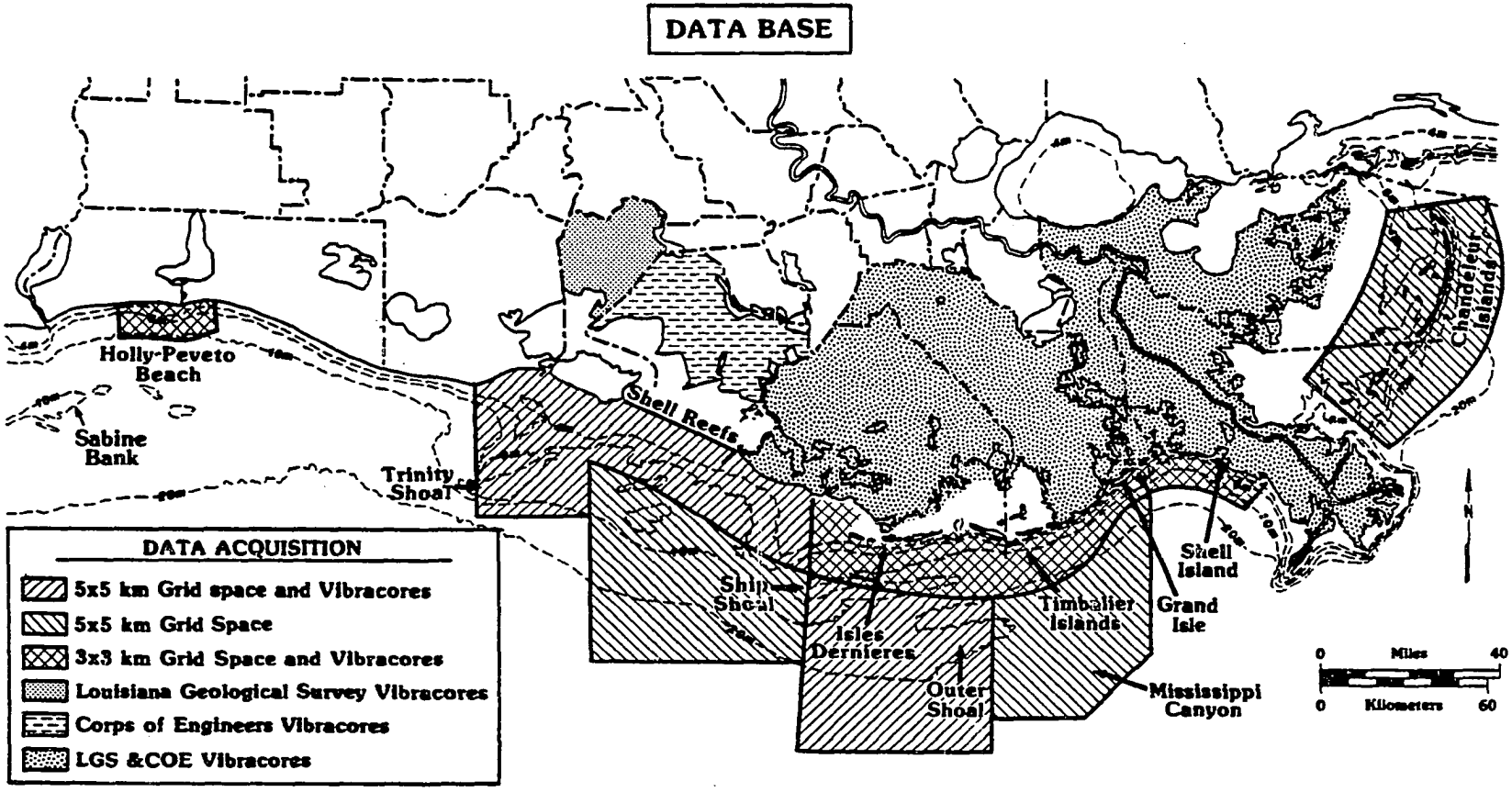

Figure 2. Location of vibracore and high resolution seismic surveys conducted by the Louisiana Geological Survey in cooperation with the U.S. Geological Survey tween 1981 and 1989.

METHODOLOGY

Seismic

Geologic framework studies rely on seismic and vibracore tools to determine the character of onshore and offshore sediments. Offshore, this is accomplished through the use of high resolution seismic profiling techniques (Figure 2; Appendix B). Among other factors, the type and intensity of reflections of the sound signal from the subbottom is a function of the lithology of the seabed and submerged strata. Sound sources are towed by a research vessel along pre-plotted tracklines through the area being explored. Trackline grids are designed based upon the amount of ship time available for the cruise, the range and fuel capacity of the research vessel, the location of coastal ports, knowledge of coastal geomorphology and historical shoreline changes, and the degree of detail required for the task at hand. In a comparison of regional seismic reflection data gathered on a relatively coarsely spaced 5.5 km grid with closely spaced lease block data, it was estimated that up to 80% of geological features can be observed on the regional grid. This 5 km by 5 km grid is sufficiently detailed for reconnaissance purposes. For actual determination of borrow sites within a specified area, greater detail is necessary and grids were spaced about 1 km by 1 km.

Navigation data is recorded in real time aboard ship and stored on magnetic tape. These data are later processed into a trackline map at a given scale, depending upon the size of the area being surveyed. Interpretations of the seismic profiles are plotted onto mylar overlays of the trackline charts and preliminary maps of geologic targets were made. Because resolution and penetration of seismic signals in the seabed are partly functions of the frequency of the sound signal itself, two types of seismic sources were employed. Using two devices provides the ability to have one high frequency system with better resolution in the upper sediments while a second, lower frequency device can give greater penetration to deeper strata. Additionally, attenuation of the seismic signal due to absorption of the sound by the material of the seabed is related to lithology. Coarser deposits attenuate more of the signal at higher frequencies. Thus, accurate determination of the thickness of a sand section may require a lower frequency device for full penetration. The characteristic of shell beds is the almost total reflection of the sound signal. Fine-grained sediments generally produced the best reflections, except

when rich in organic material, which results in high attenuation of the signal.

In this study, a Datasonics 3.5 kHz subbottom profiler was used as the high frequency tool, while an ORE Geopulse was used to provide greater penetration. Vertical resolution of these two tools is about 0.5 m and 1.5 m, respectively. Penetration averaged about 10 m for the 3.5 kHz device, and reached greater than 50 m for the Geopulse. In each case, data quality were usually poorest in shallow water nearshore. The return signals were split traced on an EPC 3200 recorder at sweep rates of 1.8 second for each channel, resulting in an effective display of 1.4 second for the entire record. Filter settings for the ORE Geopulse were variable, depending upon the area surveyed. All data were recorded on magnetic tape on a Hewlett Packard 4300 reel-to-reel recorder for subsequent playback. Navigation was accomplished by using a Northstar 600 Loran-C receiver corrected with a Morrow XYP-200 real time Loran plotter. Navigation data were recorded on magnetic tape on a Texas Instruments Silent 700, and processed into trackline maps by the U.S. Geological Survey in Corpus Christi, Texas, and Woods Hole, Massachusetts. Seismic interpretations were plotted onto the trackline charts on mylar overlays at scales of 1:80,000.

Seismic profiles were collected in cooperatively funded cruises in 1982, 1983, 1984, 1985, 1986, 1987, 1988, and 1989 (Appendix B). Participating agencies were the U.S. Geological Survey, U.S. Minerals Management Service, the Terrebonne Parish government, and the Louisiana Geological Survey. All cruises were performed aboard the R/V R. J. Russell, R/V Acadiana, or R/V Coli of the Louisiana Universities' Marine Consortium in Cocodrie, LA.

Vibracore

Vibracoring is used extensively by the Louisiana Geological Survey to obtain shallow, undisturbed cores from unconsolidated fluvial, deltaic, coastal, and shallow marine sediments (Figure 2; Appendix C). Vibracoring techniques can be performed both on land or in water up to 20 m deep. Vibracoring on land involves less labor and equipment and, as a result, is less expensive and faster than coring in water. The vibracore unit employed in this project is a Dreyer concrete vibrator powered by a 5 HP Briggs and Straton gasoline engine. The unit includes high frequency vibrations of 20-40 cycles/s transmitted through a 4.3 m cable to an aluminum vibrating head. The head is attached to a 10 cm

diameter, 9 m long aluminum core pipe which is vertically erected at the coring site. Sediment penetration is accomplished through liquefaction of a thin layer of sediment as the core pipe is driven downward to a desired depth or until refusal occurs. The unfilled portion of the core pipe is filled with water and capped with a plastic and rubber vacuum test plug to provide a suction which prevents loss of the core during extraction of the pipe. The core pipe is retrieved through the use of a hand operated winch and tripod system. Vibracore sections are transported back to the Vibracore Lab for processing that includes initial storage, splitting, analysis, and archiving.

Vibracoring in both shallow (<1.5 m) and deep (1.5-30 m) water involved many of the same techniques previously described. However, deep water coring involves the use of a system developed by Alpine Ocean Seismic Survey. This system is capable of obtaining cores 10-15 m length. A 15 m long aluminum tower supported by 1.3 m pads, serves as a guide for a pneumatic vibrator that drives the core pipe into the substrate. Cores are retained in clear plastic liners inserted in a metal core pipe. To obtain the maximum depth, two 7.5 m lengths of plastic liner are spliced together to obtain a complete 15 m in one attempt. Hydraulic jetting is used to achieve deeper penetration and longer recovery lengths in sediments that cannot be fully penetrated in one attempt, or to obtain cores of better quality. In this procedure, a new liner is inserted inside the core pipe after the first vibracore attempt is complete. The vibracore rig again is placed on the water bottom very close to the spot where the first run was completed. High pressure water is pumped via a 5 cm diameter hose down through the core pipe, washing away the sediment and allowing the core pipe to penetrate to the depth at which the first ended. Then the water pressure is turned off and the air is turned on to the vibrator, thus driving the core pipe the second 7.5 meters or to refusal.

The core analysis begins by splitting the vibracore in half using a circular saw equipped with a 19 cm carbide-tipped steel blade and an aluminum guide designed so the saw will follow a straight path over the length of the core pipe. A steel wire is then pulled lengthwise through the core pipe along the saw cut dividing the core into equal halves. The first half is cleaned, trimmed with an osmotic knife, described, then wrapped in plastic, and archived for future reference. The other half of the core is processed for grain size samples, radiocarbon dating materials, x-ray radiograph slabs, and epoxy relief

peels. Each vibracore is sampled for sediment grain size analysis at an interval averaging 1-2 m except when sand bodies over 1 m thick are encountered. Here, the sampling interval for the sand bodies averages 0.5 m or less. The sediment samples collected from the vibracores are processed for grain size analysis. Analysis of sedimentary structures and facies within the core is accomplished through visual examination of the core itself, the use of epoxy relief peels, and x-ray radiographs of sections. The information from cores is recorded on a standardized description sheet, which accommodates information concerning sedimentary structures, textural characteristics, bedding thickness, particle size, and additional analyses performed on the core.

Sediment samples are placed in a glass beaker and dried in a Fisher Isotemp oven at an average temperature of 65°C. Higher temperatures were avoided to prevent any clays in the samples from baking. The subsamples normally dried overnight (16 hours) and were allowed to attain equilibrium the next morning by cooling in the room for at least one hour before weighing. The subsamples were completely disaggregated using a mortar and pestle prior to sieving. A set of cast acrylic sieves with mesh sizes ranging from 1.25 phi (medium sand) to 4.00 phi (very fine sand) were assembled at a 0.25 phi interval. Sediments finer than 4.00 phi were combined and considered the fine size fraction (silt and clay) of the sample. The sieves were systematically cleaned before each sample was processed, then stacked with the coarsest sieve on top and the finest on the bottom. The subsample was added to the top and the entire nest of sieves was placed in a sonic sieving unit, which vibrated the subsample for a nominal sieving time of two minutes. Upon completion of the sieving, each sieve was inverted and cleaned. The trapped sediment grains from each sieve were emptied onto a large sheet of paper and transferred to a labeled, preweighed beaker. The beakers and sediment-filled beakers were weighed using a Sartorius electronic digital balance to an accuracy of 0.001 gm. The individual weights per phi interval were entered into a FORTRAN 77 program developed to calculate grain size statistics using a microcomputer at Louisiana Geological Survey. This program calculates Folk, Inman, and moment measure statistics (mean, sorting, skewness, and kurtosis); textural descriptions; phi percentiles; weight values; weight percents; and cumulative percentages. Cumulative frequency curves for the grain size samples were produced from the initial data using a commercial spreadsheet computer program in

combination with a flat bed plotter. When organic-rich samples were encountered, they were radiocarbon dated using a commercial vendor (Appendix D).

Facies

The sediment which comprise a complete Mississippi River delta cycle sequence can be divided into regressive and transgressive facies. Terminology used to describe these deposits is derived from LeBlanc (1972), Coleman and Prior (1982), Gerdes (1985), Penland et al. (1988a), and Kosters (1989). Seismic and vibracore analyses in the Mississippi River delta plain led to the identification of two major sets of sedimentary facies in the lower Mississippi River delta plain and in the offshore areas. Each facies type was identified on the basis of lithology, texture, faunal assemblages, stratigraphic position, and sedimentary structures. The major facies identified include a regressive set comprised of prodelta, delta front, distributary, beach ridge and fresh marsh as well as a transgressive set comprised of sand sheet, shoal, barrier, lagoon, and salt marsh.

Prodelta

The prodelta facies is the depositional platform of a delta complex representing the initial phase of mud accumulation on the inner shelf (Figure 3). Prodelta deposits consist of massive clays with poorly sorted silt and sand laminations. Mean grain sizes were observed from 6.9-8.1ø with sorting ranging 1.7-2.6ø. The sand content varied 2-13%. Prodelta sequences typically coarsen-upward increasing in silt and sand content reflecting the advance of a prograding distributary. Laminated silty clays grade upward into starved-ripple laminated silts and silty sands encased in prodelta muds. Rafted organic fragments are common. Due to high sedimentation rates, burrowing structures are generally absent. Shells and shell fragments are rare.

Delta Front

The delta front represents progradation in close proximity to the distributary channel (Figure 4). Delta front deposits are coarser than prodelta deposits due to the increasing influence of the approaching distributary mouth. The delta front facies coarsens upward, the basal contact is gradational with the underlying prodelta facies. Distributary channels are found truncating the top of many delta

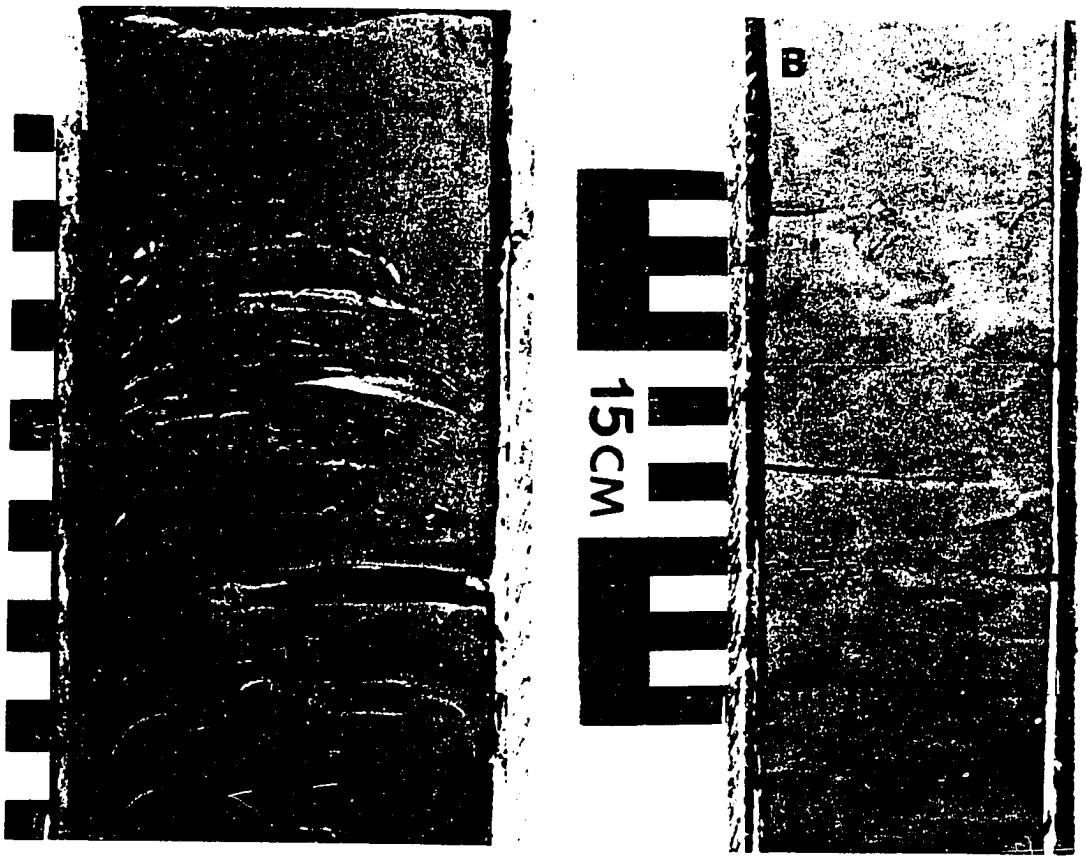

Figure 3. Representative photographs of the prodelta facies: (A) parallel laminated silty clay, (B) massive-appearing silty clay.

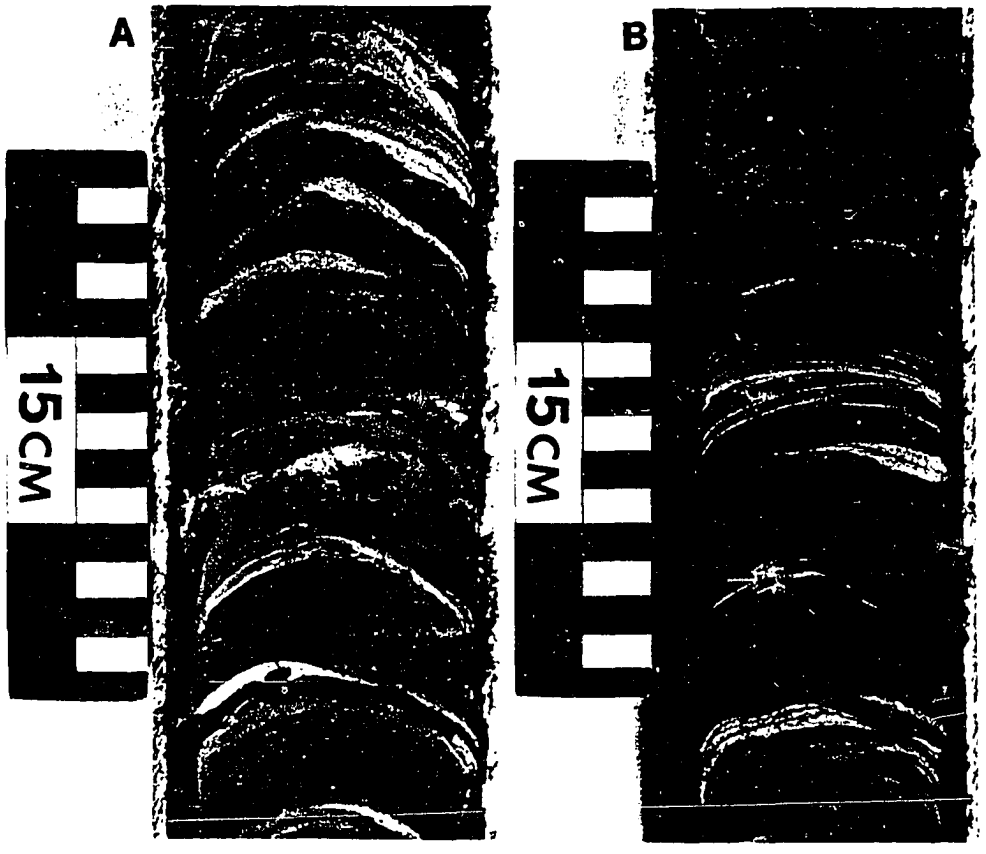

Figure 4. Representative photographs of the delta front facies: (A) parallel laminations of silt and sand in a silty clay matrix, (B) starved silt and sand ripple laminations, small scale lenticular beds, and parallel laminations of silt in a silty clay matrix. Concavity in bedding and laminae is due to coring deformation.

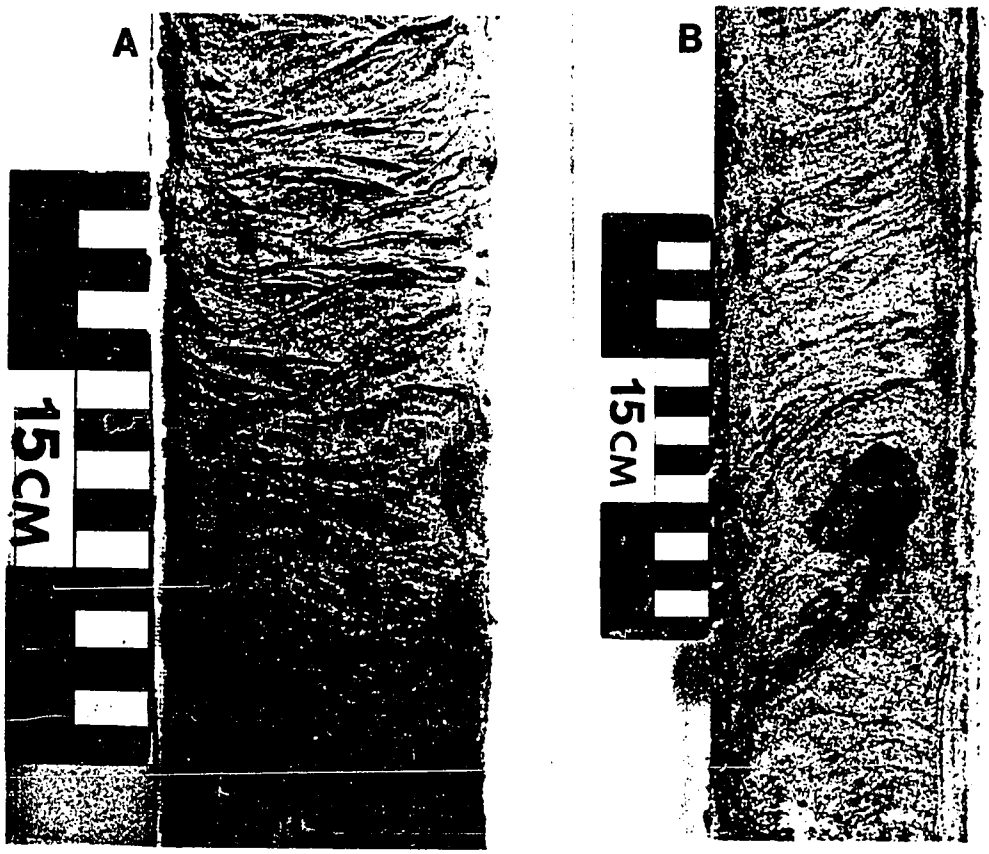

Figure 5. Representative photographs of the distributary facies: (A) climbing ripple cross-laminations, and (B) mud clast in climbing ripple laminations and flaser bedding.

6.8ø and standard deviation of 1.25-2.32ø. Delta front deposits are 19-27% sand. Laminated and rippled silty clay form the lower half of most delta front sequences which grade upward into silty/sandy wavy and lenticular ripples. Starved ripple laminations and rafted organics are common. Burrowing and shells are absent, suggesting that sedimentation rates are persistent enough to preclude the development of significant faunal communications.

Distributary

The distributary facies represent the environments of deposition associated with the main distributary and include coarse and fine grain channel fill, levee, overbank, and distributary mouth bar environments (Figure 5). Mean grain size of the distributary sediments ranges from 3.0-5.0ø with a standard deviation of 0.5-2.1ø. This fine sand to silt deposit is well sorted to poorly sorted with a sand content of 29-98%. Distributary progradation is continuous with peak periods of rhythmic deposition associated with floods. The base of distributary sequences are erosional due to channel cutting. Climbing ripple laminations, ripple-drift cross-laminations, and low-angle laminations are the most prevalent sedimentary structures. Rafted organics, flaser laminations, and mud rip-up clasts are common. Some burrowing and shells are found in distributary sequences marking a period of rapid sand deposition followed by distributary abandonment, waning flow conditions, and deposition of fine-grained channel fill.

Beach Ridge

Beach ridge plains are found on the updrift side of prograding distributary systems which intercept sediment being transport alongshore (Figures 6 and 7). A typical beach ridge sequence is a coarsening-upward deposit of shoreface sediments overlain by foreshore and washover deposits (Gerdes, 1982). The mean grain size is 3.03-3.68ø with a standard deviation of 0.23-0.42ø. Lower shoreface deposits are dominantly laminated fine-sand with scattered burrows throughout. In some cases, heavily bioturbated, massive silty sands are found on the lower shoreface. Upward in the beach ridge sequence, burrowing decreases and the predominantly laminated bedding gives way to ripple and ripple drift cross-bedding. Detrial organics and shell fragments are common.

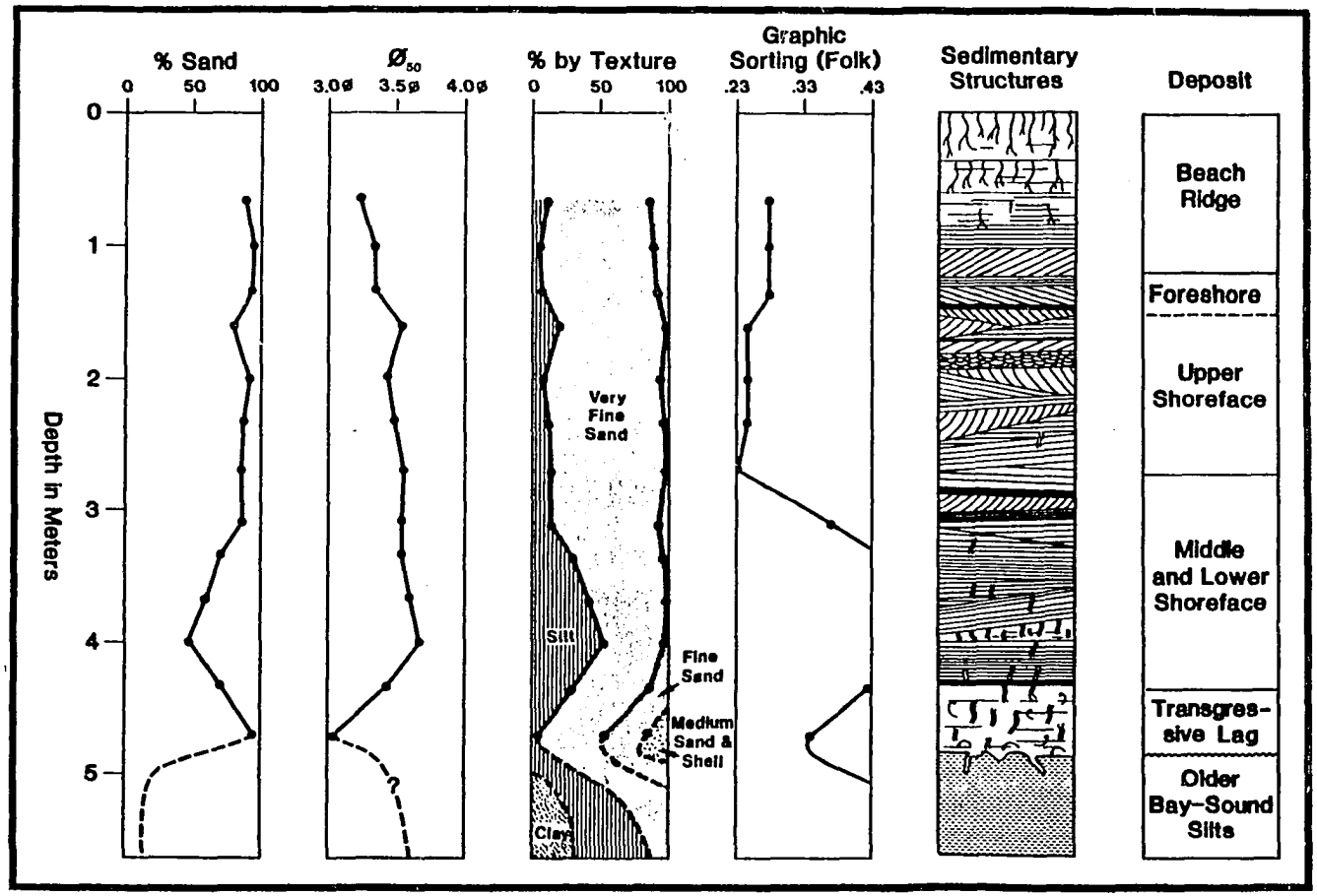

Figure 6. Beach ridge stratigraphic sequence from the Cheniere Caminada beach ridge plain (Gerdes, 1982).

UPPER SHOREFACE

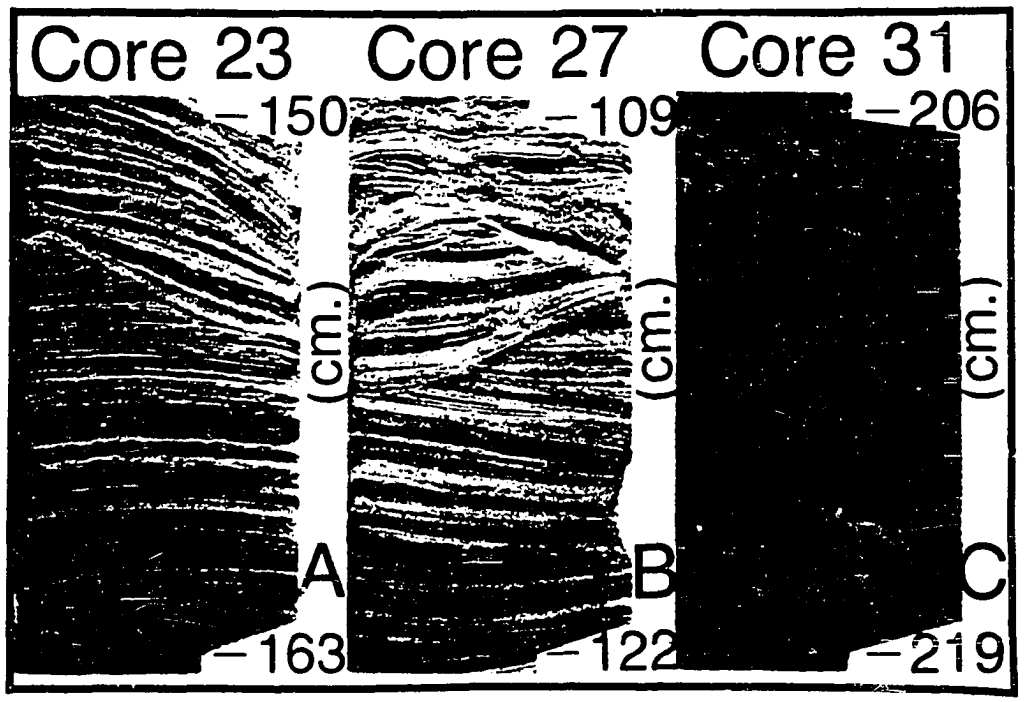

LOWER SHOREFACE

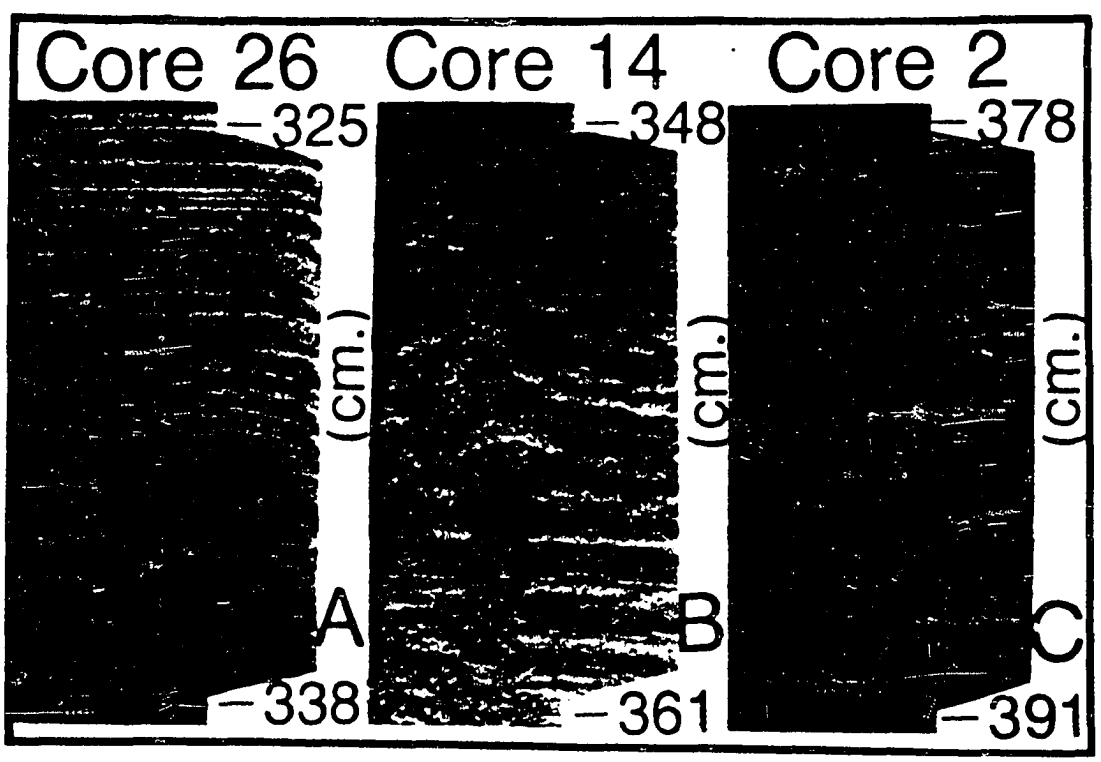

Figure 7. Photographs of a Cheniere Caminada beach ridge sequence illustrating the upper and lower shoreface deposits (Gerdes, 1982).

Figure 8. Photograph of organic-rich fresh marsh deposits.

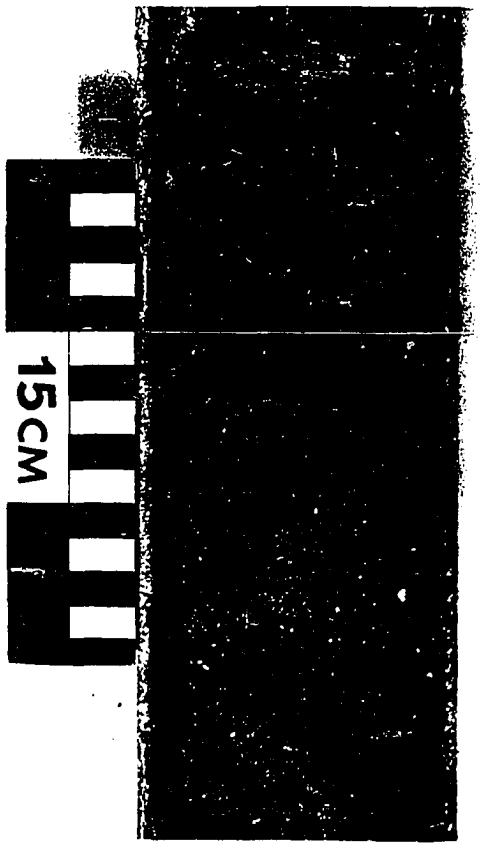

Figure 9. Massive-appearing sand sheet with mud-lined burrow traces and a thin layer of burrowed silty clay (scale is in cm).

Fresh Marsh

Fresh marshes represent the establishment of herbaceous vegetation on emergent distributary and delta front surfaces (Figure 8). *Sagittaria spp.*, *Eleocharis spp.*, and *Bacopa monniri* are the dominant vegetation found in fresh marsh areas (Kosters 1989). Fresh marshes are characterized by thick organic soils of rooted marsh with a matrix of silty clay lenses and detrital organic layers. The organic content of fresh marsh sediments typically are 35 - 75%. This humic peat is rooted with few recognizable plant fragments.

Sand Sheet

The sand sheet facies represent thin sand deposits on the shoreface and inner shelf offshore of a barrier shoreline produced by storm deposition (Figure 9). Grain size of sand sheet deposits ranges 2.7-3.2ϕ with a standard deviation of 1.7-2.3ϕ. The sand sheet is often massive in appearance but can contain graded bedding and flasers. Horizontal and low-angle planar laminations with burrows, principally Callianassa, can also be found as well as shell fragments.

Shoal

The shoal deposit is used to describe massive marine sand bodies sourced from the transgression and submergence of a former barrier island. Ship Shoal is the best example. The shoal deposit can be subdivided into three distinct facies, shoal crest, shoal front, and shoal base. The shoal crest facies is a clean, moderately sorted, fine- to medium-grained sand with a mean size of 1.51-2.57ϕ with a standard deviation of 0.51-1.65ϕ (Figure 10). The shoal crest is 95-100% sand. At Ship Shoal the shoal crest coarsens upward with faint horizontal and subhorizontal laminations. The most common burrowing type found in Callianassa. Graded beds, wave ripple laminations, low angle planar laminations, and trough cross beds are the primary structures. Clasts of lithified beach sediments, *Crassostrea* sp. shell, and *Rangia* sp. shell are found. Modern marine shells found include *Mulinia* sp. and *Olivella* sp. The shoal front represents the depositional landward slope of an inner shelf shoal (Figure 11). It consists of moderately sorted fine- to very fine-grained sand. Mean size ranges 2.71-3.16ϕ with a standard deviation of 0.51-0.94ϕ. The shoal front deposit is 75-95% sand. Low-angle planar and horizontal laminations and flaser bedding are the primary structures. Callianassa and Skilithos

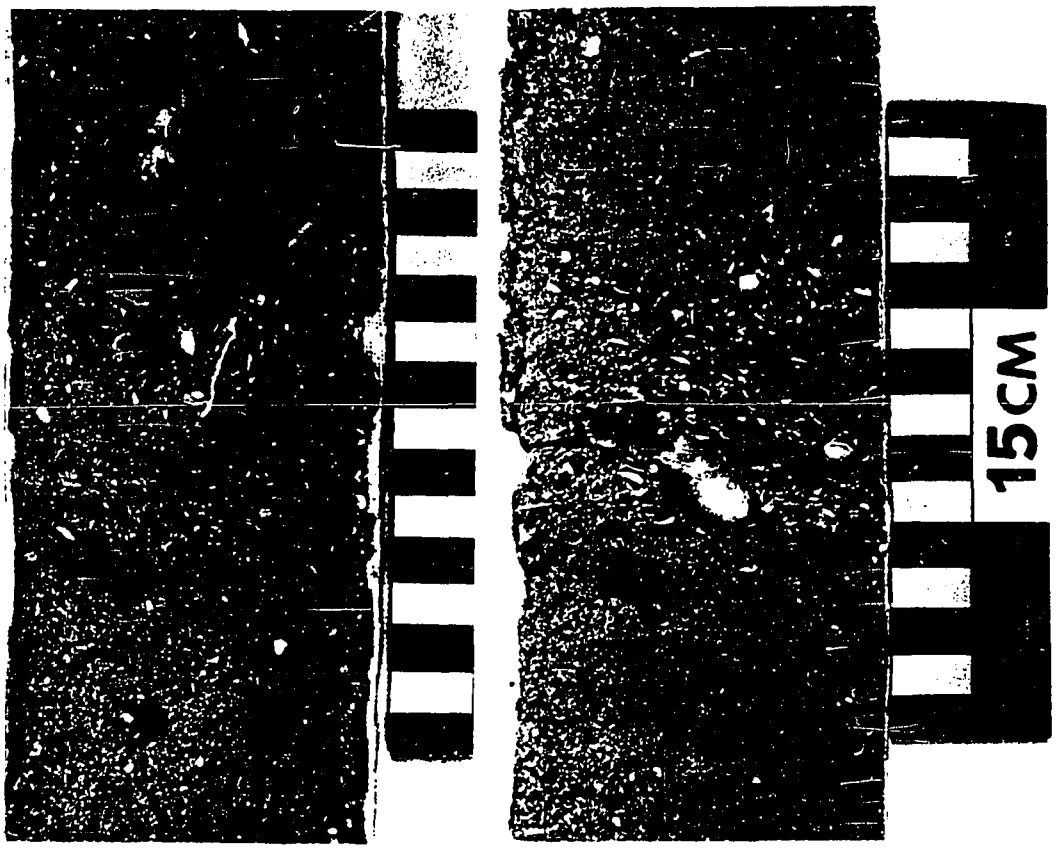

Figure 10. Representative photographs of the shoal crest facies: (A) normally graded bed of *Mulinia* sp. and *Olivella* sp. shells and sand and (B) graded bed with beachrock clasts and *Crassostrea* sp. shell fragments (scale is in cm).

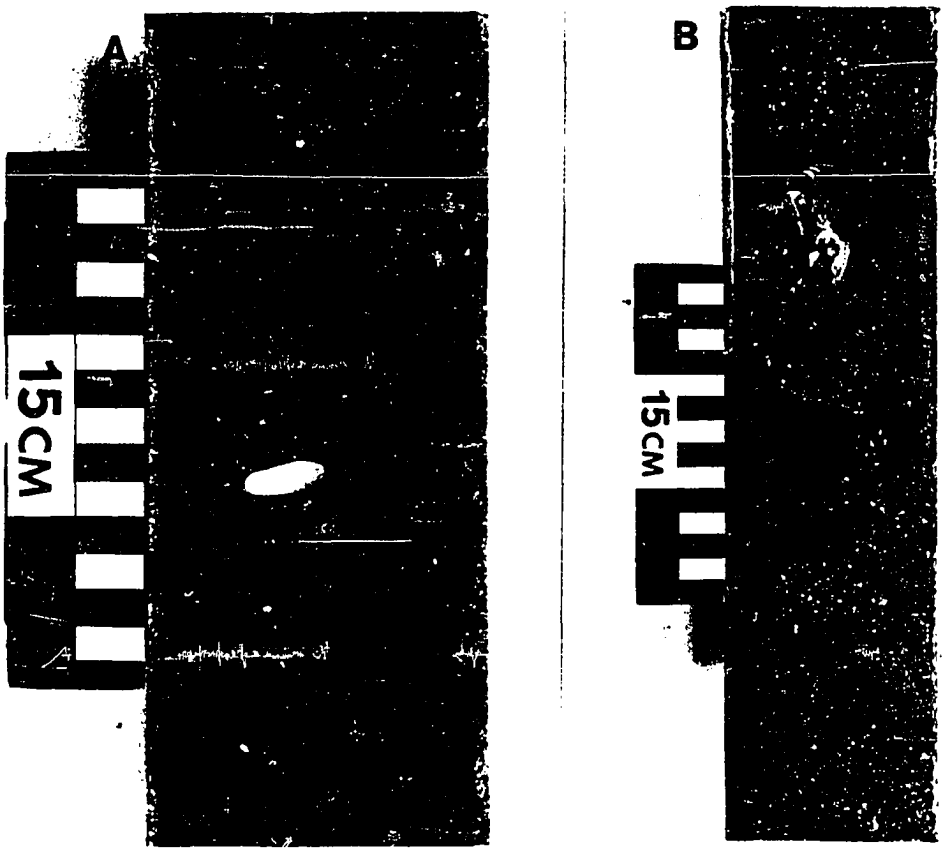

Figure 11. Representative photographs of the shoal front facies: (A) vertical Ophiomorpha burrow trace within massive-appearing sand with *Olivella* sp. shells and (B) beachrock clasts and *Crassostrea* sp. shell in massive-appearing sand.

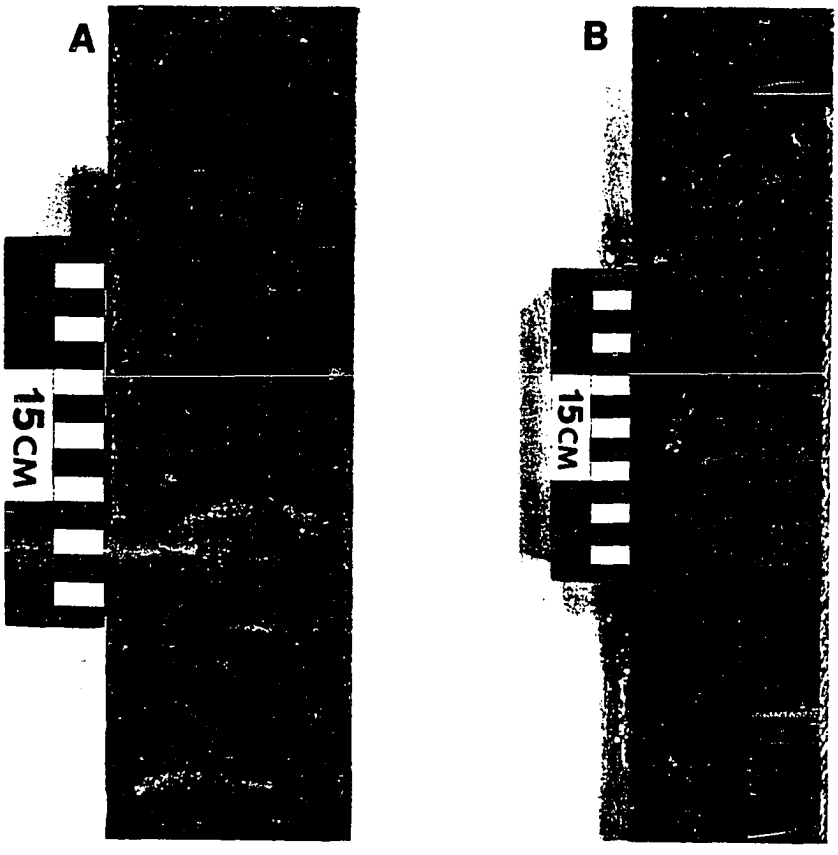

Figure 12. Representative photographs of the shoal base facies: (A) interbedded lenticular- and wavy-bedded sands and laminated muds and (B) contact between shoal front and shoal base facies.

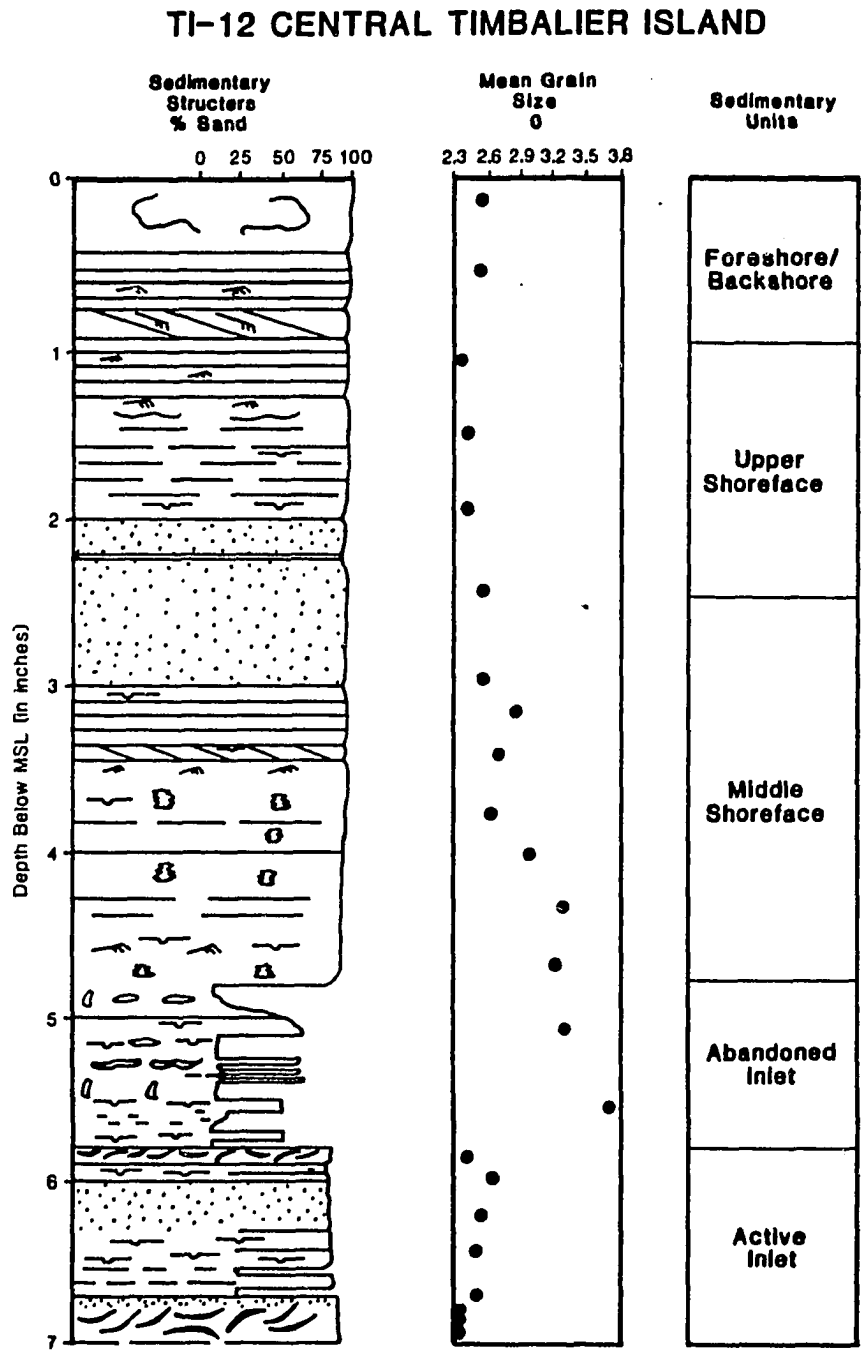

Figure 13. A recurved spit-dominated barrier facies sequence from Timbalier Island (Isacks, 1989).

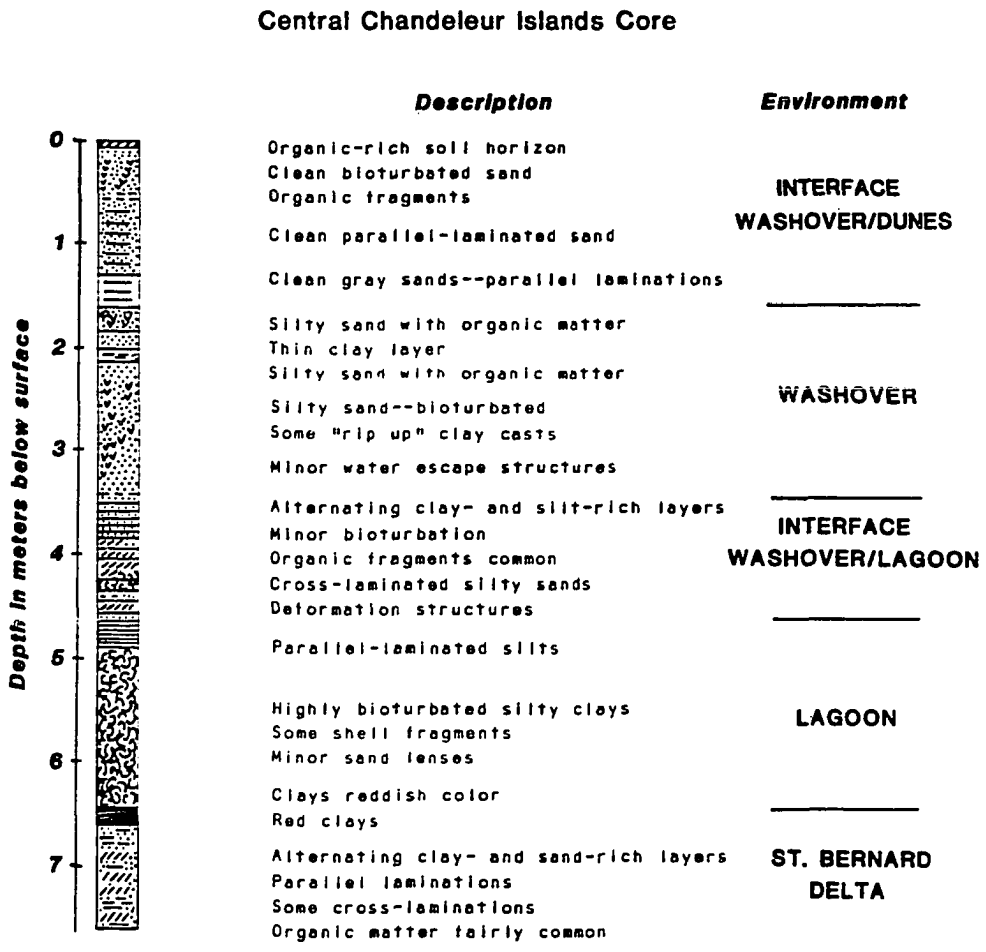

Figure 14. A washover-dominated barrier facies sequence from the Chandeleur Islands, Louisiana (van Heerden et al., 1985).

burrows are abundant in the shoal front facies. Clasts of lithified beach sediments, *Crassostrea* sp. shell, and *Rangia* sp. shell are common. *Mulinia* sp. and *Olivella* sp. are the common marine shells found. The shoal base facies represent the depositional base of the landward depositional slope of an inner shelf shoal (Figure 12). Interbedded layers of silty clay and lenticular-to-wavy bedded, poorly sorted, very fine-grained sand characterized these facies. The mean grain size ranges between 3.1-3.6ϕ with a standard deviation of 1.2-1.5ϕ, the sand content is 50-75%. Wavy and lenticular bedding and low-angle planar laminations are the primary structures. Callianassa and Skilithos are the common burrow types. Clasts of beach rock, *Crassostrea* sp. and *Rangia* sp. shell are common. The primary marine shells are *Mulinia* sp. and *Olivella* sp.

Barrier

The barrier facies represents the deposits which comprise the sand component of a transgressive barrier island system. The primary sedimentary types are recurved spit, tidal inlet, washover, beach, and dune. Two primary barrier sequences were recognized in the barrier islands surrounding the Mississippi River delta plain. The first is a recurved spit sequence which fine-upwards from tidal channel deposits overlain by ebb tidal delta and spit platform deposits followed by beach and dune deposits (Figure 13). The second is a washover dominated sequence which coarsens upward from flood tidal delta deposits overlain by washover, beach, and dune deposits (Figure 14). The mean grain size of the barrier facies is 2.64-3.72ϕ with a standard deviation of 0.23-0.42ϕ. The sand content ranges from 85 to 100%. The primary physical structures range from trough cross-beds, low-angle planar bedding, horizontal laminations, graded storm beds, to a variety of ripple types. Callianassa and Skilithos burrows are the most common. The primary marine shells are *Mulinia* sp. and *Olivella* sp. Clasts of beach rock, *Crassostrea* sp. and *Rangia* sp. shell are common.

Lagoon

The lagoon facies is used to describe sediments deposited in backbarrier waterbodies similar to Terrebonne Bay or Chandeleur Sound (Figure 15). Brackish-water organisms such as the *Rangia* sp. have built many reefs in the upper ends of interdistributary bays and *Crassostrea* sp. reefs are distributed throughout the more saline lower ends of the bay behind the barrier shorelines. Where salt water

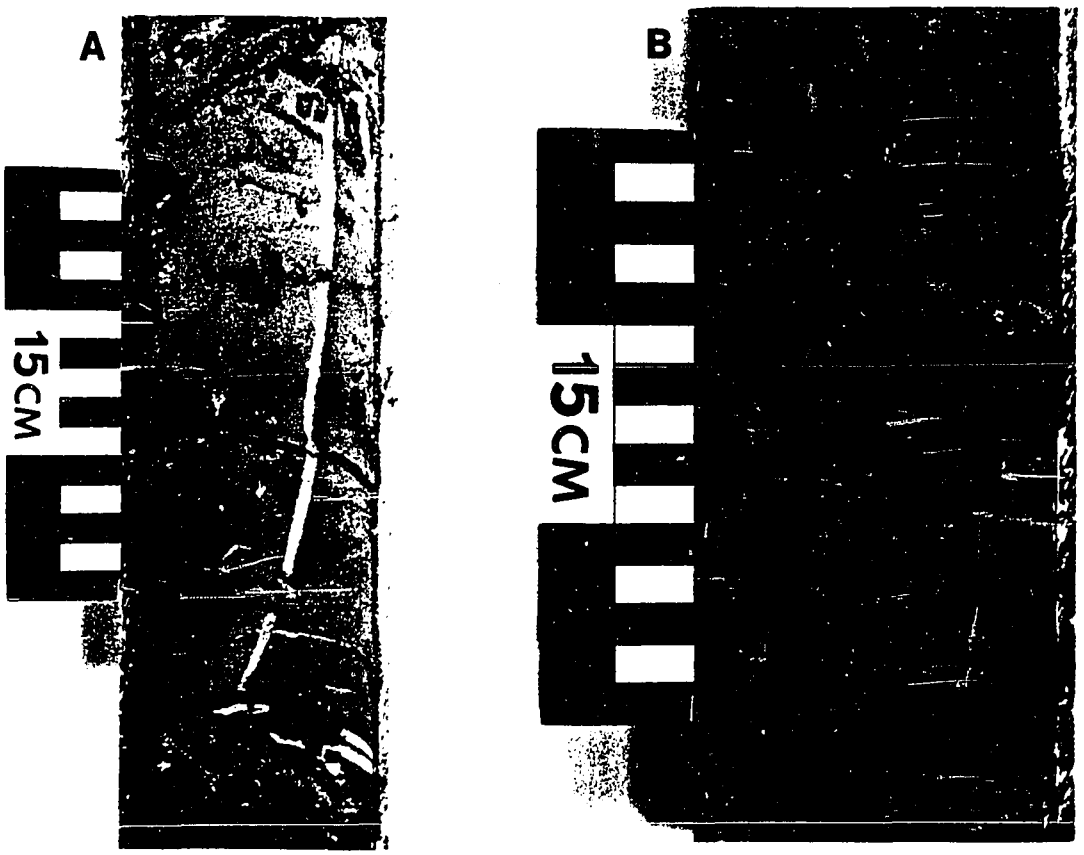

Figure 15. Representative photographs of the lagoonal facies: (A) laminated silty clay with sand- and shell-filled Skilithos burrows and (B) large and small burrows filled with sand in laminated silty clays.

Figure 16. Representative photographs of salt marsh facies from the margins of Lake Pelto and Terrebonne Bay.

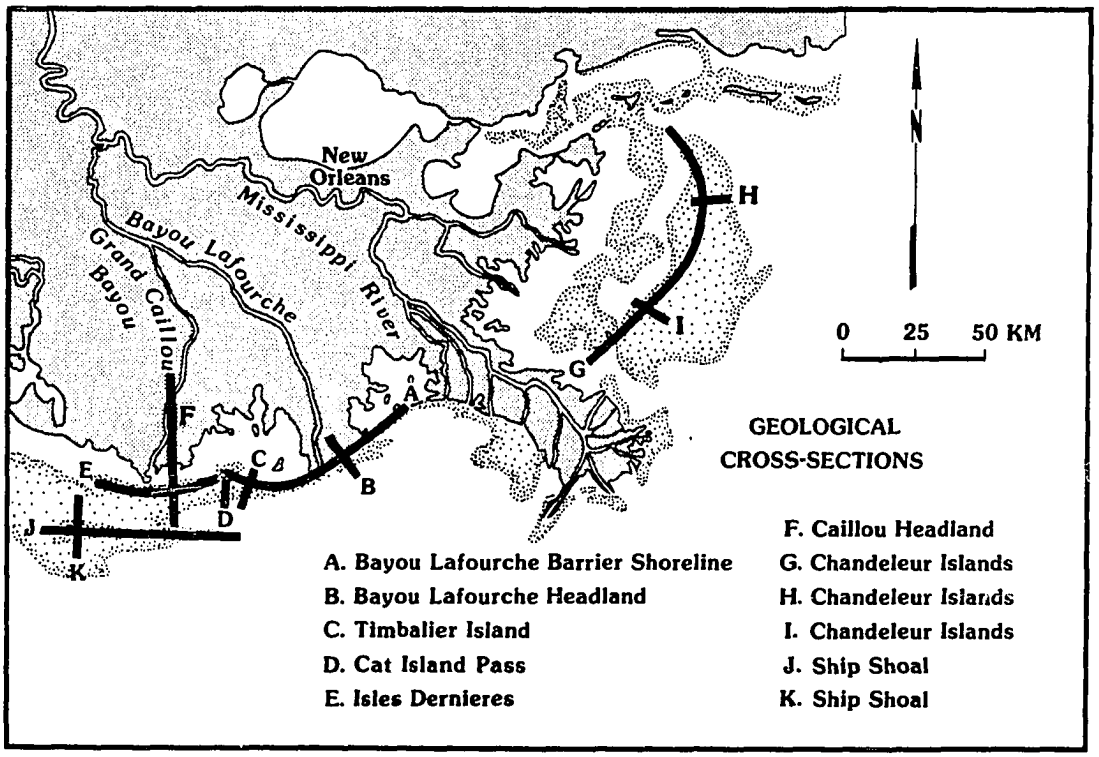

Figure 17. Location map and explanation of the geologic cross sections presented in the text. The cross sections were built from the following data bases: seismic and vibracore data from the Louisiana Geological Survey (unpubl. data), U.S. Army Corps of Engineers (1962, 1972, 1975), Neese (1984), Gerdes (1985), Conaster (1969), Frazier et al. (1978), Kolb and Van Lopik (1958), Penland and Suter (1983), Penland et al. (1986b, 1987b, 1988a, 1988b, 1988c), and Suter and Penland (1987).

reaches into the supper ends of the bay, the *Rangia* sp. die out and are replaced by the more salt-tolerant *Crassostrea*sp. Fine-grained sediment accumulate in this setting and the considerable biologic activity produces a bioturbated mud sequence. Storm processes rework surface sediment and shell reefs producing graded storm bedding. The mean grain size of the lagoonal facies ranged from 4.3-5.5ϕ with a standard deviation of 1.71-2.3ϕ. The sand content is 5-30%. The lagoonal facies is a burrowed silty clay containing parallel and ripple laminations of silt and shell. Vertical and horizontal burrows filled with sand and shell are common.

Salt Marsh

The salt marsh facies is used to describe the sediments which accumulate in the *Spartina alterniflora* dominated salt marshes surrounding backbarrier bays and sounds (Figure 16). Other common plants are *Juncus roemerianus, Distichlis spicata,* and *spartina patens.* Salt marsh sediments are characterized by rooted silty clay deposits containing detrital organic layers, burrows, and low-angular to horizontal laminations. The organic content is 5-35% (Kosters, 1989).

Geologic Cross Sections

The geologic cross sections were built from new seismic and vibracore data collected as well as from existing geotechnical reports, Louisiana Geological Survey, theses, dissertations, U.S. Army Corps of Engineers' reports, journal publications, and conference proceedings. The geologic strike section of the Bayou Lafourche shoreline (A) in Figure 17 was built with vibracores/borings from Gerdes (1985), Conaster (1969), Louisiana Geological Survey, and the U.S. Army Corps of Engineers (1975, 1980). The geologic dip section (B) through the Cheniere Caminada beach ridge plain in the Bayou Lafourche headland was built with vibracores from Gerdes (1985) and the Louisiana Geological Survey. The geologic dip section (C) was built using borings from the U.S. Army Corps of Engineers (1962, 1975) and seismic data from the Louisiana Geological Survey. The seismic dip section (D) is built from Louisiana Geological Survey seismic data (Suter and Penland, 1987). The geologic strike section (E) of the Isles Dernieres is built from vibracores/borings from Neese (1984), U.S. Army Corps of Engineers (1962, 1975), and Louisiana Geological Survey. The regional dip section (F) through the Terrebonne coastal region was built using LGS seismic and vibracores. The Chandeleur Island strike

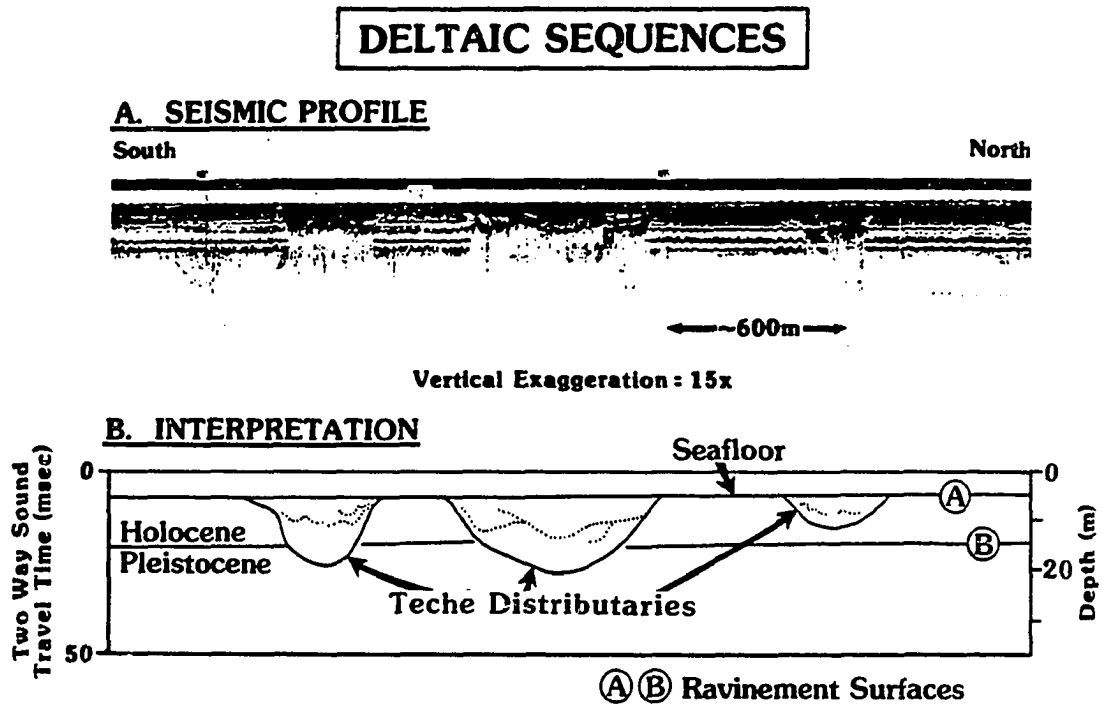

Figure 18. Interpreted seismic section from the Trinity Shoal area illustrating multiple ravinement surfaces, Holocene/Pleistocene contact, and the Teche distributaries of the Late Holocene delta plain.

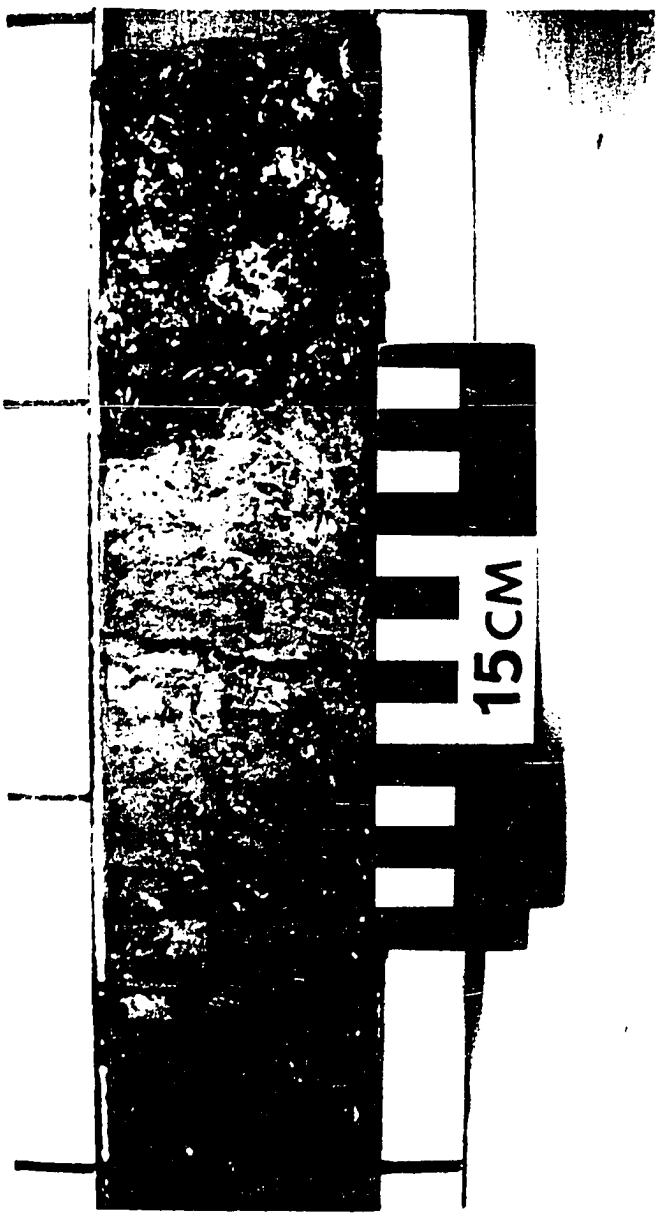

Figure 19. Vibracore photograph from the Terrebonne coastal region illustrating the contact between the Modern and Late Holocene delta plains. Prodelta muds overlie a ravinement surface truncating a lagoonal sequence marked by a transgressive lag of sand and reworked *Rangia* sp. shells.

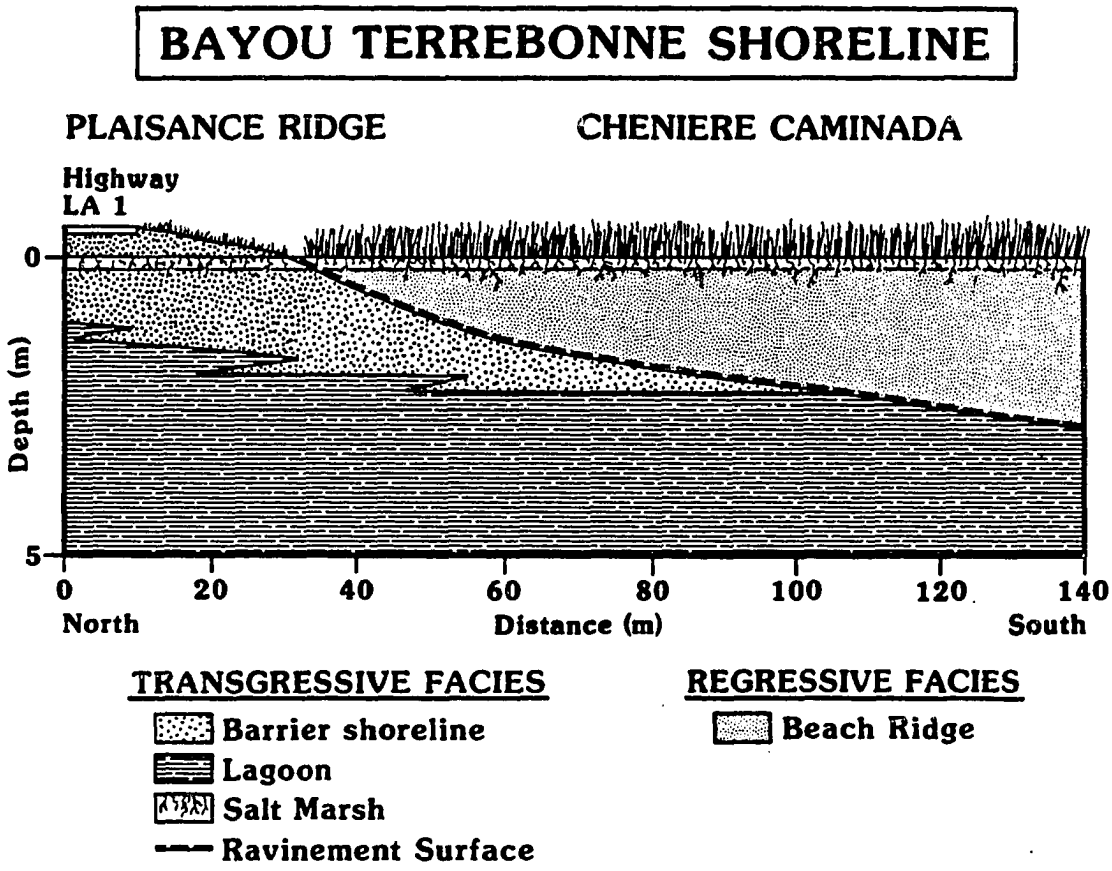

Figure 20. Diagram illustrates a dip cross section exposed in a sand pit showing the contact between the Bayou Terrebonne and Bayou Lafourche delta lobes with the large Lafourche delta complex.

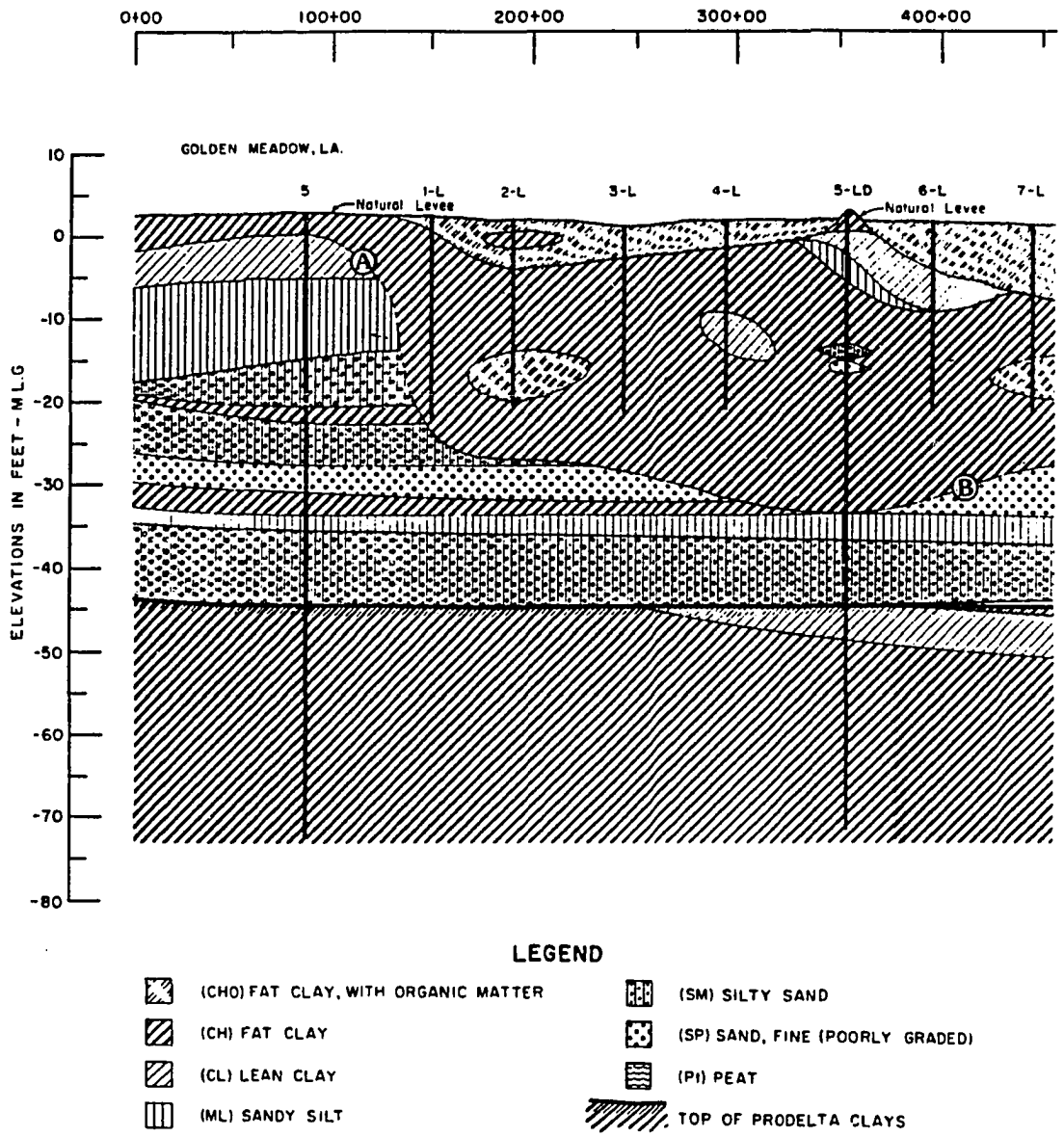

Figure 21. Diagram shows the regional ravinement surface recognized in an USACE cross section (1962a) which separates the Modern and Late Holocene delta plain. (A) Teche shoreline and (B) Teche ravinement surface.

section (G) was derived from Frazier et al. (1978) supplemented by LGS vibracores. The Ship shoal cross sections (J, K) were built using LGS seismic and vibracores data, this is also the case for Trinity Shoal.

The seismic, vibracores, and cross sections are designed to illustrate the depositional sequences which make up the facies architecture of the barrier island and delta plain systems of the Mississippi River. The term depositional sequence is used to describe "a stratigraphic unit composed of a relatively conformable succession of genetically related strata and bounded at its top and base by unconformities or their correlative conformities" (Mitchum, 1977). In this study, ravinement surfaces served as the major unconformity upon which depositional sequences were delineated and mapped. A ravinement surface is generated by shoreline and shoreface erosion during transgression (Swift, 1979; Nummedal and Swift, 1987). Ravinement surfaces are recognized as high amplitude reflectors in seismic, stratigraphic unconformities marked by a sandy/shelly transgressive lag in core, or as a paleo-transgressive shoreline expressed by surface morphology and outcrop in borrow pits.

Figure 18 illustrates an interpreted seismic section from the Trinity Shoal region depicting multiple ravinement surfaces, the Holocene/Pleistocene boundary, and three Bayou Teche distributaries truncated by shoreface erosion. In Figure 19 a photograph of a ravinement surface in the Terrebonne coastal region illustrates the contact between the Modern and Late Holocene delta plains. Figure 20 is a schematic drawing of the Plaisance sand mine along Highway 1, in Lafourche Parish adjacent to the north side of the Cheniere Caminada beach ridge plain, showing the ravinement surface between the Bayou Terrebonne and Bayou Lafourche delta lobes within the Lafourche delta complex. These figures serve to point out the importance of the ravinement surface as a sequence boundary as well as to how to recognize this unconformity (Figure 18, 19, and 20). It is interesting to note that many of the design studies by the USACE in support of navigation projects mapped ravinement surfaces in cross section without recognizing them as such, this only goes to show how easy it is to identify a ravinement surface. Figure 21 is an example of a USACE cross section in Barataria basin near Golden Meadow which mapped the position of the Teche shoreline and ravinement.

BARRIER ISLAND EVOLUTION

Mississippi River Sedimentation

Mississippi River sediment accumulate in deltaic depositional sequences consisting of a regressive, or constructional phase followed by a transgressive or destructive phase (Figure 22). Scruton (1960) used the term *delta cycle* to refer to these alternating phases of deltaic evolution. Many studies have focused on the regressive phase (Russell et al., 1936; Fisk, 1944; Kolb and Van Lopik, 1958), resulting in the development of a composite Mississippi delta stratigraphic column that emphasizes the deep-water Balize delta (Coleman and Wright, 1975) and the importance of sediment accumulated during transgression in abandoned delta systems is not emphasized.

The objective of this chapter is to provide a comprehensive model for the transgressive phase of Mississippi River delta plain depositional systems. Previous research has identified many of the components of an abandoned Mississippi River delta complex (Coleman and Gagliano, 1964) and the stratigraphic relationship between the regressive and transgressive phases of the deltaic sequence (Frazier, 1967; LeBlanc, 1972). The present study provides a detailed description of transgression in abandoned Holocene Mississippi River delta complexes, and an evolutionary model that links delta complexes into an ordered spatial and temporal sequence of development. The evolutionary model is based on a synthesis of vibracores, seismic profiles, and soil borings, supplemented by an analysis of more than 45 historical coastal charts dating back to the early 1700s (Appendices B, C, D, E, and F). Compilation and analysis of the vibracore and seismic data resulted in the development of cross sections depicting major facies relationships, sequence boundaries, and regional ravinement surfaces (Figure 17). The historical coastal charts provide information on shoreline changes, shoreface erosion, and the morphology of the coastline at different dates.

Difficulties arise with terminology in a study that covers both geomorphology and stratigraphy and integrates findings on deltaic and coastal sedimentary environments. The term *delta* is used to indicate a landform. The sediments that are deposited in a deltaic environment constitute a parasequence that accumulates locally in a single delta or as several deltas grouped together in a *delta complex*. A complete Mississippi River deltaic depositional sequence consists of a regressive component and a transgressive component. The term, *regressive*, is used to describe "a seaward

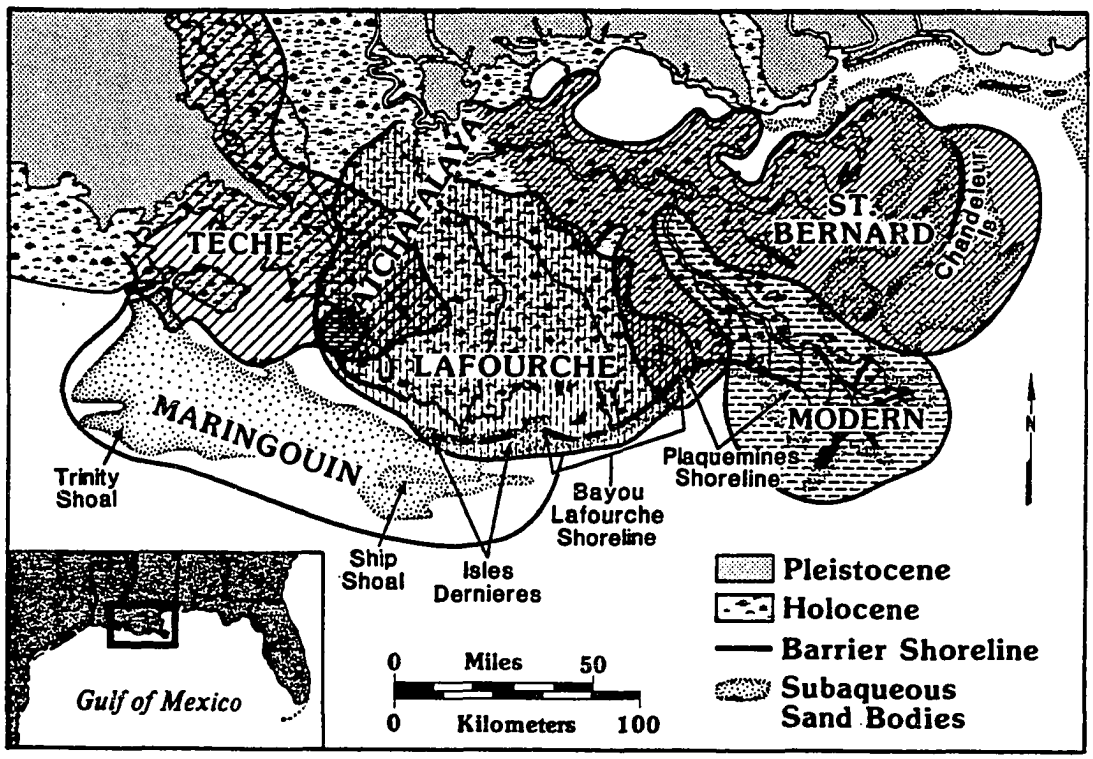

Figure 22. Location map of the Holocene Mississippi River delta plain showing the distribution of transgressive barriers and shoals. Over the last 7000 years, the Mississippi River has built a delta plain consisting of six delta complexes; four are abandoned (Maringouin, Teche, St. Bernard, and Lafourche), and two are active (Modern and Atchafalaya). More than 75 percent of the Mississippi River delta plain is abandoned and is in various stages of transgression due to submergence (modified from Frazier, 1967, 1974).

movement of the shoreline indicated by seaward migration of the littoral facies" (Mitchum, 1977). The term, *transgressive* is used to describe "a landward movement of the shoreline indicated by landward migration of the littoral facies" (Mitchum, 1977). Although initially difficult to concieve of in a deltaic setting, transgressive sedimentation is an integral part of river-dominated, cyclic, deltaic sequences such as those formed by the Mississippi River, where such sedimentation can contribute a significant proportion to the total sequence thickness. This study concentrates on sandy barrier and shoal systems, recognizing that the term *barrier* implies the existence of lagoonal, wetland, or estuarine environments and that such environments predominantly occur during transgressive rather than regressive phase (Kraft, 1971).

Apart from the Modern delta complex located in deep water near the shelf edge, Holocene Mississippi River sediments have accumulated in shallow water, shelf-phase delta complexes. The delta-building process consists of prodelta platform formation, followed by distributary progradation and bifurcation, which results in delta plain establishment. This process continues until the distributary course is no longer hydraulically efficient. Abandonment occurs in favor or a more efficient course, initiating the transgressive phase of the *delta cycle*. The abandoned delta complex subsides, and coastal processes rework the seaward margin, generating a sandy barrier shoreline backed by bays and lagoons (Kwon, 1969; Penland et al., 1981). Each transgressive depositional system is derived from a single abandoned delta or delta complex (Figure 22).

According to Frazier (1967), the Mississippi River has built six major delta complexes consisting of more than 18 smaller deltas over the last 7,000. During this time (Figure 22), delta complex building began in the area of Cocodrie (Maringouin) and switched sequentially west near Marsh Island (Teche), east near New Orleans (St. Bernard), west again south of Donaldsonville (Lafourche), then southeast of Belle Chase (Modern), and finally back to the west, below Morgan City (Atchafalaya) according to Frazier (1967). Today, the delta plain can be divided into two distinct geomorphic regions, active deltas and abandoned deltas. Delta building is restricted to the Modern delta complex and the Atchafalaya delta complex. The four remaining complexes, the Maringouin, Teche, St. Bernard, and Lafourche, are abandoned. In addition, the Plaquemines delta of the Modern complex is abandoned.

Transgressive Depositional Systems

Bayou Lafourche Barrier System

Geomorphology

The Bayou Lafourche transgressive depositional system consists of a central erosional headland fronted by the Caminada-Moreau coast with a pair of recurved spits and flanking barrier islands on either side, the Caminada Pass spit and Grand Isle to the east and Timbalier Islands to the west (Figure 23). Behind the flanking barriers lie two restricted interdistributary bays Barataria Bay and Timbalier Bay. Since the abandonment of the Bayou Lafourche delta some 300 yBP, shoreface erosion has actively supplied sand for flanking barrier development (Gerdes, 1985). The primary sand sources are the Bayou Lafourche distributaries and the Chenier Caminada beach ridge plain (Penland et al., 1986a).

The Caminada-Moreau coast is a thin, discontinuous mainland beach with marsh outcropping on the lower beach face. Sediment abundance increases downdrift to the east and west, as evidenced by washover terraces that eventually coalesce farther downdrift to form a higher more continuous dune terrace and eventually a continuous foredune ridge on the margins of the headland (Ritchie and Penland, 1985). The Caminada Pass spit was formed by downdrift spit accretion through lateral migration away from the Bayou Lafourche erosional headlands. The Timbalier Islands and Grand Isle developed through this same process (Penland et al. 1981). Washover sheets and multiple washover channels are common on the updrift, erosional end of Timbalier Island. Downdrift, longshore bars become more numerous and better developed because of increasing sediment abundance. Dune ridges form by onshore bar migration and welding, followed by aeolian reworking and dune development (Ritchie and Penland, 1988).

A historical map comparison for the years 1887-1978 shows retreat of over 3 km on the erosional headland in the vicinity of Bayou Lafourche and Bay Marchand, and westward lateral migration of over 5 km at Timbalier Island (Figure 24). A similar pattern of lateral barrier island migration is seen at Grand Isle. This pattern of longshore spit building and breaching illustrates Gilbert's (1885) model of barrier island formation. Once detached from the mainland, flanking barrier islands migrate by updrift erosion and downdrift spit building. The recurved spit morphology

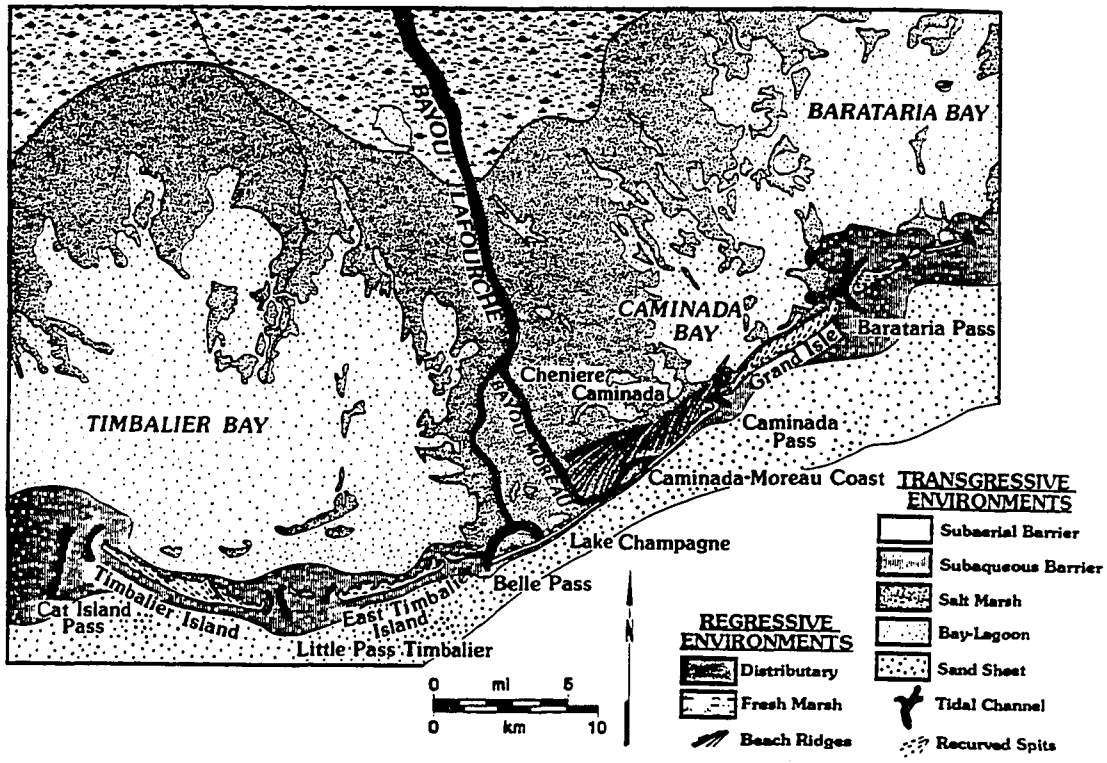

Figure 23. The Bayou Lafourche transgressive depositional system consists of (1) the Bayou Lafourche headland containing Cheniere Caminada, (2) the flanking barriers of the Caminada Pass spit and Grand Isle to the east, (3) the Timbalier Islands to the west, and (4) two restricted interdistributary bays, Barataria Bay and Timbalier Bay (Penland et al., 1988a).

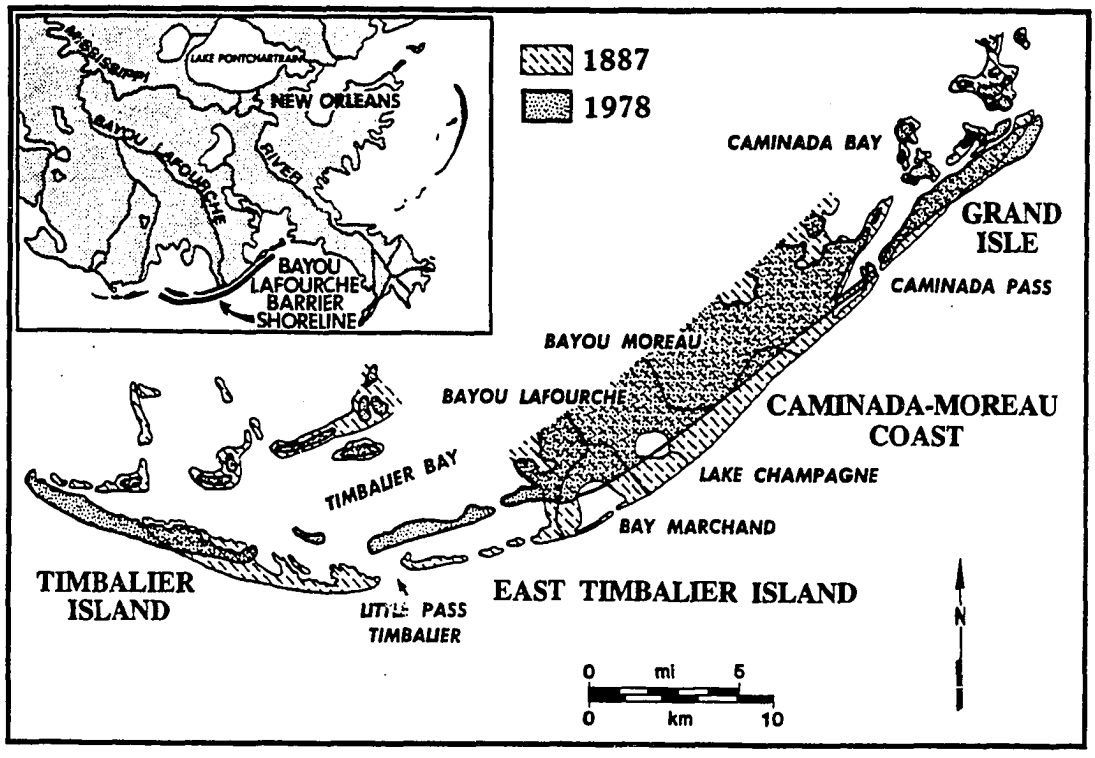

Figure 24. Coastal changes in the Bayou Lafourche barrier shoreline between 1887 and 1978 (Penland and Boyd, 1981).

of Timbalier Island reflects this process.

Flanking barrier island growth and breaching have led to the development of large tidal inlets at Cat Island Pass, Little Pass Timbalier, Caminada Pass, and Barataria Pass. Due to submergence and land loss, the Timbalier, Caminada, and Barataria bays are continually increasing in size and depth, resulting in an increase in the volume of water stored within these restricted interdistributary bays. Therefore, the volume of water exchanged through tidal inlets during a tidal cycle increases, leading to increases in inlet cross sectional area, tidal current velocity, and sediment storage capacity. The tidal prism/tidal inlet relationship represents an important process affecting barrier island shape and tidal inlet sediment dispersal, evolution, and sand body development. A long-term increase in tidal prism volume will eventually lead to a situation in which the volume of sediment stored within the tidal inlet is comparable to, if not more than, the volume of sediment stored within the adjacent flanking barrier islands. As the tidal prism increases, the morphology tidal inlets changes from wave-dominated with flood tidal deltas to tide-dominated with large ebb tidal deltas (Levin et al. 1983; Suter and Penland, 1987).

Stratigraphy

Along the Caminada-Moreau coast, distributaries associated with Bayou Lafourche and Bayou Moreau are seen in the subsurface and are depicted in the stratigraphic strike section of Figure 25A. Between Bayou Moreau and Caminada Pass spit, Cheniere Caminada beach ridges are exposed on the eroding surface. The Bayou Lafourche barrier sand body thickens downdrift from 1-2 m thick in the central headland to 4-5 m thick at Grand Isle, and reaches a maximum thickness of 5-6 m near Cat Island Pass at Timbalier Island.

A stratigraphic dip section through the central Bayou lafourche erosional headland, Figure 25B, shows the facies relationship between the eroding shoreface and distributary and beach ridge sand bodies. The Caminada-Moreau barrier is a prism of washover sediment 1-2 m thick. A thin sequence of organic-poor salt marsh deposits overlying organic-rich fresh marsh outcrops on the eroding beach face. The relatively thin nature of the salt marshes overlying the headland reflects the initial effects of submergence and salt water intrusion acting on the Bayou Lafourche delta. A stratigraphic dip section through Timbalier island west of the headland shows this sand body overlies

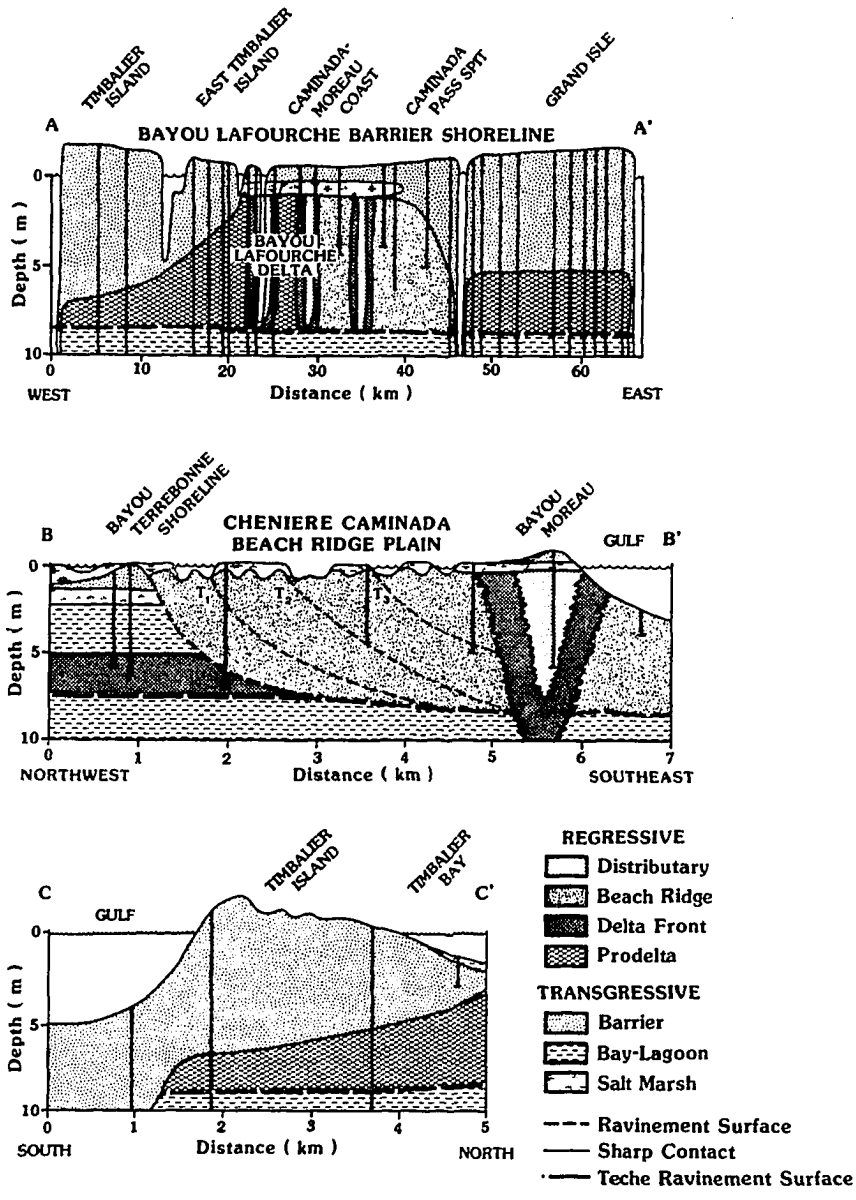

Figure 25. (A) Stratigraphic strike section A-A' is of the Bayou Lafourche barrier shoreline (Figure 17). The shelf phase Bayou Lafourche delta lies on a shallow ravinement surface 7-8 m in the subsurface. Distributary and beach ridge sand bodies core the headland and supply sand through shoreface erosion for flanking barrier development. The transgressive barrier sands increase in thickness from 1-2 m at the headland to over 5 m at the downdrift ends of the flanking barrier islands. (B) Stratigraphic dip section B-B' from the central portion of the Bayou Lafourche delta headland shows the Cheniere Caminada beach ridge plain lying seaward of the transgressive Bayou Terrebonne shoreline and interfingering with the Bayou Moreau distributary as it meanders away from the coast (modified from Gerdes, 1985). (C) Stratigraphic dip section C-C' is from Timbalier Bay across Timbalier Island and onto the inner shelf. Timbalier Island represents a flanking barrier island composed of recurved spit and tidal channel deposits derived from the eroding Bayou Lafourche delta headland (Penland et al., 1988d).

a sequence of regressive deltaic muds (Figure 25C). The sand body, which has a maximum thickness of 5-6 m, pinches out seaward on the erosional shoreface and interfingers landward with a sequence of restricted interdistributary bay muds. Surficial sediment samples show a thin sand sheet spreading seaward of the shoreline (Krawiec, 1966).

Isolated, filled tidal channel scars are found offshore of the Timbalier Islands, marking the retreat path of the Bayou Lafourche barrier system (Suter and Penland, 1987). A seismic strike section (Figure 26) depicts westward-dipping clinoforms within a tidal channel sequence 8-10 m thick associated with the westward migration of Timbalier Island and Cat Island Pass. Large tidal sand bodies are also found east of the Bayou Lafourche headland, where the ebb tidal deltas of Caminada Pass and Barataria Pass extended 2 km of 6 km offshore of Grand Isle and are 3 km and 8 km wide, respectively. Tidal channel depths range from 10-20 m, and localized scour holes are up to 50 m at channel junctions (USACE, 1972; Shamban, 1985).

Isles Dernieres Barrier System

Geomorphology

The symmetrical, 32-km long Isles Dernieres barrier island arc formed in response to the abandonment of the Bayou Petit Caillou delta within the Lafourche delta complex approximately 420 yBP (Penland et al., 1987b) (Figure 27; Appendix D). Typical barrier widths are 1.5-2.0 km in the central island arc and 0.5-1.0 km in the downdrift flanks which are dominated by recurved spits. The Isles Dernieres have fragmented into four smaller islands separated by tidal inlets. These inlets are 300-1200 m wide and 6-18 m deep. Inlet morphology varies from wave-dominated to tide-dominated depending on the size of the tidal prism. Wine Island shoal, a former barrier island, is the easternmost island member. Remnants of the Cheniere Caillou beach ridge plain, associated with the progradation of the Bayou Petit Caillou distributaries, from the core of the east-central portion of the barrier island arc. Cheniere Caillou consists of a series of partially submerged beach ridges that spread seaward on their western margin against Caillou headland distributaries.

The recent shoreline history of the Isles Dernieres is one of rapid barrier island detachment, island fragmentation, and land loss. The transition of the Isles Dernieres from an erosional headland with flanking barrier islands to a barrier island arc is illustrated by the historical map comparison in Figure

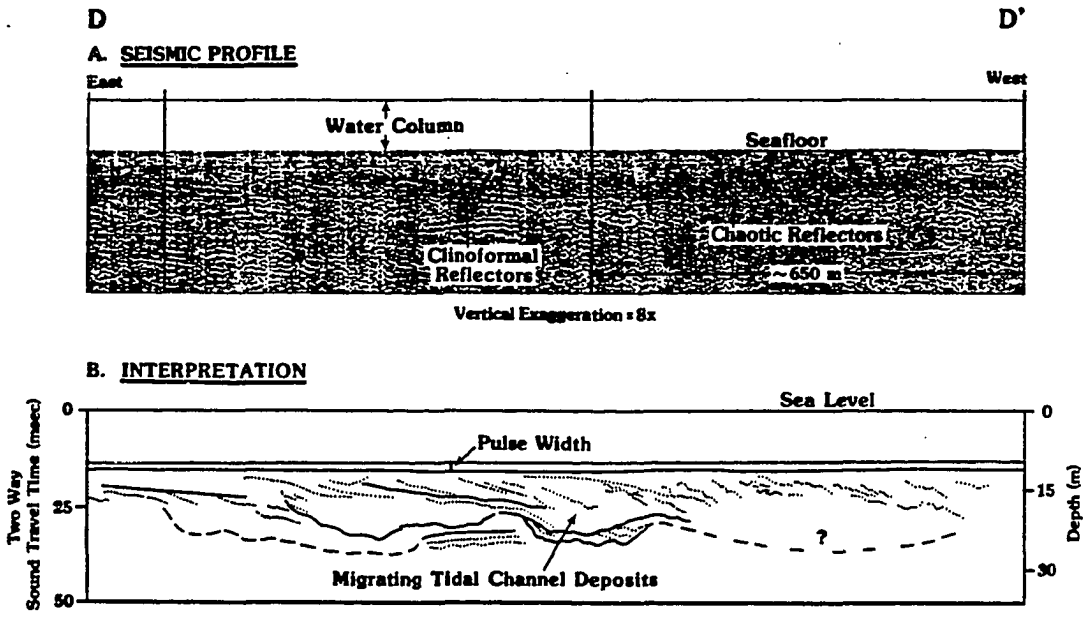

Figure 26. High resolution seismic profile and interpretative drawing along strike section D-D' through the tidal inlet scar of Cat Island pass. Westward-dipping clinoforms characterize the tidal inlet deposits generated by the westward migration of Cat Island Pass; sequences reach thicknesses of 10 m or more (modified from Suter and Penland, 1987).

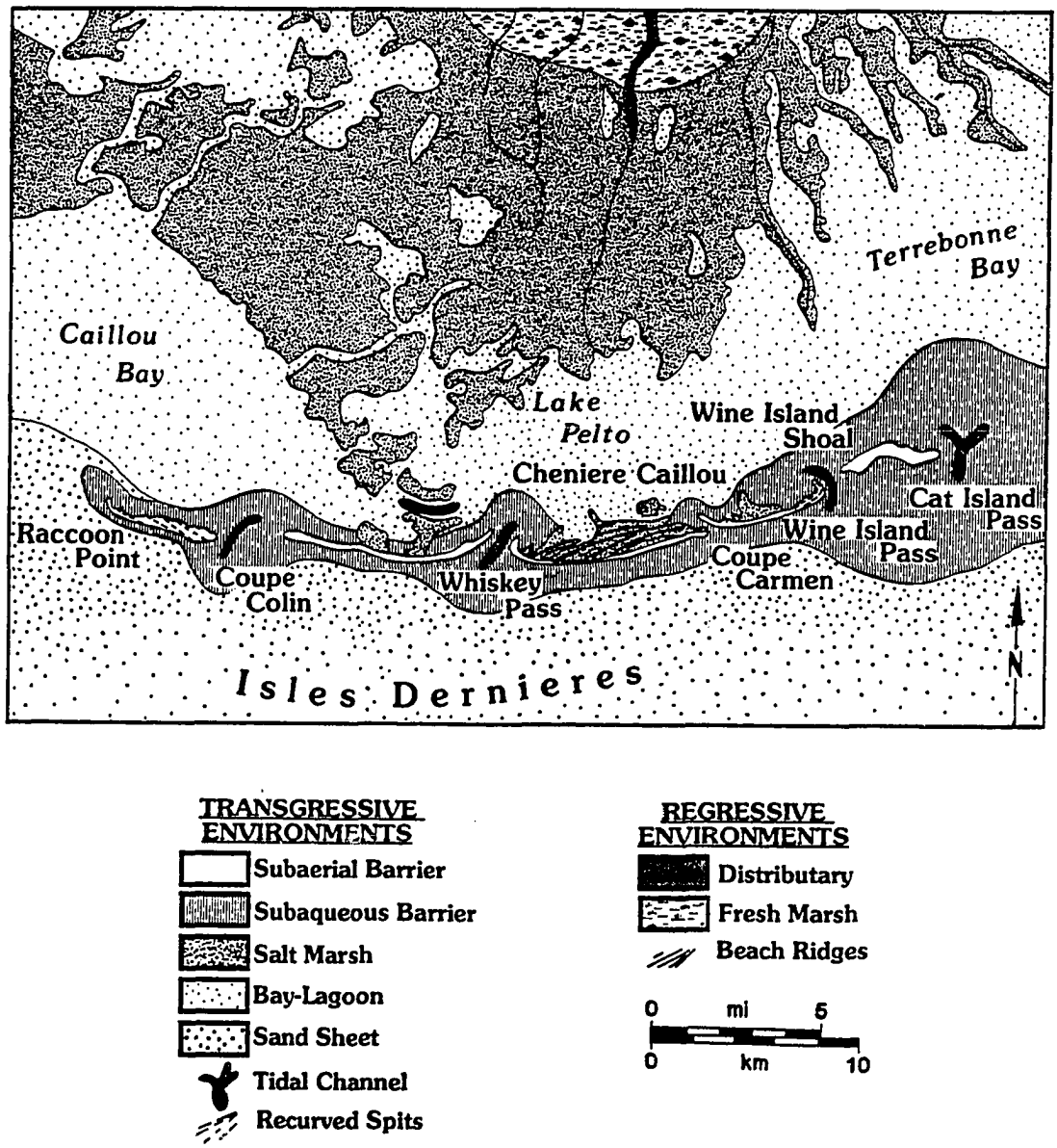

Figure 27. The Isles Dernieres barrier system consists of four island fragments that originated from a single island in 1853. Today the morphology of these small island remnants is dominated by recurved spits. This young barrier island arc is cored by distributaries and beach ridges associated with Bayou Petit Caillou delta in the Cheniere Caillou area (Penland et al., 1988a).

28. In 1853, Caillou Boca, Pelto Bay, and Big Pelto Bay separated the Isles Dernieres from the adjacent mainland by less than 500 m at the narrowest point. By 1978, these bays had coalesced and increased in size threefold to form the modern day Lake Pelto. The northern shore of Lake Pelto had greater land loss during this time period and retreated faster than the Gulf shoreline, resulting in the detachment of the Isles Dernieres from the mainland by more than 7 km of open water. The Isles Dernieres have steadily decreased in size over time from 34.8 km^2 in 1887 to 10.2 km^2 in 1979 (Penland and Boyd, 1981).

Stratigraphy

The stratigraphic strike section in Figure 29 shows that the subsurface of the Isles Dernieres consists of a complex set of interfingering distributary, interdistributary, and beach ridge facies overlain by a sequence of lagoonal and barrier shoreline facies. A set of bifurcating distributaries 4-5 m thick associated with the Bayou Petit Caillou delta extends seaward under the east-central portion of the Isles Dernieres and interfingers with the Cheniere Caillou beach ridge plain (Penland et al., 1985). The Cheniere Caillou beach ridge plain is 5-6 m thick and interfingers with regressive prodelta and delta front deposits lying on an older ravinement surface. The top of this beach ridge sequence lies about 2 m below mean sea level. In the central Isles Dernieres, the Bayou Petit Caillou delta is overlain by a thin sequence of washover sands resting on lagoonal deposits 1-2 m thick. The barrier sand body increases in thickness to 4-5 m toward Wide island and Raccoon Point. The bulk of the transgressive barrier sands are stored west of the central headland in recurved spits and ebb tidal deltas associated with Coupe Colin and Raccoon Island. The present barrier island arc sand body and backbarrier deposits pinch out on the upper shoreface and overlie the regressive core of the submerged Bayou Petit Caillou delta.

Figure 30 shows a vibracore dip section across Lake Pelto from the mainland Terrebonne salt marshes, seaward across the Isles Dernieres, illustrating the relationship between the underlying Bayou Petit Caillou delta facies and the overlying transgressive Isles Dernieres facies. The fine-grained lagoon sequence averages 1-2 m thick and the adjacent salt marshes around Lake Pelto are typically 1 m thick. Beneath these transgressive deposits lie regressive distributary and beach ridge deposits which supplied the sands for the development of the Isles Dernieres. The Isles Dernieres

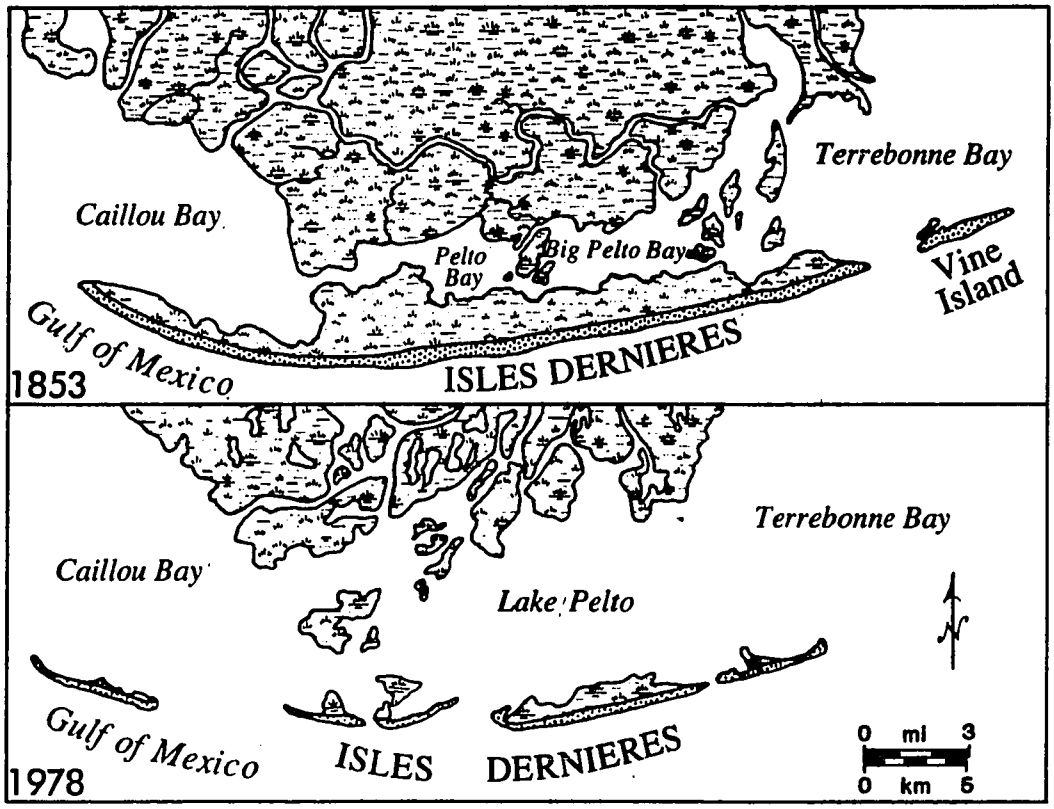

Figure 28. The shoreline changes in the Isles Dernieres barrier system between 1853 and 1978 illustrate the transition, through Hoyt's (1967) mainland detachment submergence process, from an erosional headland with flanking barriers to a barrier island (Penland et al., 1981).

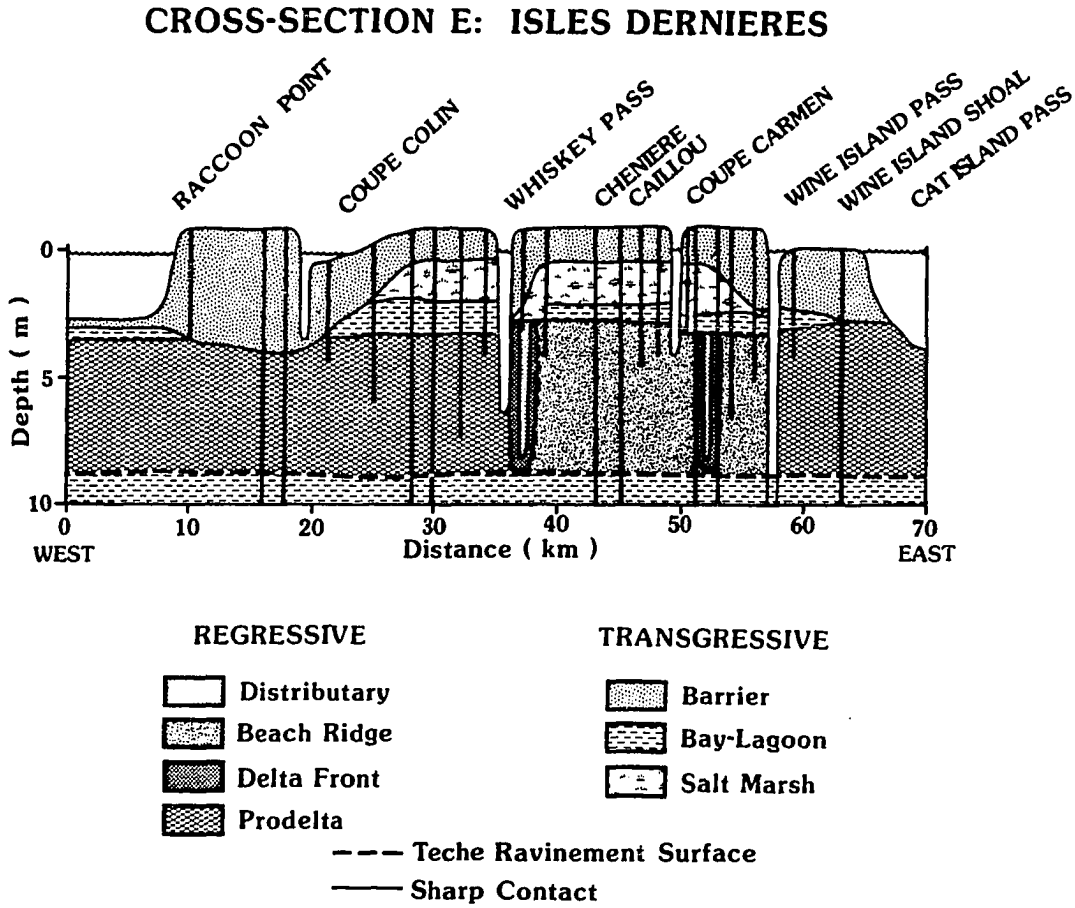

Figure 29. The Isles Dernieres barrier island arc in strike section E-E' is cored by a sequence of distributary and beach ridge sand bodies associated with the shelf-phase Bayou Petit Caillou (Figure 17). The transgressive barrier sands increase in thickness from 1-2 m over the central headland and from 5-6 m at the downdrift end of recurved spits. This delta of the larger lafourche delta complex lies on a ravinement surface 7-8 m in the subsurface.

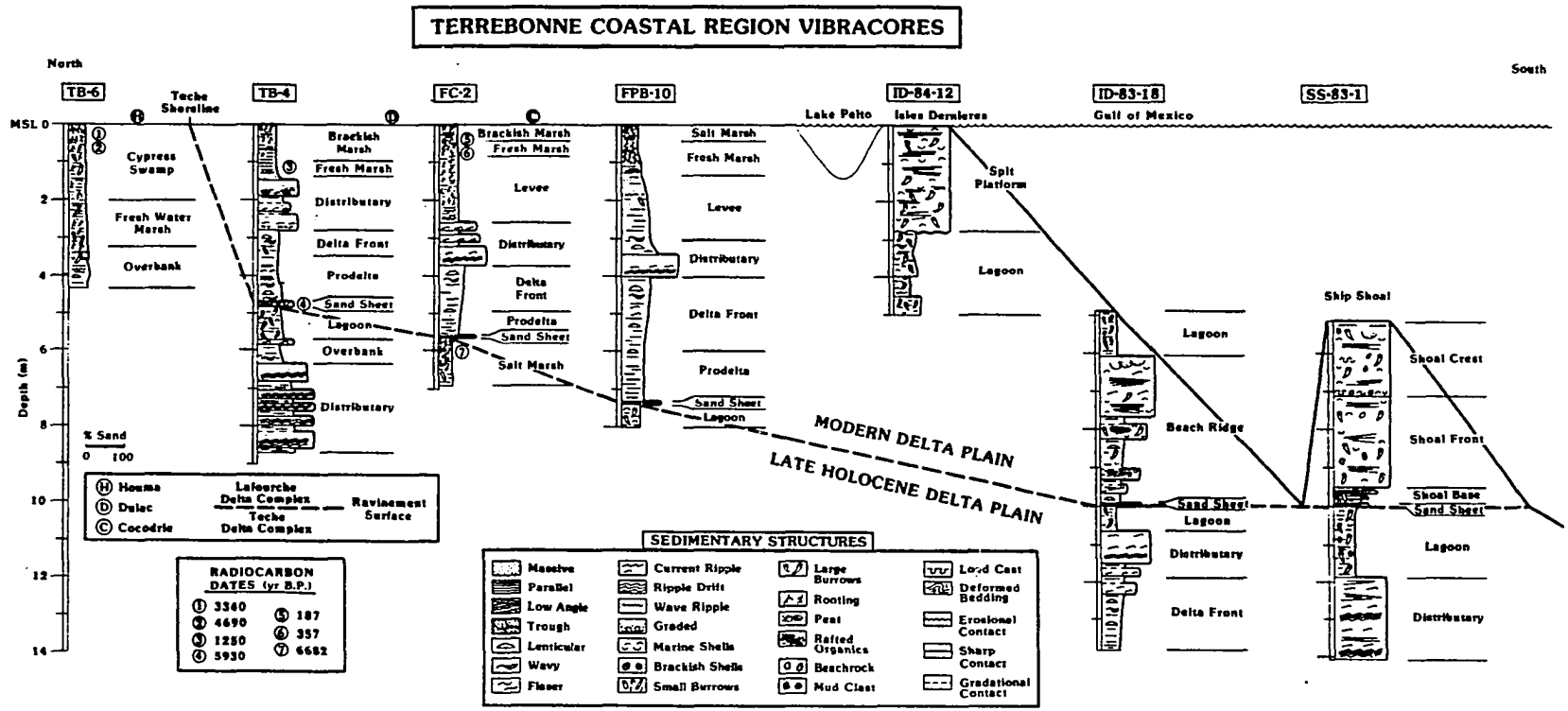

Figure 30. Diagram illustrates a vibracore dip section (F-F') of the complete shelf-phase Bayou Petit Caillou delta from the Teche shoreline south to the Isles Dernieres barrier island arc. This shallow water delta lies on a ravinement surface 7-8 m in the subsurface near the Isles Dernieres that merges updip to a relict transgressive barrier shoreline. Note the total thickness of this deltaic sequence and the significance of the transgressive sequence component that becomes thicker toward the coast (Penland et al., 1988a).

consist of a 2-3 m thick sequence of recurved spit sands overlying a sequence of lagoonal muds 2 m thick.

Within the Isles Dernieres, Whiskey Pass and Coupe Carmen are shallow, wave-dominated inlets with well-developed, flood tidal delta sand bodies 1-2 m thick (Neese, 1984; Penland et al., 1985). Maximum channel depths are 3-5 m. Coupe Colin and Wine Island Pass are mixed energy inlets with tidal delta sand bodies confined to the inlet throat. Vibracores and high-resolution seismic profiles reveal that the Wine Island Pass ebb tidal delta is 6 m thick and pinches out seaward, overlying tidal channel scars.

Chandeleur Barrier System

Geomorphology

The oldest transgressive barrier island arc found in the Mississippi River delta plain is the Chandeleur Islands (Figure 31). The asymmetric shape of the chandeleur Islands is due to their oblique orientation to the dominant southeast wave approach which leads to the preferential transport of sediment northward (Kahn, 1980; Kahn and Roberts, 1982; Penland et al., 1985). The Chandeleur Islands are more than 75 km long, and island widths range from 200 m to over 2500 m. Northward, large flood tidal delta and washover fans separated by hummocky dune fields dominate barrier island morphology. The wide beaches and multiple bars in the surf zone reflect an abundance of sediment. Southward, the islands become narrower, the dunes taller, and the flood tidal deltas and washover fans give way to discontinuous washover terraces and flats. Farther south, the island arc fragments into a series of small, ephemeral islands and shoals separated by tidal inlets. Chandeleur-Breton Sound averages 3-5 m deep and separates the Chandeleur Island arc from the retreating mainland shoreline by more than 25 km of open water.

For the last 100 years, the Chandeleur Islands have retreated landward during fluctuating periods of land loss and gain to the total island area. Retreat rates along the Gulf shoreline are greater than 15 m/yr in the southern island arc and decrease northward to less than 5 m/yr. The Chandeleur Islands have experienced an average land loss rate of 0.11 km^2/yr since 1879 (Penland and Boyd, 1981). Periods of high and low hurricane frequency correspond to periods of high and low land loss. Constructive fair-weather processes lead to island recovery, followed by an increase

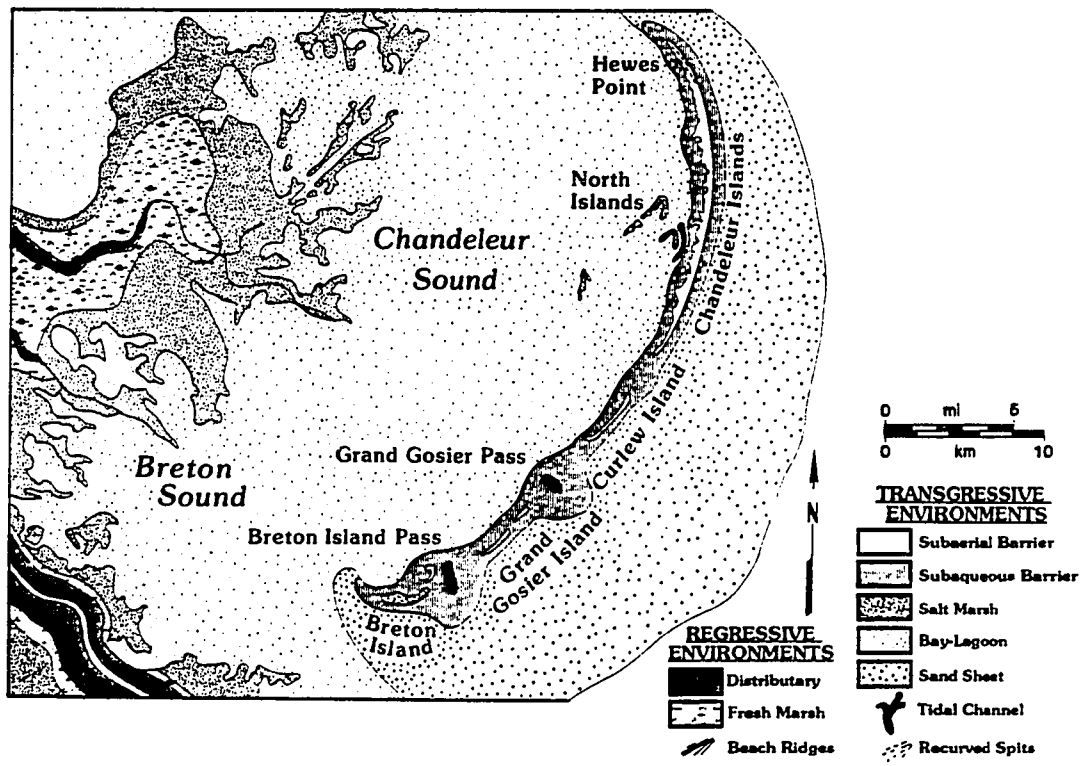

Figure 31. The Chandeleur transgressive depositional system represents the largest barrier island arc on the Mississippi River delta plain. Associated with the St. Bernard delta complex, this barrier island arc sand body is 75 km long and separated from the mainland by an intradeltaic lagoon 25 km wide (Penland et al., 1988a).

in island area. However, the historical rate of recovery is not sufficient to maintain the Chandeleur Islands against the frequency of hurricane impact. As a result, these islands experience a net long-term land loss. The mainland shoreline retreat rates exceed those of the Gulf shoreline of the Chandeleur Islands, indicating that the detachment process continue.

Stratigraphy

In strike section, the Chandeleur Islands sand body overlies a thick sequence of lagoonal deposits resting on the regressive St. Bernard delta complex (Figure 32). The distributary headlands, once the major sand sources, now lie on the lower shoreface and inner shelf and extend seaward under the central and southern Chandeleur Islands. Here, three major distributaries occur beneath the thin and discontinuous barrier island arc. Towards the north, the Chandeleur Islands sand body is thicker and more continuous and overlies a sequence of lagoonal deposits that increases in thickness northward from 2-7 m. The base of the Chandeleur Island transgressive depositional system averages 6-8 m below mean sea level. At tidal inlets, deep, isolated sand-filled sequences can develop because of channel migration. In areas where recurved spits build into deep water, thick sand bodies develop with the basal portions lying below the advancing ravinement surface, which has an average depth of 5-8 m (Penland et al., 1985).

The dip section shown in Figure 32B illustrates the facies relationships between the eroding shoreface and the regressive/transgressive components of the St. Bernard delta complex in the northern Chandeleur Islands. The barrier island arc sand body overlying lagoonal muds pinches out seaward on the erosional shoreface. Landward, flood tidal delta and washover sands overlie and interfinger with the lagoonal muds of Chandeleur Sound. The northern barrier island arc consists of a coarsening-upward sequence of lagoonal, flood tidal delta and washover deposits capped by beach and dune sands. Average sand body thickness is 5-7 m, increasing to over 10 m where local dune fields occur. A thin sand sheet spreads more than 5 km seaward of the Chandeleur Islands.

Farther south, the dip section shown in Figure 32C extends from Breton Sound seaward across the subaqueous shoal portion of the southern Chandeleur Islands. In contrast to the northern dip section, here the subaerial superstructure of the barrier island arc built of flood-tidal delta deposits has been submerged but is reworked by shoreface erosion. The sand body is 4-5 m thick

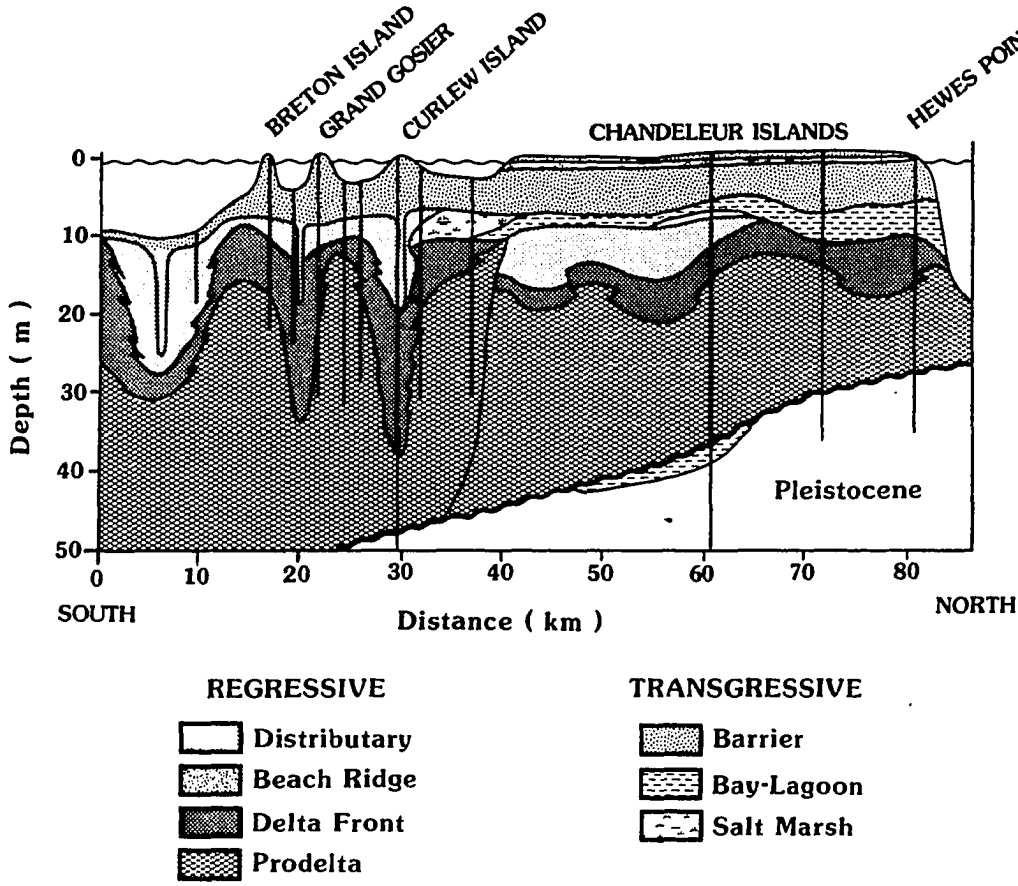

Figure 32. (A) Strike section G-G' illustrates the relatively uniform 5-10 m sand body thickness of the Chandeleur Islands. A sequence of lagoonal muds 2-4 m thick separates the basal flood tidal delta sands from the underlying surface of the St. Bernard delta plain. The St. Bernard distributaries lies under the southern half of the Chandeleur Island (modified from Frazier et al., 1978).

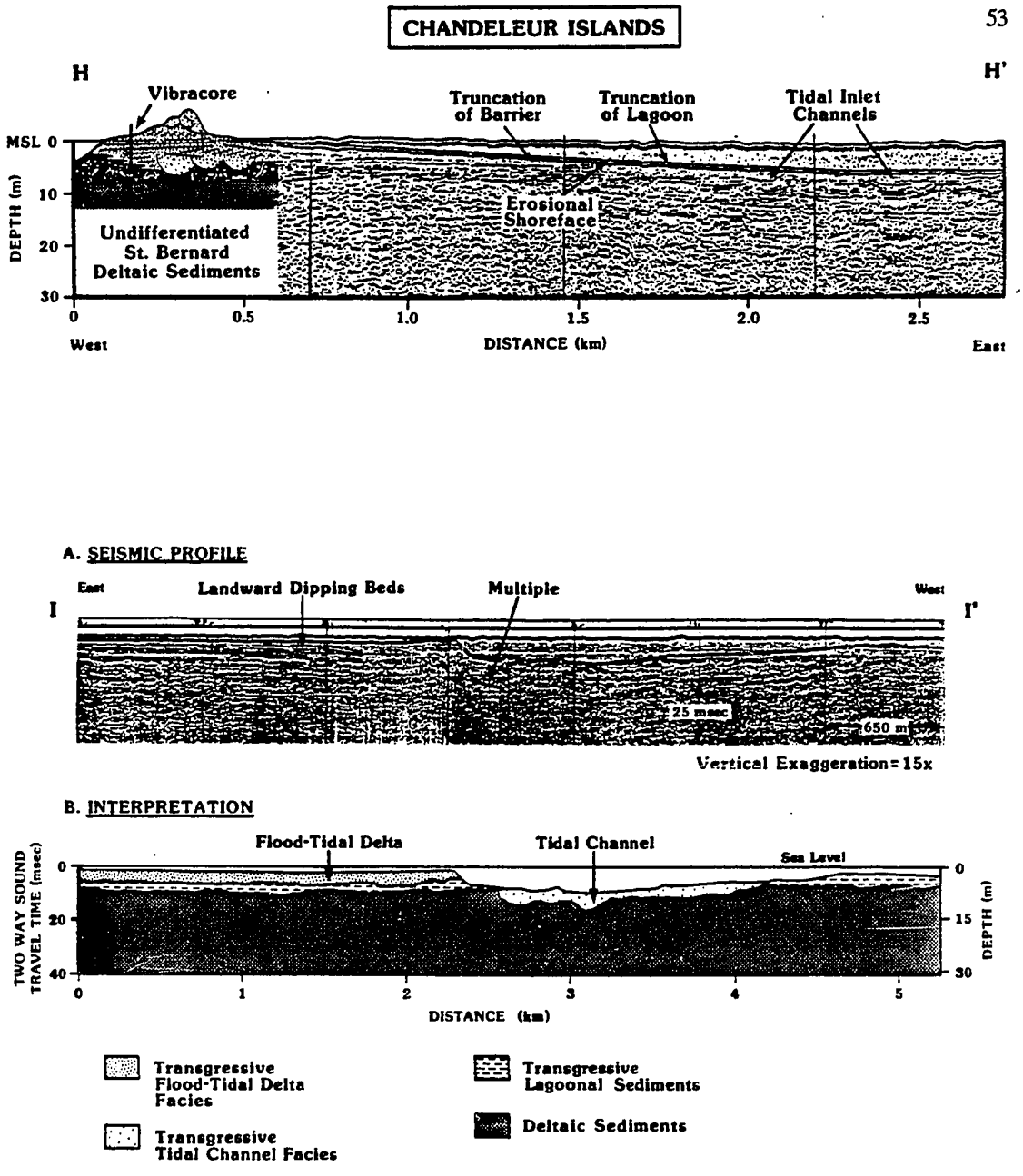

Figure 32. (B) Dip section H-H' illustrates the transgressive facies relationships through the northern Chandeleur Islands. Flood tidal delta sands interfinger with the lagoonal muds of Chandeleur Sound. Offshore, the barrier island sand body is truncated by shoreface erosion, and tidal inlet scars occur through the retreat path. (C) Dip section I-I' illustrates the facies relationships on the southern Chandeleur Islands, where the morphology is dominated by flood tidal deltas and sand shoals. This seismic section shows landward-dipping clinoforms within the flood tidal delta sand body overlying lagoonal muds of Breton Sound. A tidal channel is deflected against the landward margin of this flood tidal delta before it turns seaward at the south end of Grand Gosier Island (Penland et al., 1988a).

and pinches out on the lower shoreface. Landward, clinoforms within the flood tidal delta dip westward and overlie a 2-3 m thick sequence of lagoonal muds, which extends seaward under the southern Chandeleur Islands and is exposed on the inner shelf in the retreat path (Figure 32I.)

Ship Shoal System

Geomorphology

Ship Shoal is approximately 50 km long with widths ranging from 5 to 7 km in the central shoal area to 8-12 km at the eastern and western ends (Figure 33). Relief varies from 7 m in the west to 5 m in the east, and corresponding shoal crest water depths range from 3 m in the west to 8 m in the east. On the inner shelf, in water depths less than 10 m, the landward-oriented asymmetry of Ship Shoal indicates that it is migrating landward (towards the north). The shoal crest is asymmetric shoreward with landward slopes of 1:750 and seaward slopes of 1:900. Westward this asymmetry becomes more pronounced, landward slopes increase to 1:90, and seaward slopes decrease to 1:2100.

A comparison of bathymetric profiles taken between 1887 and 1983 indicates that Ship Shoal migrated more than 1000 m landward and the rates of movement were greatest in the west (Cuomo, 1984). The greater landward migration rates in the western region are attributable to the shoal crest's extension into the zone of shoreface wave activity. Rates of landward shoal migration vary from 15 m/yr in the west, to 9 m/yr in the central shoal area, to 7 m/yr in the east. This pattern of landward shoal migration emphasizes the fact that after a barrier sand body submerges, it continues to be actively reworked and driven landward across the continental shelf, forming a marine sand body.

Stratigraphy

Ship Shoal is uniform in thickness along strike section (Figure 34A); the entire transgressive sequence averages 5-6 m thick through its 50 km length. The higher energy shoal crest facies increases slightly in thickness in shallower water over the western shoal, yet overall geometry remains uniform (Penland et al., 1986b). A dip section reveals that the shore-parallel crest of central Ship Shoal overlies the Maringouin delta complex (Figure 34B). Shoal crest deposits are 1-2 m thick and the shoal front deposits are 2.0-3.5 m thick. The shoal base deposits are approximately 1-2 m thick.

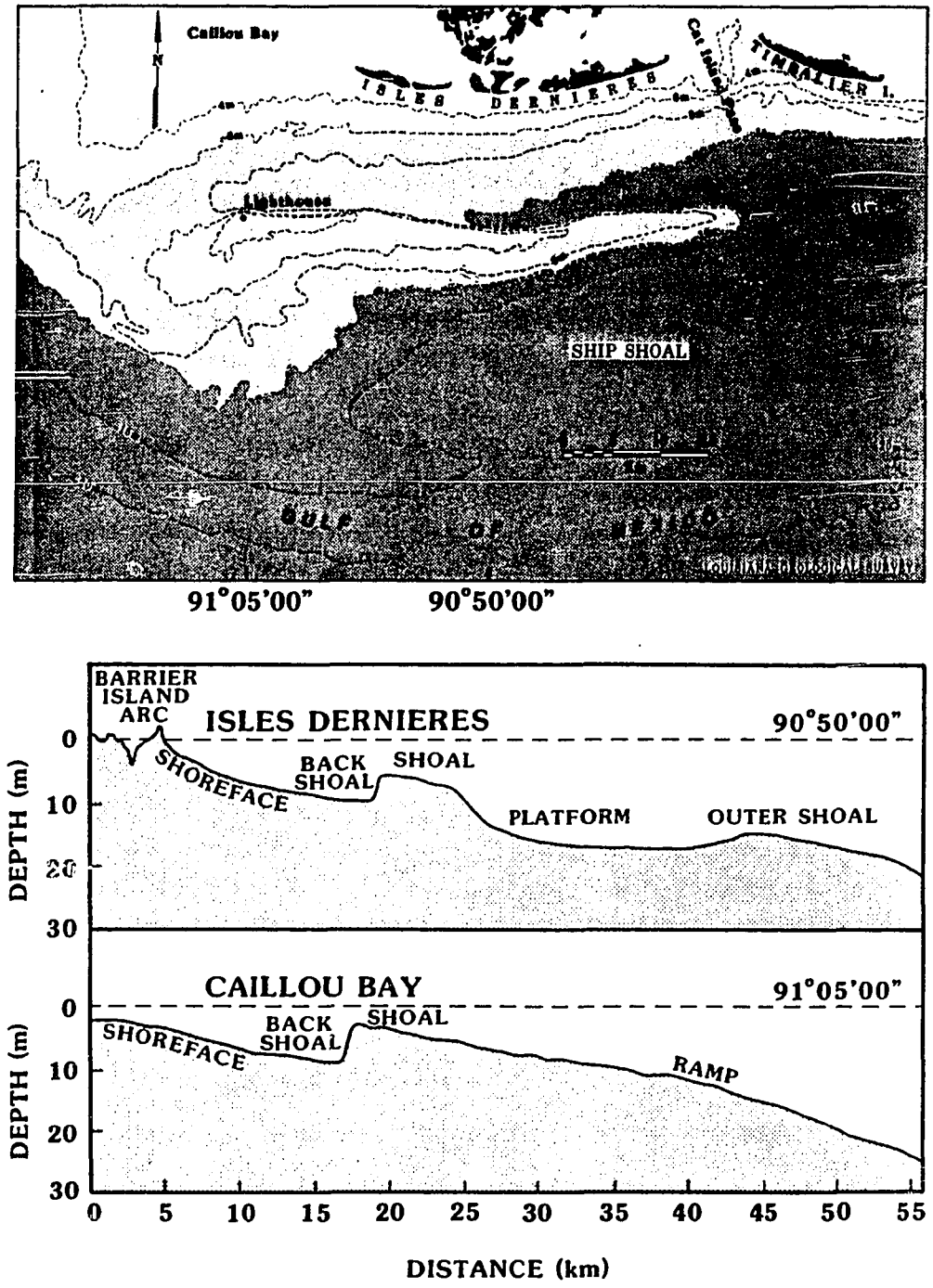

Figure 33. Ship Shoal, associated with the Maringouin delta complex, represents the oldest transgressive sand body in the Holocene Mississippi River delta plain. More than 50 km long, Ship Shoal has an inner shelf relief of 4-6 m. The geometry of the Ship shoal sand body is skewed landward, indicating that it is migrating onshore across the inner shelf (Penland et al., 1986b).

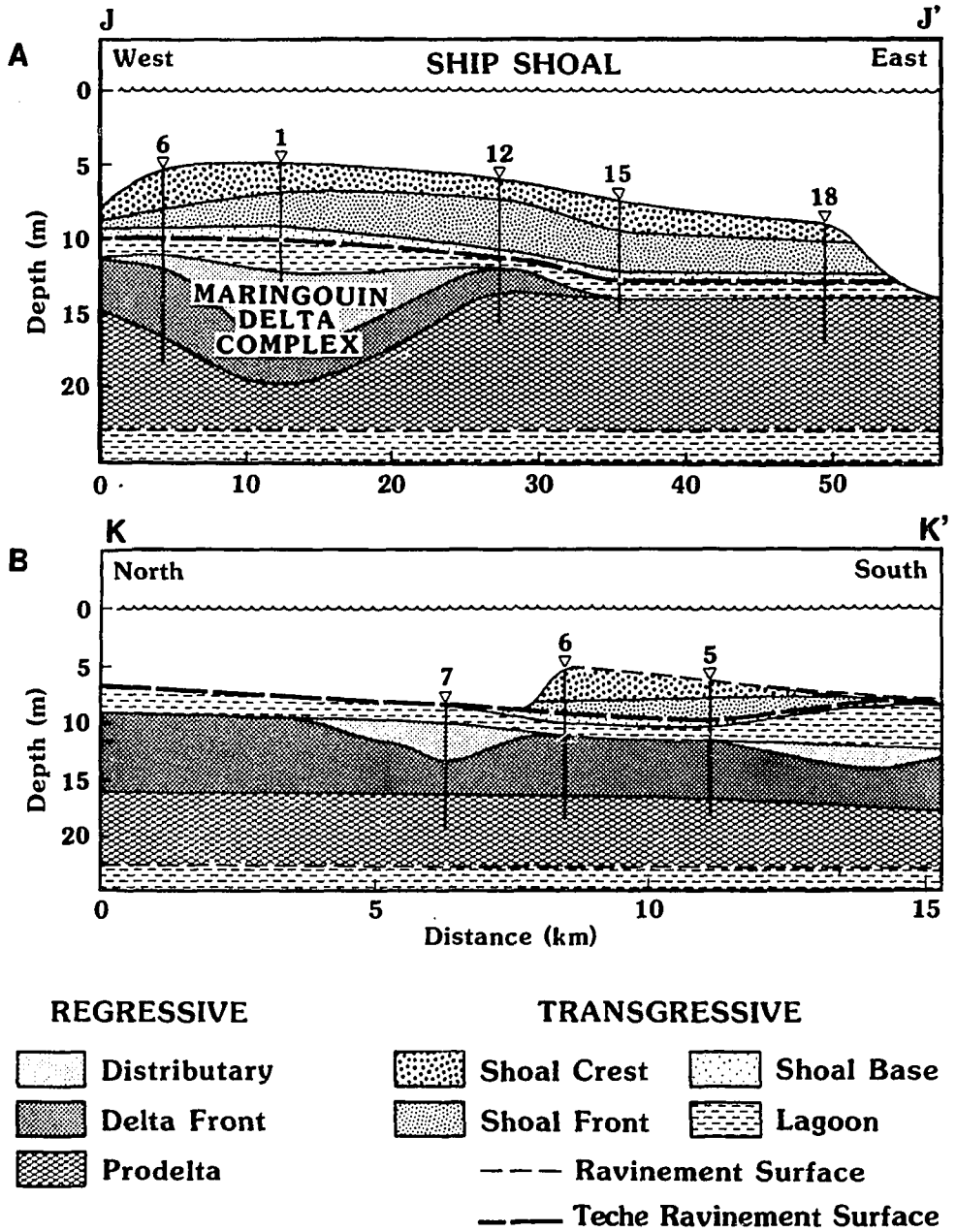

Figure 34. (A) Strike section J-J' illustrates the facies relationship between the surface of the Maringouin delta complex and the overlying Ship Shoal transgressive sequence. Stratigraphic boundaries are derived from a composite of vibracores (upper boundaries) and seismic data (lower boundaries). The sand body geometry of Ship Shoal is a uniform 4-5 m along its entire 75 km length. The original headland of the Maringouin delta complex underlies the western end of Ship Shoal. (B) Dip section K-K' illustrates the facies relationship across Ship Shoal and the adjacent inner shelf. Ship Shoal is composed of sand derived from the shoreface and inner shelf reworking of a submerged barrier island arc (Penland et al., 1988b).

Lagoonal deposits 1.0-1.5 m thick are found underlying Ship Shoal throughout the region.

The main Maringouin distributaries extend seaward underneath the western half of Ship Shoal (Figure 34A). The strike section shows that this zone of distributaries is about 10 km wide and 1-6 m thick. These distributaries lie on a regional unconformity associated with an older transgressed delta complex deposited at a lower sea level stand. The base of shoreface erosion is below the 10 m isobath in the western shoal region, indicating that the entire sand body is being truncated along the seaward shoal margin and reworked into a marine sand body.

Vibracores document that Ship Shoal and the underlying Maringouin delta complex represent a genetically related depositional sequence. The vertical stacking of facies documents the landward migration of Ship Shoal. No *in situ* barrier shoreline deposits were found within the sand body of Ship Shoal, while *in situ* lagoonal muds are present beneath the shoal and exposed landward on the flat inner shelf, which is the ravinement surface upon which Ship Shoal is migrating. The stratigraphic position of Ship Shoal indicates that it is a transgressive sand body that has migrated to its present position under conditions of sea level rise, shoreface erosion, and submergence.

Clasts of lithified beach sands, *Crassostrea* sp. shell, and *Rangia* sp. shell are common constituents of the vibracored transgressive and sequences. These clasts are well rounded, polished fragments indicating possible exposure to a high-energy environment, such as a surf zone, during their depositional history. Lithified beach sands are found along all of the transgressive barrier shorelines of the Mississippi River delta plain (Roberts and Whelan, 1975). *Crassostrea* sp. reefs commonly occur throughout the backbarrier lagoon and the lagoon shore of flanking barrier islands and barrier island arcs. *Rangia* sp. shell reefs were once common along the inland margins of transgressive backbarrier bays and lagoons. The occurrence of the reworked clasts and lagoonal muds indicates that Ship Shoal is a marine sand body originating from the transgression and submergence of a former barrier shoreline.

Transgressive Depositional Systems Model

Mississippi River delta complexes have followed a sequential pattern of development characterized by shifting shallow water depocenters (Figure 22). The transgressive depositional systems that evolve in abandoned delta complexes follow a corresponding pattern of sequential development, determined by the age of the delta complex from which they are derived. The geomorphic and stratigraphic features characterizing each transgressive depositional system reflect its position in the evolutionary sequence. This sequence begins when marine processes transform an abandoned delta complex into stage 1, an *erosional headland with flanking barriers* (Figure 35). Flanking barriers are built from headland sand sources supplied by shoreface erosion through Gilbert's (1885) spit-breaching process. Relative sea level rise, land loss, and shoreface erosion lead to submergence and the separation of the stage 1 barrier shoreline from the mainland by Hoyt's (1967) detachment process, forming stage 2, the *barrier island arc*. The final evolutionary stage occurs when relative sea level rise and overwash processes overcome the ability of the barrier island arc to maintain its subaerial integrity; submergence of the barrier island arc eventually occurs, initiating stage 3, *inner shelf shoals*. Following submergence, the former barrier island arc sand body continues to be reworked into a marine sand body to the shoreface and inner continental shelf. This process is termed *transgressive submergence*.

Stage 1: Erosional Headlands and Flanking Barriers Islands

Depositional Environments and Processes

Stage 1 transgressive depositional systems consist of (1) an erosional headland, (2) a mainland beach, (3) flanking spits and barrier islands, (4) tidal inlets and deltas, (5) restricted interdistributary bays, and (6) a sand sheet (Figure 35).

In Stage 1, the sand dispersal pattern consist of a longshore transport divergence in the central headland. Distributary and beach ridge sand bodies lie on the upper shoreface and are truncated by shoreface retreat, supplying sand for flanking barrier development. Sand is transported away from the headland and accumulate in recurved spits and flanking barrier islands. During storm impacts, sand is transported seaward onto the inner shelf and landward into washover fans. The flanking barriers migrate away from the erosional headland through downdrift, recurved spit growth

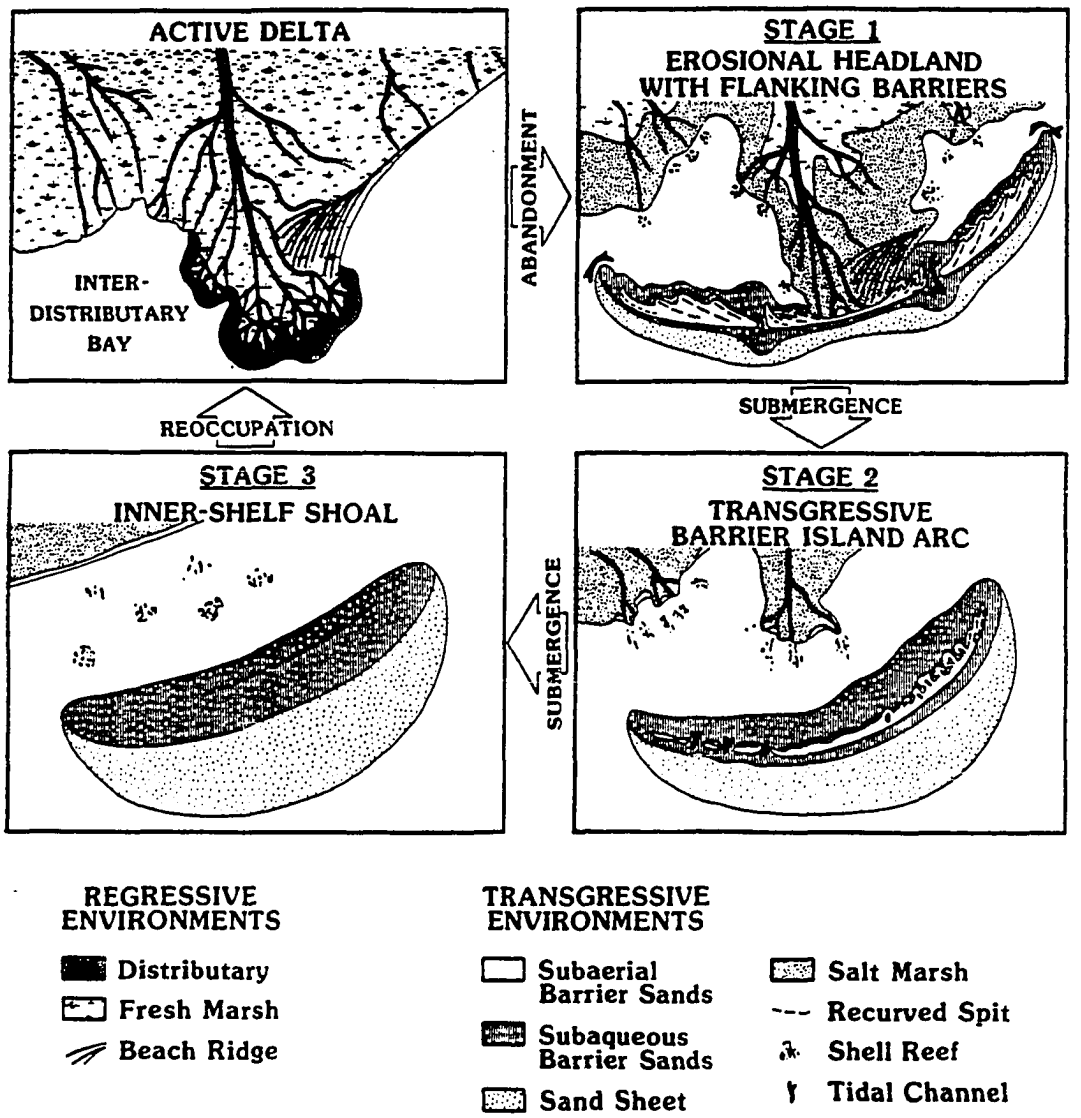

Figure 35. The genesis and evolution of transgressive depositional systems in the Mississippi River delta plain are best summarized by this three-stage geomorphic model, which begins with stage 1, *erosional headland and flanking barriers* . next is stage 2, *transgressive barrier island arc*. The sequence ends with stage 3, *inner shelf shoals* (Penland et al., 1988a).

and/or updrift erosion. The recurved spit morphology of the flanking barrier islands reflects the importance of the updrift sand sources in the central erosional headland.

Flanking barrier migration encloses subsiding interdistributary bays. The sandy superstructure of flanking barriers in Stage 1 is built by the lateral migration of tidal inlets and their subsequent infilling by spit platform deposits. Tidal inlets are significant sediment sinks in Stage 1 barriers, as frontal and lateral migration result in sediment loss from the active dispersal system. Examples of Stage 1 transgressive depositional systems include the Bayou Lafourche barrier system, derived from the Lafourche delta complex, and the younger Plaquemines barrier system, derived from the Modern delta complex.

Stage 2: Barrier Island Arc

Depositional Environments and Processes

The Stage 2 transgressive depositional environments consist of (1) a barrier island arc, (2) tidal inlets, (3) a lagoon, and (4) an inner shelf sand sheet (Figure 35). A Stage 2 barrier island arc develops from a Stage 1 erosional headland with flanking barriers by the process of mainland detachment through submergence, as described by Hoyt (1967). Long-term subsidence leads to submergence of the erosional headland, and backbarrier marshes and restricted interdistributary bays coalesce to form larger interdeltaic lagoons.

The transgressive barrier island arc primarily comprises flood tidal delta and washover fan environments, which are colonized by salt marsh and mangroves along the lagoon margin. Discontinuous dune fields occur on these surfaces. Recurved spits occur at the downdrift end of individual islands. Tidal inlet morphology varies between mixed-energy and wave-dominated, depending on tidal prism size. As barrier island arcs continue to develop, the majority of the tidal flow is exchanged around the island margin. As a result, tidal influence on barrier shoreline morphology is diminished, and the barrier island arc shape becomes wave-dominated. Seaward of the barrier island arc lies a well-developed retreat path of tidal inlet scars capped by an inner shelf sand sheet.

Sediment dispersal consists of longshore transport away from a divergence zone, where the greatest shoreline erosion occurs, decreasing downdrift in each direction. Sediment accumulates in

recurved spits, flood tidal deltas, washover fans, dunes, and tidal inlets along the barrier island arc. During storms, coarse-grained sediments are transported offshore and to the inner shelf sand sheet. Storm overwash transports sand landward through tidal inlets and into flood tidal deltas and washover fans. Examples of Stage 2 transgressive depositional systems include the Isles Dernieres, derived from the Lafourche delta complex, and the Chandeleur Islands, derived form the St. Bernard delta complex.

Stage 3: Inner Shelf Shoals

Depositional Environments and Processes

The shoals identified on the inner shelf of the Mississippi River delta plain (Figure 22) are landward-retreating sand bodies. Landward shoal migration takes place through the erosion of the seaward shoal slope and deposition on the landward shoal slope. Stage 3 transgressive depositional systems are composed of five major components: 1) shoal crest, 2) shoal front, 3) shoal base, 4) sand sheet, and 5) mainland shoreline. The shoal crest is the zone of maximum wave energy. Stage 3 inner shelf shoals extend into the shoreface zone of fair-weather and storm-wave processes; as a result, the shoal crest experiences sediment dispersal nearly year round. The shoal front and shoal base represent the leading edge of landward shoal migration. Seaward, a sand sheet marks the shoal retreat path.

Stage 3, the inner shelf shoal, develops from the transgression and submergence of Stage 2 barrier island arcs (Figure 35). Long-term relative sea level rise combined with repeated storm impacts and a diminishing sand supply eventually overcome the ability of the barrier island arc to maintain its subaerial integrity. Ensuing transgression and subsidence eventually lead to complete barrier island arc submergence, forming Stage 3, an inner shelf shoal. This process results in the submergence of the barrier island arc, producing a sand shoal cored by a suite of coastal facies lying on the shoreface and inner shelf. Marine processes continue to drive the sand shoal landward through shoreface erosion, reworking the coastal facies into a sand shoal cored by maine facies. Examples of Stage 3 transgressive depositional systems are Trinity Shoal, associated with Teche delta complex, and Ship Shoal, associated with the Maringouin delta complex.

DELTA PLAIN DEVELOPMENT

Recognition of Multiple Delta Plains

Fisk (1944) produced the first depositional model of the Mississippi River delta plain. This model depicts a single Holocene delta plain 4250 years old consisting of six delta complexes (Figure 36). From oldest to youngest, these are Maringouin, Teche, Lafourche, St. Bernard, and Modern Mississippi. Within these delta complexes, Fisk (1944) identified 20 individual stages. Kolb and Van Lopik (1958) presented a simplified depositional model for the Mississippi River delta plain, 5400 years old, consisting of seven delta complexes: the Sale-Cypremort, Cocodrie, Teche, St.Bernard, Lafourche, Plaquemines, and Balize, in order of decreasing age (Figure 37). The most recent depositional model of the Mississippi River delta plain was developed by Frazier (1967, 1974), which depicts a single Holocene delta plain 7250 years old, consisting of sixteen separate delta lobes organized into five delta complexes (Figure 38). From oldest to the youngest, these are the Maringouin, Teche, St. Bernard, Lafourche. Plaquemines-Modern delta complexes. The term *delta plain* is used in this chapter to describe a set of delta complexes deposited during a period of relative stable sea level. The term *delta complex* is used to describe a set of smaller delta lobes that are tied to a common distributary and are built by the delta-switching process.

In developing the model presented in the "Barrier Island Evolution" chapter, an extensive offshore and onshore data set of seismic profiles and vibracores were collected to provide the opportunity to ground truth the single Holocene delta plain model concept of Fisk (1944), Kolb and Van Lopik (1958), and Frazier (1967). Data from the Marsh Island and Trinity Shoal region were the first indicators that the single Holocene delta plain concept was more complex than what was previously thought. This area is mapped as the Teche delta complex overlapping the Maringouin delta complex by Frazier (1967), however the seismic and vibracore data show in fact that these are the same delta complex and not two separate complexes (Appendix B, C, D, and E). In addition, the top of this submerged delta complex represents a ravinement surface which can be traced updip to the Marsh Island and Atchafalaya Bay shorelines.

Working in the Terrebonne coastal region to the east, onshore vibracores were correlated with offshore seismic and vibracore data between Houma and Ship Shoal in order to build the cross

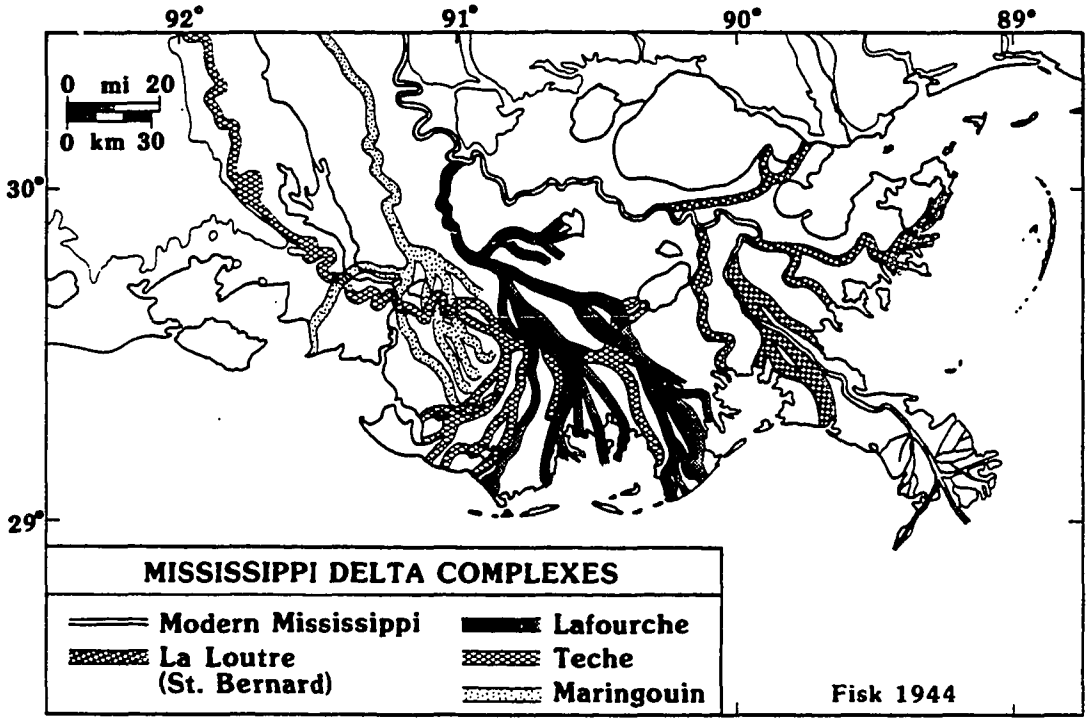

Figure 36. Diagram depicting Fisk's (1944) chronostratigraphic model of the single Holocene Mississippi River delta plain.

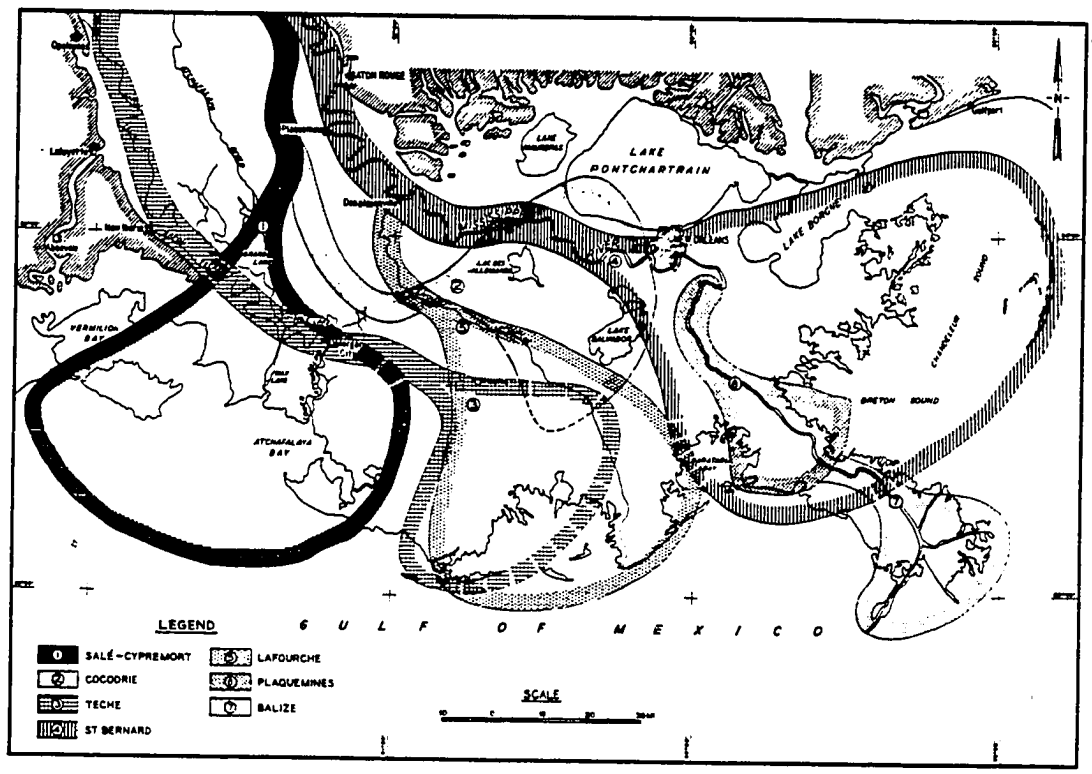

Figure 37. Diagram depicting Kolb and Van Lopik's (1958) chronostratigraphic model of the single Holocene Mississippi River delta plain.

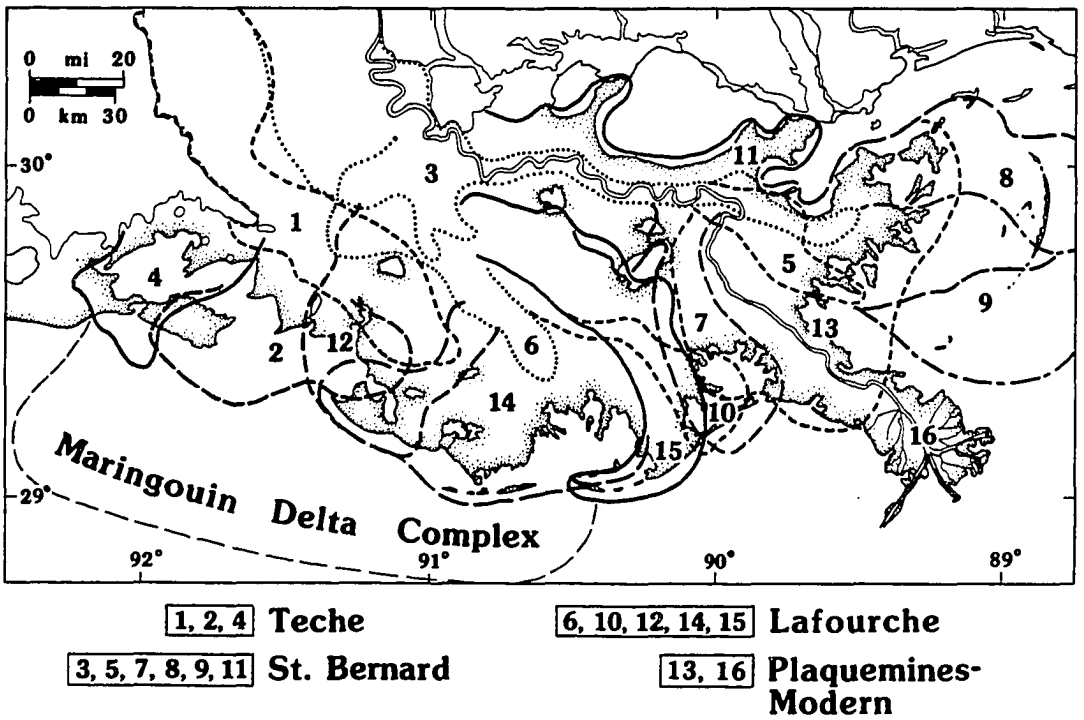

Figure 38. Diagram depicting Frazier's (1967) chronostratigraphic model of the single Holocene Mississippi River delta plain.

section depicted in Figure 39. This cross section shows the Lafourche and Teche delta complexes are separated by a regional ravinement surface indicating the Teche delta complex is not associated with the same delta plain as is the Lafourche delta complex. The ravinement surface in the Trinity Shoal area was traced east to the ravinement surface separating the Lafourche and Teche delta complexes. Updip, this shoreface erosion surface can be traced to the relict Teche shoreline south of Houma. It appears that the Teche shoreline is an eastward continuation of the Vermilion Bay/Atchafalaya Bay shoreline now buried by the Lafourche delta complex. Landward of the Teche shoreline, the typical marsh sequence range 3-4 m thick with radiometric dates of 4000-7000 yBP. Seaward of the Teche shoreline, marsh sequence are thin, 1-2 m, and are typically 1000-3000 years in age. These old, thick marshes reflect a period of sustained marsh aggradation landward of a retreating shoreline. The facies architecture and age relationship suggest relative sea level rose 5-6 m in about 1000 years. The young thin marshes reflect development since delta plain formation and relative sea level stabilization about 3000 years ago. This trend of old, thick marshes separated from young thin marshes by a relict transgressive shoreline can be traced through Barataria basin into the St. Bernard barrier complex. The significance of the Teche shoreline, Teche ravinement surface, and Ship Shoal is that these features are evidence of a 5-6 m relative sea level rise event which achieved highstand about 3000 years ago. As a consequence, a regional transgression took place preventing the Mississippi River from significantly prograding its delta plain until relative rates of sea level rise fell below a critical threshold value allowing delta plain development to occur. The recognition of the features allowed the subdivision of the single Holocene delta plain into the Modern and Late Holocene delta plains. A comparison of the cross sections in Figures 39 and 40 illustrate the concept of a single delta plain (A) and multiple delta plains (B). The cross section from Fisk (1955) depicts a single Holocene delta plain in the Terrebonne coastal region (Figure 40). The second cross section in Figure 39 is a refinement of the first cross section by subdividing this 30 m section into two delta plains termed the Modern and Late Holocene based on new seismic, vibracore, and radiometric data (Penland et al., 1987b; Penland et al., 1987c; Penland et al., 1988b).

The recognition of the Teche ravinement surface truncating a series of different aged delta complexes from Trinity shoal east to the St. Bernard delta complex and merging updips to a relict

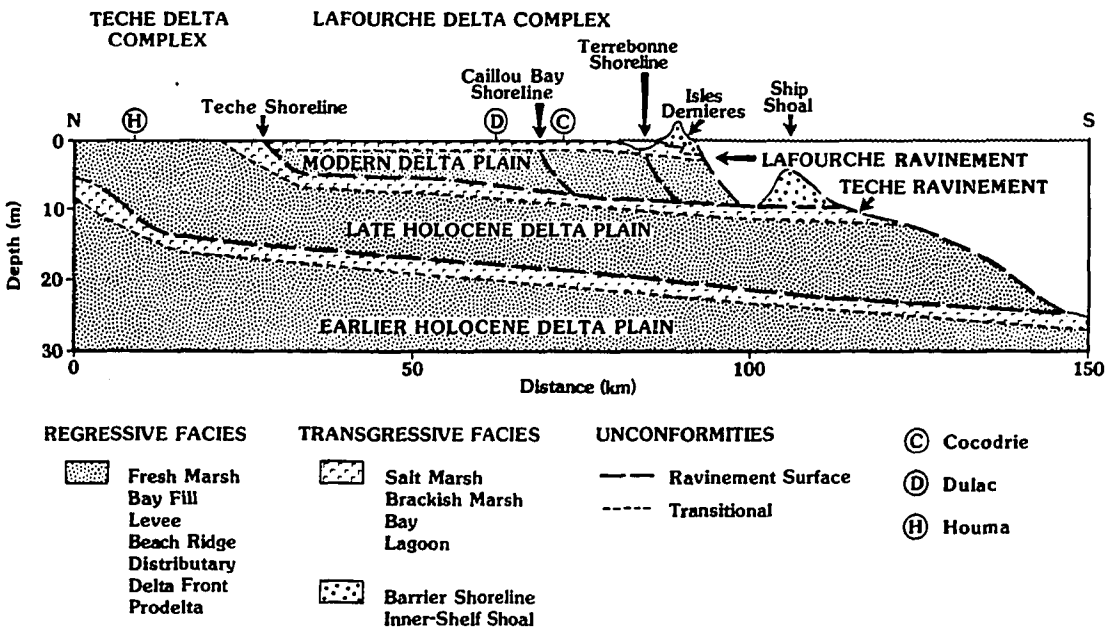

Figure 39. Geologic cross section in the Terrebonne coastal region showing the stacking of the Late Holocene and Modern delta plains separated by a regional ravinement surface, see figure 3 for location.

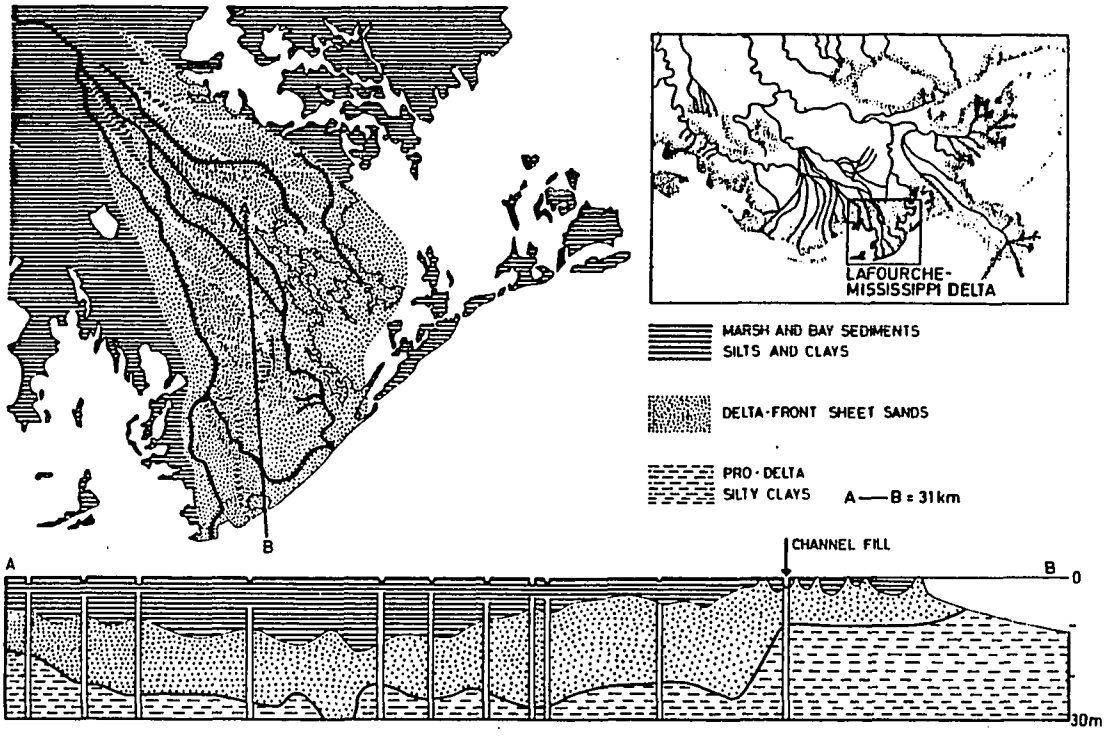

Figure 40. Fisk's (1955) cross section through the Terrebonne coastal region as in figure 21 illustrating the original single Holocene delta plain concept.

transgressive shoreline supports the concept of a eustatic driven pulse of sea level rise 4000 - 3000 years ago and multiple delta plains. In the Trinity Shoal region, Frazier (1967) originally mapped this area as a single Holocene delta plain consisting of the Maringouin delta complex overlain by the Teche delta complex (Figure 38). However, a seismic profile and vibracore from this area depicts only a single delta plain lying on the Pleistocene Prairie surface (Figure 41). This diagram clearly illustrates that the Pleistocene Prairie deposits are truncated by a ravinement surface overlain by a single delta plain parasequence truncated by Teche ravinement surface. Thus, instead of two overlying delta complexes as interpreted by Frazier (1967), only a single delta complex parasequence associated with the Late Holocene, plain can be observed (Figure 41). It is interesting to note that a fresh layer of Atchafalaya River prodelta muds now lie on the Teche ravinement surface representing the initial stage in the establishment of the Modern delta plain in this region.

The Teche ravinement surface can be traced towards the east where it essentially represents the surface of the inner shelf as far as Point Au Fer. At Point Au Fer the Teche ravinement is covered by a thin deposit of deltaic sediments associated with the Bayou du Large delta lobe of the Lafourche delta complex associated with the Modern delta plain (Figure 42). This diagram illustrates, the Late Holocene delta plain parasequence truncated by the Teche ravinement surface and which is overlain by the Modern delta plain parasequence. The Teche ravinement can be traced further towards the east beneath the Isles Dernieres and Bayou Lafourche barrier shorelines (Figures 25 and 29). Figure 30 is a regional dip cross section in the Terrebonne Parish region that ties the strike cross sections in Figure 25 and 29 onshore to the relict Teche transgressive shoreline and offshore to Ship Shoal and Teche ravinement surface as depicted in Figure 39.

The Teche ravinement surface is very persistent and not only can be easily recognized in seismic and vibracore but this surface can be delineated in engineering studies by the U.S. Army Corps of Engineers (USACE 1962a,b,c). In the eastern Terrebonne basin and western Barataria basin the USACE conducted three studies to identify the best location for the Bayou Lafourche and Lafourche-Jump waterway. The three regional dip cross sections in Figures 43, 44, and 45 all recognized the Teche ravinement surface. Figure 43 is located on the western margin of Bayou Lafourche running parallel to this distributary course. This diagram depicts the Teche ravinement

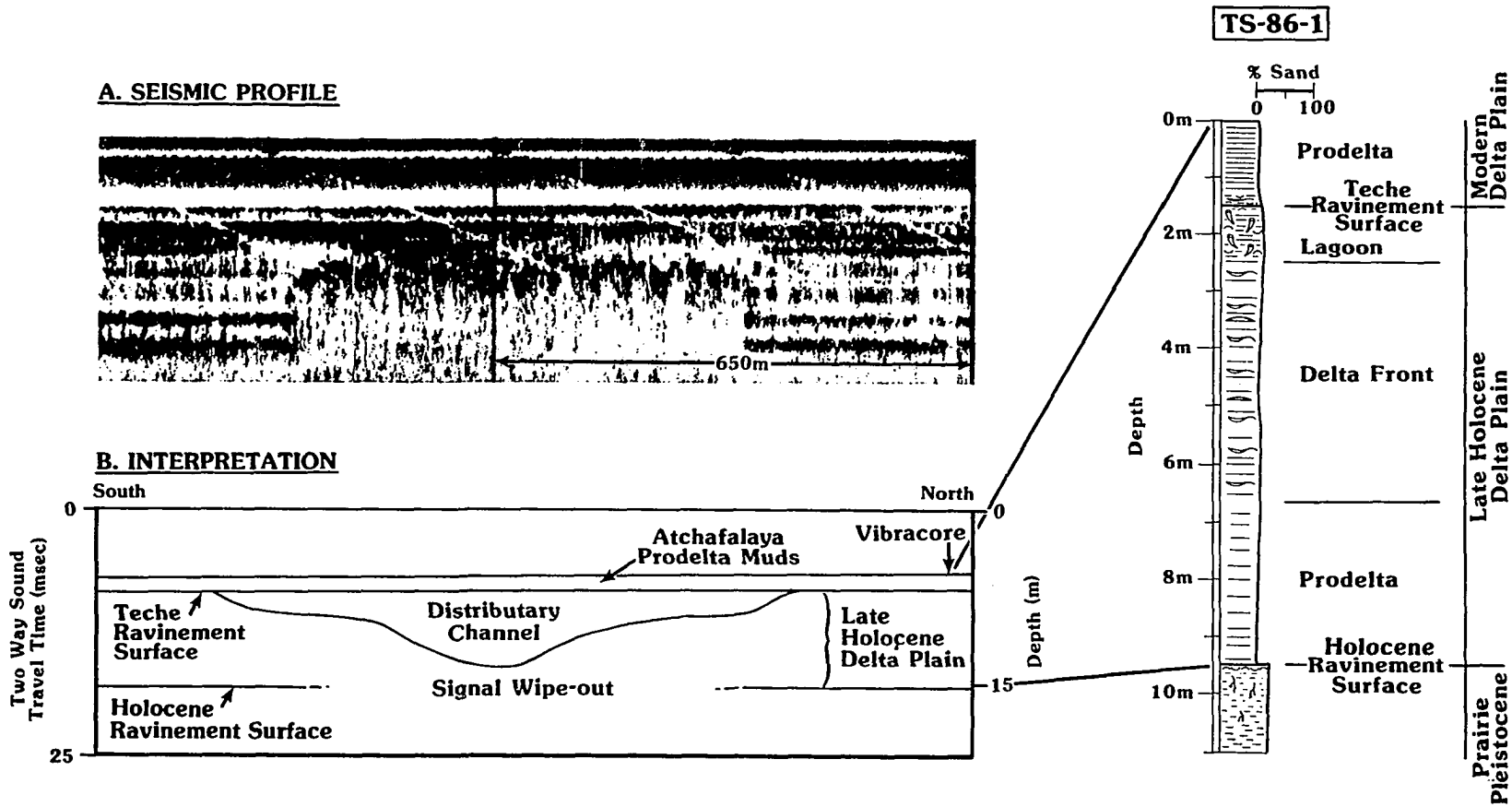

Figure 41. Seismic and vibracore data illustrating the stratigraphic relationship of the Late Holocene delta plain in the Trinity Shoal area (see Figure E-15 for location).

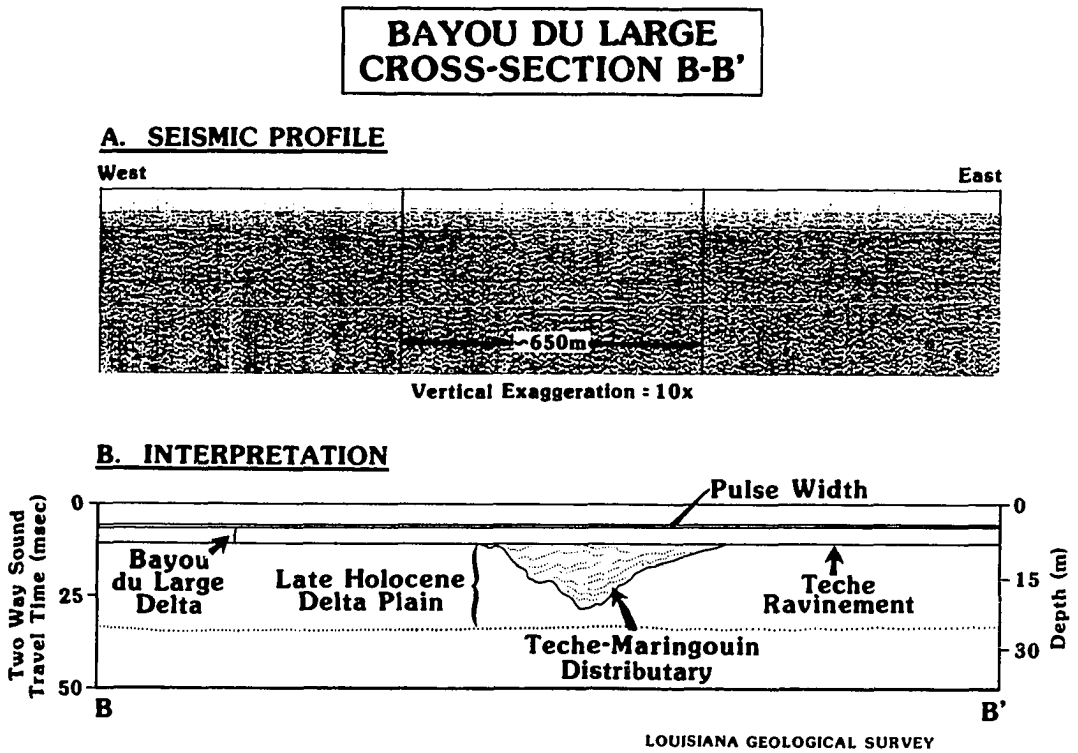

Figure 42. Seismic section offshore of Point Au Fer illustrating the Late Holocene delta plain, the Teche ravinement surface, and the Modern delta plain (see Figure E-15 for location).

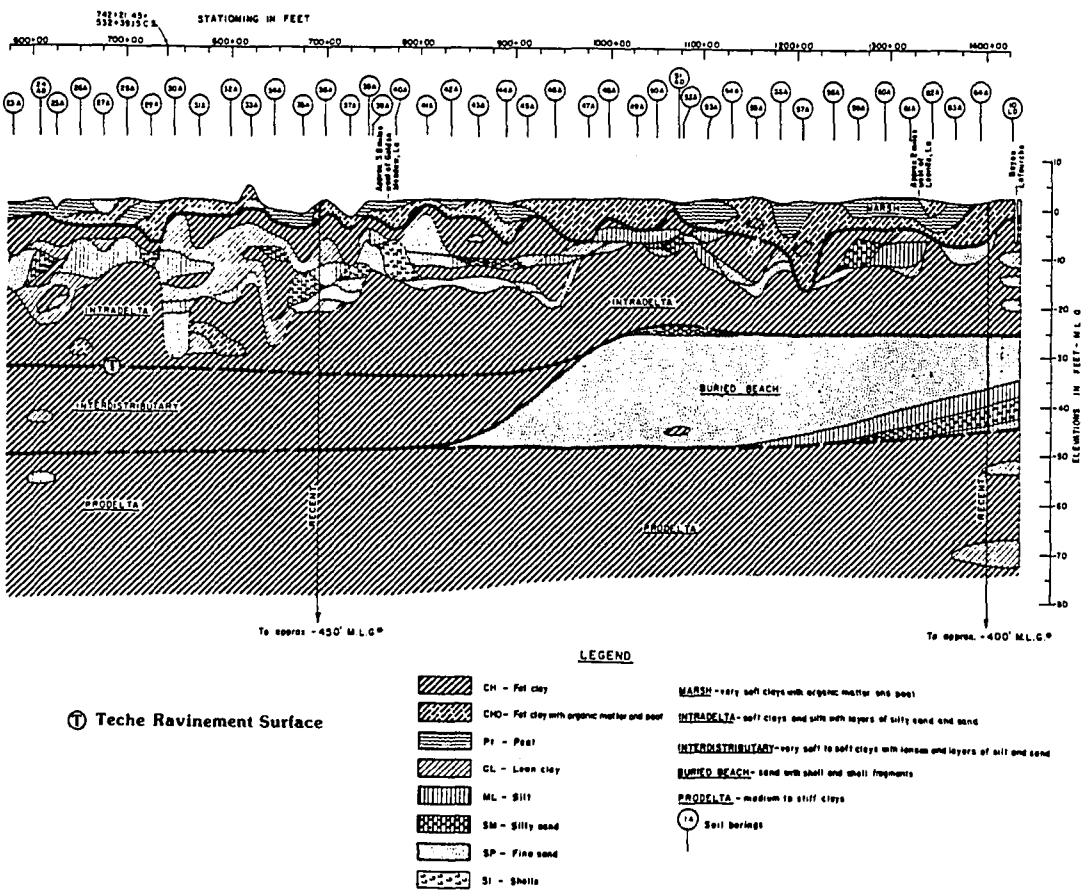

Figure 43. An USACE (1962a) engineering cross section illustrating the Teche shoreline and ravinement surface (see Figure E-15 for location).

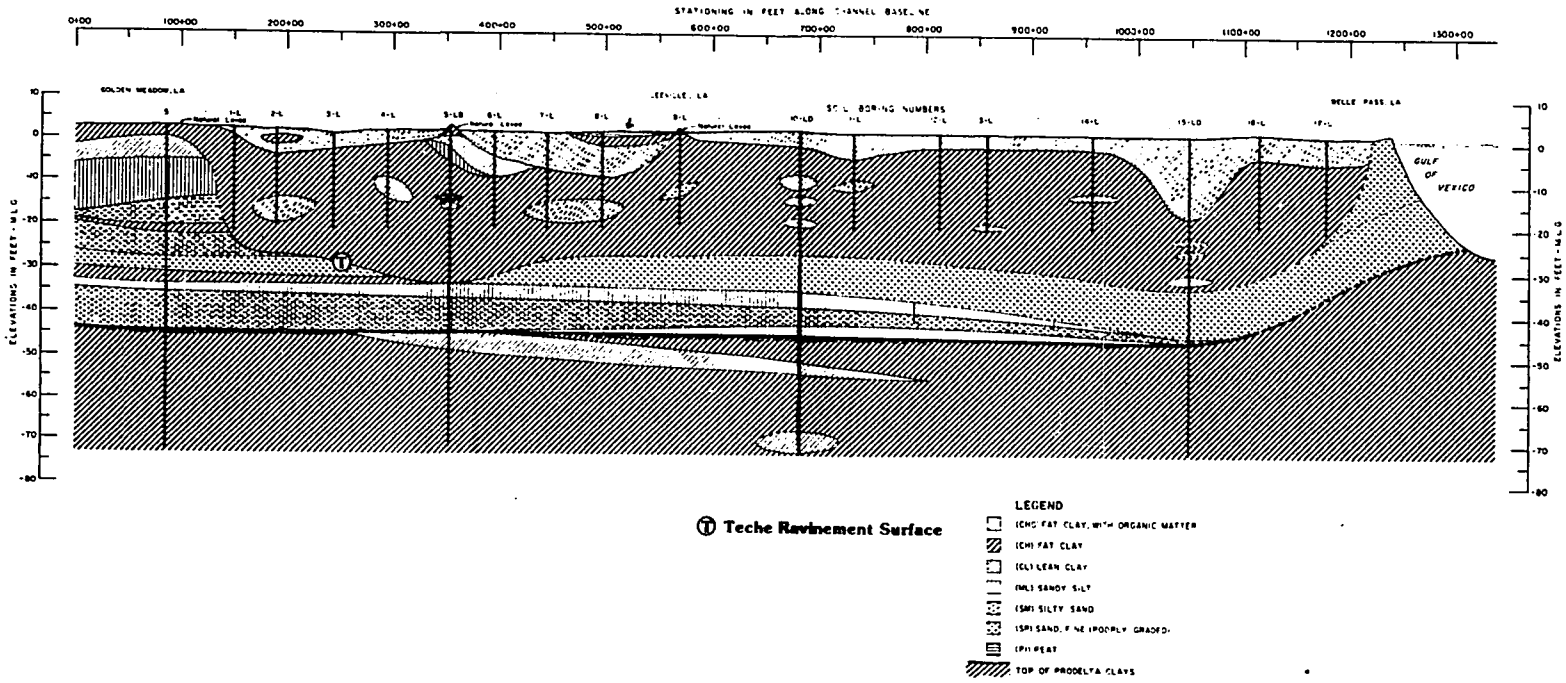

Figure 44. An USACE (1962b) engineering cross section illustrating the Teche shoreline and ravinement surface (see Figure E-15 for location).

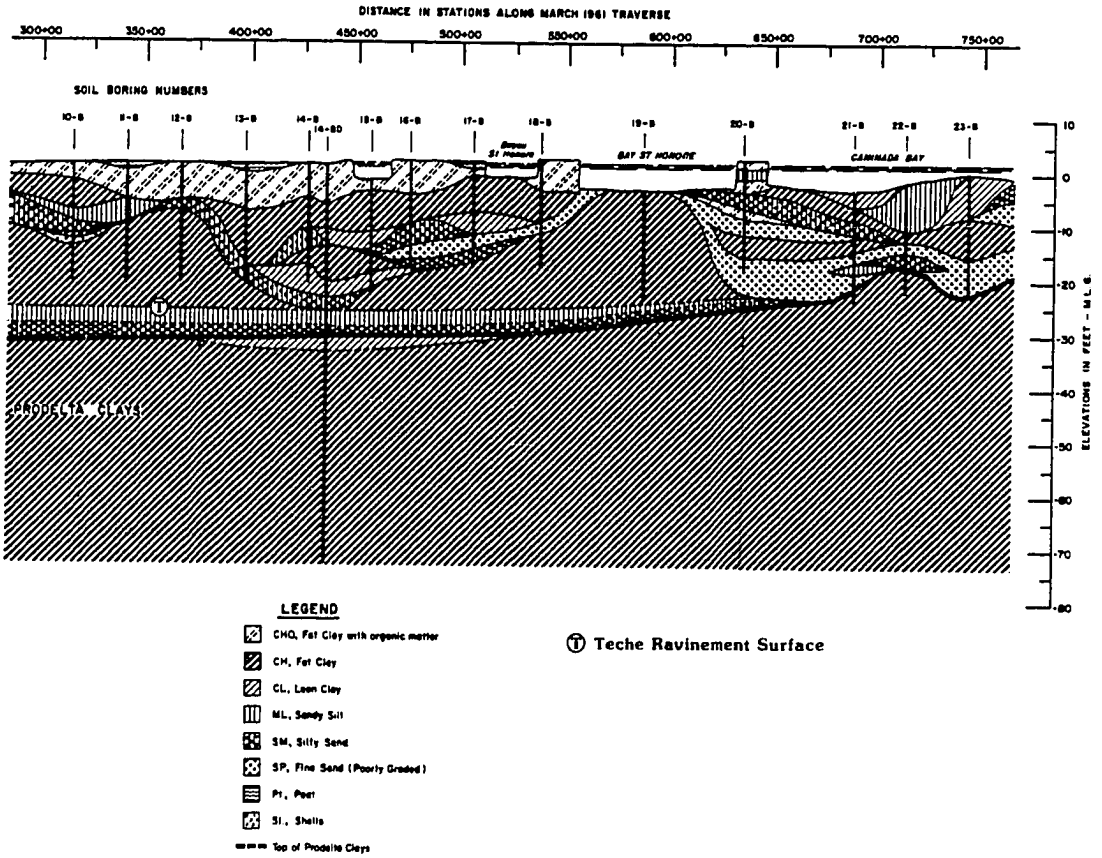

Figure 45. An USACE (1962c) engineering cross section illustrating the Teche ravinement surface (see Figure E-15 for location).

surface as well as a buried transgressive shoreline near Little Lake on the west side of Leeville. Figure 44 is located on the east side of the Bayou Lafourche channel between Belle Pass and Golden Meadow. This diagram also illustrates the Teche ravinement and a relict erosional shoreface in the vicinity of Golden Meadow in the Barataria Basin. Figure 45 is an oblique dip cross section between Grand Isle, Caminada Bay, and Leeville. This diagram also illustrates the regional extent of the Teche ravinement surface.

In lower Barataria Bay, the seismic profile in Figure 46 shows the eastern continuation of the Teche ravinement surface which is predominant reflector on high resolution seismic profiles. The Teche ravinement surface in Barataria Bay can be traced updip to the Teche shoreline located on the north side of Little Lake. Kosters (1986) isopach map of the marsh sediments in the Barataria basin illustrates the relationship between the Teche shoreline and marsh thickness. As observed in the Terrebonne basin, landward of the Teche shoreline one finds thick old marshes and seaward of it one finds thin young marshes. Eastward out of the Barataria Basin, Frazier et al. (1978) mapped the location of a transgressive shoreline buried by the St. Bernard delta complex (Figure 48). This shoreline strikes NE/SW between Creole Gap and the position of the Teche shoreline in the eastern Barataria Basin. This unnamed barrier sandy body lies in the subsurface of the Modern delta plain, marking the former shoreline position of the Eastern delta complex of the Late Holocene delta plain.

Figure 41 - 48 as well as Figures 25, 29, 30, 34, and 39 all support the concept of the Teche shoreline and ravinement surface and the concept of the Modern and Lake Holocene delta plains.

New Holocene Geologic Framework

Relative sea level in the northern Gulf of Mexico during the late Wisconsinan lowstand fell to depths of -130 m below present sea level exposing the continental shelf and producing a set of shelf margin deltas (Berryhill, 1986; Berryhill and Suter, 1986; Kindinger, 1989) supplied by the Mississippi River between 10,000 and 25,000 yBP (Coleman et al., 1983; Bouma et al., 1986; Mazzulo, 1986). During the lowstand, the Mississippi River incised a trench across the continental shelf and together with tributary streams and subaerial weathering process, produced an erosional unconformity on the Pleistocene Prairie terrace marked by a widespread oxidation surface (Fisk, 1944). Sediments were largely restricted to infilling the Mississippi Canyon during the period 11,000-18,000 yBP.

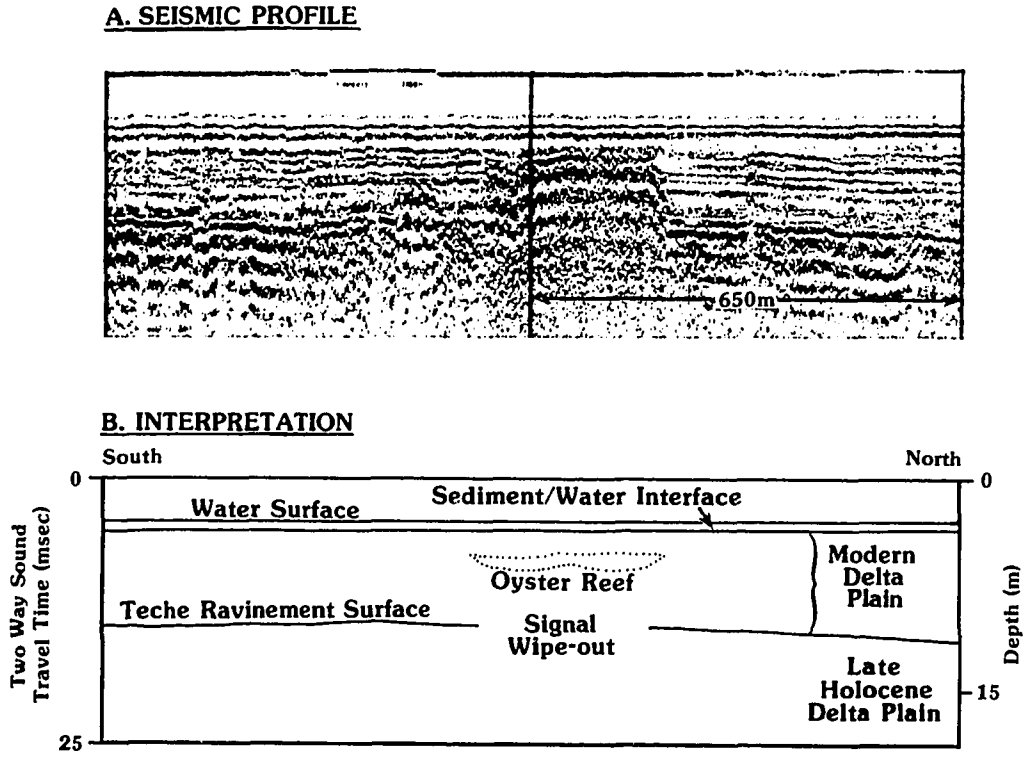

Figure 46. Seismic profile in Barataria Bay illustrating the Teche ravinement surface (see Figure E-15 for location).

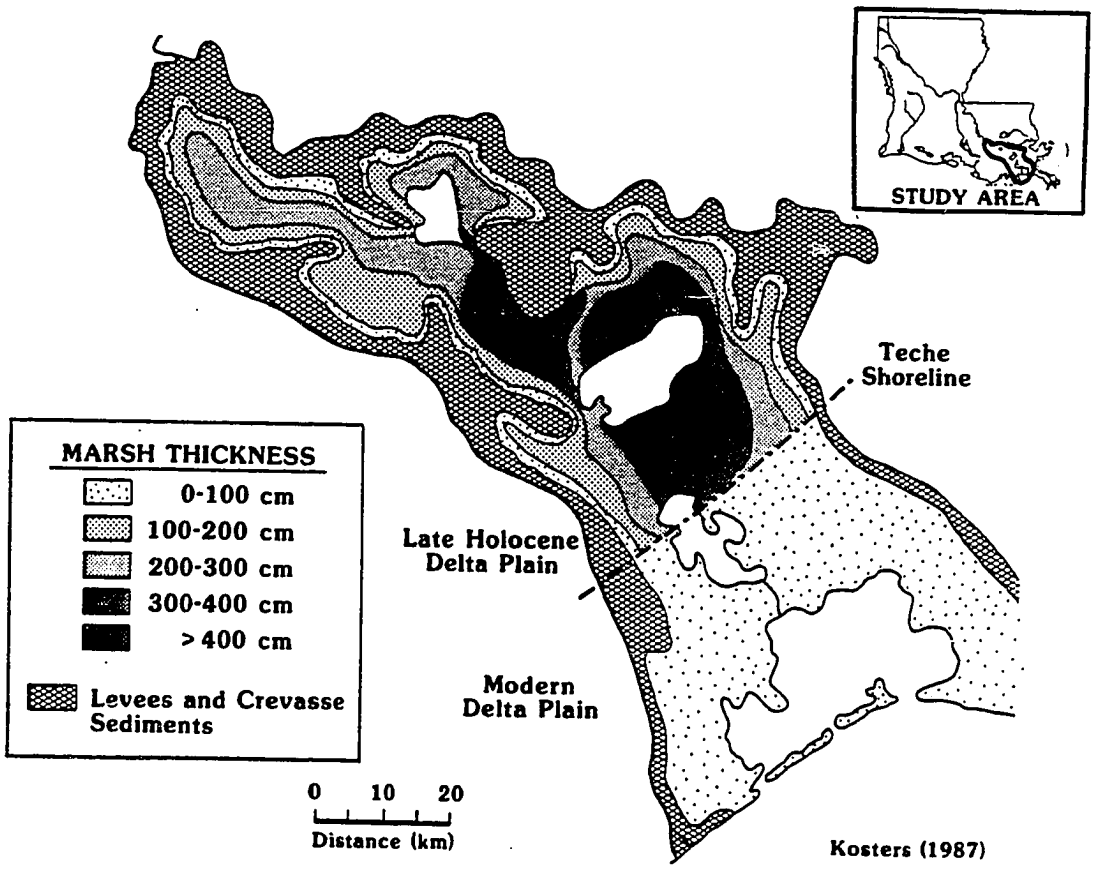

Figure 47. Isopach map of the marsh thickness in Barataria Basin (Kosters, 1986)

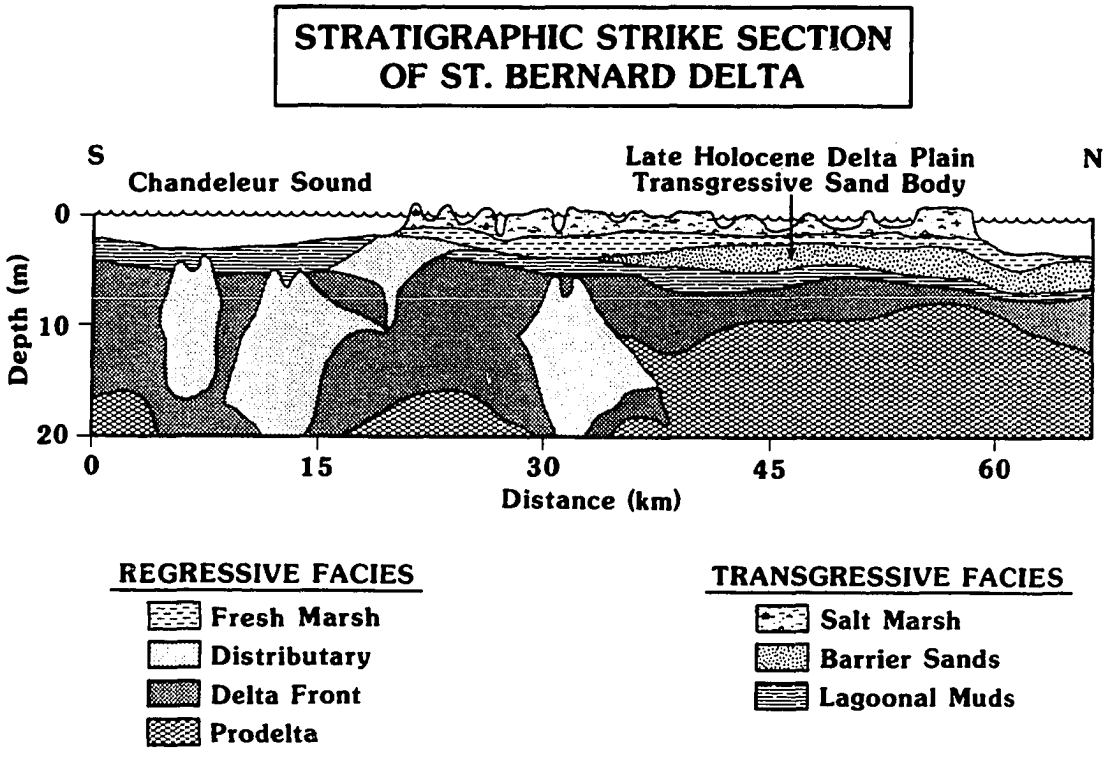

Figure 48. Frazier et al. (1978)'s strike cross section of the buried Teche shoreline in the St. Bernard delta complex (see Figure E-15 for location).

Between 11,000 yBP and present, the Mississippi River was no longer totally confined to the canyon and proceeded to develop a series of shelf-phase delta plains on the outer- to mid-continental shelf during the Holocene transgression (Fisk and McClelland, 1959; Suter et al., 1987; Boyd et al., 1988; Boyd et al., 1989).

The sediment volume supplied by the Mississippi River to its delta plain appears to have been unable to keep pace with the relative sea level rise that drove the Holocene transgression. Individual shelf-phase delta plains, coupled with these stillstands backstepped landward across the present continental shelf. The establishment of individual delta plains, built of smaller complexes by the delta switching process, indicates the existence of several periods when the rate of sea level rise slowed or archived a stillstand during the Holocene transgression. As rates of relative sea level rise again increased, these earlier Holocene shelf-phase delta plains were transgressed and submerged producing large sand shoals marking the former shoreline position (Penland et al., 1989). These Holocene shelf-phase deltas plains progressively onlap the Prairie Pleistocene unconformity.

Each shelf-phase delta plain lies on a ravinement surface and consists of a regressive and transgressive component (Penland et al., 1988a). The regressive component is built predominantly of distributary sands encased in prodelta muds capped by freshwater marsh deposits. The second component of this shelf-phase delta sequence is transgressive and consists of salt marsh and lagoonal deposits overlain by a barrier shoreline or shelf sand body. Lying along the -10 m isobath, Trinity Shoal and Ship Shoal represent the Late Holocene shoreline trend associated with a $\pm$4000-7000 yBP stillstand (Penland et al., 1989). The end of the Holocene transgression is marked by the culmination of the eustatic rise in sea level about $\pm$3000 yBP when the Late Holocene delta plain shoreline retreated to the mouth of the Mississippi River alluvial valley (Gould and McFarlan, 1959; McFarlan, 1961; Coleman and Smith 1964; Bernard and LeBlanc, 1965). Associated with the current stillstand over the last 3000 years, the shoreline of the Modern shelf-phase delta plain extends between Point Au Fer and Hewes Point. The exact timing of the eustatic highstand is debatable, but it appears to have begun around 3000 yBP (Gould and McFarlan 1959; McFarlan, 1961 and Coleman and Smith 1964). This position at the close of the Holocene transgression represents a maximum highstand of sea level (time of maximum flooding). The subsequent development of the Modern delta plain

consisted of a series of prograding delta complexes which advanced the shoreline (Fisk, 1944; Kolb and Van Lopik, 1958; Frazier, 1967).

Late Holocene Delta Plain

The Late Holocene delta plain consists of the Maringouin and Teche delta complexes offshore of south-central Louisiana. The Late Holocene delta plain was deposited during a sea level stillstand about 5-6 m below present sea level about 4000-7000 yBP. The Teche shoreline represents an eastward subsurface continuation of the Marsh Island and Atchafalaya Bay shoreline, buried by the Modern delta plain. The Teche shoreline was generated by a rapid 5-6 m rise in sea level 4000-3000 yBP. During this sea level rise period the Mississippi River was actively aggrading its delta plain landward of the retreating Teche shoreline and little delta progradation took place. The surface of the Late Holocene delta plain is truncated by a regional ravinement surface (A) which can be traced onshore, updip, beneath the Modern delta plain to the Teche shoreline (Figure 49). This same ravinement surface merges with the shoreline associated with Marsh Island, Vermilion Bay, West Cote Blanche Bay, East Cote Blanche Bay, and Atchafalaya Bay, all located west of the Modern delta plain. The base of the Late Holocene delta plain lies on a ravinement surface (B) found 22-26 m in the subsurface, truncating the top of an earlier Holocene delta plain.

Trinity Shoal is the westernmost member of the Late Holocene shoreline trend defined by the -10 m isobath (Figure 50). Located 40 km offshore of Cheniere Au Tigre and Marsh Island, Trinity Shoal is a lunate sand body 30 km long and 5-10 km wide (Suter et al., 1985; Penland et al., 1989). Trinity Shoal was built by the transgressive submergence of the Bayou Cypremort-Sale delta complex of the larger Late Holocene shelf-phase delta plain. It lies in 7-10 m of water and has an inner shelf relief of 2-4 m. The morphology of the seaward margin of Trinity Shoal is very similar in slope to an eroding shoreface. Surface sediments were mapped at 75-100% very fine sand by Frazier (1974). Krawiec (1966) mapped the median phi diameter of Trinity Shoal sands at 3.4-3.8 phi with secondary amounts of shell and organics.

The vibracores collected from Trinity Shoal indicate it is a submerged transgressive barrier shoreline undergoing shoreface reworking into a marine sand body (Figure 51). A distinct marine sand body overlies the barrier shoreline core of Trinity Shoal. The marine sand body is distinguished

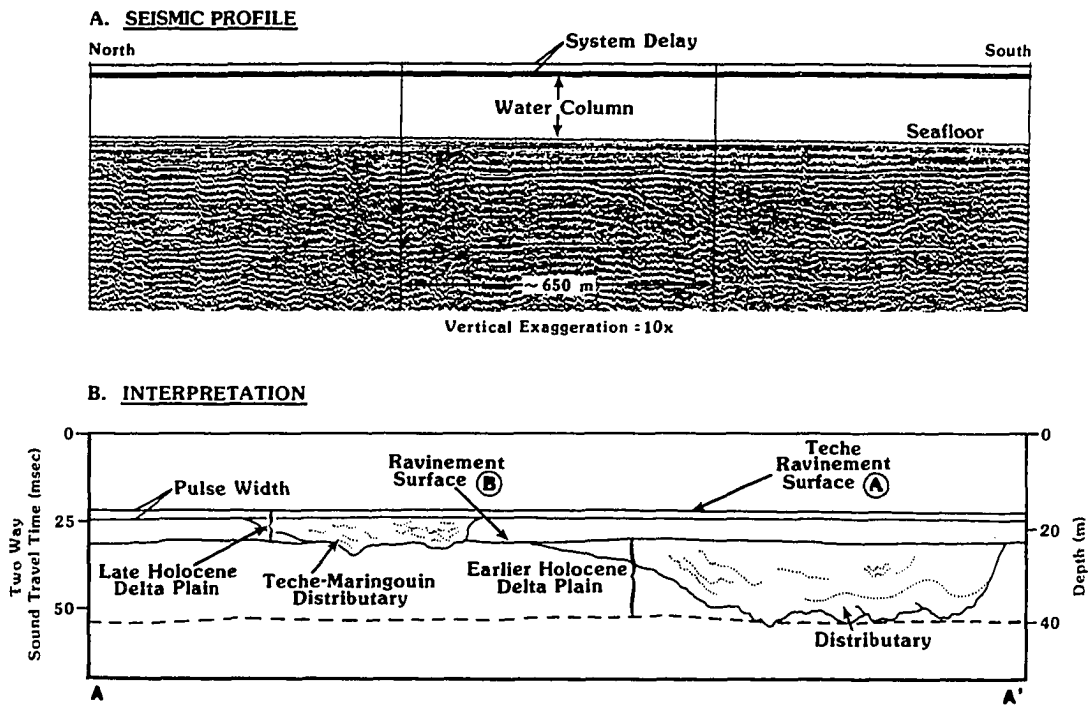

Figure 49. A high resolution seismic profile illustrating two ravinement surfaces bounding the Teche delta complex of the Late Holocene delta plain (Penland et al., 1987b).

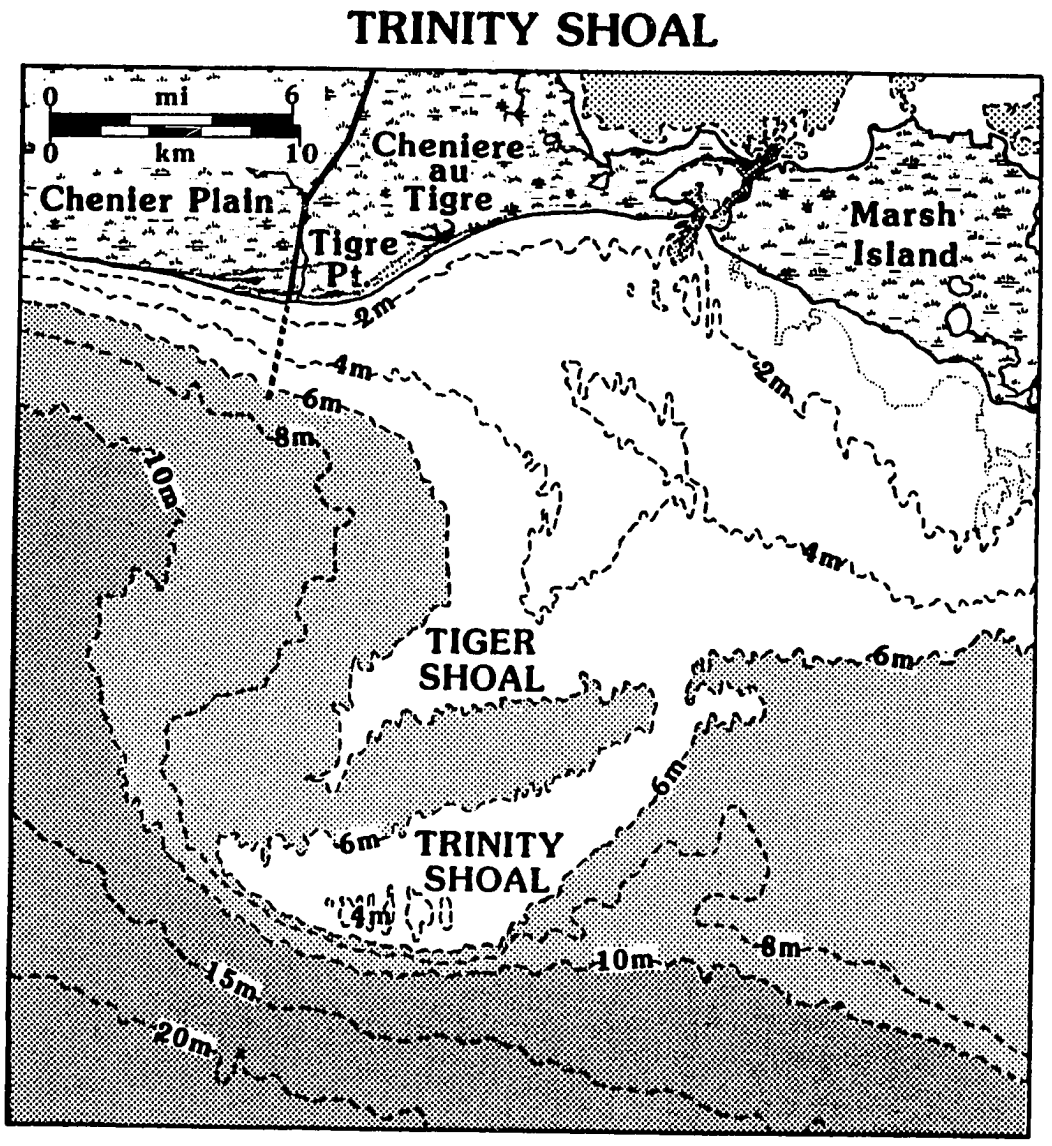

Figure 50. Location diagram of Trinity Shoal (Penland et al., 1989a).

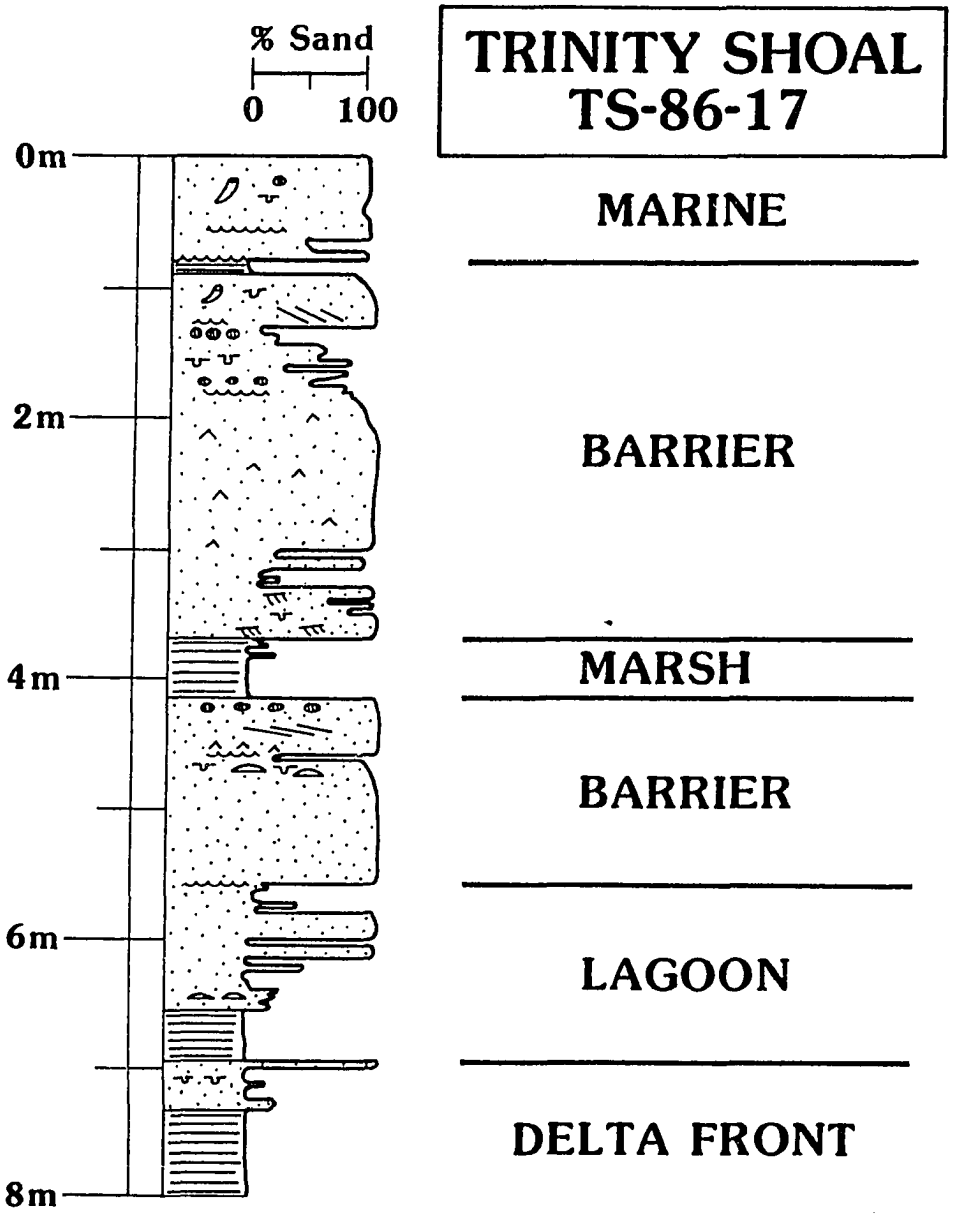

Figure 51. Representative vibracore log from Trinity Shoal (Penland et al., 1989a).

by the lack of mud laminations, its massive appearance, and its position in the parasequence. The contact between the underlying lagoonal muds and overlying barrier sands is 1-2 m thick and represents a coarsening upward interface between the flood tidal delta/washover deposits and the lagoonal muds. The geometry of the barrier sand body suggests the presence of a flood tidal delta and channel complex reaching a thickness of 5-6 m (Figure 52). The shoal sands capping Trinity Shoal thicken landward from 1-2 m. A comparison of the shelf bathymetry with a net sand isopach map indicates that the morphology of Trinity Shoal is not represented by its sand body geometry (Suter et al., 1985). This appears to be a function of tidal inlet channels present in the shoal sand body which occur below the depth of the adjacent sea floor surrounding the shoal. High resolution seismic profiles have suggested the presence of tidal inlet channeling in the Trinity Shoal sand body.

Ship Shoal is the eastern member of the Late Holocene shoreline trend defined by the -10 m isobath (Penland et al., 1986a). Located 20 km offshore of the Isles Dernieres, Ship Shoal is a shore-parallel sand body 50 km long with widths ranging from 5-7 km in the central shoal area. Ship Shoal migrated more than 1 km landward at rates of 7-15 m/yr. The median grain size diameter on the crest of the Ship Shoal range from 2.73-3.20 phi with a standard deviation of 0.28-0.44 phi. The surface lithology of Ship Shoal was mapped at 75-100% fine sand by Frazier (1974); this zone coincides with the 7-8 m isobath.

Analysis of vibracores and high resolution seismic data from Ship Shoal show a uniform sand body along strike (Figure 34). The entire transgressive sequence averages 5-6 m thick through its 50 km length and consists of shoal crest, shoal front, and shoal base marine deposits (Figure 53). The higher-energy shoal crest facies increases slightly in thickness in shallower water over the western shoal. Shoal crest deposits are 1-2 m and the shoal front deposits are 2.0-3.5 m thick. The shoal base deposits thicken eastward from approximately 1-2 m. In contrast to Trinity Shoal, the base of Ship Shoal is a flat and very sharp contact produced by the inner shelf shoal migration onto the continental shelf ravinement surface. Lagoonal deposits 1.0-1.5 m thick are found underlying Ship Shoal throughout the region below the ravinement surface. No in situ barrier shoreline deposits were found within the sand body of Ship Shoal. In situ lagoonal muds are present beneath the shoal and exposed landward on the flat inner shelf, which is the ravinement surface upon which Ship Shoal is

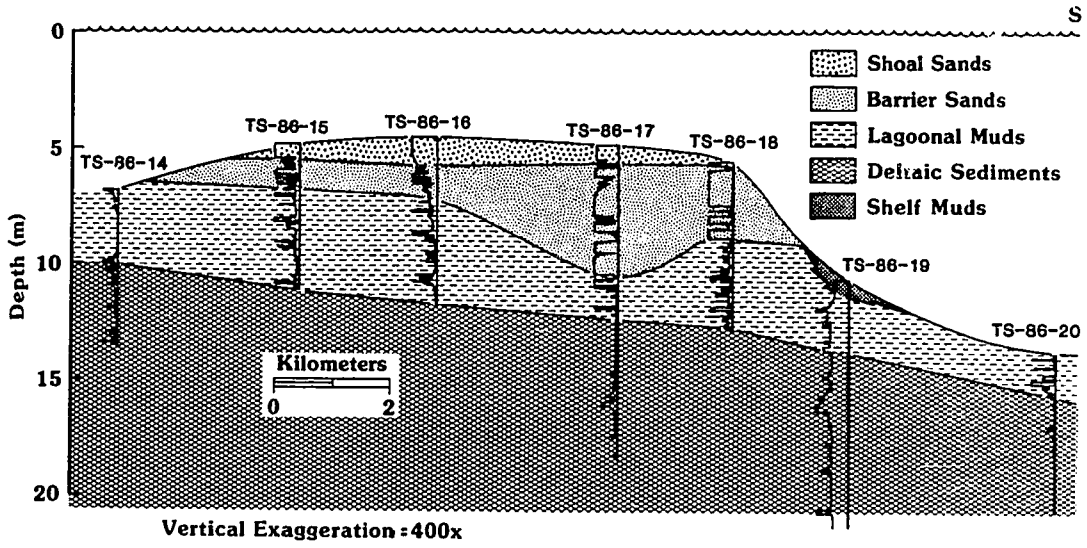

Figure 52. Representative dip section through Trinity Shoal (Penland et al., 1989a).

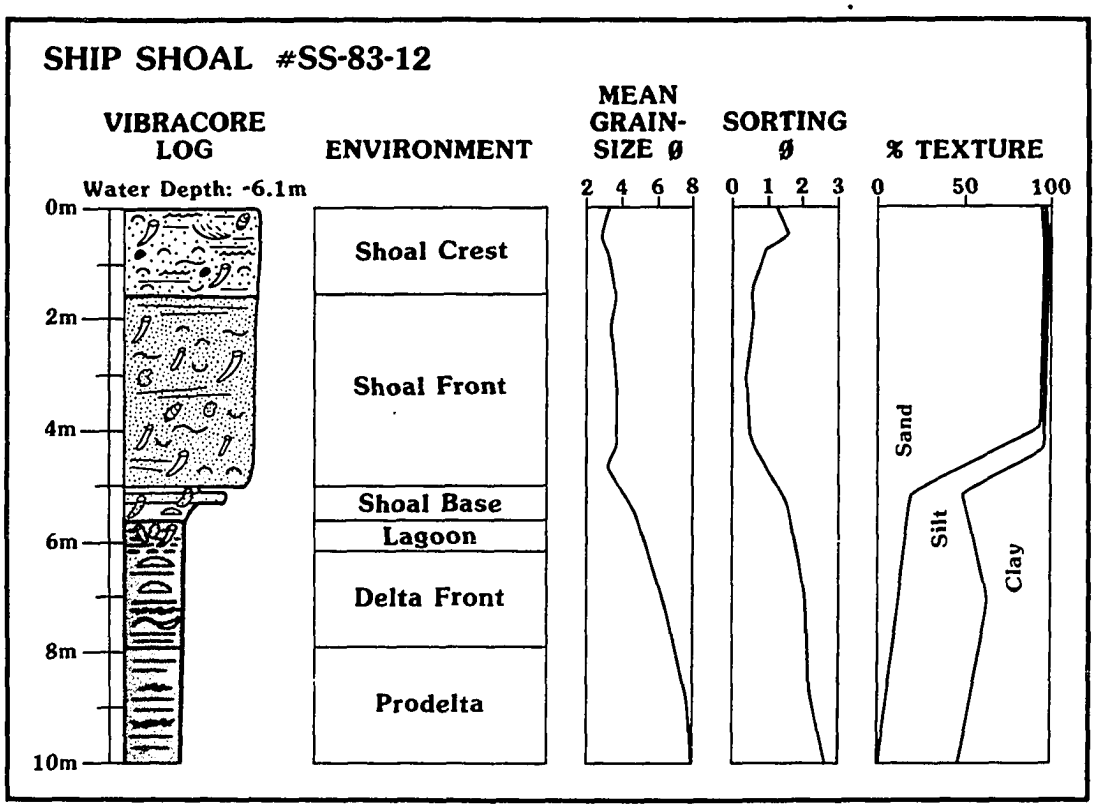

Figure 53. Representative vibracore log from Ship Shoal (Penland et al., 1989b).

migrating. The occurrence of reworked litified clasts of beach sand and *Crassostrea* sp. and *Rangia* sp. shell indicated that Ship Shoal is a marine sand body originating from the transgression and submergence of a former barrier shoreline. The comparison of the bathymetry and net sand isopach of Ship Shoal indicates shoal morphology is representative of its sand body geometry (Penland et al., 1986b). This geomorphic relationship is a function of shoal migration onto the flat inner shelf ravinement surface.

An unnamed barrier sand body lies in the subsurface of the Modern delta plain, marking the former shoreline of the Eastern delta complex of the Late Holocene delta plain in St. Bernard parish. This sand body represents the Teche shoreline which strikes towards the southwest into the central portion of the Barataria basin where the thicknesses of the Late Holocene and Modern marshes are markedly different (Figure 47). Marshes north of the Teche shoreline reach thicknesses exceeding 4 m in some areas of the Late Holocene delta plain. These thick marshes north of the Teche shoreline developed under conditions of rapid sea level rise and sustained delta plain aggradation landward of a retreating shoreline. The marshes south of the Teche shoreline formed under conditions of stable sea level and rapid delta complex progradation once sea level had stabilized. Attempts to date, to delineate the trend of Trinity Shoal and Ship Shoal farther eastward have been unsuccessful.

Modern Delta Plain

The Modern delta plain lies over the submerged Late Holocene delta plain south of the Teche shoreline. The St. Bernard and Lafourche delta complexes are abandoned and are in various stages of barrier shoreline transgression. The deep water Modern and shallow water Atchafalaya delta complexes are active now and are building seaward of the Teche shoreline which was established about 3000 yBP, when the transgression of the distal Late Holocene delta plain ended (McIntire, 1958; Weinstein and Gagliano, 1982; Appendix D).

The St. Bernard delta complex represents the oldest portion of the Modern delta plain. Abandoned about 1500 years ago, this delta complex represents an advanced stage of barrier shoreline development (Figure 54). Three distinct deltas, the Bayou Terre aux Beoufs delta lobe and the Chandeleur shoreline is associated with the younger Bayou La Loutre delta lobe. Extensive

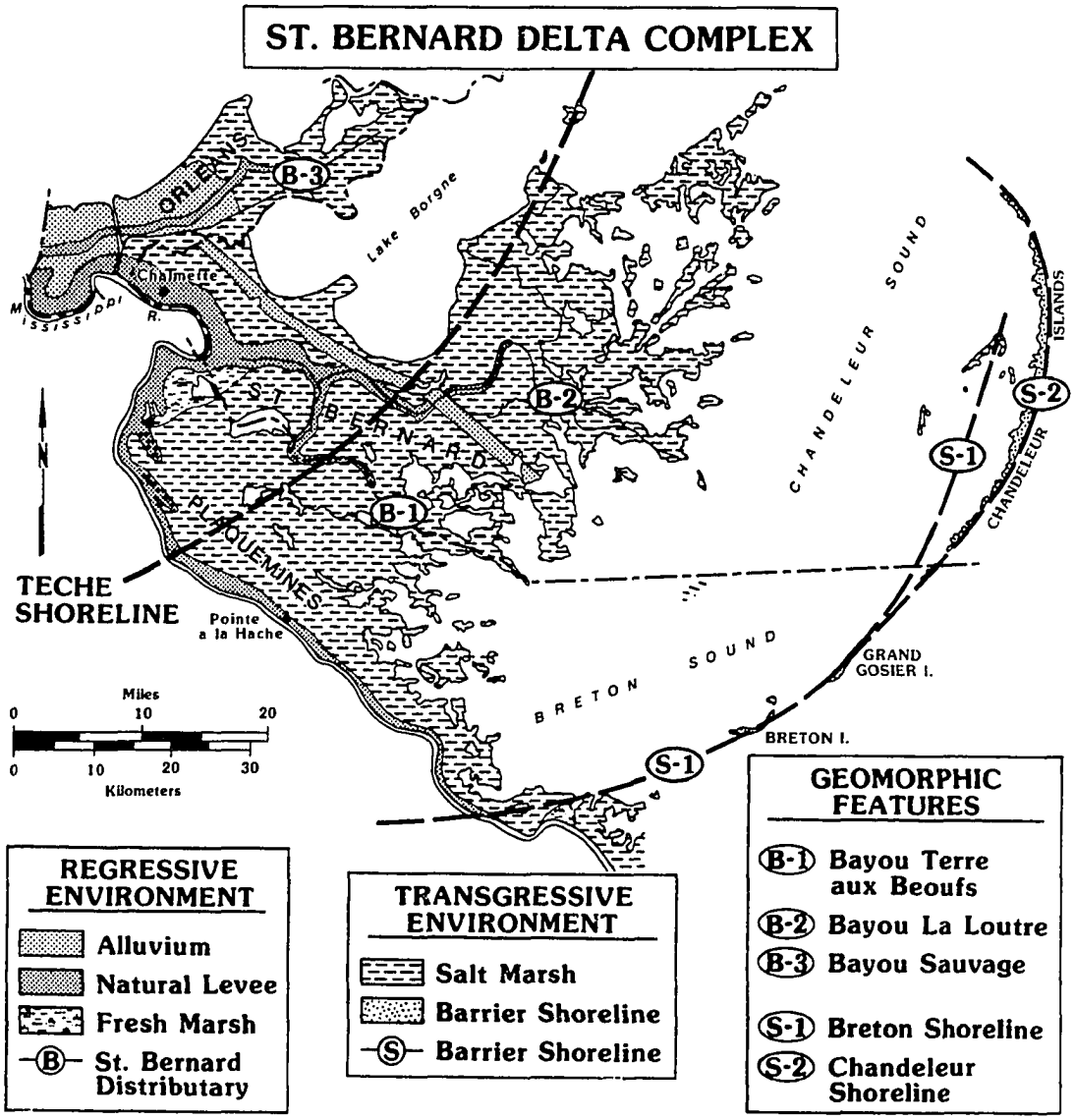

Figure 54. Geomorphic diagram of the St. Bernard delta complex.

submergence and transgression of this delta complex has led to the coalescence of the Breton and Chandeleur shorelines as well as their detachment from the mainland by the growth of Chandeleur and Breton sounds.

The Lafourche delta complex occupies most of the western portion of the Modern delta plain. This delta complex consists of four abandoned delta lobes ranging from 300-1220 years in age based on radiocarbon data (Penland et al., 1988b). Two distinct transgressive shorelines can be identified buried within the Lafourche delta complex: the Caillou Bayou and Terrebonne shorelines, associated with the Bayou de Large delta and the Bayou Terrebonne delta, respectively (Figure 55). The Bayou Grand Caillou delta built seaward of the Terrebonne shoreline south of Cocodrie about 900 years ago. Abandonment occurred about 400 years ago, resulting in the formation of the Isles Dernieres barrier island arc. Concurrently, the Bayou Lafourche delta built seaward of the Terrebonne shoreline about 700 years ago. Abandonment occurred about 300 years ago, resulting in the formation of the Bayou Lafourche erosional headland and the flanking barriers of Timbalier Island and Grand Isle.

The Modern delta complex represents the transition from a multidistributary shallow water delta lobe, the Plaquemines, to an elongate deep water delta lobe, the Balize (Figure 56). The Plaquemines delta, whose principal distributaries are Bayou Robinson, Grand Bayou, and Dry Cypress Bayou, began building seaward of the Teche shoreline about 900 years ago and continued southward across pre-existing Breton shoreline, resulting in the progradation of the Cheniere Ronquille beach ridge plain. Abandonment of the delta erosional headlands with flanking barriers which coalesced to form the Plaquemines barrier shoreline. Beginning in the early 1700s, the Balize delta lobe prograded onto the continental shelf. Concurrent with this growth was the development of artificial levees on the Mississippi River which constricted the channel and allowed this delta lobe to build out into deep water. The Balize delta would not have reached its current configuration under natural conditions because of the extreme hydraulic inefficiency of this course.

The most recent delta complex to begin building on the Louisiana coast is the Atchafalaya (Van Heerden and Roberts, 1988). The Atchafalaya River has been depositing a series of lacustrine deltas farther inland within the larger Atchafalaya basin since the 1850s. After the 1973 floods, a

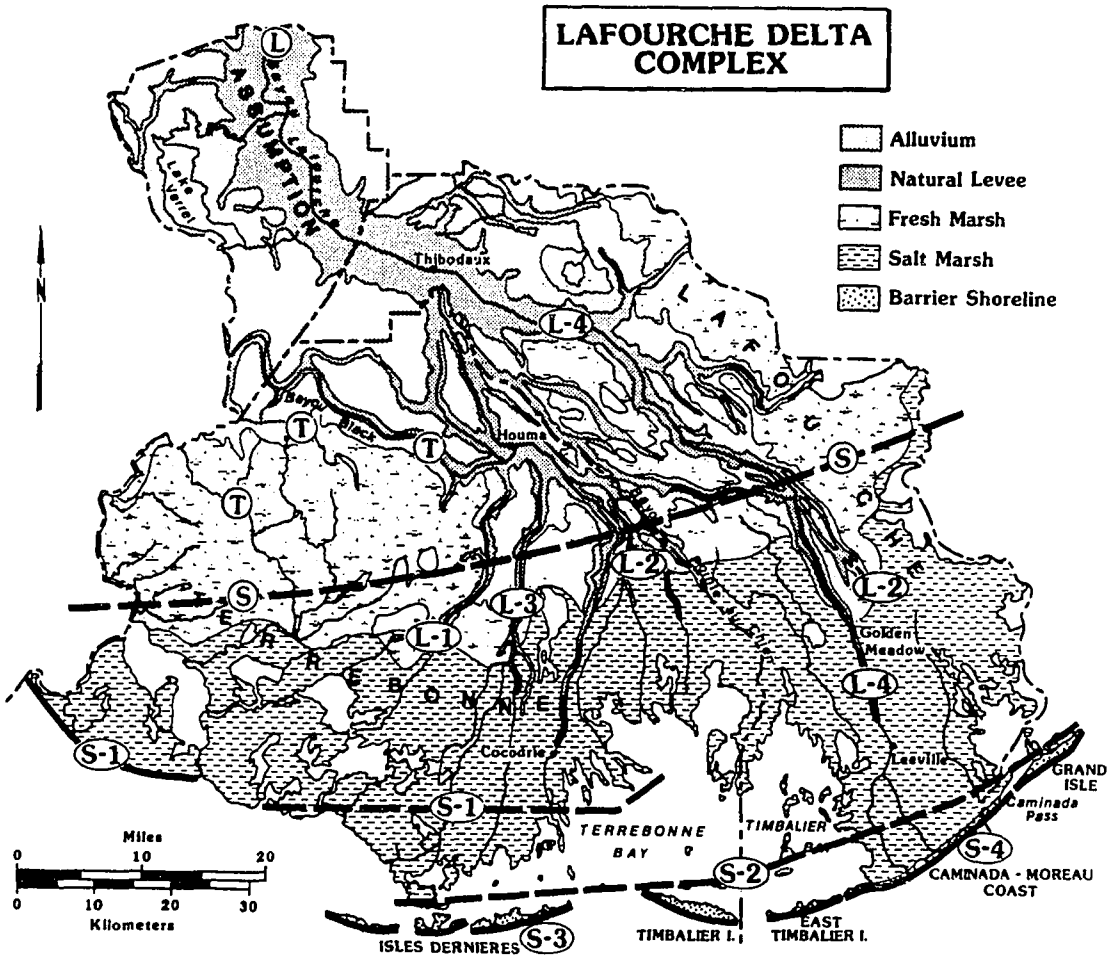

GEOMORPHIC FEATURES

(T) Teche Deltas	(S) Teche Shoreline
(L-1) Bayou du Large	(S-1) Caillou Bay Shoreline
(L-2) Bayou Terrebonne	(S-2) Terrebonne Shoreline
(L-3) Bayou Grand Caillou	(S-3) Isles Dernieres
(L-4) Bayou Lafourche	(S-4) Lafourche Shoreline

Figure 55. Geomorphic diagram of the Lafourche delta complex.

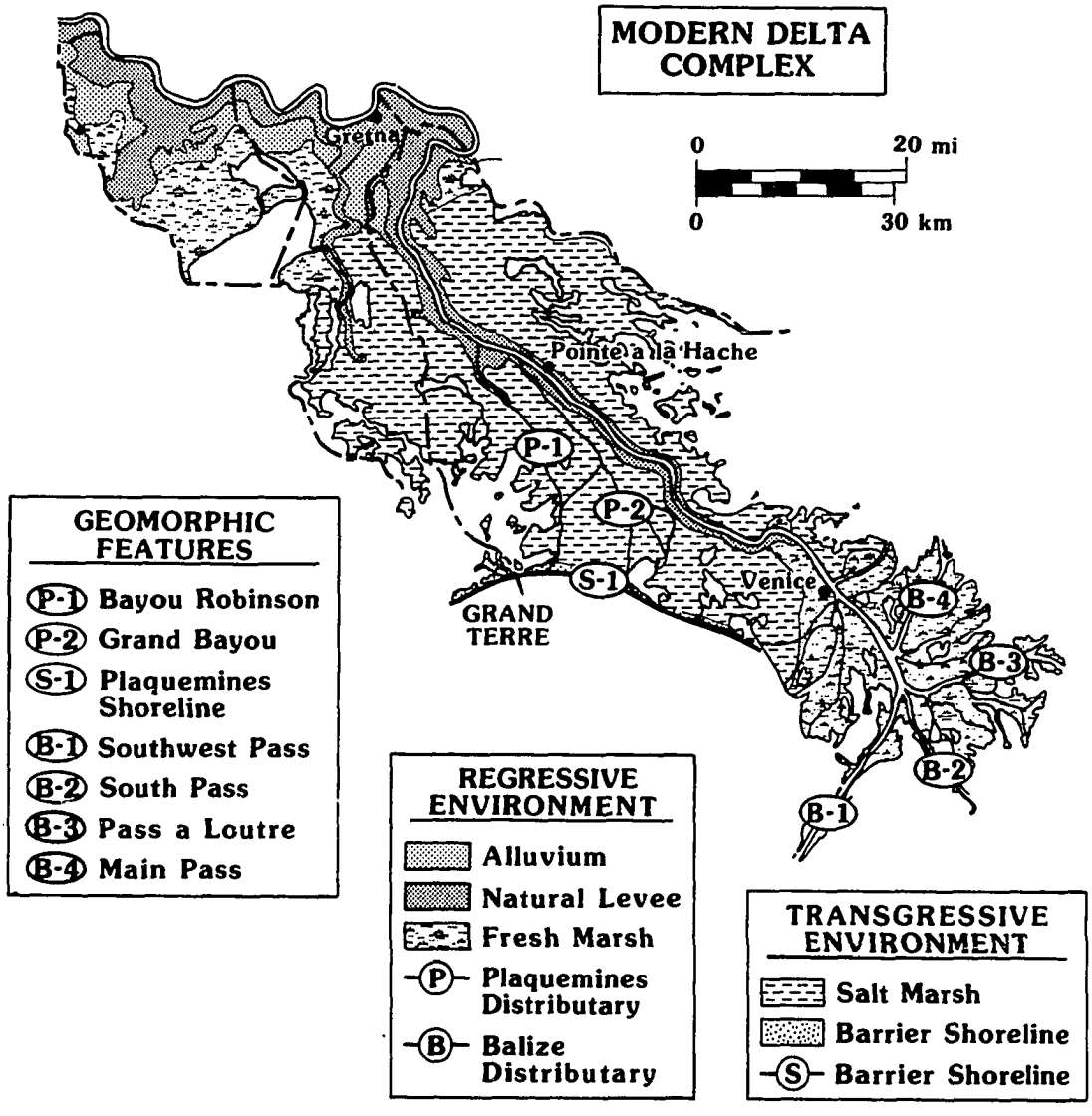

Figure 56. Geomorphic diagram of the Modern delta complex.

subaerial delta lobe began to form within Atchafalaya Bay. Atchafalaya River sedimentation represents the newest progradation of a major shallow water complex in Louisiana.

CHENIER PLAIN FORMATION

Holocene Geologic Framework

The chenier plain of the Mississippi River (Figure 57) is a classic locality of alternating coarse clastic ridges and mudflats, first described by Russell and Howe (1935) and Howe et al. (1936). The term *chenier* is derived from the Cajun term "chene" for live oak, the dominant species found on the crests of the higher ridges. The Mississippi River chenier plain is described as stretching 200 km from Sabine Pass, Texas to Southwest Point, Louisiana, and ranging between 20 and 30 km wide, with elevations of 2-6 m. Several coastal plain rivers dissect the chenier plain, including the Sabine, Calcasieu, and the Mermentau rivers. White and Grand lakes dominate the eastern landscape, and Calcasieu and Sabine lakes are prominent features in the west. The Louisiana chenier plain consists of more than five major sets of ridges, which in cross section thicken seaward to about 6-8 m at the shoreface and lie on the Pleistocene Prairie terrace.

The chenier plain evolved during the Holocene as a sequence of prograding mudflats intermittently reworked into sandy or shelly ridges (Russell and Howe, 1935; Hoyt, 1970). Episodes of mudflat progradation are tied to pulses of sediments transported westward across the inner continental shelf during periods when a major distributary of the Mississippi River was located in the western portion of the delta plain. The chenier plain can be divided into stratigraphically distinct cheniers, beach ridges, recurved spits, and vegetated mudflats (Figure 58).

Russell and Howe (1935) and Howe et al. (1935) presented the first major physiographic descriptions of this area and using aerial photographs to map the ridge and mudflat trends. These pioneering scientists described the chenier plain as a Holocene sequence of prograding mud flats intermittently reworked into ridges of sand and shell. Pulses of Mississippi River sediment, transported by longshore currents, were though responsible for the various stages of progradation. When the Mississippi River discharged sediment near the present chenier plain, the shoreline advanced seaward by mudflat progradation. When the course of the Mississippi River switched away from the chenier plain, marine processes reworked the mudflats to produce a shore-parallel shell and sand chenier ridge overlying marsh sediments (Figure 59).

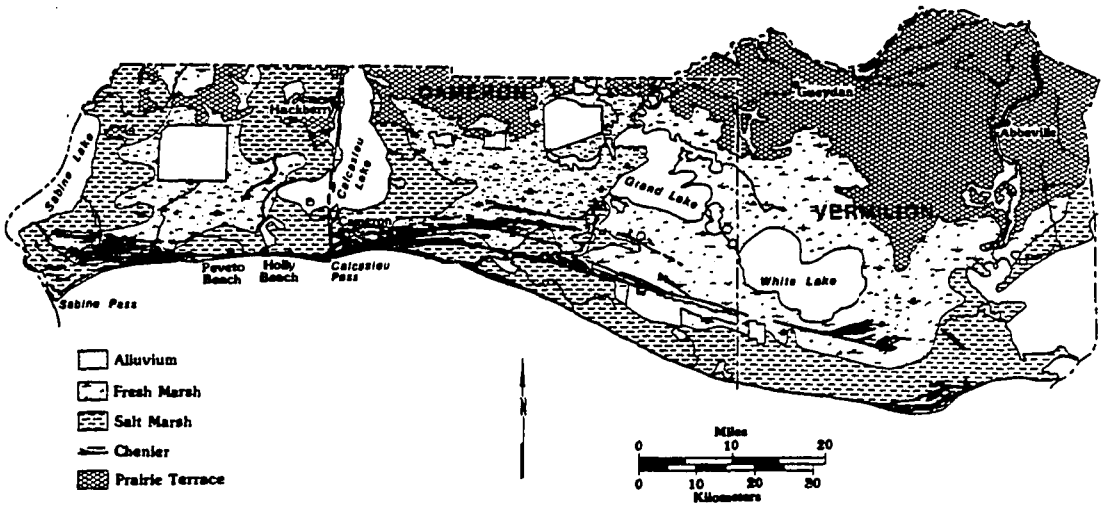

Figure 57. Location diagram of the Mississippi River chenier plain.

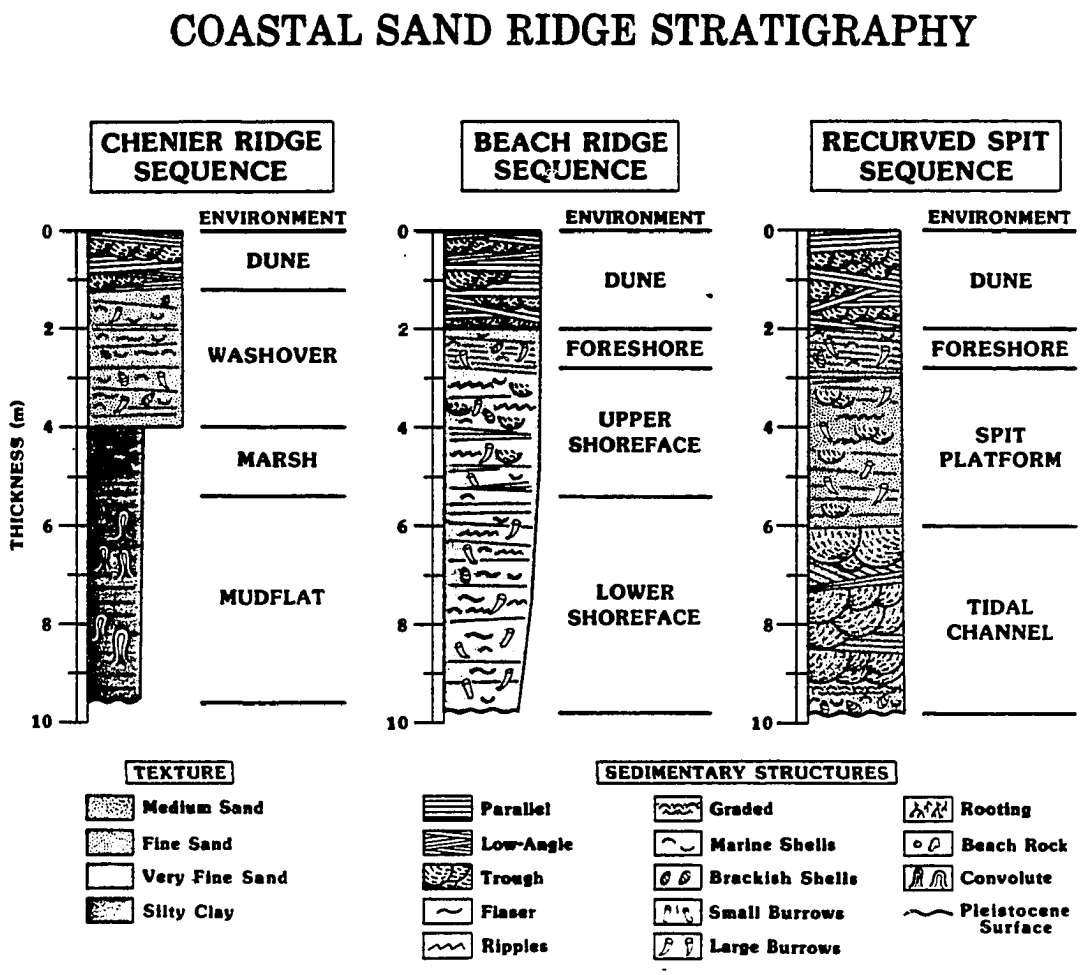

Figure 58. Stratigraphic model for chenier, beach ridge and recurved spit sequences (Penland and Suter, 1989).

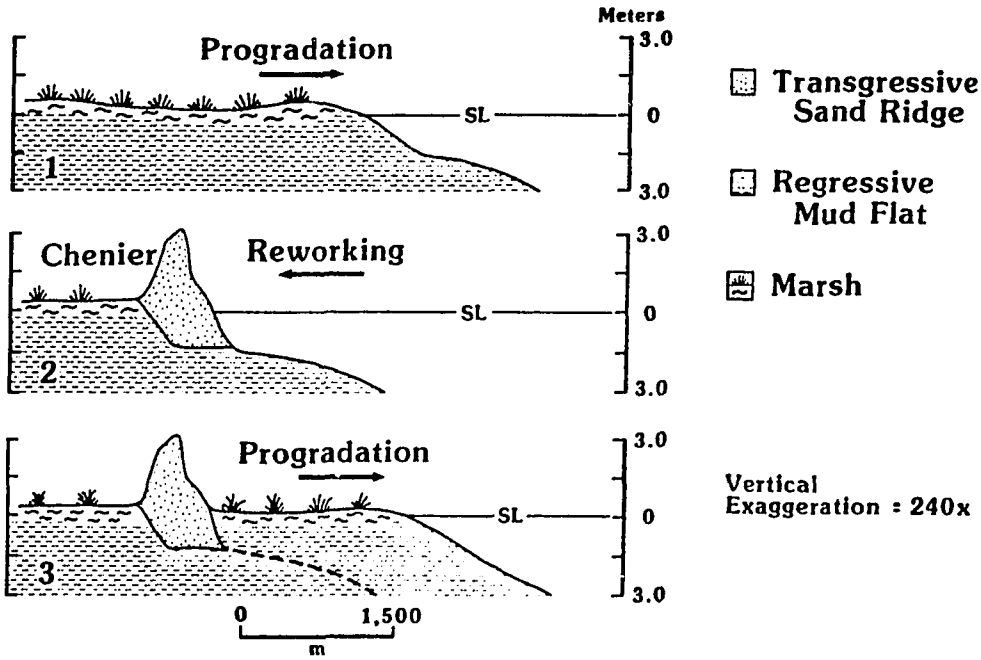

Figure 59. Process-response model for chenier ridge and mudflat development by Hoyt (1964).

Fisk (1948) conducted the first comprehensive geologic investigation of the chenier plain. Using engineering borings, Fisk (1948) mapped the Pleistocene Prairie terrace and the geometry of the Holocene chenier plain. He delineated basic facies patterns in the coastal marshlands and correlated their development with eustasy and with the shifting patterns of Mississippi River sedimentation. His report presented the most comprehensive set of stratigraphic cross sections for the chenier plain (Figures 60 and 61).

Byrne et al. (1959) completed a detailed facies investigation of the Mississippi River chenier plain and Gould and McFarlan (1959) presented a study of the geologic history area. Byrne et al. (1959) delineated the sedimentary facies that constitute the stratigraphy of the chenier plain using the dominant fauna. The zones, named after the dominant foraminifera, are 1) *Streblus* , 2) *Streblus-Elphidium* , 3) *Quinqueloculina* , and 4) *Trochammina* . They subdivided the stratigraphy on the basis of faunal assemblages and textural analyses into 1) basal transgressive deposits, 2) gulf-bottom sand and silty clay, 3) gulf-bottom silty clay, 4) bay-bottom and mud-flat clayey silt, 5) bay-mouth silt, 6) marsh organic clay and silt, and 7) chenier sand and shell.

Gould and McFarlan (1959) used a radiocarbon chronology to focus on the regional development of the chenier plain. The Holocene highstand was dated around 3000 yBP with the shoreline located along the Pleistocene Prairie Terrace, after which the progradation of the mud flats began. They delineated four major chenier shorelines: 1) the Little Chenier-Little Pecan Island trend (2800 yBP), 2) the Creole-Pumpkin Ridge-Tiger Island trend (2100 yBP), 3) the Oak Grove-Grand Chenier-pecan Island trend (1100 yBP), and 4) the western modern shoreline-eastern Mulberry island trend (less than 600 yBP). A direct correlation was made between each of these ridge systems and major delta complex abandonment events in the Mississippi River delta plain: the shoreline of 2800 yBP was correlated with the Teche abandonment, the shoreline of 2100 yBP was correlated with the St. Bernard abandonment, the shoreline of 1100 yBP was correlated with the Bayou Barataria abandonment, and the shoreline of 600 yBP was correlated with the Lafourche abandonment according to Gould and McFarlan (1959). The most recent episode of mud flat progradation is tied to the outbuilding of the Atchafalaya River delta (Morgan et al., 1953).

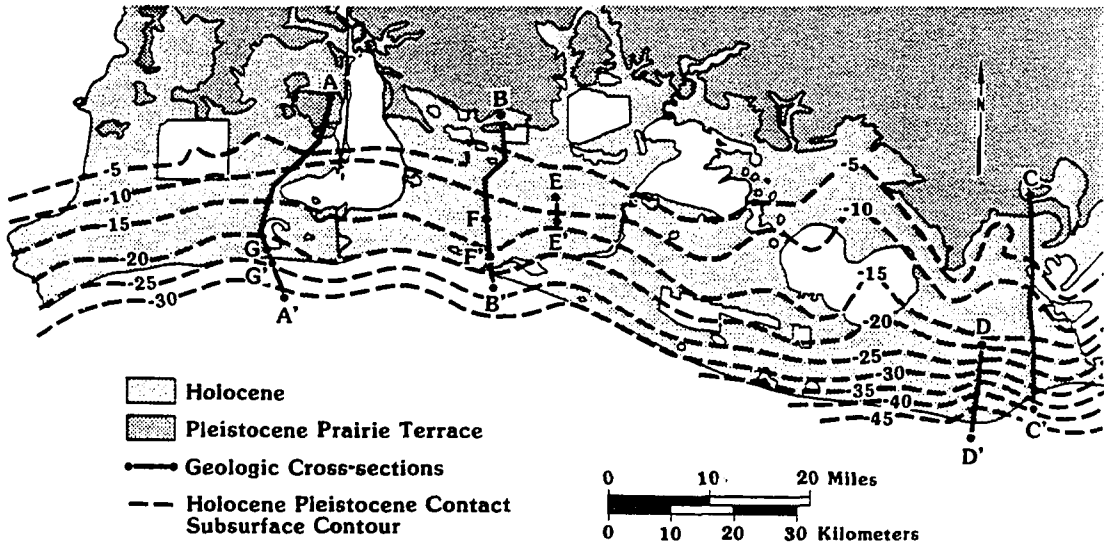

Figure 60. Location of regional cross sections and the geometry of Holocene chenier plain sequence (Fisk, 1948).

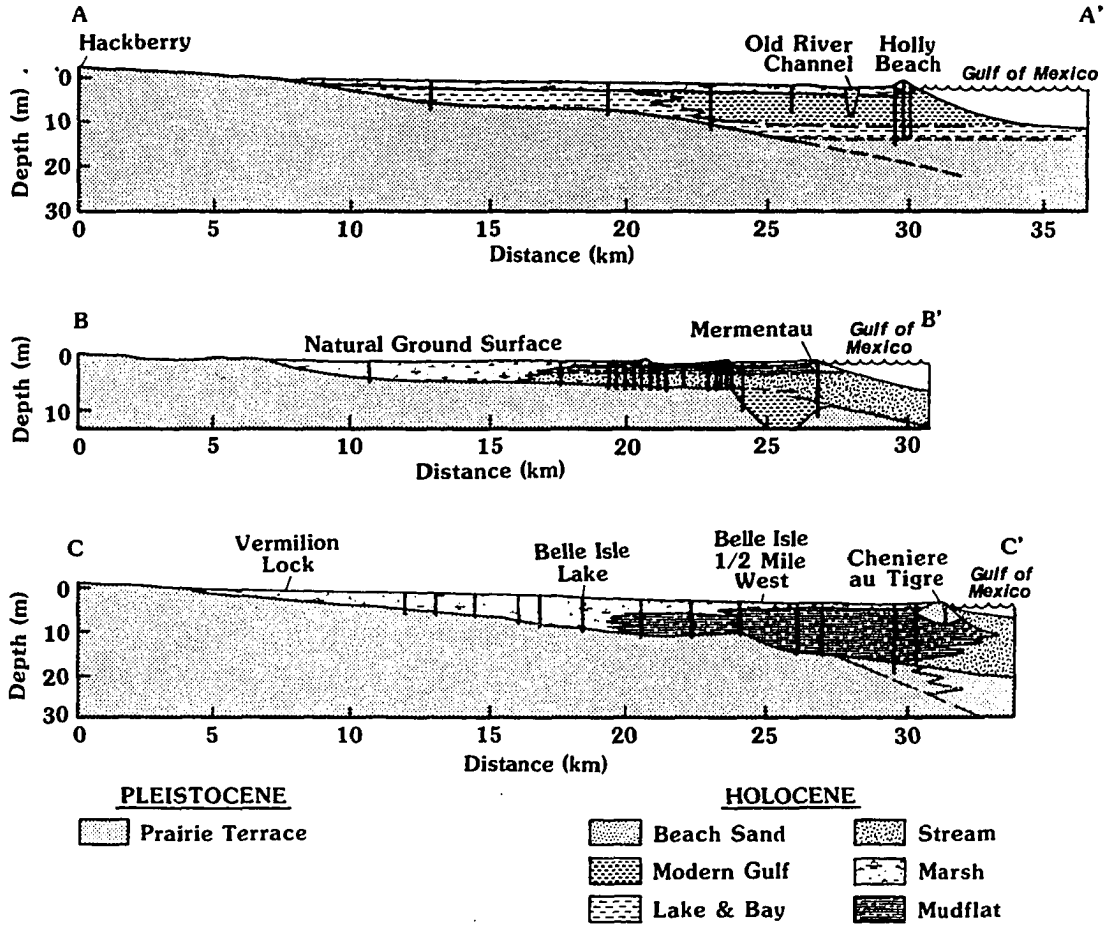

Figure 61. Representative regional stratigraphic dip oriented cross sections of the eastern and western chenier plain Calcasieu and headland (modified from Fisk, 1948).

New Holocene Geologic Framework

New seismic, vibracore, and radiocarbon data from the Mississippi River delta plain indicates this chronology can be refined in light of the recognition of the Late Holocene and Modern delta plains (Penland et al., 1987; Boyd et al., 1988), in contrast with the original single Holocene delta plain model (Fisk, 1944; Kolb and Van Lopik, 1958; Frazier, 1967). Analysis of these new data indicates that the individual Teche and Maringouin delta complexes (now called the Teche) of the Frazier (1967) model were in fact the same delta plain. A regional ravinement surface was discovered separating the Teche delta complex from the Lafourche delta complex (Penland et al., 1988b). This ravinement surface can be traced updip to an ancient transgressive shoreline termed the Teche shoreline, which can be mapped through the St. Bernard, Modern, and Lafourche delta complexes to the Atchafalaya Bay shoreline (Figure 48). The Teche basin shoreline is the modern equivalent of this regional transgressive shoreline and the Atchafalaya delta complex is building across it. This shoreline represents a major transgressive event about 4000-3000 yBP when sea level rose 5-6 m, submerging the coast of the Late Holocene delta plain and producing a shoreline parallel trend of sand shoals between Ship Shoal and Sabine Bank. The Late Holocene delta plain, including the Teche delta complex, dates to a temporary stillstand, 7000-4000 yBP, followed by rapid transgression. A stillstand at about 3000 yBP led to the formation of the Modern delta plain consisting of the St. Bernard, Lafourche, Modern, and Atchafalaya delta complexes. This new interpretation suggests a major revision of the timing and process of chenier plain formation (Figure 62).

First, this stacked delta plain interpretation indicates that the Little Chenier-Little Pecan Island trend cannot be linked to the Teche delta complex switching event because they are associated with different sea level stillstands and different aged delta plain. The Little Chenier-Little Pecan Island trend appears to represent the Holocene transgression highstand shoreline instead of the Pleistocene/Holocene contract. The absence of shoreline features along the Prairie Terrace, old thick marshes behind this ridge, and the concentration of Tchefuncte Indian middens on this ridge support this interpretation (McIntire, 1958). Thus, the landward margin of the Holocene marsh overlying the Prairie Terrace is not the highstand shoreline, it represents the leading edge of the Holocene

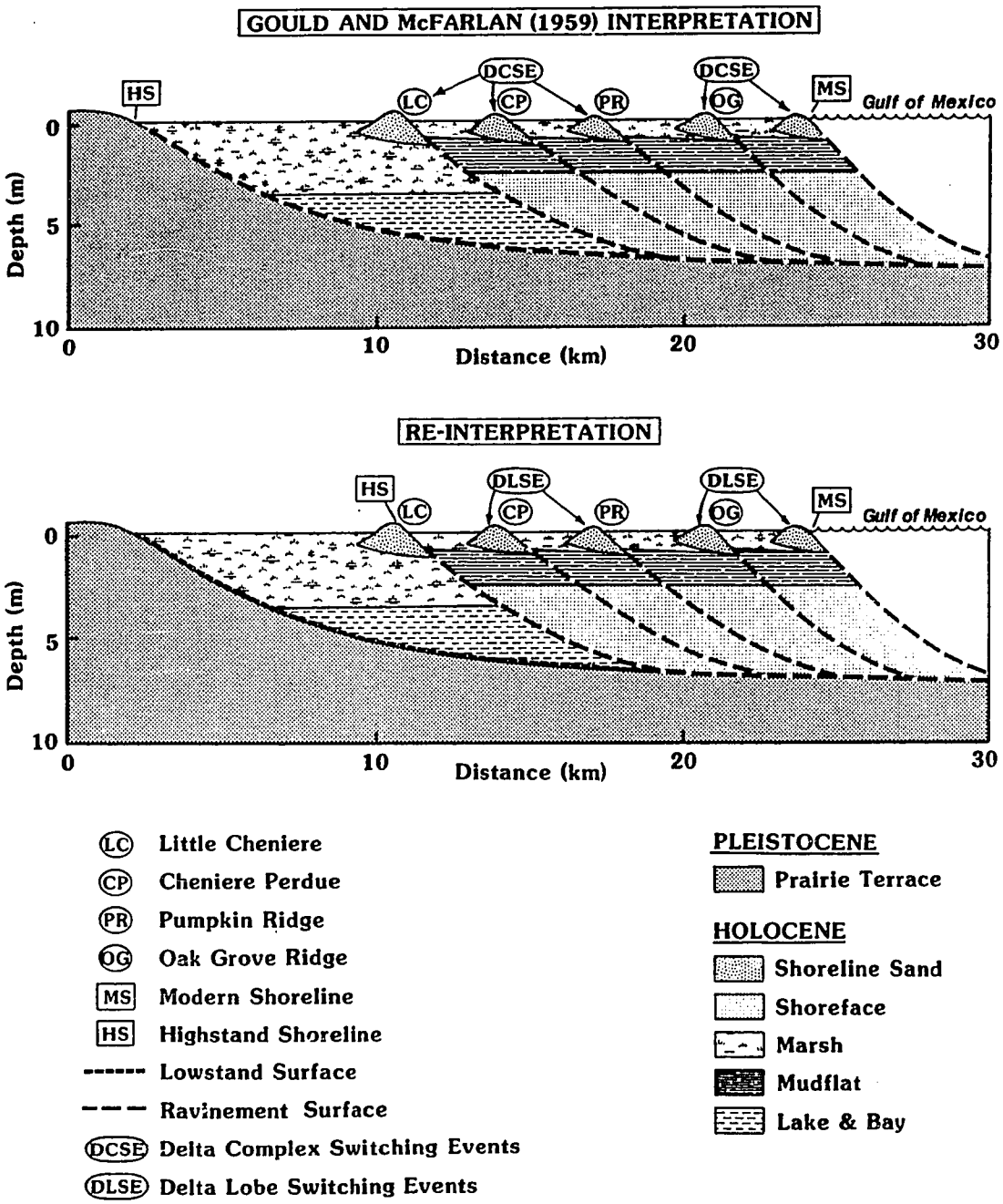

Figure 62. Previous and new chronostratigraphic models for the Mississippi River chenier plain (Penland and Suter, 1989a).

transgression.

Second, if the timing of the chenier plain is not tied to the Teche delta complex, then is the precise linking of the chenier process model to delta complex switching valid? Significant mud flat progradation seems to require a westerly position of the Mississippi River, but the numerous different forms and ages of the cheniers do not correspond well to the timing of major delta complex switching. Occurrence of individual ridges is probably tied to delta lobe switching within the Lafourche delta complex and variations in sediment supply from local rivers.

DISCUSSION

Barrier Island Evolution

Barrier Island Transgression, Submergence, and Stratigraphy

The mechanism controlling barrier island formation have been debated since the early nineteenth century. Few models have allowed an evaluation of the processes controlling barrier island formation or an understanding of how the alternative mechanisms are related. The well-defined evolutionary sequence of abandoned Mississippi delta complexes provides direct evidence of barrier origin and displays the major mechanisms proposed for barrier island formation (Figure 35). In stage 1, Gilbert's (1885) concept of longshore spit building and subsequent breaching is the dominant mode of barrier island genesis. The primary source of sediment available for barrier shoreline development comes from erosion of deltaic headlands and subsequent longshore transport of sand into flanking barrier spits. Spits are breached by storm overwash processes. Submergence ensures the increasing backbarrier tidal prism necessary to maintain storm breaches and lead to tidal inlet development and flanking barrier island formation.

The formation of flanking barriers by Gilbert's (1885) spit-breaching process produces a characteristic stratigraphic signature (Figure 63). This sequence reflects the lateral migration of flanking barriers away from headland sand sources. During stage 1, spits first develop at the margins of the erosion headland and build laterally downdrift, forcing tidal channels to migrate or infill. Spit building leads to the stacking of tidal channel and spit deposits. Flanking barrier stratigraphy reflects the importance of spit and tidal inlet processes, erosional shoreface retreat, and the erosional headland sand source. The *flanking barrier island sequence* is a fining-upward sequence dominated by tidal channel sand and shell overlain with recurved spit platform sands capped by a thin sequence of beach, washover, and dune deposits. The contact between the base of the stage 1 sequence and underlying regressive deltaic muds is an erosional tidal channel surface.

Evolution from stage 1 to stage 2 demonstrates Hoyt's (1967) concept of barrier island formation by mainland detachment through coastal submergence (Figure 28). While coastal reworking is forming barriers at the seaward margin of an abandoned delta complex, rapid subsidence acts to submerge the backbarrier deltaic plain. The formation of barrier islands in this environmental then

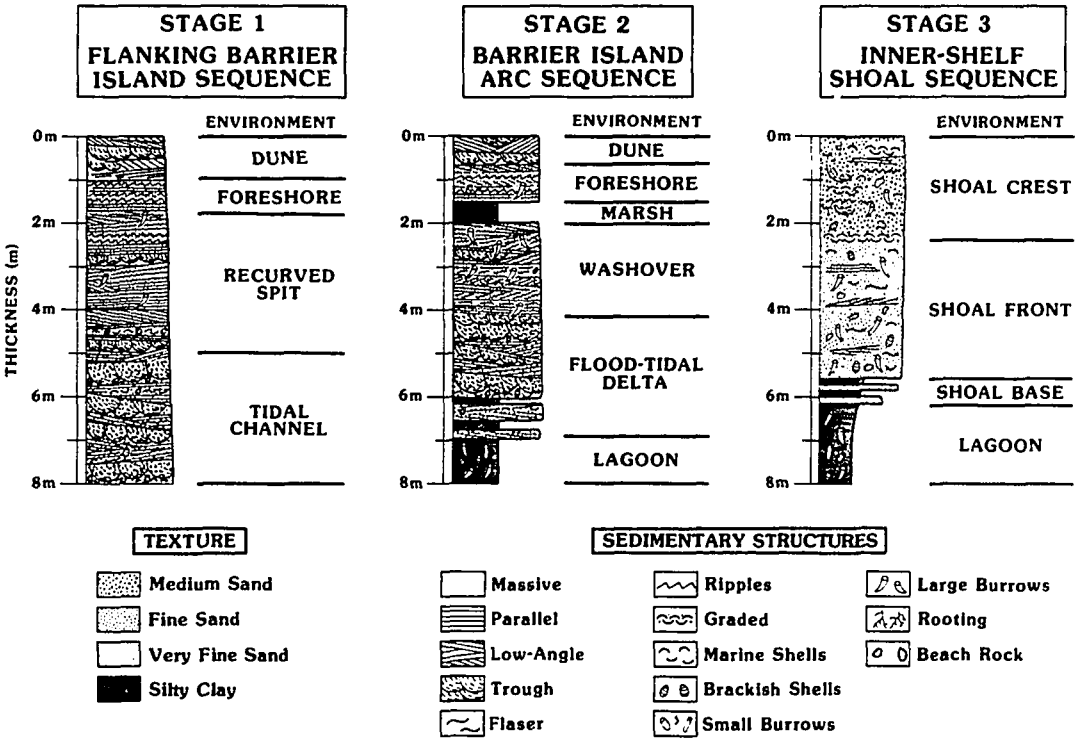

Figure 63. Generalized composite stratigraphic sequences for each stage of transgressive barrier and shoal sand body development. The *flanking barrier island sequence* reflects the importance of shoreface erosion, recurved spit building, and tidal channel migration during transgression. The *barrier island arc sequence* reflects the importance of flood tidal delta and overwash processes during submergence. The *inner shelf shoal sequence* reflects the importance of shoreface erosion and inner shelf reworking following barrier island arc submergence (Penland et al., 1988a).

becomes a question of rate of submergence and landward retreat of the mainland shoreline versus rate of barrier shoreline retreat. The gradient of the mainland behind the Chandeleur Islands and the Isles Dernieres ranges from flat to a seaward slope of about 1:5,000. A relative sea level rise of 50 cm/100 yr produces submergence and landward retreat of the mainland shoreline at rates greater than 25 m/yr; average barrier shoreline retreat rates are less than 20 m/yr. Landward retreat of the mainland shoreline is not a linear process but consists of progressive enlargement of lakes, distributaries, tidal channels, and interdistributary bays, followed by eventual coalescing to form larger transgressive open water bays and lagoons.

The formation of barrier island arcs by Hoyt's (1967) mainland detachment process through submergence produces a characteristic coarsening-upward stratigraphic signature, the *barrier island arc sequence* (Figure 63). This sequence consists of lagoonal muds grading upward into interbedded lagoonal muds and flood tidal delta sands to washover sands capped by beach, washover, and dune sediments. The contact between the stage 2 sequence and the underlying regressive muds is gradational, representing the transition of a freshwater delta plain to saltwater marshes, bays, and lagoons. This sequence reflects landward barrier migration in response to relative sea level rise, in combination with tidal inlet and overwash processes. In stage 2, barrier island arcs have migrated landward past the position of the ancestral erosional headland and flanking barrier shoreline and are composed of material eroded and reworked from distributary and former stage 1 sand bodes. The stratigraphy of transgressive barrier island arcs is distinctly different from that of tide-dominated stage 1 flanking barriers and reflects the importance of submergence, wave-dominated tidal inlet and overwash processes, and barrier sand recycling.

The evolution from stage 2 to stage 3 by the transgression and submergence of a former barrier island arc eventually produces a marine sand body (Figure 63). The inner shelf shoal sequence coarsens upward from shoal base silt and sand, rapidly grading into shoal front sand, capped by shoal crest sand and shell. The base of the inner shelf shoal lies on a ravinement surface. Stage 3 inner shelf shoal stratigraphy reflects the importance of inner shelf shoal reworking and shoal sand cycling. This results from the limited range of sediment size available in the Holocene Mississippi delta. Other comparable sequences may display trends with more pronounced variability.

Transgressive Shoreline and Continental Shelf Sand Bodies

The term *transgressive submergence* best describes the process of shoreline and shelf sand generation and presentation on the Mississippi River delta plain. Transgression occurs when the shoreline migrates landward in a horizontal sense in response to delta complex abandonment, leading to erosion and reworking during shoreline and shoreface retreat. Submergence refers to the vertical relationship between sea level and a fixed spot on the surface of a sedimentary sequence. Submergence occurs when the depth of water increases over that spot as a result of eustatic, isostatic, or tectonic processes (Mathews, 1984). A high rate of submergence characterizes transgression in abandoned Mississippi River delta complexes and leads to marine sand body generation. Other mechanisms described as producing sand deposits during shoreline transgression, namely *shoreface retreat* and *in-place drowning*, do not adequately characterize either the process or the stratigraphic signature of shoreline transgression identified in the retreat path of abandoned Mississippi River delta complexes (Mathews, 1984). These models were developed to explain the transgressive stratigraphy of the U.S. Atlantic continental shelf.

Shoreface retreat (Fisher, 1961; Kraft, 1971; Swift, 1975, 1976) refers to a process whereby the base of the shoreface translates landward, truncating pre-existing facies. The stratigraphic signature of shoreface retreat is an erosional diastem, a ravinement surface overlain by a thin, often discontinuous sand sheet. Vertical and landward translation of the shoreface allows basal segments of the lagoon and barrier sediments to be preserved (Swift, 1975; Field and Duane, 1976).

In-place drowning (Sanders and Kumar, 1975; Rampino and Sanders, 1980) describes a process whereby both barrier and lagoonal sediments accrete vertically, keeping pace with relative sea level rise. Rapid relative sea level rise results in transgression of the barrier and generation of a new shoreline farther landward. Both barrier and lagoonal deposits are only slightly reworked and drowned in situ. The stratigraphic signature of in-place drowning consists of a thickened lagoon and barrier sand sequence preserved largely intact and perhaps overlain by an erosional diastem.

The process of *transgressive submergence* and the stratigraphic sequence for stage 3 inner shelf shoals are not well described by either *shoreface retreat* or *in-place drowning*. The characteristics of each transgressive sequence depend on the process variable combination that

operates in the local environment, whether it be *shoreface retreat, in-place drowning, transgressive submergence*, or some other mechanism. There is not one generally applicable model, but rather a spectrum of transgressive stratigraphies corresponding to a range of process-variable combinations. The controlling variables differentiating transgressive submergence from other models are high rates of relative sea level rise, low gradient continental shelves with limited local sand sources, and a storm-dominated process environment. It operates when submergence is rapid enough to inundate the barriers while they continue to undergo transgression and shoreface retreat. *Transgressive submergence* is a new mechanism for describing the evolution of shoreline and shelf sands in the Gulf of Mexico (Figure 64).

Deltaic Stratigraphy

Classic studies of the Mississippi River delta plain (Russell et al., 1936; Kolb and Van Lopik, 1958; Fisk, 1955, 1961; Frazier, 1967; Coleman and Wright, 1975) have emphasized the regressive component of the delta sequence. The facies present in the transgressive part of the sequence have not previously been described comprehensively, although transgressive sedimentation occupies the majority of the depositional surface of the Holocene delta plain. It generates a widespread marker sequence consisting of lagoonal muds, barrier sand bodies, sand shoals, and organic deposits formed in salt-to-brackish marshes.

This three-stage model identifies and emphasized the transgressive component of the delta cycle and explains the generation and evolution of a transgressive depositional system through the process of *transgressive submergence.* A complete shallow water delta sequence consists of a regressive-transgressive couplet. Figure 65 shows a complete shallow water Mississippi delta sequence, based on the Maringouin delta complex. Here, due to the lack of accommodation space, the regressive sediments are seen to be substantially thinner than for the equivalent sequence developed in the Balize deep water delta (Coleman and Wright, 1975). Completion of the delta sequence requires the addition of overlying lagoonal and shoal facies. The transgressive sediments are volumetrically significant, contributing up to 50 percent of the composite sequence thickness. Preservation potential of this complete shallow water deltaic sequence is likely to be high, either through submergence below the zone of active reworking or by burial during a new regressive phase.

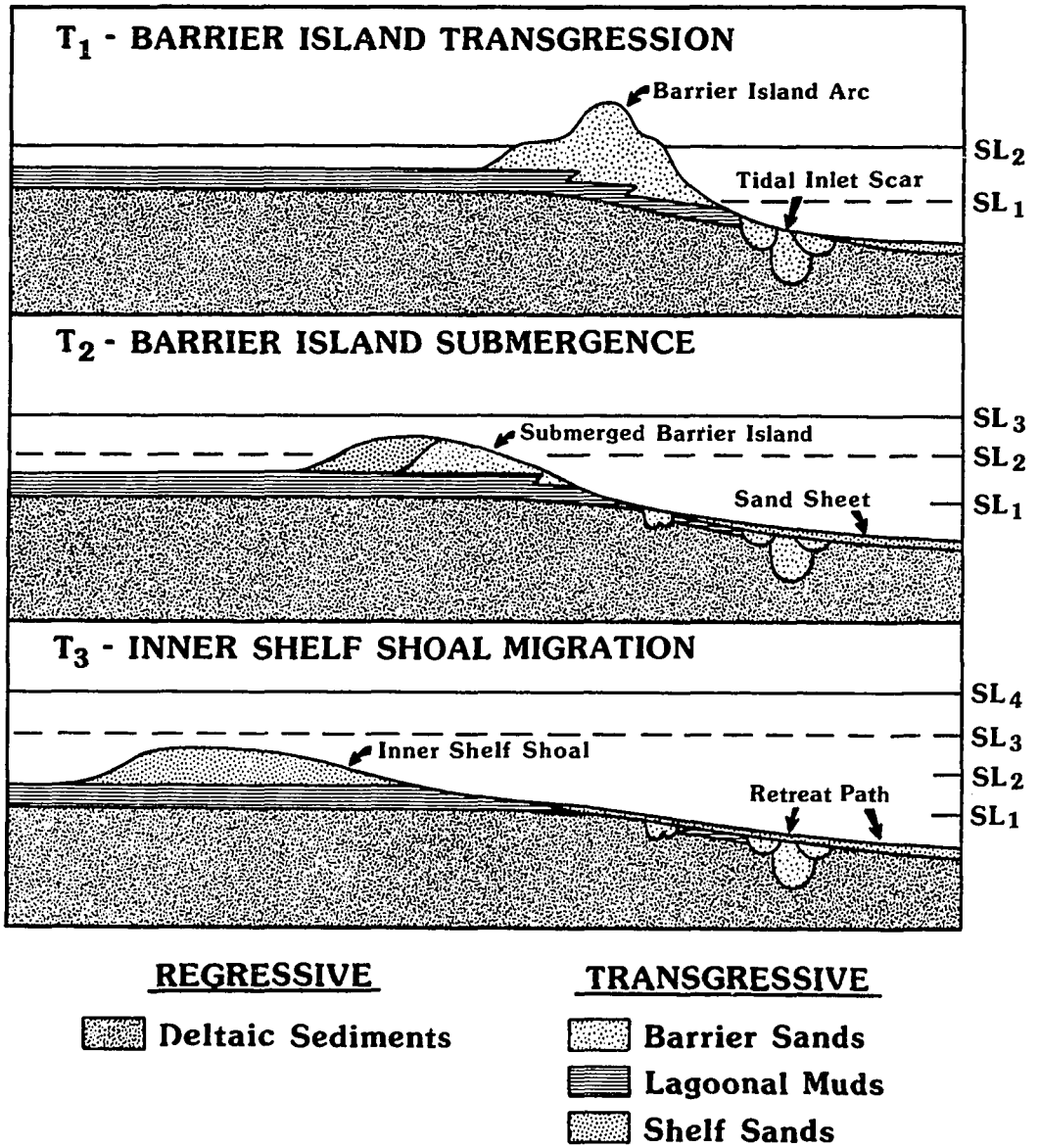

Figure 64. This stratigraphic model illustrates the *transgressive submergence* process in which a marine inner shelf sand shoal is generated by the reworking of a submerged barrier island arc sand body associated with an abandoned delta complex (Penland et al., 1988a).

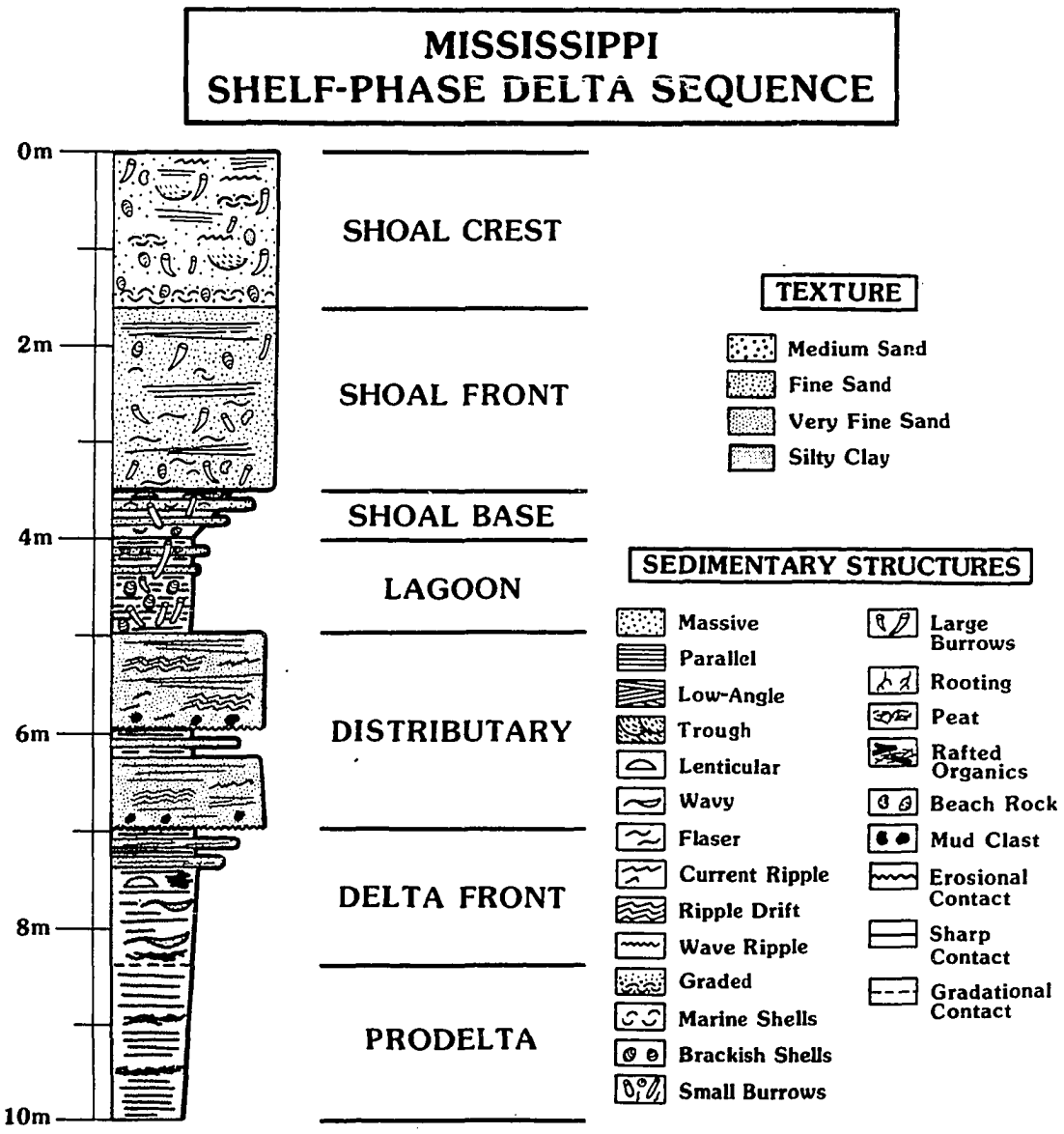

Figure 65. A generalized stratigraphic model for an abandoned shelf-phase Mississippi River delta complex illustrates the significance of the transgressive component. In this new stratigraphic sequence, shelf-phase delta complexes, which differ considerably from the tradition deepwater Mississippi River delta complex model, are seen as the primary depositional constituents of the Holocene Mississippi River delta plain (Penland et al., 1988a).

Delta Plain Development

Sea Level History

The relative sea level curve in Figure 66 depicts the depositional history of the Late Holocene and Modern delta plains over the last 7,000 years. The Late Holocene delta plain, consisting of three delta complexes, was built during a standstill in relative sea level about 7000-4000 yBP. The Late Holocene transgression between 4000 yBP and 3000 yBP led to the complete transgression and submergence of the distal Late Holocene delta plain, generating the Teche shoreline. During this period, deltaic sedimentation consisted mainly of aggradation of the alluvial valley landward of the retreating Teche shoreline, and little active progradation took place. With a relative stillstand in sea level beginning about 3000 years ago, the Mississippi River began building the currently active Modern delta plain.

The depositional model in Figure 60 depicts the development of the Late Holocene and Modern delta plains as a function of sea level changes and the delta switching process. Both delta plains are separated by a regional ravinement surface, traceable from the Atchafalaya Bay east through the St. Bernard delta complex, that merges updip with the Teche shoreline. A rapid 5-6 m rise in relative sea level between 4000 and 3000 yBP resulted in the transgressive submergence of the Late Holocene delta plain, generating Ship Shoal, Trinity Shoal and the Teche shoreline and the Teche ravinement surface. During this period relative sea level rise was of such magnitude that the sediment supply from the Mississippi River to the coastline could not prograde any delta complexes except during sea level stillstands. After 3000 yBP, the current stillstand occurred, resulting in the progradation of the Modern delta plain.

New Depositional Model

The most recently and widely accepted chronostratigraphic model for the Mississippi River delta plain is from Frazier (1967), depicting a single Holocene delta plain consisting of six individual delta complexes. This extensive data set of vibracores, high resolution seismic profiles, and new radiocarbon dates afforded the opportunity to test and refine the previous models (Appendices B, C, D, E, and F). It is important to note that the major difference between the research presented here and that of our earlier colleagues is the extensive offshore data coverage of the submerged portions

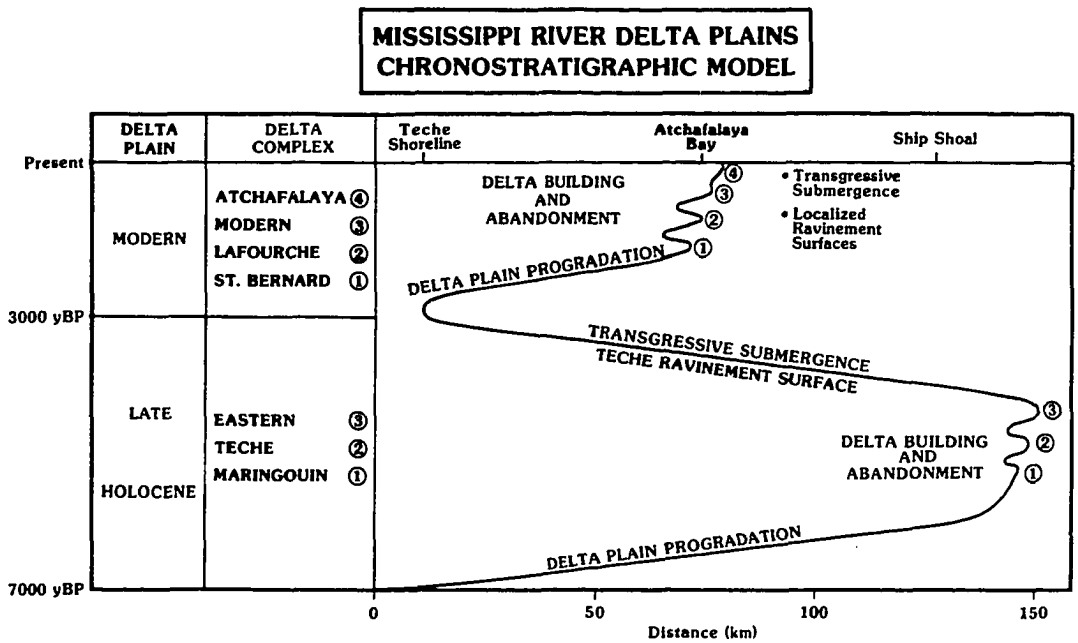

Figure 66. Diagram depicts sea level history for the Late Holocene and Modern delta plains (Penland et al., 1987).

of these delta plain, which the previous studies lacked. Vibracore and seismic data were used to identify ravinement surfaces and correlate them regionally.

The recognition of the regional Teche shoreline and ravinement surface was the key to the reinterpretation of the Mississippi delta plain stratigraphy. The Teche ravinement surface separates two imbricated delta plains developed at different sea level stillstands with an intervening hiatus of about 1000 years. In this new interpretation, the Maringouin and Teche delta complexes of the single Holocene delta plain of Frazier (1967) are actually the same delta complex and were not part of the Modern deltaic sediment package because the delta complex lies below the Teche ravinement surface, and thus are associated with the Late Holocene delta plain. Mapping of the Teche ravinement surface led to the identification of separate Late Holocene and Modern delta plains (Figure 67).

The chenier plain of southwestern Louisiana is located downdrift of the Mississippi River and represents a marginal deltaic plain composed of prograding mud flats separated by transgressive shorelines. Originally, the progradation of the chenier plain was tied to the Teche delta complex of Frazier's (1967) single Holocene delta model, which was active 7000-4000 yBP. The chenier plain cannot be correlated with these delta complexes because they are associated with the Late Holocene delta plain which, was active when sea level was 6 m lower. These dates better correlate with the initial progradation of the Modern delta plain. The age of the most landward ridge of the chenier plain supports the timing of the end of the Teche transgression about 3000 yBP.

The age relationships and distribution of archaeological sites throughout the Mississippi River delta plain and the chenier plain support the pattern of coastal development presented by this new chronostratigraphic model. Landward (north) of the Teche shoreline on the Late Holocene delta plain, a diverse mixture of Indian middens from Archaic (>1500 B.C.) to Natchez (1700 A.D.) in age arc found (McIntire, 1958). Seaward (south) of the Teche shoreline on the Modern delta plain, only younger Indian middens are found, ranging from Tchefuncte (500 B.C.) to Natchez (1700 A.D.). This distribution supports the theory that the Teche transgression was regional and ended by generating the Teche shoreline and its western extension, Little Chenier Ridge, the oldest and landward-most ridge in the chenier plain. In addition, the occupation intervals of individual delta complexes by ancient Indians correlate very closely with the delta complex chronology of the Modern delta plain,

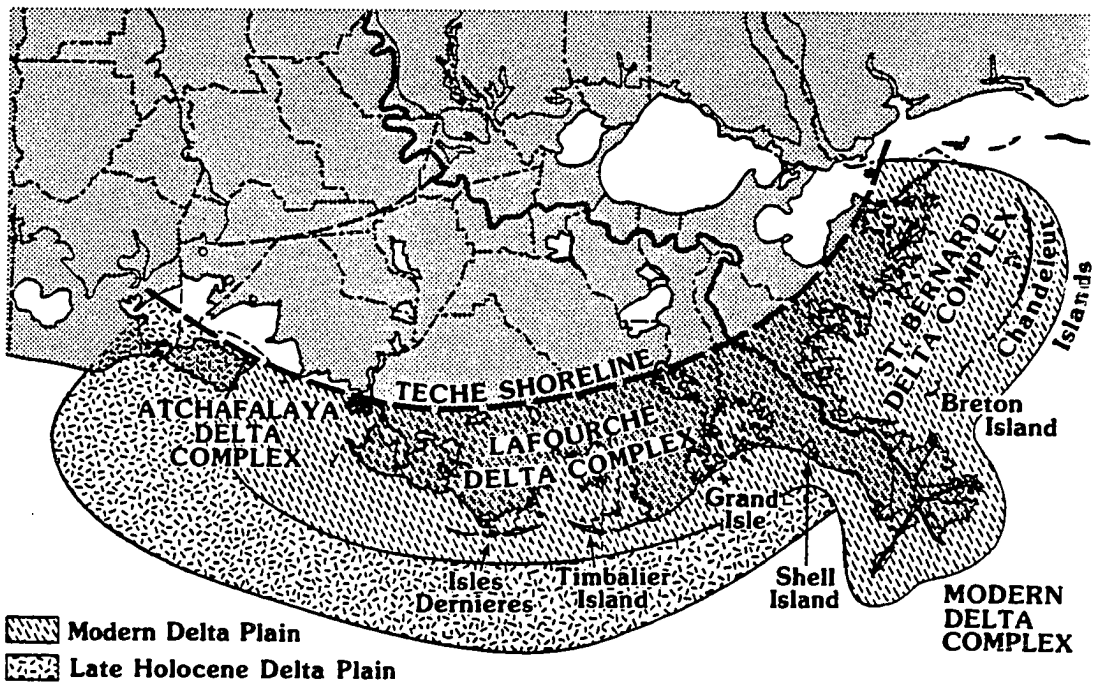

Figure 67. Diagram depicting the Late Holocene and Modern delta plains (Penland et al., 1987).

supporting the concept of two delta plains deposited at two different sea levels.

Delta Plain Facies Models

Fisk (1955) and Kolb and Van Lopik (1958) identified two morphologic types of delta complexes in the Mississippi River delta plain: shoal water and deep water delta complexes. Fisk (1955) used the Bayou Lafourche delta complex as an example of a shoal water delta and proposed that in situations where a delta complex progrades into shallow water, the distributary mouth bar sands coalesce to form a laterally continuous delta-front sheet sand. According to Fisk's (1955) classification and Frazier's (1967) chronology, all of the Mississippi River delta complexes are shoal water deltas except the Modern delta complex.

The Balize lobe of the Modern delta complex is the only deep water Mississippi River delta complex, currently prograding off the edge of the continental shelf into water depths exceeding 150 m. This continued progradation under conditions of decreasing hydraulic efficiency results from channel stabilization by an extensive levee system. The present configuration would not have been achieved under natural conditions because most of the flow would have diverted to the Atchafalaya River by the early 1900s. Thus, the current Mississippi delta facies model is based upon a deep water delta development under artificial conditions.

Coleman and Wright (1975) presented a composite, idealized sequence for the Mississippi River delta plain based on the deep water Modern delta complex (Figure 68). This model depicts a coarsening-up, regressive sequence of prodelta muds grading into distributary sands capped by thin bay and marsh deposits, with thicknesses ranging between 60 m and 150 m. The regressive component of the delta cycle model is emphasized and no transgressive component, which would be generated during the abandoned phase of the delta cycle, is included. Analysis of the Louisiana Geological Survey vibracore and seismic database indicates that deep water deltaic deposits as depicted by the above sequence are not found elsewhere (Appendices B, C, D, E, and F). It appears that shallow water deltaic sequences, 10-15 m thick, are the most common constituents of the Mississippi River delta plain.

Seismic and vibracore data indicate that the shallow water Lafourche delta complex is representative of the other delta complexes constituting the Lake Holocene and Modern delta plain

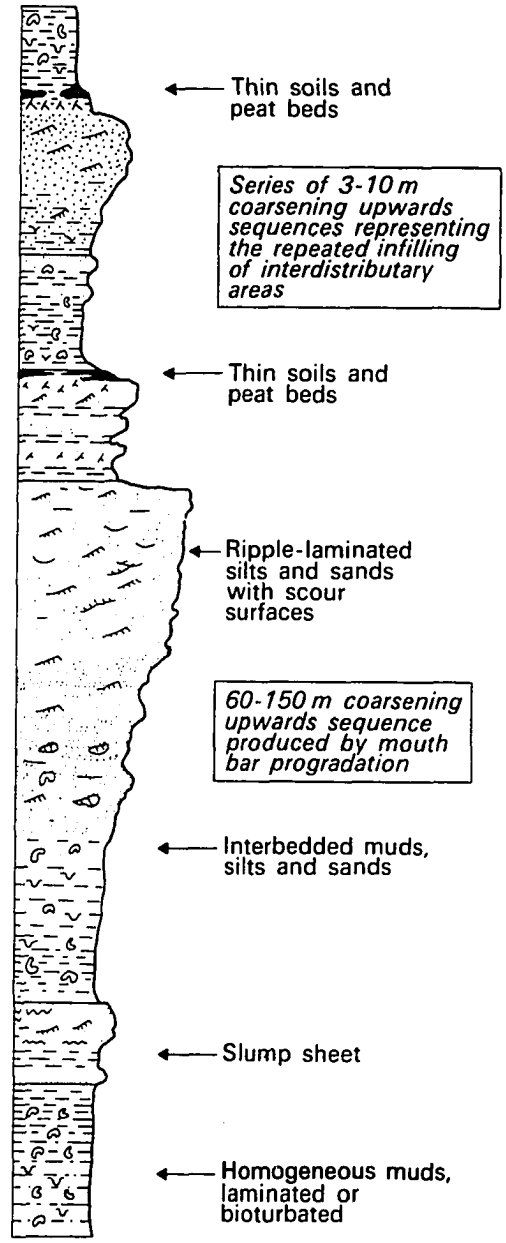

Figure 68. An idealized stratigraphic sequence for the Balize delta lobe of the Modern delta complex.

(Appendices E and F). The Lafourche delta complex model of a shallow water delta plain depicts a sequence 10-12 m thick except at distributary channels, where the thickness may exceed 12 m. The morphology is dominated by multiple this shallow water delta complex is terminated by a series of overlapping shorelines, beach ridge plains and smaller individual delta lobes.

The idealized, shelf-phase deltaic sequence best described the stratigraphy generated by the Mississippi River delta cycle for the Late Holocene and Modern delta plains. The thick deep water delta complex model and sequence are representative of a shelf margin delta. A fully developed shallow water delta sequence consists of a regressive component (50-70 percent) of prodelta, delta front, and distributary facies capped by a transgressive component (30-50 percent) consisting of lagoonal muds truncated by a ravinement surface upon which an inner shelf shoal rests. Only the lower portions of the regressive sequence are preserved because the upper portion is reworked by transgression and submergence. The inner shelf shoal derives from the shoreface reworking of a submerged barrier shoreline. The shelf phase model differs significantly from the delta-water delta models in the thickness of the sequences, the facies sequence, and the volumetric importance of the transgressive component.

These new chronostratigraphic model for the Late Holocene and Modern delta plains emphasized the importance of shelf-phase delta complexes, sea level control, delta switching, and the distributary chronology, deltaic stratigraphy, and the timing of the generation of the chenier plain in western Louisiana.

Eustacy and Subsidence

The balance between sediment supply and relative sea level change controls the development and stability of the coastline. Assuming relative sea level rise during the Holocene transgression was constant, this produces a rate of 0.7 cm/yr using 130 m as the lowstand withdrawal elevation. According to this scenario, highstand was achieved about 5000-7000 years ago at which time the Mississippi River began building its single modern delta plain. However, the existence of earlier Holocene delta plains seaward on the continental shelf terminated by large sand shoals indicates the rise of sea level during the Holocene transgression was not constant and that stillstands took place. The occurrence of these shoals indicates that a threshold value for eustacy exist, at which a particular

rate of rise produces either coastal retreat or progradation. Under current sea level rise conditions, compactional subsidence ranges from >0.62 cm/yr for young sediments to <0.18 cm/yr for older sediments based on data from the Terrebonne coastal region (Penland et al., 1988b). Under these conditions, the Mississippi River has built a delta plain of four smaller delta complexes over the last ±3000 years. The timing of these stillstands is based on previous work by Frazier (1974), who mapped a stillstand at 10,000-8,000 yBP and at ± 7000-4000 yBP. Coleman and Smith (1964), McFarlan (1961), and Gould and McFarlan (1959) all suggest the current stillstand started 3000 yBP (Figure 69). The recognition of regional ravinement surfaces separating the individual delta plains and the stratigraphic relationship between the overlying shoals and underlying delta plains indicate a hiatus in delta plain development took place during the Holocene transgression. New radiocarbon dates lying below the Late Holocene ravinement surface clearly indicate a stillstand in the period 7000-4000 yBP. The 3000 year timing for each delta plain is used because each is made of three complexes which typically require about 800-1200 years to build (Frazier, 1967).

Because three major stillstands took place between 10,000 and 3,000 yBP, less time was available for sea level to rise 20 m; therefore the rate of rise must be higher than the average rate indicated for the Holocene transgression. During the period 10,000-3000 yBP, a 20 m rise in sea level occurred incorporating two periods of rapid relative sea level rise. Assuming the Early (10,000-8,000 yBP) and Late (7000-4000 yBP) Holocene stillstands each lasted 3000 years, this allows only 2000 years available to accomplish a 20 m rise in sea level, at a rate of 1 cm/yr. If these transgressive events are only 500 years in duration, as some radiometric data suggest, the sea level rise rates would increase to 2 cm/yr (Appendix D). The relative sea level rise rates suggest that threshold value for regional coastal erosion, land loss, and submergence to occur in the Mississippi River delta plain is at rates greater than 2 cm/yr.

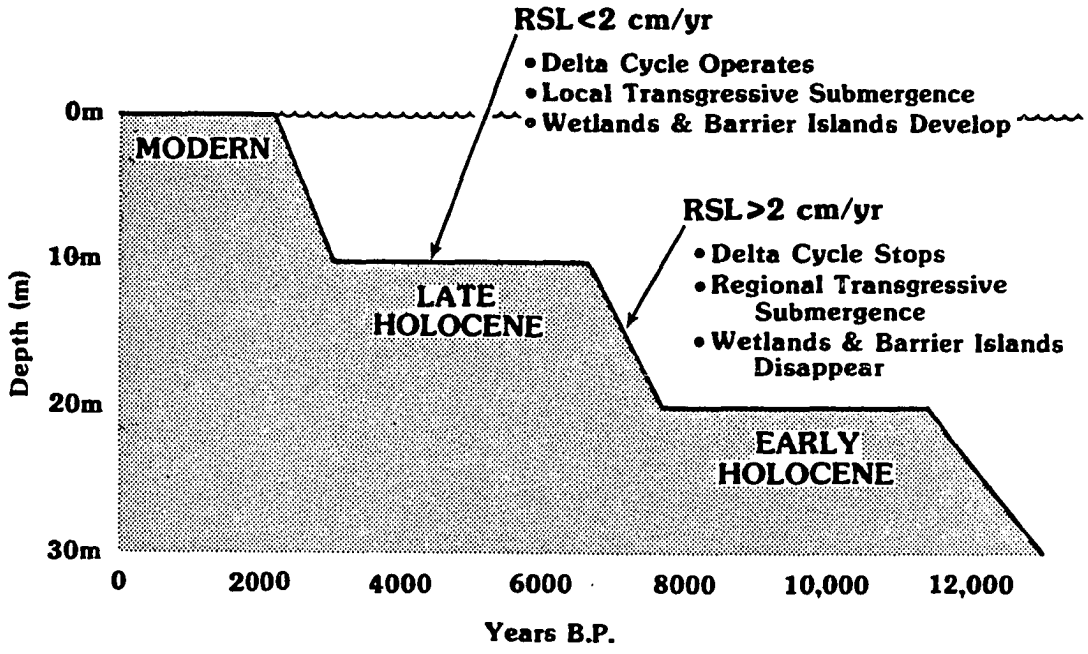

Figure 69. Diagram depicts the relationship between sea level history and coastal stability.

Chenier Plain Formation

Chronostratigraphy

The timing and the process of formation of the chenier plain was re-evaluated in the light of new chronostratigraphic findings in the Mississippi River delta plain (Figure 55). A regional transgression occurred between approximately 3000 BP and 4000 yBP, leading to the transgressive submergence of the Late Holocene delta plain, producing the regional Teche shoreline. The timing of the end of this transgression conforms to the age of the most landward ridge in the chenier plain, the Little Chenier-Little Pecan Island trend. This ridge trend was originally interpreted as representing the Teche delta complex switching event with the landward Holocene/Pleistocene contact representing the highstand shoreline. The implication of this new interpretation is that the Little Chenier-Little Pecan Island trend represents the maximum flooding shoreline, a continuation of the Teche shoreline separating the Late Holocene and Recent delta plains, and that the Holocene/Pleistocene contact represents the leading edge of the marshes transgressing onto the Prairie Terrace. Significant mudflat progradation seems to require a westerly position of the Mississippi River but the numerous different forms and ages of cheniers do not correspond well to the timing of major delta complex switching. Progradation of the chenier plain appears to be associated with building of the Recent delta plain and not the Teche complex of the Late Holocene delta plain. The occurrence of individual ridges appears to be primarily tied to delta lobe switching within the Lafourche complex and variations in sediment supply from local rivers. The recent development of the Atchafalaya delta complex to the west is the closest position of an active distributary to the chenier plain since sea level stabilization; a new episode of rapid mudflat progradation is thus taking place.

CONCLUSIONS

A new three-stage model illustrates the depositional history of abandoned Mississippi River deltas from stage 1, *erosional headland with flanking barriers*, to stage 2) *transgressive barrier island arcs*, followed by stage 3, an *inner shelf shoal*, through a process termed *transgressive submergence*. This three-stage model illustrates the formation of barrier islands through both spit breaching and mainland detachment processes. Each stage of the model has a distinctive morphostratigraphy. Transgressive submergence is a new mechanism for describing the evolution of barrier shoreline shelf sand bodies. In the Gulf of Mexico it results from high rates of relative sea level rise on low-gradient continental shelves with limited sand sources in storm-dominated environment. Sand bodies are submerged as they continue to undergo transgression and shoreface retreat. Transgressive depositional systems in river-dominated delta plains are vertically and spatially significant components of a shallow water deltaic depositional sequence. These shallow-water, shelf-phase delta complexes, which differ considerably from those included in the traditional deep water Mississippi delta model, are the primary depositional constituents of the Holocene Mississippi River delta plain. Recognition of the regional Teche shoreline and ravinement surface led to the identification of the Late Holocene and Modern delta plains instead of the single Holocene delta plain model described by Frazier (1967). The Early, Late Holocene, and Modern delta plains were built during conditions of relatively stable sea level, $\pm$11,000-8000 yBP, 7000-4000 yBP and 3000-0 yBP, respectively. During this period Mississippi River sedimentation was characterized by delta complex progradation onto the inner continental shelf. Sea level during the Teche transgression, 4000-3000 yBP, rose about 5-6 m from the position of the Late Holocene sea level to the Modern sea level at a rate of about 1-2 cm/yr. Mississippi River sedimentation during the Teche transgression was characterized by delta plain aggradation landward of a regionally retreating shoreline. Analysis of the regional seismic and vibracore database indicates the shelf-phase shallow water delta complex model as represented by the Lafourche delta complex is the most appropriate depositional model for the Late Holocene and Modern delta plains. The shallow water delta complex sequence emphasizes the regressive and transgressive components of the delta cycle and the thin character of these sequences, 10-15 m thick. The thick, artificially leveed deep water Modern delta complex is not an appropriate model to

describe shelf-phase Mississippi River delta complexes. The chronostratigraphy of the chenier plain is re-defined by the recognition of the Late Holocene and Modern delta plains of the Mississippi River delta. The Little Chenier-Little Pecan Island trend represents the highstand shoreline instead of the landward Pleistocene/Holocene contact and the individual mudflat/chenier systems are linked to delta lobe switching in the Lafourche delta complex instead of delta complex switching in the larger delta plain.

BIBLIOGRAPHY

Berryhill, H. L., Jr., 1986. Use of high-resolution reflection profiling techniques for identifying major Late Quaternary continental shelf/slope facies in H. L. Berryhill, Jr., ed., Late Quaternary Facies and Structure, Northern Gulf of Mexico: AAPG Studies in Geology 23, p. 1-11.

Berryhill, H. L., Jr., and Suter, J. R., 1986. Deltas. in H. L. Berryhill, Jr., ed., Late Quaternary Facies and Structure, Northern Gulf of Mexico: AAPG Studies in Geology 23, p. 131-190.

Bouma, A. H., Coleman, J. M., and Meyer, A. H., 1986. Introduction, objectives and principle results of Deep Sea Drilling project Leg 96. in A. H. Bouma, et al., eds., Deep Sea Drilling Project Leg 96 Initial Report, p. 533-540.

Boyd, R., Suter, J. R., and Penland, S., 1988. Implications of modern sedimentary environments for sequence stratigraphy. in D. P. James and D. A. Leckie, eds., Sequences, Stratigraphy, Sedimentology: Surface and Subsurface. Canadian Society of Petroleum Geologists Memoir 15, p. 33-36.

Byrne, J. V., Leroy, D. O., and Riley, C. M., 1959. The chenier plain and its stratigraphy, southwestern Louisiana. GCAGS Transactions, v. 9:1-23.

Coleman, J. M., 1966. Recent Peat Deposits of Vermilion, Iberia and St. Mary Parishes, Louisiana. Louisiana State University, Oh.D. Dissertation, 113 p.

Coleman, J. M., 1988. Dynamic changes and processes in the Mississippi River deltaic plain: America Bull., v. 100:999-1015.

Coleman, J. M. and Gagliano, S. M., 1964. Cyclic sedimentation in the Mississippi River deltaic plain: GCAGS Transactions, v. 14:67-82.

Coleman, J. M. and Prior, D. B., 1980. Deltaic sand bodies: AAPG Continuing Education Course Note Series No. 15, 171 p.

Coleman, J. M. and Prior, D. B., 1982. Deltaic environments. in P. A. Scholle and D. Spearing, eds., Sandstone Depositional Environments, AAPG Memoir 31, p. 139-178.

Coleman, J. M. and Roberts, H. H., 1988a. Sedimentary development of the Louisiana continental shell related to sea level cycles: part I - sedimentary sequences. Geo-Marine Letters, v. 8:63-108.

Coleman, J. M. and Roberts, H. H., 1988b. Sedimentary development of the Louisiana continental shell related to sea level cycles: part I - sedimentary sequences. Geo-Marine Letters, v. 8:109-119.

Coleman, J. M. and Smith, W. G., 1964. Late Recent rise of sea level. Geol. Soc. of America Bull., v. 75:833-840.

Coleman, J. M. and Wright, L. D., 1975. Modern river deltas: variability of processes and sand bodies. in M. L. Broussard, ed., Deltas - Models for Exploration. Houston Geological Society, p. 99-150.

Coleman, J. M., Gagliano, S. M., and Webb, J. R., 1964. Minor sedimentary structures in a prograding distributary. Mar. Geol. v. 1:240-258.

Coleman, J. M., Prior, D. B., and Lindsay, J. F., 1983. Deltaic influences on shelf edge instability processes. in D. J. Stanley and G. T. Moore, eds., The Shelf Break; Critical Influence on Continental Margin. SEPM Special Publications 33, p. 121-1337.

Coleman, J. M., Suhayda, J. N., Whelan, T., III, and Wright, L. D., 1974. Mass movements of Mississippi River delta sediments. GCAGS Transactions, v. 24:49-68.

Conaster, W. E., 1969. The Grand Isle barrier island complex. Tulane University, Ph.D. Dissertation, 138 p.

Cuomo, R. F. 1984. The geologic and morphologic evolution of Ship Soal, northern Gulf of Mexico. Louisiana State University, Master of Science Thesis, 249 p.

Field, M. E., and Duane, D. B., 1976. Post-Pleistocene history of the United States inner continental shelf: significance to the origin of barrier islands. Geol. Soc. America Bull., v. 87:691-702.

Fisher, A. G., 1961. Stratigraphic record of transgressing seas in light of sedimentation in the Atlantic coast of New Jersey. AAPG Bull., v. 45:1656-1666.

Fisk, H. N., 1944. Geologic Investigation of the Alluvial Valley of the Lower Mississippi, U.S. Army Corps of Engineers, 78 p.

Fisk, H. N., 1947. Fine-Grained Alluvial Deposits and Their Effects on Mississippi River Activity. U.S. Army Corps of Engineers, 82 p.

Fisk, H. N., 1948. Geology of Lower Mermentau River Basin and Control Structure Sites: Definite Project Report, Mermentau River, Louisiana. U.S. Army Corps of Engineers, 64 p.

Fisk, H. N., 1952. Geological Investigation of the Atchafalaya Basin and Problems of Mississippi River Diversion. U.S. Army Corps of engineers, 145 p.

Fisk, H. N., 1955. Sand facies of recent Mississippi delta deposits. Fourth World Petroleum Cong. Rome Proceedings, Sec. 1-C, p. 377-398.

Fisk, H. N., 1960. Recent Mississippi sedimentation and peat accumulation. in Cong. Av. Etudes de Stratigraphie et de Geologie due Carbonifere, 4th Heerlen, Compte rendu, Maastricht, Netherlands, p. 189-199.

Fisk, H. N., 1961. Bar-finger sands of the Mississippi delta. in Geometry of Sandstone Bodies. American Association of Petroleum Geologists, p. 29-52.

Fisk, H. N. and McClelland, B., 1959. Geology of continental shelf off Louisiana, its influence on offshore foundation design. Geol. Soc. of America Bull., v. 70:1369-1394.

Fisk, H. N., McFarlan, E., Jr., Kolb, C. R., and Wilbert, L. J., Jr., 1954. Sedimentary framework of the modern Mississippi delta. Jour. of Sed. Pet., v. 24(2):76-99.

Frazier, D. E., 1967. Recent deltaic deposits of the Mississippi River: their development and chronology. GCAGS Transactions, v. 27:287-315.

Frazier, D. E., 1974. Depositional Episodes: Their Relationship to the Quaternary Stratigraphic Framework in the Northwestern Portion of the Gulf basin. Texas Bureau of Economic Geology Geological Circular 74-1, 28 p.

Frazier, D. E., Osanik, A., and Elski, W. C., 1978. Environments of peat accumulation - coastal Louisiana. in W. R. Kaiser, ed., Proceedings of the Gulf Coast Lignite Conference: Geology, Utilization, and Environmental Aspects, p. 5-20.

Gerdes, R. G., 1982. Stratigraphy and History of Development of the Caminada-Moreau Beach Ridge Plain, Southeast Louisiana. Louisiana State University, Master of Science Thesis, 184 p.

Gerdes, R. G., 1985. The Caminada-Moreau beach ridge plain. in S. Penland and R. Boyd, eds., Transgressive depositional environments of the Mississippi delta plain. Louisiana Geological

Survey Guidebook Series, p. 127-140.

Gilbert, G. K., 1885. The topography features of lake shores. in U.S. Geological Survey 5th Annual Report, p. 87-88.

Gould, H. R. and McFarlan, E., 1959. Geological history of the chenier plain, southwestern Louisiana: GCAGS Transactions, v. 9:262-270.

Howe, H. V., Russell, R. J., McGuirt, J. H., Croft, B. C., and Stephenson, M. B., 1935. Reports on the Geology of Cameron and Vermilion Parishes. Louisiana Geological Survey, Geological Bulletin No. 6, 242 p.

Hoyt, H. H., 1967. Barrier island formation. Geol. Soc. of America Bull., v. 78:1125-1135.

Hoyt, H. H., 1970. Development and migration of barrier islands, northern Gulf of Mexico, discussion. Geol. Soc. of America Bull., v. 81:3779-3782.

Isacks, T. S., 1989. Geologic Evolution and Sedimentary Facies of the Timbalier Islands, Louisiana. Louisiana State University, Master of Science Thesis, 189 p.

Kahn, J. H., 1980. The role of hurricanes in the long-term degradation of the Chandeleur Islands, Louisiana. Louisiana State University, Master of Science Thesis, 99 p.

Kahn, J. H. and Roberts, H. H., 1982. Variations in storm surge response along a microtidal transgressive barrier island arc. Sedimentary Geology, v. 33:129-146.

Kaczarowski, R. T. and Gernant, R. E., 1980. Stratigraphy and coastal processes of the Louisiana chenier plain. GCAGS Field Guide, 72 p.

Kindinger, J. L., 1989. Upper Pleistocene to Recent shelf and upper slope deposits of offshore Mississippi-Alabama. in R. A. Morton and D. Nummedal, eds., Shelf Sedimentation, Shelf Sequences, and Related Hydrocarbon Accumulation. Gulf Coast Section-SEPM, Proceedings. 7th Annual Research Conference, p. 163-174.

Kolb, C. R. and Van Lopik, J. R., 1958. Geology of the Mississippi River Deltaic Plain, Southeast Louisiana. U.S. Army Corps of Engineers, Technical Report 3-483, 120 p.

Kolb, C. R. and Van Lopik, J. R., 1966. Depositional environments of the Mississippi River deltaic plain - southeastern Louisiana. in M. L. Shirley and J. A. Ragsdale, eds., Deltas in Their Geologic Framework. Houston Geological Society, p. 17-61.

Kosters, E. C., 1987. Parameters of peat formation in the Mississippi Delta. Louisiana State University, Ph.D. Dissertation, 255 p.

Kosters, E. C., 1989. Organic-clastic facies relationships and chronostratigraphy of the Barataria interlobe basin, Mississippi delta plain. Jour. of Sed. Pet., v. 59(1):98-113.

Krawiec, W., 1966. Recent sediments of the Louisiana inner continental shelf. Rice University, Ph.D. Dissertation, 50 p.

Kraft, J. C., 1971. Sedimentary facies patterns and geologic history of a Holocene marine transgression. Geol. Soc. of America Bull., v. 82:2131-2158.

Kwon, H. J., 1969. Barrier islands of the northern Gulf of Mexico coast, sediment source and development: Louisiana State University Press, Coastal Studies Series No. 25, 51 p.

LeBlanc, R. J., 1972. Geometry of sandstone reservoir bodies (with discussion) in underground waste management and environmental implications. AAPG Memoir No. 18, p. 133-190.

Levin, D., Nummedal, D., Penland, S., and Howard, P., 1983. Tidal inlet evolution on a transgressive deltaic coast. American Association of Petroleum Geologists, v. 67(3):113.

Matthews, R. K., 1984. Dynamic Stratigraphy: Englewood Cliffs, N. J., Prentice Hall, 489 p.

Mazzulo, J., 1986. Sources of sand for the Mississippi Fan. in A. H. Bouma, et al. Deep Sea Drilling Project Leg 96, Initial Report, p. 533-540.

McFarlan, F. Jr., 1961. Radiocarbon dating of Late Quaternary deposits, south Louisiana. Geol. Soc. of America Bull., v. 72:129-158.

McIntire, W. G., 1958. Prehistoric Indian settlements of the changing Mississippi River delta. Louisiana State University Press, Coastal Studies Series No. 1, 82 p.

Mitchum, R. M., Jr., 1977. Glossary of terms used in seismic stratigraphy. in C. E. Payton, ed., Seismic Stratigraphy-Applications to Hydrocarbon Exploration. AAPG Memoir 26, p. 205-212.

Morgan, J. P., Van Lopik, J. R., and Nichols, L. G., 1953. Occurrence and development of mud flats along the western Louisiana coast. Louisiana State University Press, Coastal Studies Series No. 2, 53 p.

Morgan, J. P. and Shaver, R. H., 1970. Deltaic Sedimentation: Modern and Ancient. SEPM, Special Publication No. 5, 312 p.

Neese, K. J., 1984. Stratigraphy and geologic evolution of Isles Dernieres, Terrebonne Parish, Louisiana. Louisiana State University, Master of Science Thesis, 127 p.

Nummedal, D. and Swift, D. J. P., 1987. Transgressive stratigraphy at sequence-bound unconformities: some principals derived from Holocene and Cretaceous examples. in D. Nummedal, Pilkey, Orrin H., Howard, J. D., eds., Sea level Fluctuation and Coastal Evolution. SEPM Special Publication No. 41, p. 241-260.

Penland, S. and Boyd, R., 1981. Shoreline changes on the Louisiana barrier coast. IEEE Oceans. 81:209-219.

Penland, S. and Suter, J. R., 1983. Transgressive coastal facies preserved in barrier island arc retreat paths in the Mississippi River delta plain: GCAGS Transactions, v. 33:367-382.

Penland, S. and Suter, J. R., 1989a. Geomorphology of the Mississippi River chenier plain. Mar. Geol., v. 90:231-258.

Penland, S. and Suter, J. R., 1989b. New chronostratigraphic model for Mississippi River chenier plain (abstract). AAPG, v. 73(3):398.

Penland, S., Kosters, E. C., and Suter, J. R., 1987c. A new depositional model for the Mississippi River delta plain. AAPG, v. 71:423.

Penland, S., Boyd, R., Nummedal, D., and Roberts, H. H., 1981. Deltaic barrier development on the Louisiana coast. GCAGS Transactions, v. 31:471-476.

Penland, S., Boyd, R., and Suter, J. R., 1988a. Transgressive depositional systems of the Mississippi delta plain: A model for barrier shoreline and shelf sand development. Jour. of Sed. Pet., v. 58(6):932-949.

Penland, S., Ritchie, W., Boyd, R., Gerdes, R. G., and Suter, J. R., 1986a. The Bayou Lafourche delta, Mississippi River delta plain, Louisiana. Geol. Soc. America Centennial Field Guide - Southeastern Section, p. 447-452.

Penland, S. Suter, J. R., and Boyd, R., 1985a. Barrier island arcs along abandoned Mississippi River deltas. Mar. Geol., v. 63:197-233.

Penland, S., Suter, J. R., and Boyd, R., 1986a. Inner shelf shoal formation through transgressive barrier submergence. AAPG, v. 70:361.

Penland, S., Suter, J. R., and Kosters, E. C., 1987d. A new chronostratigraphic model for the Mississippi River delta plain. SEPM Annual Mid-year Meeting, Abstracts, v. 4:64.

Penland, S., Suter, J. R., and McBride, R. A., 1987b. Delta plain development and sea level history in the Terrebonne coastal region, Louisiana. Coastal Sediments '87, American Society of Civil Engineers, p. 1689-1705.

Penland, S., Suter, J. R., and McBride, R. A., 1988b. Reconnaissance investigation of shoreface and inner shelf sand resources in Terrebonne Parish: Point Au Fer to Timbalier Island. Louisiana Geological Survey Open-File Report 88-06, 62 p.

Penland, S. and Suter, J. R., 1988. A new depositional model for the Mississippi River delta plain. Sequences, stratigraphy, sedimentology: surface and subsurface. Canadian Society of Petroleum Geologists, Memoir 15, p. 581.

Penland, S., Suter, J. R., and McBride, R. A., Williams, S. Jeffress, Kindinger, J. L., and Boyd, R., 1989. Holocene sand shoals offshore of the Mississippi River delta plain. GCAGS Transactions, v. 39, p. 471-480.

Penland, S., Suter, J. R., and Moslow, T. F., 1986b. Inner shelf shoal sedimentary facies and sequences: Ship Shoal, northern Gulf of Mexico. in Moslow, T. F. and Rhodes, E. G., eds., Modern and Ancient Shelf Clastics: A Core Workshop. SEPM Core Workshop No. 9, p. 73-123.

Rampino, M. R. and Sanders, J. E., 1980. Holocene transgression in southcentral Long Island, New York: Jour. of Sed. Pet., v. 50:1063-1080.

Ritchie, W. and Penland, S., 1985. Overwash process-response characteristics of landforms along the Caminada-Moreau coast, Louisiana. in Penland, S. and Boyd, R., eds., transgressive Depositional Environments of the Mississippi River Delta Plain. Louisiana Geological Survey, Guidebook Series, 262 p.

Ritchie, W. and Penland, S., 1988. Rapid dune changes associated with overwash processes on the deltaic coast of south Louisiana. Mar. Geol., v. 81:97-122.

Roberts, H. H., and Whelan III, T., 1975. Methane-derived carbonate cements in barrier and beach sands of a subtropical delta complex. Geochimica et Cosmochimica Acta, v. 39:1085-1089.

Russell, R. J., 1936. Physiography of the Lower Mississippi River Delta. Louisiana Geological Survey, Geological Bulletin No. 8, 484 p.

Russell, R. J. and Howe, H. V., 1935. Cheniers of southwestern Louisiana. Geog. Rev., 25(3):449-461.

Russell, R. J. and Russell, R. D., 1939. Mississippi River delta sedimentation. in P. D. Trask, ed., Recent Marine Sediments. AAPG, p. 153-177.

Sanders, J. E. and Kumar, N., 1975. Evidence of shoreface retreat and in-place "drowning" during Holocene submergence of barriers, shelf off of Fire Island, New York. Geol. Soc. of America Bull., v. 86:65-76.

Scruton, F. P., 1960. Delta building and the deltaic sequence. in Shepard, F. P., Phleger, F. B., and van Andel, T. H., eds., Recent Sediments, Northwest Gulf of Mexico. AAPG Symposium Volume, p. 82-102.

Shamban, A. J., 1985. Historical evolution and coastal morphology of Barataria Pass, Louisiana. Louisiana State University, Master of Science Thesis, 156 p.

Suter, J. R., Berryhill, H. L., Jr., and Penland S., 1985. Environments of Sand Deposition, southwest Louisiana continental shelf. GCAGS Transactions, v. 35:495-504.

Suter, J. R. and Penland, S., 1987. A preliminary assessment of sand and aggregate resources in three areas of the Louisiana inner shelf: Timbalier Island, Chandeleur Islands, and Trinity Shoal. Louisiana Geological Survey, Open-File Report 87-04, 58 p.

Swift, D. J. P., 1975. Barrier island genesis: evidence from the central Atlantic shelf, eastern U.S.A. Sed. Geol., 14(1):1-44.

Tillman, R. W. and Martinson, R. S., 1984. The Shannon shelf ridge sandstone complex, Salt Creek anticline area, Powder River basin, Wyoming. in Tillman, R. W. and Siemers, C. T., eds., Siliciclastic Shelf Sediments. SEPM Special Publication No. 34, p. 85-142.

Trowbridge, A. C., 1930. Building of the Mississippi delta. AAPG Bulletin, v. 14:867-901.

U.S. Army Corps of Engineers, 1962. Belle Pass to Raccoon Point, Louisiana: Beach erosion control study. New Orleans District, U.S. Army Corps of Engineers, 64 p.

U.S. Army Corps of Engineers, 1962a. Bayou Lafourche and Lafourche-Jump Waterway, Louisiana: Design Memorandum No. 1 - General Design. New Orleans District, 29 p.

U.S. Army Corps of Engineers, 1962b. Bayou Lafourche and Lafourche-Jump Waterway, Louisiana: Design Memorandum Supplement No. 1 - General Design. New Orleans District, 20 p.

U.S. Army Corps of Engineers, 1962b. Bayou Lafourche and Lafourche-Jump Waterway, Louisiana: Design Memorandum Supplement No. 1 - General Design. New Orleans District, 20 p.

U.S. Army Corps of Engineers, 1967. Bayou Lafourche and Lafourche-Jump Waterway, Louisiana: Design Memorandum No. 2 - General Design. New Orleans District, 31 p.

U.S. Army Corps of Engineers (USACE), 1972. Grand Isle and Vicinity Louisiana Review Report: Beach Erosion and Hurricane Protection. New Orleans District, 62 p.

U.S. Army Corps of Engineers (USACE), 1975. Louisiana Coastal Area Study - Barrier Islands from Raccoon Point to Belle Pass. Abridged Report on Beach Erosion Control Study: New Orleans District, 44 p.

U.S. Army Corps of Engineers, 1980. Grand Isle and Vicinity Louisiana Phase II: General Design Memorandum-Beach Erosion Control and Hurricane Protection. New Orleans District, 32 p.

Van Heerden, I. Ll. Penland, S., and Boyd, R. 1985. A transgressive stratigraphic sequence from the central Chandeleur Islands, Louisiana. in Penland, S. and Boyd, R., eds., Transgressive Depositional Environments of the Mississippi River Delta Plain. Louisiana Geological Survey, Guidebook Series, p. 189-201.

Van Heerden, I. Ll. and Roberts, H. H., 1980. The Atchafalaya delta - Louisiana's new prograding coast. GCAGS Transactions, v. 30:497-506.

Van Heerden, I. Ll. and Roberts, H. H., 1988. Facies development of Atchafalaya delta, Louisiana: a Modern Bayhead delta. AAPG Bulletin, v. 72:439-453.

Van Wagoner, J. C., Posamentier, H. W., Mitchum, R. M., Jr., Vail, P. R. Sarag, J. F., Lovtit, T. S., and Hardenbal, J., 1988. An overview of the fundamentals of sequence stratigraphy and key

definitions. in C. K. Wilgus, B. S. Hastings, H. Posamentier, J. C., Wagoner, C. A., Ross, and C. G. Kendall, eds., Sea Level Changes: An Integrated Approach. SEPM Special Publication No. 42, p. 39-42.

Weinstein, R. A. and Gagliano, 1982. The shifting deltaic coast of the Lafourche country and its prehistoric settlement. in Uzee, P. D., ed., Lafourche Country: The People and the Land, University of Southwestern, p. 122-148.

Wells, J. T. and Kemp, G. P., 1981. Atchafalaya mud stream and recent mudflats progradation, Louisiana chenier plain. GCAGS Transactions, v. 31:409-416.

Wells, J. T. and Roberts, H. H., 1981. Fluid mud dynamics and shoreline stabilization, Louisiana chenier plain. in Proceedings of the 17th International Coastal Engineering Conference, p. 1382-1401.

Yi, Hi Il, 1987. The evolution and sedimentary sequences of the St. Bernard delta complex, Louisiana. Louisiana State University, Master of Science Thesis, 192 p.

APPENDIX A

Permission Letters

19 April 1990

Mrs. Triche Auberle
SEPM (Society for Sedimentary Geology)
P.O. Box 4756
Tulsa, Oklahoma 74159-0756
FAX 918-703-2457

Dear Ms Auberle:

This letter is a request for permission to use an article I published in the 1988 volume of the Journal of Sedimentary Geology for my Ph.D. dissertation at Louisiana State University. The article is cited as, "Penland, S. et al. 1988. Transgressive Depositional Systems of the Mississippi Delta Plain: A Model for Barrier Shoreline and Shelf Sand Development. Journal of Sedimentary Petrology, vol. 58, November, 1988, p. 932-949." I also plan to use," Penland, s. et al. 1986. Inner-shelf shoal sedimentary facies and sequences. Ship Shoal, northern Gulf of Mexico. In: Moslow and Rhodes, editors. Modern and Ancient Shelf Clastics: A Core Workshop Number 9: 73-123. I plan to use the text and figures giving full credit. Thank you for your consideration. If you have any questions, please advise. Please send your response by FAX (504-388-5328), as it will be greatly appreciated (deadline 2 May 1990).

Sincerely,

Shea Penland

Permission is hereby granted for use of the above-cited material provided proper acknowledgment of the source is given.
Date: 5/31/90
Robin J. Dixon, Executive Director
SEPM

Figure A-1. SEPM letter of permission.

Louisiana Geological Survey
P.O. Box G, University Station
LOUISIANA STATE UNIVERSITY AND AGRICULTURAL AND MECHANICAL COLLEGE
BATON ROUGE · LOUISIANA · 70893-4107
504/388-5320

19 April 1990

Mrs. Verhear
Science and Technology Divisionn
Elesiever Science Publications
P.O. Box 330
100 AH Amstgerdam
Netherlands
FAX 0111-31-205803769

Dear Mrs. Verhear:

This letter is a request for permission to use an article I published in Marine Geology in 1989 as a chapter in my dissertation at Louisiana State University. The article is cited as, "Penland, S. and Suter, S.R. 1989. Geomorphology of athe Mississippi River Chenier Plain. Marine Geology, 90(1989): 231-258". I plan to use the text and diagrmas giving full credit and acknowledgement tc Maring Geology and Elesiver Science Publishers. Please advise if you have any questions. Thank you for your consideration. Please send your response by FAX (504-388-5328), as it will be greatly appreciated (deadline 2 May 1990).

Sincerely,

Shea Penland

Permission granted subject to
permission from the author(s)
and to full acknowledgement of
the source.
Elsevier Science Publishers
Physical Sciences & Engineering Div.
24/4 1990

Figure A-2. Elsevier Science Publishers letter of permission.

Louisiana Geological Survey
P.O. Box G, University Station
LOUISIANA STATE UNIVERSITY AND AGRICULTURAL AND MECHANICAL COLLEGE
BATON ROUGE · LOUISIANA · 70893-4107
504/388-5320

19 April 1990

Ellie
Ms. ~~Ells~~ Marabello
American Society of civil Engineers
New York, New York
Phone: 212-705-7258
212-705-7712

Dear Ms. Marabello:

This letter is a request for permission to use an article I published in the ASCE Coastal Sediments '87 volume as a chapter in my Ph.D. dissertation at Louisiana State University. The article is cited as, "Penland, S. et al. 1987. Delta plain development and sea level history in the Terrebonne coastal region, Louisiana. Coastal Sediments '87, American Society of Civil Engineers, p. 1689-1755." I plan to use the text and figures giving full credit to the American Society of Civil Engineers. Thank you for your consideration. Please send your response by FAX (504-388-5328), as it will be greatly appreciated (deadline 2 May 1990).

Sincerely,

Shea Penland

Shea Penland

4/20/90

Permission granted.
Please give full credit to ASCE.
Ellie Marabello

AMERICAN SOCIETY OF CIVIL ENGINEERS
345 E 47th STREET
NEW YORK, N.Y. 10017

Figure A-3. American Society of Civil Engineers.

The Gulf Coast Association of Geological Societies

GCAGS Convention 1990
Post Office Box 52611
Lafayette, LA 70505

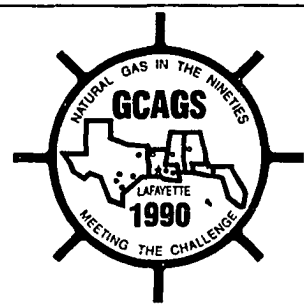

40th Annual Convention
October 17-19, 1990
Sponsored by Lafayette
Geological Society

April 25, 1990

Mr. Shea Penland
Louisiana Geological Survey
P. O. Box G
University Station
Baton Rouge, Louisiana 70893-4107

Dear Mr. Penland:

The GCAGS grants permission for you to reproduce the following material from the GCAGS Transactions:

(1) Frazier, David E. 1967, Recent Deltaic Deposits of the Mississippi River: GCAGS Transactions, Vol. 17, Figure 1, p. 289.

(2) Penland, S., et al 1989, Holocene Sand Shoals Offshore of the Mississippi River Delta Plain: GCAGS Transaction, Vol. 39, pp 471-480.

Sincerely,

Peter G. Gray
President

PGG:jdr

Figure A-4. Gulf Coast Association of Geological Societies.

APPENDIX B

Seismic Data

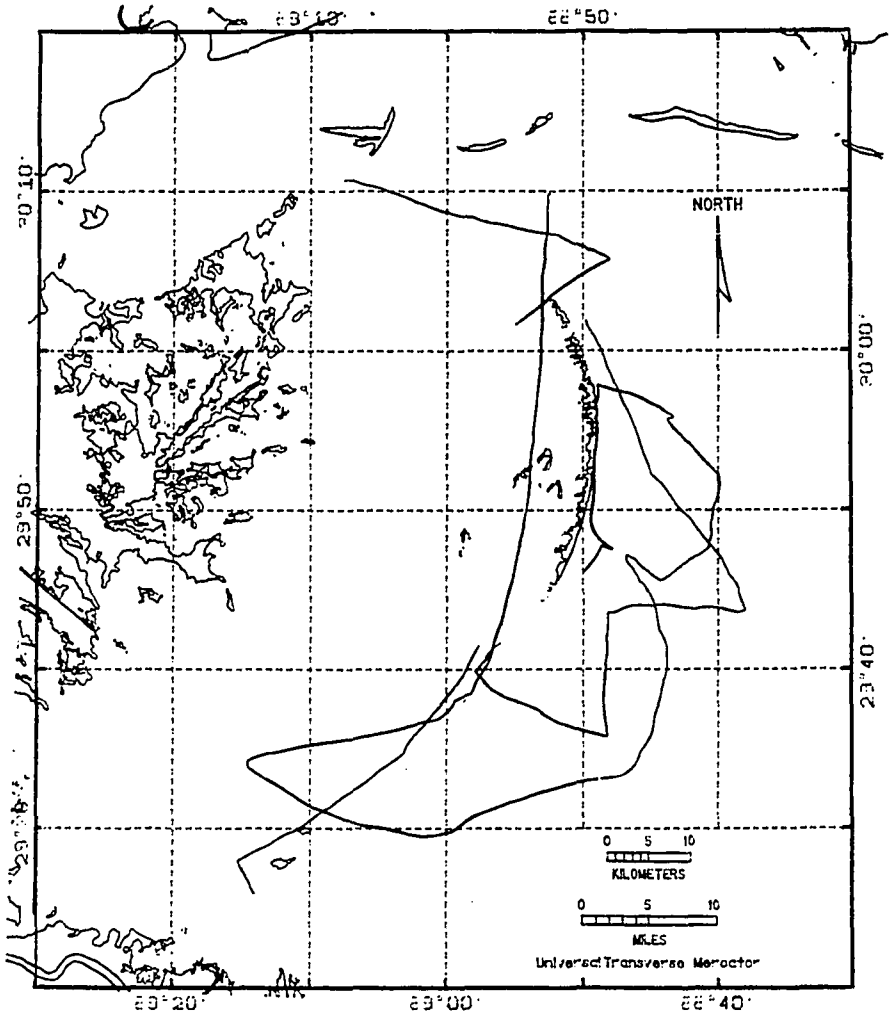

Figure B-1. The 1981 Proto-Lacoss survey in the Chandeleur Island region.

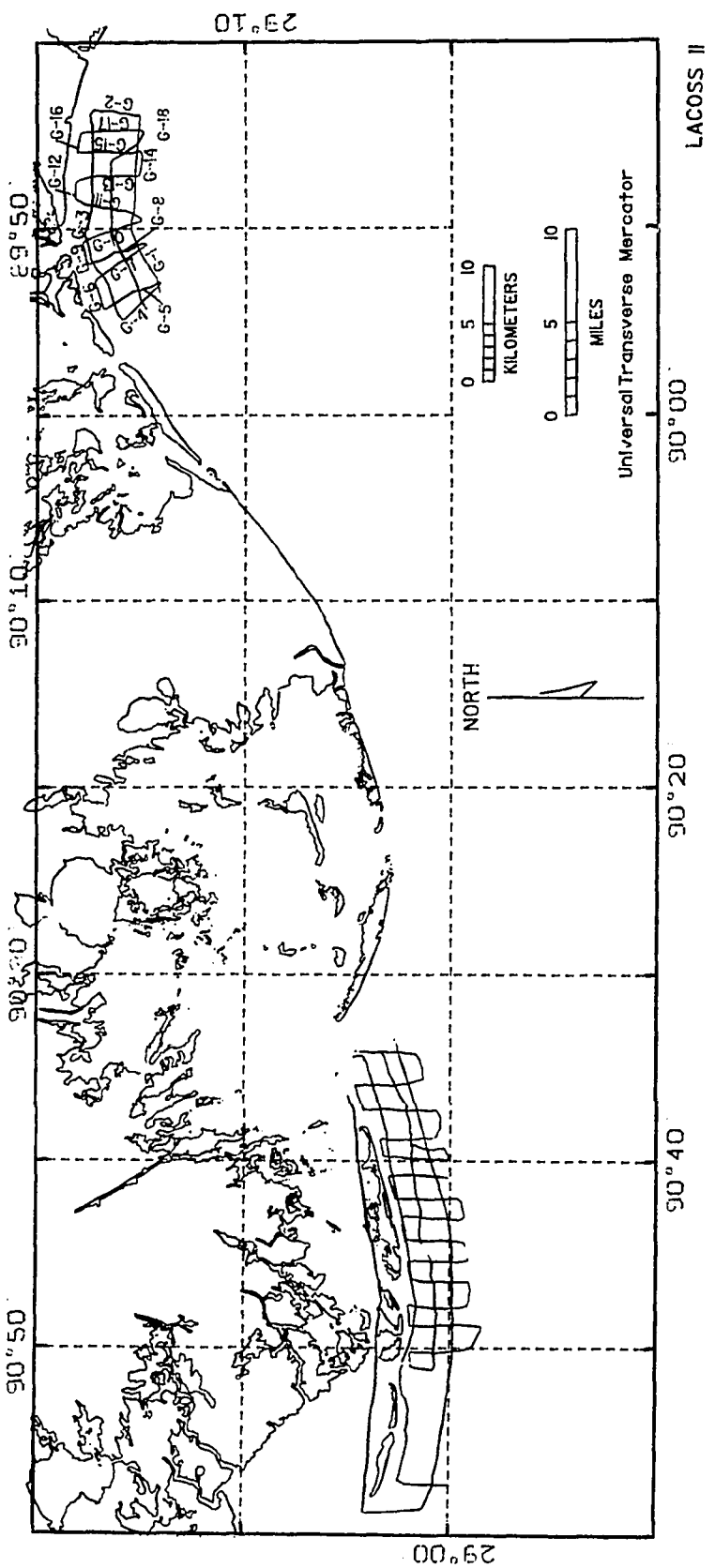

Figure B-2. The 1982 Lacoss II survey in the Cheniere Ronquille and Isles Dernieres region.

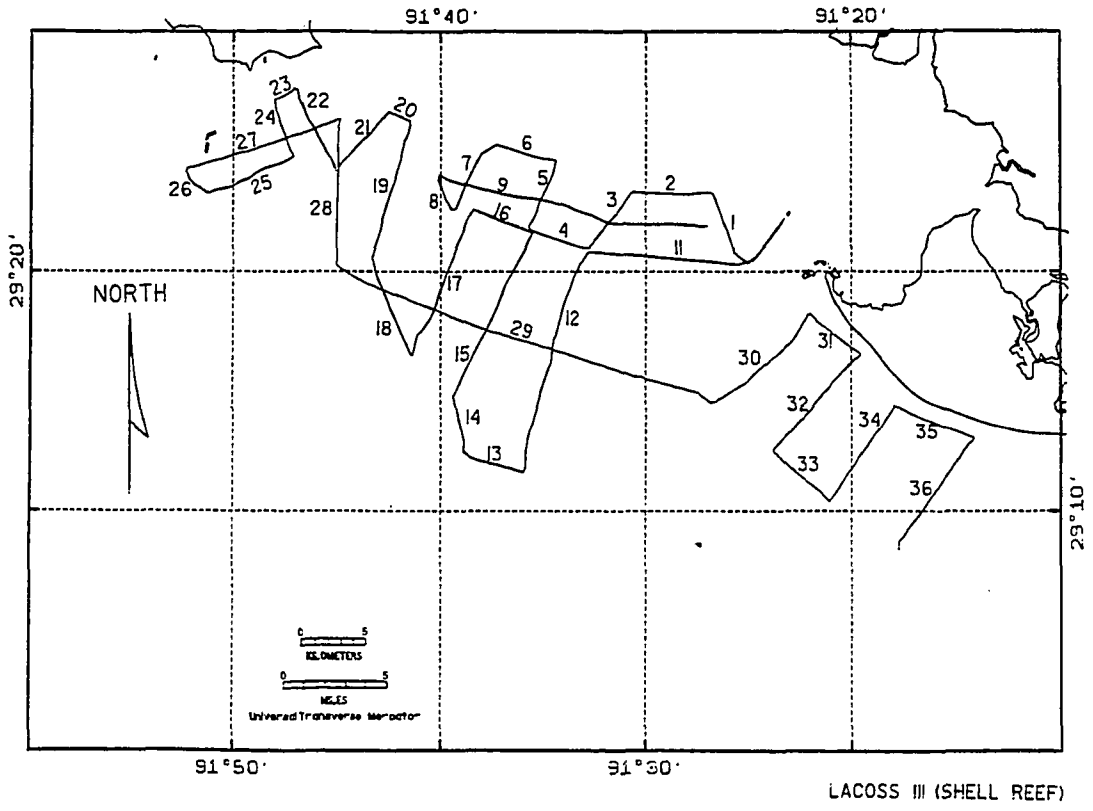

Figure B-3. The 1983 Lacoss III survey in the shell reef region.

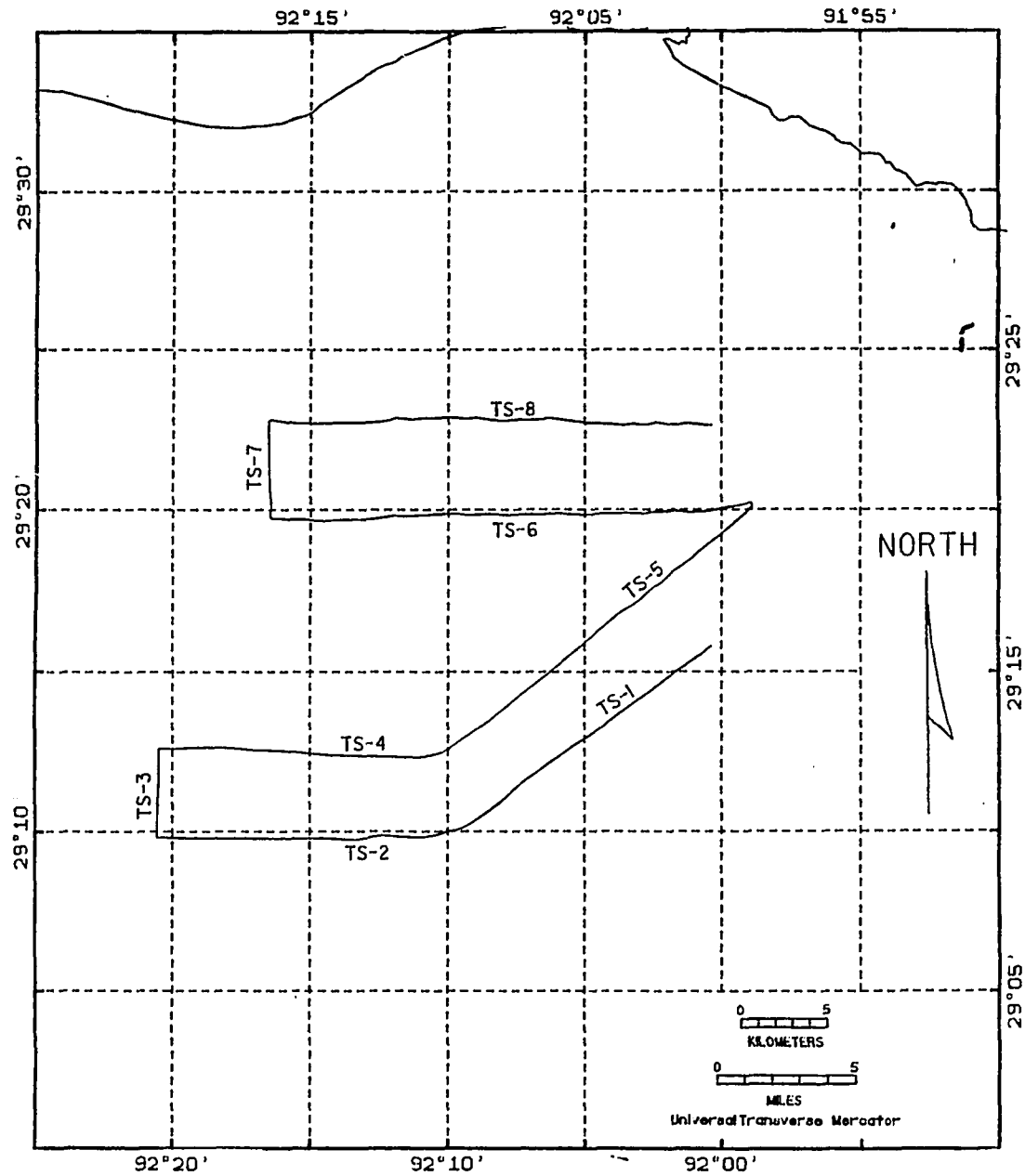

Figure B-4. The 1983 Lacoss III survey in the Trinity Shoal region.

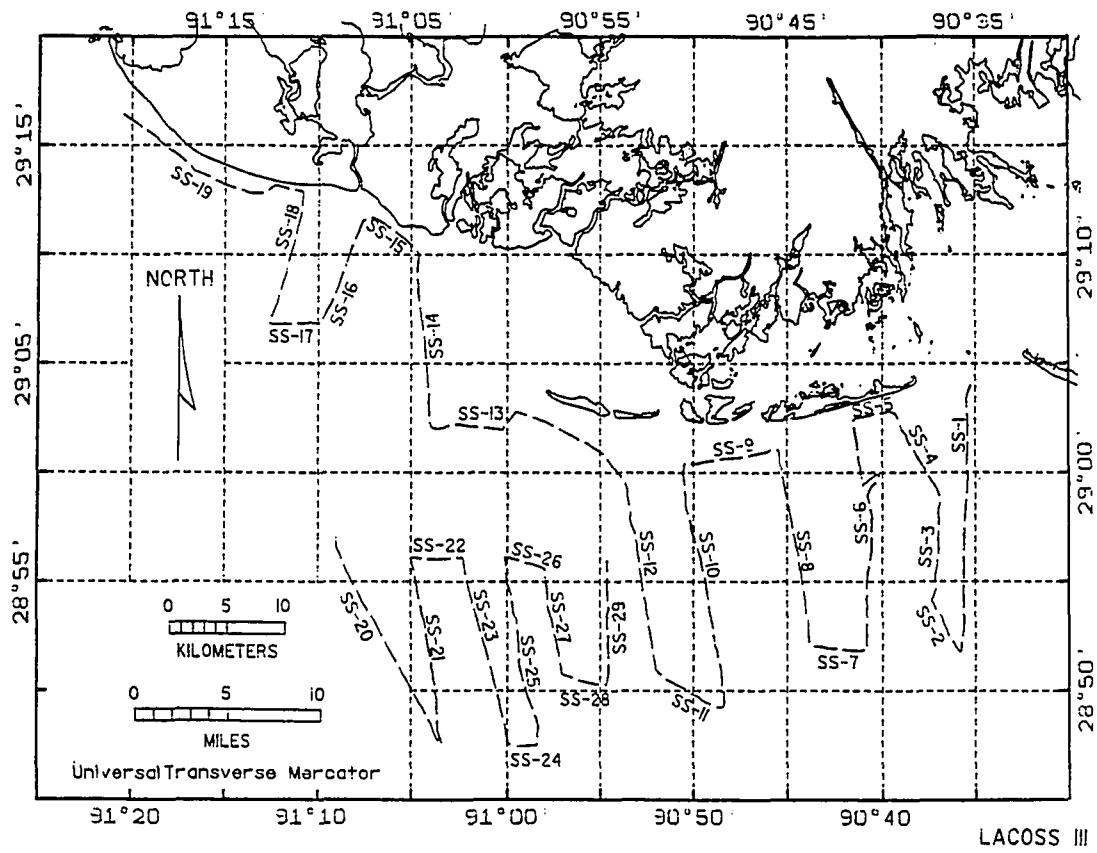

Figure B-5. The 1983 Lacoss III survey in the Ship Shoal region.

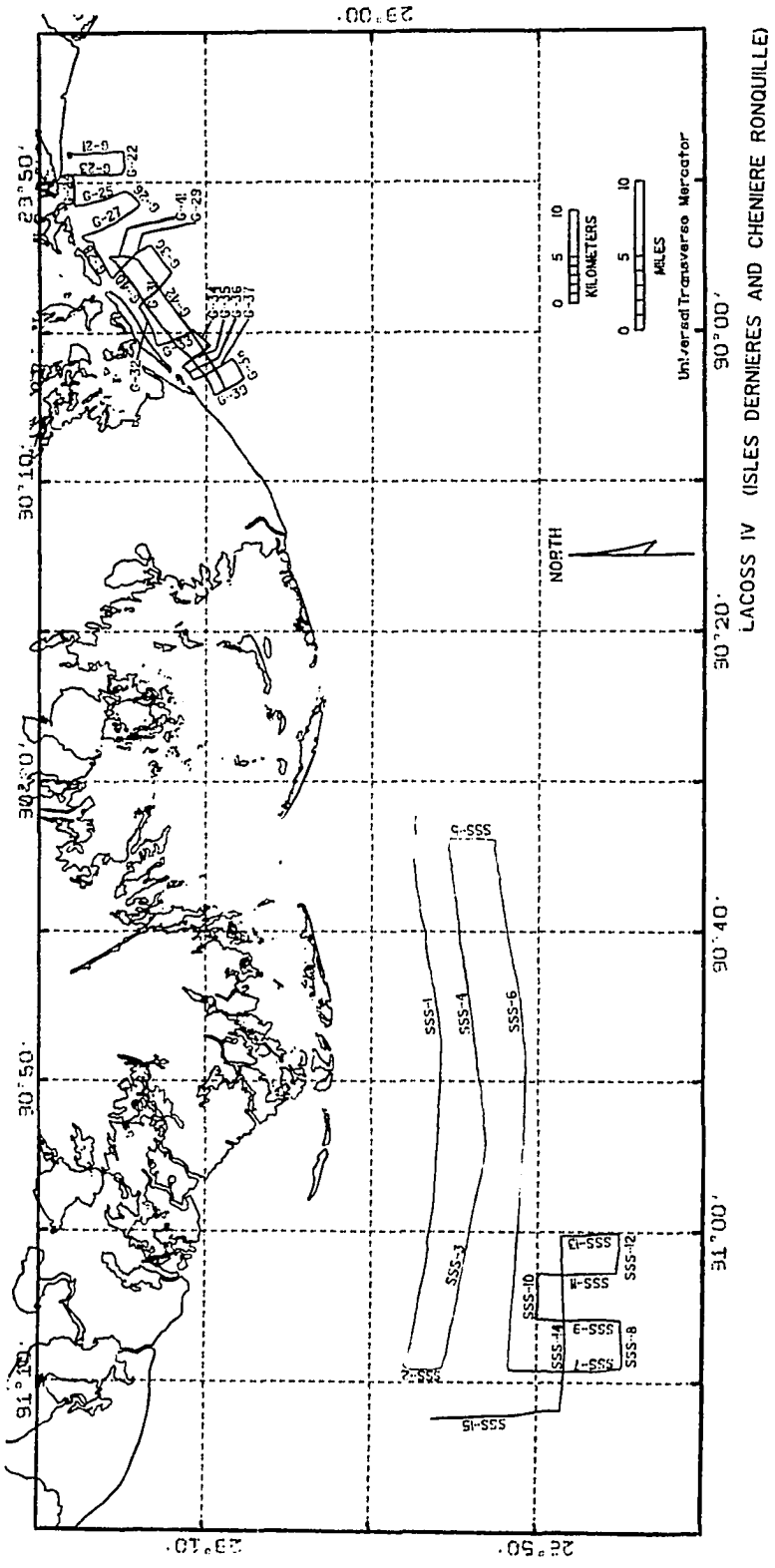

Figure B-6. The 1983 Lacoss IV survey in the Ship Shoal and Grand Isle region.

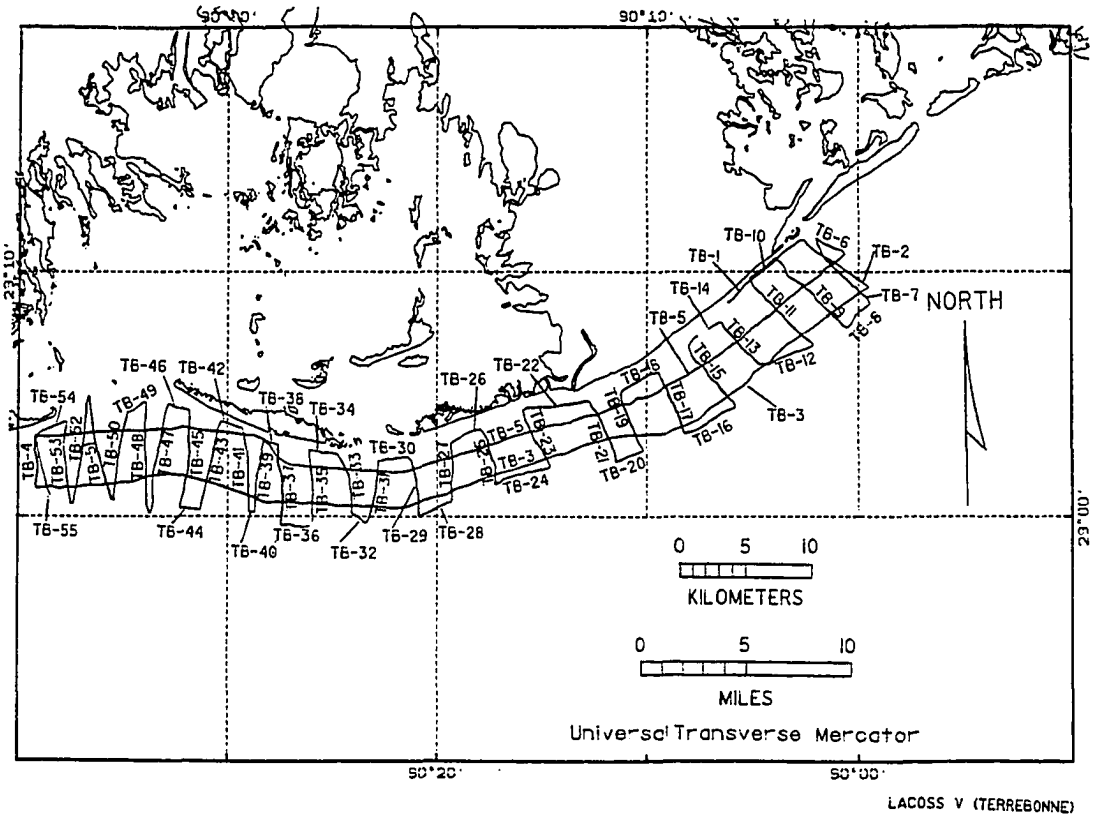

Figure B-7. The 1984 Lacoss V survey between Grand Isle and the Isles Dernieres.

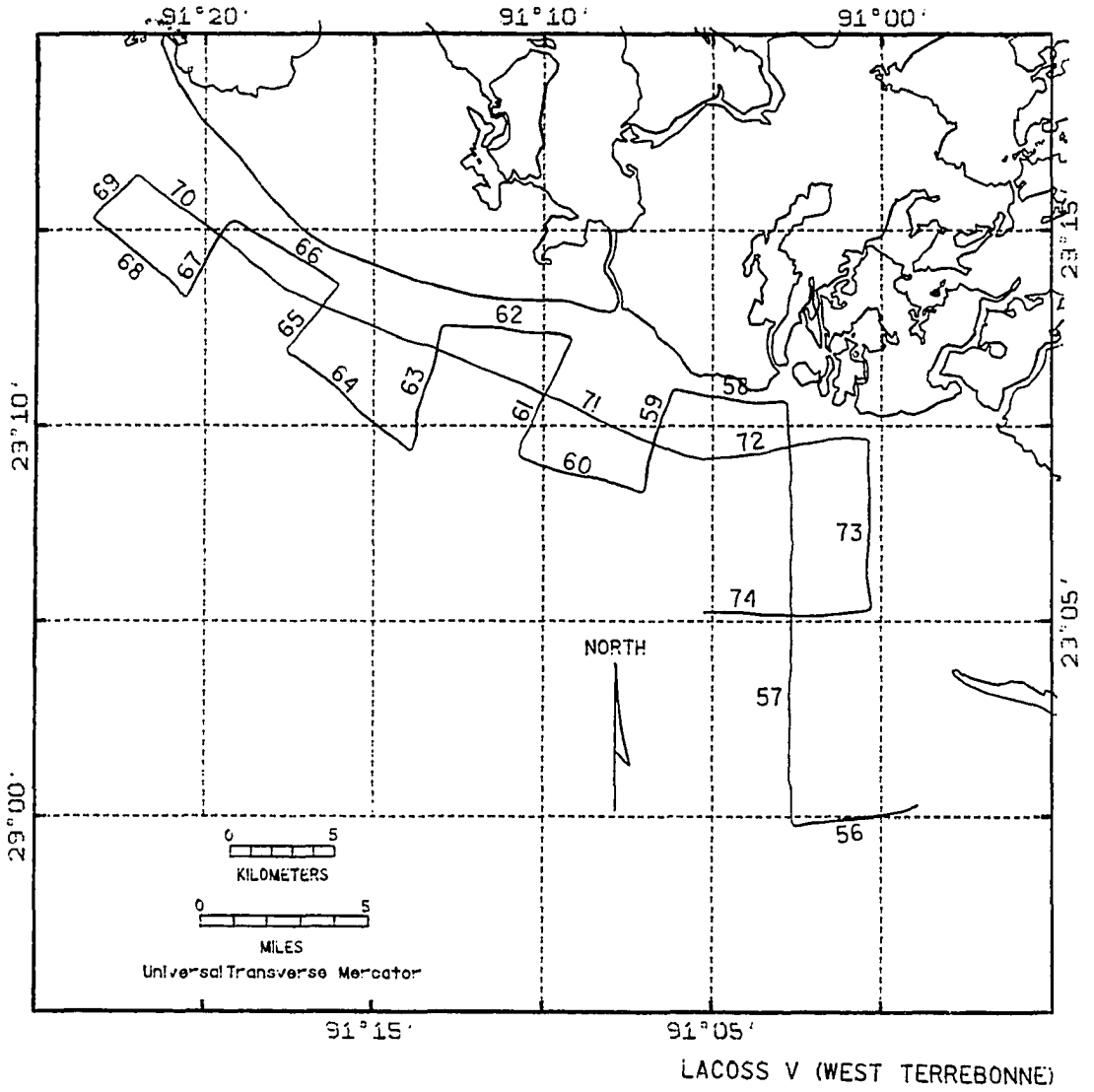

Figure B-8. The 1984 Lacoss V survey in the Point Au Fer region.

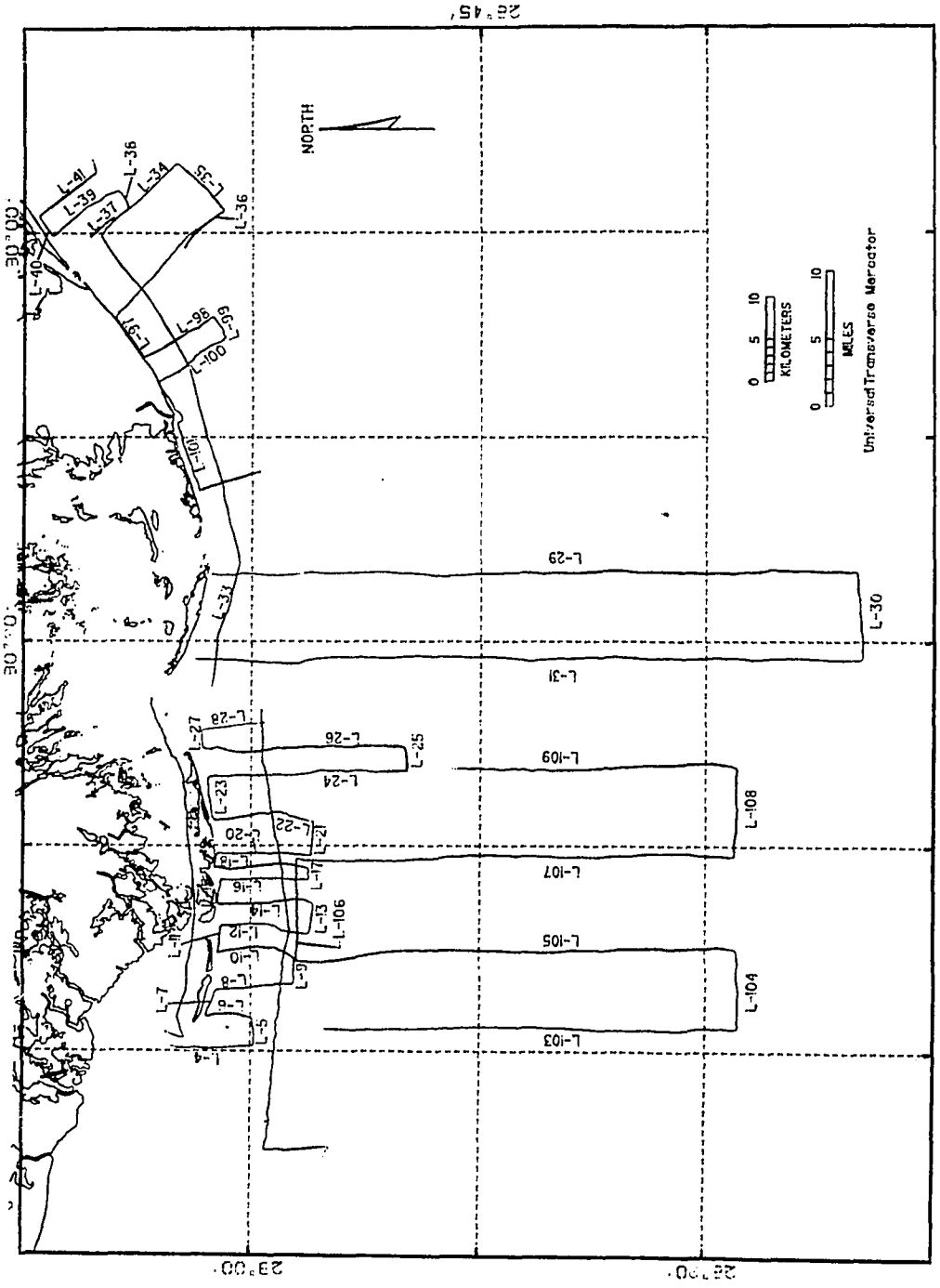

Figure B-9. The 1985 Laser survey in the Terrebonne, Ship Shoal, and Outer Shoal region.

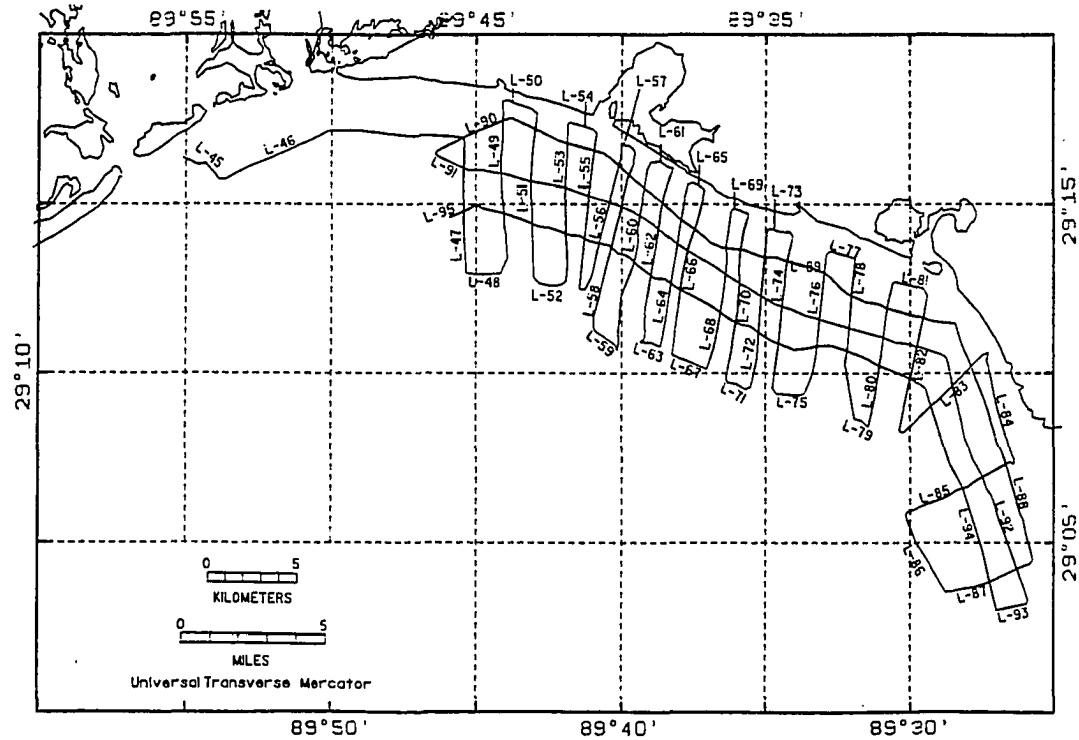

Figure B-10. The 1985 Laser survey in the Plaquemines shoreline region.

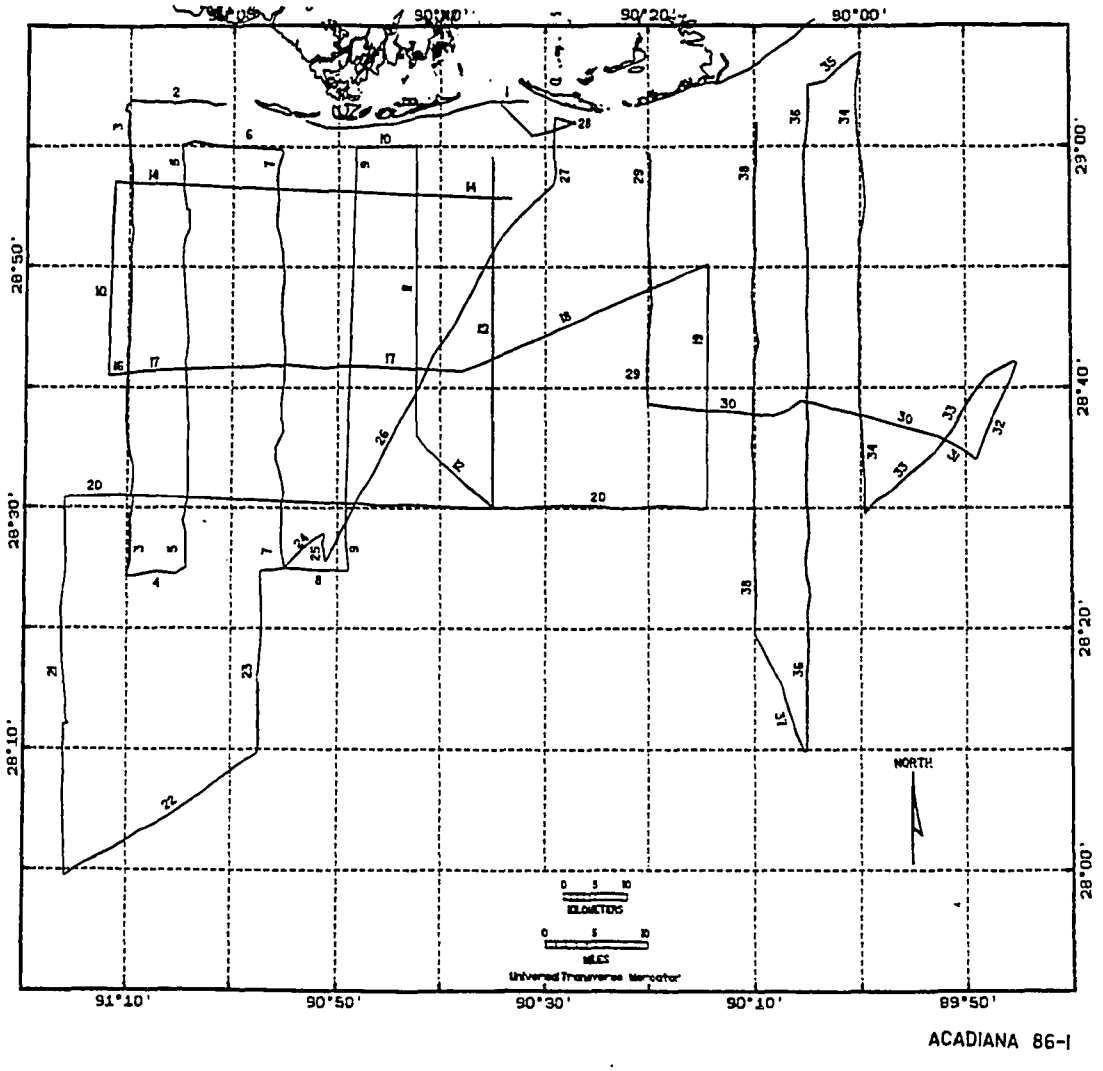

Figure B-11. The 1986-1 Acadiana survey in the Ship Shoal and Mississippi Canyon region.

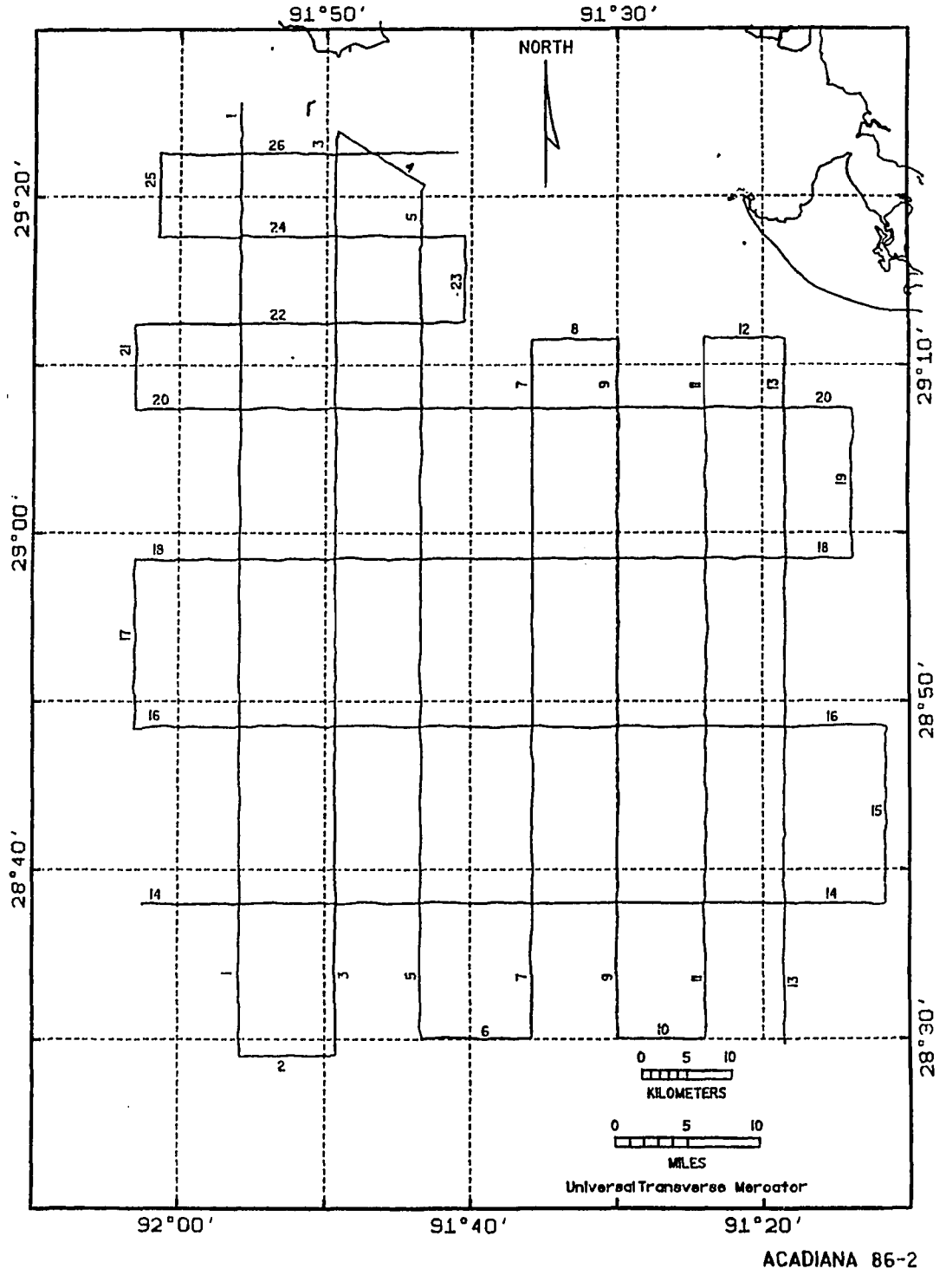

Figure B-12. The 1986-2 Acadiana survey in the shell reef area offshore of Marsh Island.

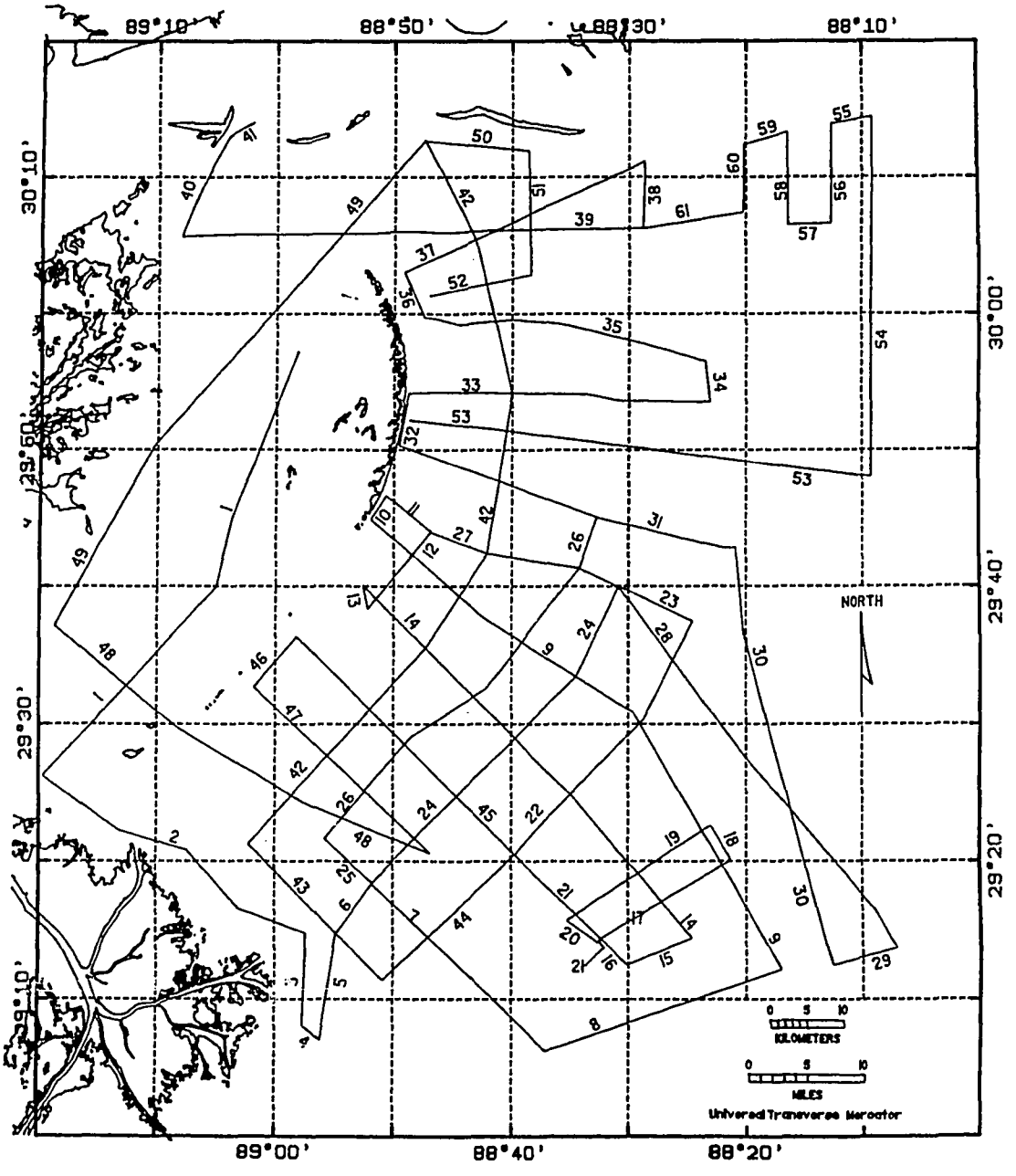

Figure B-13. The 1987 Acadiana survey in the Chandeleur Island region.

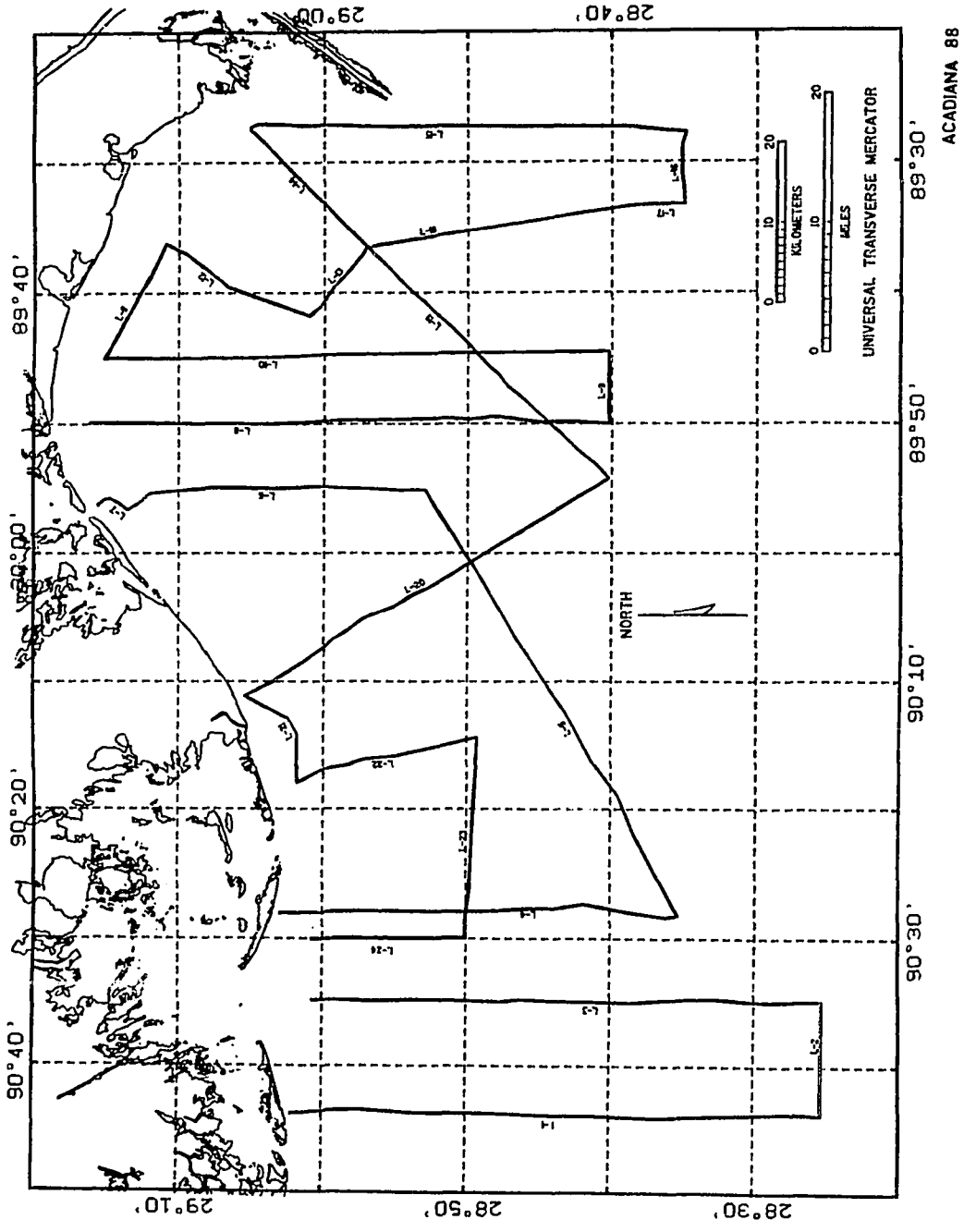

Figure B-14. The 1988 Acadiana survey in the Barataria Bight.

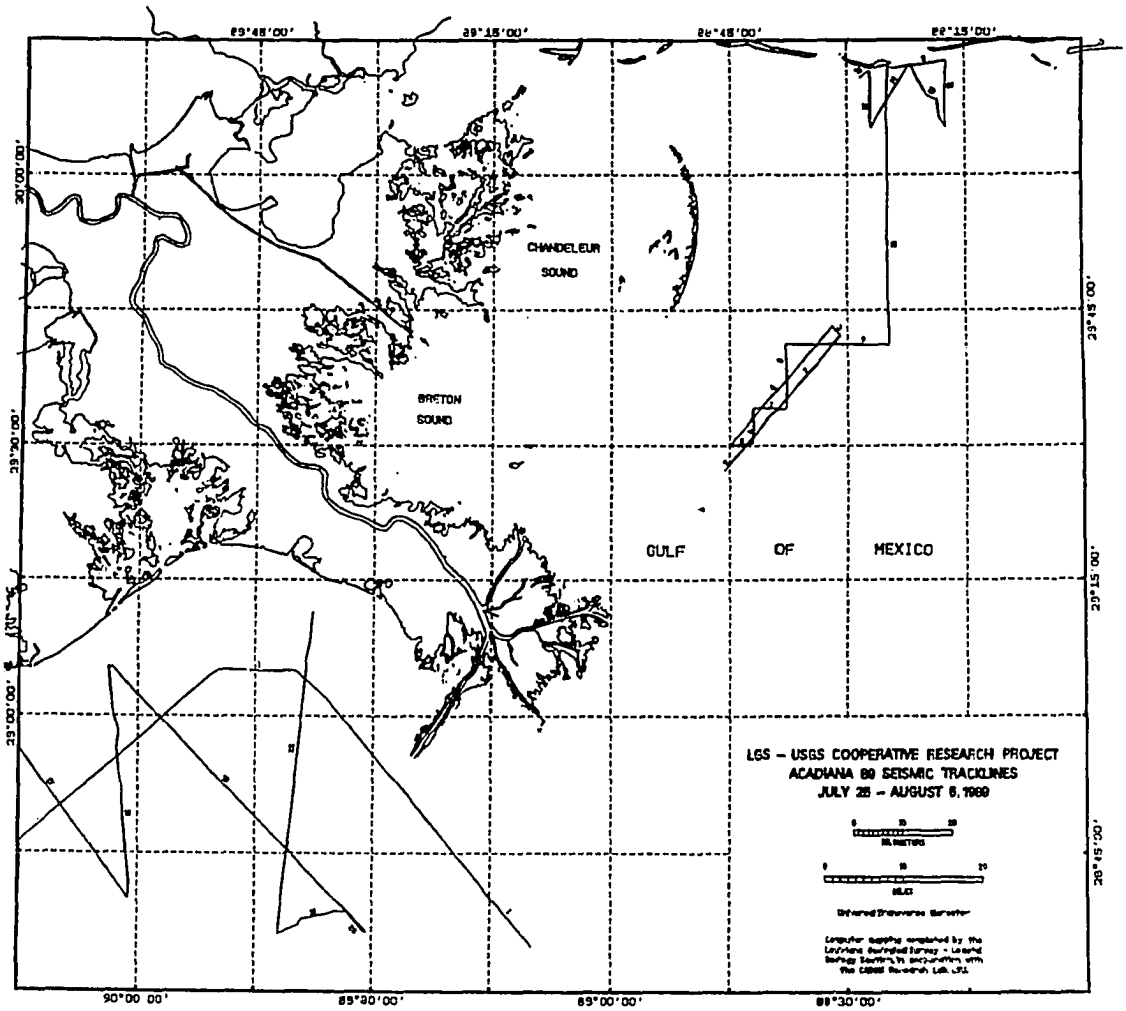

Figure B-15. The 1989 Acadiana survey in the Barataria Bight and Chandeleur Island region.

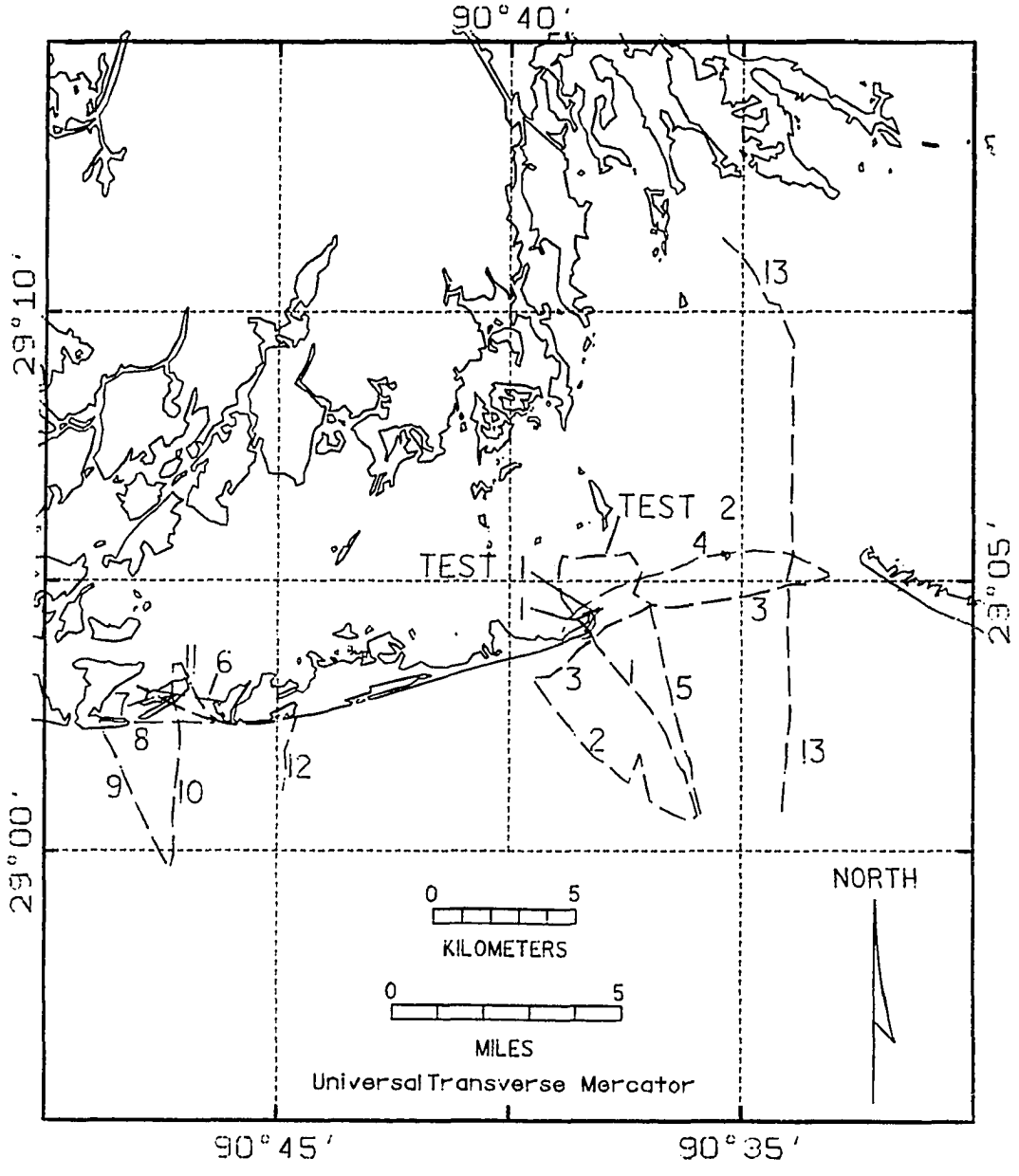

Figure B-16. The 1989 Coli survey in the Cat Island Pass region.

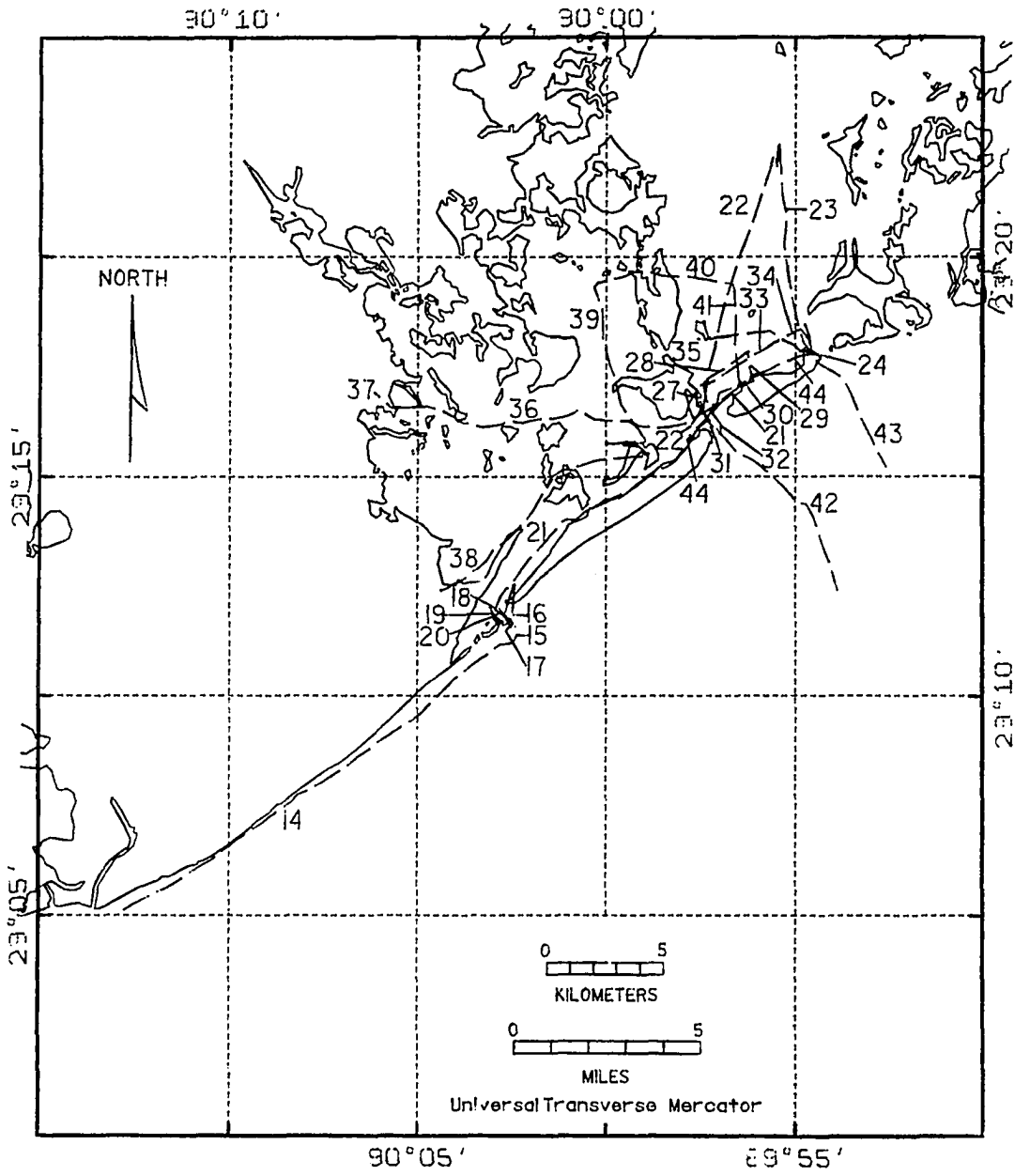

Figure B-17. The 1989 Coli survey in the Barataria Bight region.

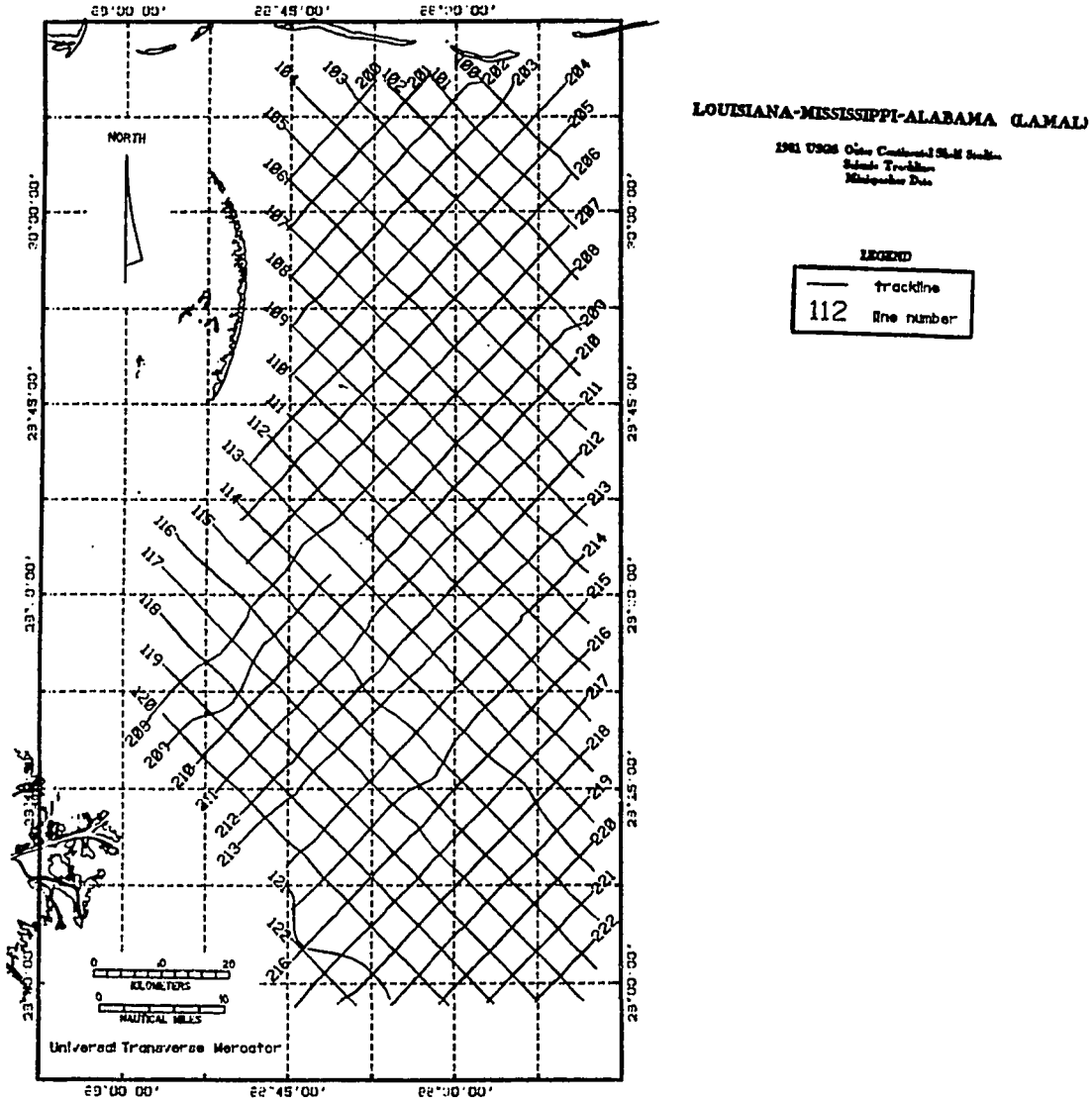

Figure B-18. The 1981 LAMAL survey in the Chandeleur, St. Bernard and Balize delta region.

APPENDIX C

Vibracore Data

The principal scientist participating in the Appendix C vibracore cruises are listed below.

Jack Kindinger - U.S. Geological Survey
Randolph A. McBride - Louisiana Geological Survey
Shea Penland - Louisiana Geological Survey
John R. Suter - Exxon
S. Jeffress Williams - Louisiana Geological Survey

SITE #	LATITUDE	LONGITUDE	WATER DEPTH (FT)
TS-86-1	29° 26' 23.36"	90° 17' 38.6"	25.0'
TS-86-2	29° 19' 29.8"	90° 17' 28.85"	21.0'
TS-86-3	29° 12' 41.47"	90° 18' 56.71"	17.0'
TS-86-4	29° 11' 25.20"	90° 20' 22.28"	30.0'
TS-86-5	29° 22' 42.20"	90° 14' 17.92"	21.0'
TS-86-6	29° 13' 32.15"	90° 15' 38.70"	13.0'
TS-86-7	29° 15' 33.28"	90° 15' 33.28"	11.0'
TS-86-8	29° 10' 30.35"	90° 15' 29.64"	16.0'
TS-86-9	29° 12' 23.74"	90° 13' 14.21"	15.0'
TS-86-10	29° 26' 04.96"	90° 11' 37.01"	17.0'
TS-86-11	29° 22' 50.84"	90° 11' 28.51"	18.0'
TS-86-12	29° 20' 24.16"	90° 11' 28.14"	17.0'
TS-86-13	29° 20' 12.40"	90° 11' 27.91"	17.0'
TS-86-14	29° 16' 29.81"	90° 11' 12.61"	22.0'
TS-86-15	29° 14' 51.26"	90° 10' 41.81"	16.0'
TS-86-16	29° 13' 18.28"	90° 10' 30.88"	19.0'
TS-86-17	29° 11' 14.23"	90° 10' 05.79"	22.5'
TS-86-18	29° 10' 15.89"	90° 09' 57.26"	18.0'
TS-86-19	29° 09' 03.31"	90° 09' 36.50"	35.0'
TS-86-20	29° 07' 12.08"	90° 09' 14.90"	45.0'
TS-86-21	29° 19' 05.88"	90° 10' 06.70"	17.0'
TS-86-22	29° 14' 15.16"	90° 05' 14.92"	23.0'
TS-86-23	29° 11' 15.20"	90° 02' 35.56"	29.0'
TS-86-24	29° 22' 53.54"	90° 05' 53.56"	16.0'
TS-86-25	29° 19' 53.60"	90° 05' 53.74"	17.0'
TS-86-26	29° 16' 48.69"	90° 03' 20.68"	24.0'
TS-86-27	29° 19' 54.61"	90° 02' 27.74"	19.0'
TS-86-28	29° 04' 12.36"	90° 08' 48.10"	52.0'
TS-86-29	29° 15' 35.71"	90° 18' 12.42"	20.0'
TS-86-30	29° 15' 24.64"	90° 05' 51.76"	17.0'

SITE #	LATITUDE	LONGITUDE	WATER DEPTH (FT)
SS-86-1	29° 01' 27.52"	90° 58' 21.34"	17.0'
SS-86-2	28° 56' 21.56"	90° 58' 27.93"	30.0'
SS-86-3	28° 55' 51.47"	90° 58' 23.97"	30.0'
SS-86-4	28° 55' 34.92"	90° 58' 24.30"	12.0'
SS-86-5	28° 47' 35.45"	90° 58' 22.87"	36.0'
SS-86-6	28° 42' 06.28"	90° 58' 14.42"	46.0'
SS-86-7	28° 37' 23.43"	90° 58' 30.12"	60.0'
SS-86-9	29° 03' 44.25"	90° 31' 15.54"	17.0'
SS-86-10	29° 55' 11.55"	90° 53' 32.95"	32.0'
SS-86-11	28° 54' 21.83"	90° 53' 27.88"	22.0'
SS-86-12	28° 51' 35.39"	90° 52' 51.89"	33.0'
SS-86-13	28° 52' 48.23"	90° 46' 04.27"	24.0'
SS-86-15	28° 37' 24.61"	90° 39' 20.42"	60.0'
SS-86-16	28° 42' 16.25"	90° 39' 26.08"	60.0'
SS-86-17	28° 45' 52.22"	90° 39' 25.66"	60.0'
SS-86-18	29° 02' 36.77"	90° 58' 17.90"	10.0'
SS-86-19	29° 01' 39.04"	90° 54' 17.19"	10.0'
SS-86-20	28° 58' 03.58"	90° 54' 53.94"	28.0'
SS-86-21	28° 45' 19.76"	90° 52' 39.38"	57.0'
SS-86-22	29° 01' 25.05"	90° 47' 29.20"	15.0'
SS-86-23	29° 02' 01.93"	90° 51' 35.71"	10.0'
SS-86-24	28° 51' 58.64"	90° 37' 47.62"	55.0'
SS-86-25	28° 55' 30.08"	90° 37' 47.91"	25.0'
SS-86-26	28° 54' 12.28"	90° 58' 23.86"	18.0'
SS-86-27	28° 54' 42.36"	90° 58' 24.51"	
SS-86-28	28° 54' 57.91"	90° 44' 15.19"	22.0'
SS-86-29	28° 54' 18.22"	90° 44' 11.26"	22.0'
SS-86-30	28° 53' 41.75"	90° 44' 00.20"	28.0'
SS-86-31	28° 52' 57.51"	90° 43' 54.70"	34.0'
SS-86-32	28° 51' 53.62"	90° 58' 11.75"	32.0'

SITE #	LATITUDE	LONGITUDE	WATER DEPTH (FT)
SS-83-0	28° 56' 20.0"	90° 59' 10.8"	34'
SS-83-1	28° 55' 10.6"	90° 59' 54.0"	17'
SS-83-2	28° 55' 0.8"	91° 0' 3.9"	20'
SS-83-3	28° 53' 0.0"	90° 59' 40.0"	25'
SS-83-4	28° 51' 43.0"	91° 04' 06"	25'
SS-83-5	28° 53' 16.0"	91° 04' 18"	21'
SS-83-6	28° 54' 45.0"	91° 04' 14"	17'
SS-83-7	28° 56' 0.0"	91° 04' 52"	28'
SS-83-11	28° 55' 59.5"	90° 49' 50.3"	35'
SS-83-12	28° 54' 5.3"	90° 49' 50.7"	20'
SS-83-13	28° 51' 25.0"	90° 48' 17.0"	46'
SS-83-14	28° 56' 58.2"	90° 44' 51.1"	35'
SS-83-15	28° 54' 49.0"	90° 44' 49.3"	25'
SS-83-16	28° 52' 48.6"	90° 44' 49.6"	34'
SS-83-17	28° 56' 57.9"	90° 35' 58.9"	41'
SS-83-18	28° 56' 58.2"	90° 36' 31.8"	30'
SS-83-19	28° 53' 49.7"	90° 36' 0.0"	49'

SITE #	LATITUDE	LONGITUDE	WATER DEPTH (FT)
ID-83-2	28° 00' 36.0"	90° 55' 23.0"	21'
ID-83-3	29° 59' 50.0"	90° 50' 12.0"	26'
ID-83-4	29° 59' 52.9"	90° 46' 41.7"	26'
ID-83-5	28° 4' 3.3"	90° 34' 56.8"	20'
ID-83-6	28° 2' 57.1"	90° 40' 4.7"	16'
ID-83-7	28° 1' 46.6"	90° 46' 51.2"	15'
ID-83-9	28° 1' 18.6"	90° 35' 37.5"	30'
ID-83-10	28° 2' 45.9"	90° 35' 58.0"	17'
ID-83-11	28° 4' 5.1"	90° 36' 14.6"	15'
ID-83-12	28° 1' 22.0"	90° 37' 17.3"	29'
ID-83-13	28° 0' 35.3"	90° 38' 45.7"	30'
ID-83-14	28° 2' 7.9"	90° 38' 56.2"	18'
ID-83-15	28° 1' 50.0"	90° 39' 58.0"	22'
ID-83-16	28° 0' 8.1"	90° 39' 59.1"	31'
ID-83-17	28° 0' 27.7"	90° 40' 49.6"	30'
ID-83-18	28° 2' 57.8"	90° 40' 54.3"	16'
ID-83-19	28° 1' 50.2"	90° 42' 7.5"	21'
ID-83-20	28° 0' 28.3"	90° 42' 9.0"	28'
ID-83-21	28° 1' 30.0"	90° 43' 5.2"	18'
ID-83-22	28° 0' 56.2"	90° 44' 18.6"	22'
ID-83-23	29° 59' 16.8"	90° 44' 24.6"	31'
ID-83-24	28° 0' 40.1"	90° 48' 49.4"	22'
ID-83-25	29° 58' 59.9"	90° 48' 49.7"	29'

CAT ISLAND PASS AREA

SITE #	LATITUDE	LONGITUDE	WATER DEPTH (FT)
CIP-86-1	29° 04.03'	90° 43.68'	8.5'
CIP-86-2	29° 03.88'	90° 42.62'	13.0'
CIP-86-3	29° 04.30'	90° 40.33'	11.0'
CIP-86-4	29° 04.29'	90° 38.76'	9.5'
CIP-86-5	29° 04.34'	90° 38.35'	14.0'
CIP-86-6	29° 04.75'	90° 29.14'	10.0'
CIP-86-7	29° 05.55'	90° 31.61'	4.5'
CIP-86-8	29° 05.70'	90° 28.20'	6.0'
CIP-86-9	29° 05.83'	90° 28.74'	5.0'
CIP-86-10	29° 04.99'	90° 29.95'	8.0'
CIP-86-11	29° 05.49'	90° 33.56'	12.0'
CIP-86-12	29° 05.69'	90° 35.63'	11.0'
CIP-86-13	29° 05.46'	90° 35.83'	8.0'
CIP-86-14	29° 05.35'	90° 36.10'	4.0'
CIP-86-15	29° 04.87'	90° 35.79'	12.0'
CIP-86-16	29° 05.72'	90° 37.48'	8.0'
CIP-86-17	29° 05.38'	90° 37.23'	8.0'
CIP-86-18	29° 05.86'	90° 36.90'	7.5'
CIP-86-19	29° 05.54'	90° 36.83'	6.0'

SHELL REEF AREA

SITE #	LATITUDE	LONGITUDE	WATER DEPTH (FT)
SR-86-1	29° 24' 34.41"	91° 51' 27.35"	10.0'
SR-86-2	29° 19' 41.26"	91° 43' 56.20"	15.0'
SR-86-3	29° 13' 19.56"	91° 42' 19.48"	20.0'
SR-86-4	29° 06' 26.02"	91° 42' 18.41"	15.0'
SR-86-5	29° 01' 23.29"	91° 41' 19.56"	34.0'
SR-86-6	29° 07' 59.64"	91° 38' 46.53"	17.0'
SR-86-7	29° 22' 48.09"	91° 34' 08.97"	12.0'
SR-86-8	29° 21' 05.26"	91° 28' 39.30"	11.0'
SR-86-9	29° 08' 31.20"	91° 25' 30.53"	21.0'
SR-86-10	29° 13' 30.54"	91° 15' 23.62"	8.5'

POINT AU FER AREA

SITE #	LATITUDE	LONGITUDE	WATER DEPTH (FT)
SN-86-2	29° 12' 48.25"	91° 10' 18.72"	5.0'
SN-86-3	29° 06' 50.76"	91° 12' 04.12"	13.0'
SN-86-4	29° 10' 02.40"	91° 08' 24.60"	8.0'
SN-86-5	29° 10' 11.12"	91° 04' 45.88"	7.0'
SN-86-6	29° 07' 54.73'	91° 04' 36.75"	18.0'
SN-86-7	29° 04' 06.07"	91° 04' 18.53"	10.0'
SN-86-8	29° 04' 00.14"	91° 04' 01.08"	18.0'
SN-86-9	29° 01' 27.13"	91° 11' 47.97"	14.0'

SITE #	LATITUDE	LONGITUDE	WATER DEPTH (FT)
T-86-1	29° 03' 59.34"	90° 31' 45.64"	7.0'
T-86-2	29° 02' 52.85"	90° 31' 45.01"	22.0'
T-86-3	29° 01' 47.33"	90° 31' 21.78"	27.0'
T-86-4	29° 01' 03.82"	90° 32' 02.94"	30.0'
T-86-5	28° 59' 36.55"	90° 31' 29.45"	33.0'
T-86-6	29° 03' 36.59"	90° 29' 23.48"	13.0'
T-86-7	29° 02' 11.68"	90° 29' 03.52"	26.0'
T-86-8	29° 01' 15.00"	90° 29' 02.34"	28.0'
T-86-9	29° 00' 11.82"	90° 28' 51.97"	33.0'
T-86-10	29° 01' 08.50"	90° 30' 00.24"	30.0'
T-86-11	29° 02' 45.28"	90° 26' 05.63"	13.0'
T-86-12	29° 00' 13.54"	90° 25' 53.65"	32.0'
T-86-13	29° 02' 26.62"	90° 21' 23.46"	20.0'
T-86-14	29° 00' 28.16"	90° 20' 50.60"	35.0'
T-86-15	29° 03' 38.79"	90° 17' 51.40"	15.0'
T-86-16	29° 01' 11.06"	90° 17' 11.74"	31.0'
T-86-17	28° 45' 52.22"	90° 39' 25.66"	60.0'
T-86-18	29° 04' 11.95"	90° 15' 47.79"	17.0'
T-86-19	28° 56' 59.67"	90° 24' 59.63"	47.0'
T-86-20	28° 53' 17.58"	90° 24' 59.98"	59.0'
T-86-21	28° 53' 48.81"	90° 31' 13.26"	56.0'

SITE 3	LATITUDE	LONGITUDE	WATER DEPTH (FT)
CR-83-2	29° 15' 23.9"	89° 49' 13.2"	33'
CR-83-5	29° 15' 4.7"	89° 44' 17.9"	--
CR-83-6	29° 17' 18.6"	89° 43' 40.5"	--
CR-83-8	29° 17' 41.8"	89° 50' 17.5"	12'
CR-83-9	29° 17' 29.1"	89° 51' 29.5"	11'
CR-83-10	29° 16' 34.1"	89° 53' 15.8"	17'
CR-83-11	29° 15' 50.9"	89° 54' 46.7"	14'
CR-83-12	29° 14' 25.2"	89° 53' 1.5"	26'
CR-83-14	29° 16' 12.3"	89° 53' 50.0"	14'
CR-83-15	29° 17' 5.7"	89° 53' 29.6"	8'
CR-83-16	29° 17' 8.8"	89° 52' 37.8"	13'
CR-83-17	29° 16' 19.7"	89° 51' 57.0"	20'
CR-83-19	29° 15' 8.8"	89° 50' 52.9"	31'
CR-83-23	29° 17' 12.3"	89° 50' 16.9"	17'
CR-83-24	29° 16' 26.4"	89° 48' 57.6'	27'
CR-83-26	29° 18' 9.2"	89° 48' 0.1"	27'
CR-83-27	29° 15' 9.0"	89° 45' 52.5"	16'
CR-83-28	29° 16' 52.7"	89° 45' 50.3"	36'
CR-83-30	29° 18' 2.8"	89° 45' 54.4"	27'
CR-83-31	29° 18' 6.7"	89° 45' 15.8"	16'
CR-83-33	29° 15' 54.0"	89° 45' 59.9"	--
CR-83-35	29° 16' 27.2"	89° 47' 32.3"	31'
CR-83-37	29° 16' 29.8"	89° 49' 56.9"	28'
CR-83-38	29° 16' 15.9"	89° 50' 35.0"	25'
CR-83-39	29° 15' 55.6"	89° 51' 20.0"	26'
CR-83-40	29° 15' 13.1"	89° 53' 3.6"	26'
			23'

LAFOURCHE AREA

SITE #	LATITUDE	LONGITUDE	WATER DEPTH (FT)
L-86-1	29° 11' 05.83"	90° 02' 56.59"	12.0'
L-86-2	29° 10' 55.31"	90° 02' 03.36"	18.0'
L-86-3	29° 09' 49.52"	90° 00' 36.10"	32.0'
L-86-5	29° 11' 18.39"	90° 02' 02.23"	12.0'
L-86-6	29° 07' 57.62"	90° 07' 39.02"	14.0'
L-86-7	29° 08' 48.21"	90° 06' 01.48"	14.0'
L-86-8	29° 06' 53.91"	90° 03' 39.93"	39.0'
L-86-10	29° 09' 36.99"	90° 05' 03.34"	14.0'
L-86-11	29° 06' 06.54"	90° 10' 45.58"	12.0'
L-86-12	29° 03' 45.07"	90° 09' 17.62"	32.0'
L-86-13	29° 01' 48.33"	90° 07' 44.14"	58.0'

PLAQUEMINES AREA

SITE #	LATITUDE	LONGITUDE	WATER DEPTH (FT)
P-86-1	29° 9.34'	89° 34.37'	34.0'
P-86-2	29° 16' 42.08"	89° 40' 00.36"	15.0'
P-86-3	29° 14' 51.94"	89° 40' 29.98"	25.0'
P-86-4	29° 12' 37.52"	89° 41' 09.85"	38.0'
P-86-5	29° 11.56'	89° 29.28'	13.0'
P-86-6	29° 08' 33.10"	89° 30' 21.42"	27.0'
P-86-7	29° 10.16'	89° 27.81'	15.0'
P-86-8	29° 12' 47.21'	89° 37' 54.04"	28.0'
P-86-9	29° 15' 9.92"	89° 37' 01.96"	14.0'
P-86-10	29° 10.41'	89° 38.15'	36.0'
P-86-11	29° 13.42'	89° 32.57'	4.0'
P-86-12	29° 14' 0.74"	89° 58' 53.50"	11.0'
P-86-13	29° 10' 30.50"	89° 55' 45.30"	45.0'
P-86-14	29° 13' 36.61"	89° 58' 30.67'	21.0'
P-86-16	29° 14' 31.05"	89° 56' 33.50"	9.0'
P-86-18	29° 18' 23.7'	89° 48' 59.77"	11.0'
P-86-19	29° 17' 55.01"	89° 44' 09.45"	12.0'
P-86-20	29° 13' 17.62"	89° 44' 06.50"	39.0'

SITE #	LATITUDE	LONGITUDE	WATER DEPTH
MA-87-1	30° 11.24'	89° 04.88'	18'
MA-87-2	30° 05.65'	88° 55.64'	36'
MA-87-3	30° 07.22'	88° 53.20'	38'
MA-87-4	30° 09.48'	88° 53.97'	30'
MA-87-5	30° 11.16'	88° 49.00'	31'
MA-87-7	30° 13.81'	88° 52.91'	9'
MA-87-8	30° 13.39'	88° 52.78'	20'
MA-87-9	30° 12.42'	88° 52.31'	28'
MA-87-10	30° 11.50'	88° 54.41'	25'
MA-87-11	30° 12.44'	88° 55.37'	15'
MA-87-12	30° 12.05'	88° 57.14'	14'
CI-87-1	30° 06.13'	88° 53.72'	43'
CI-87-2	30° 03.85'	88° 53.32'	8'
CI-87-3	30° 05.19'	88° 49.16'	43'
CI-87-4	30° 03.54'	88° 50.40'	26'
CI-87-5	30° 02.61'	88° 51.61'	12'
CI-87-6	29° 56.36'	88° 49.03'	9'
CI-87-7	29° 53.13'	88° 49.32'	9'
CI-87-8	29° 52.02'	88° 46.97'	34'
CI-87-9	29° 46.89'	88° 49.57'	31'
CI-87-10	29° 45.93'	88° 49.78'	30'
CI-87-11	29° 45.37'	88° 49.88'	30'
CI-87-12	29° 45.0'	88° 50.90'	30'
CI-87-13	29° 44.76'	88° 52.64'	9'
CI-87-14	29° 42.97'	88° 53.11'	21'
CI-87-15	29° 36.01'	88° 57.75'	27'
CI-87-16	29° 37.32'	88° 58.84'	15'
CI-87-17	29° 31.42'	89° 04.78'	12'
CI-87-18	29° 29.21'	89° 09.60'	12'
CI-87-19	29° 28.14'	89° 07.67'	22'
CI-87-20	29° 25.58'	89° 05.28'	18'
CI-87-21	29° 23.02'	89° 01.46'	40'
CI-87-22	29° 20.68'	88° 53.20'	54'
CI-87-23	29° 24.98'	88° 52.43'	61'
CI-87-24	29° 22.56'	88° 49.66'	94'
CI-87-25	29° 26.03'	88° 45.74'	96'
CI-87-26	29° 27.51'	88° 48.38'	54'
CI-87-27	29° 29.91'	88° 47.00'	47'
CI-87-28	29° 30.89'	88° 45.02'	56'
CI-87-29	29° 33.33'	88° 41.15'	56'
CI-87-30	29° 33.77'	88° 40.37'	60'
CI-87-31	29° 34.04'	88° 35.89'	94'
CI-87-32	29° 34.90'	88° 37.12'	71'
CI-87-33	29° 35.84'	88° 39.90'	60'
CI-87-34	29° 35.59'	88° 39.00'	50'
CI-87-35	29° 36.68'	88° 38.39'	49'
CI-87-36	29° 37.83'	88° 37.09'	48'

SITE #	LATITUDE	LONGITUDE	WATER DEPTH
CI-87-37	30° 03.95'	88° 46.89'	36'
CI-87-38	30° 05.22'	88° 43.74'	48'
CI-87-39	30° 06.72'	88° 39.97'	50'
CI-87-40	30° 05.01'	88° 31.78'	60'
CI-87-41	30° 02.46'	88° 35.25'	70'
CI-87-42	30° 00.09'	88° 40.97'	58'
CI-87-43	29° 51.49'	88° 41.14'	55'
CI-87-44	29° 50.73'	88° 34.58'	82'
CI-87-45	29° 43.21'	88° 33.04'	90'
CI-87-46	29° 40.86'	88° 35.23'	70'
CI-87-47	29° 42.25'	88° 42.29'	50'
CI-87-48	29° 42.38'	88° 43.42'	55'
CI-87-49	29° 43.29'	88° 48.28'	33'
CI-87-50	29° 41.35'	88° 47.26'	46'
CI-87-51	29° 39.26'	88° 48.23'	43'
CI-87-52	29° 38.50'	88° 43.75'	52'
CI-87-53	29° 24.76'	89° 17.49'	30'
CI-87-54	29° 27.40'	89° 18.80'	25'
CI-87-55	29° 30.98'	89° 14.61'	12'
CI-87-56	29° 36.81'	89° 08.64'	15'
CI-87-57	29° 39.16'	89° 05.94'	13'
CI-87-58	29° 42.36'	89° 04.47'	11'
CI-87-59	29° 46.25'	89° 02.76'	12'
CI-87-60	29° 47.13'	89° 02.61'	12'
CI-87-61	29° 47.66'	89° 02.34'	12'
CI-87-62	29° 48.78'	89° 01.60'	12'
CI-87-63	29° 53.13'	88° 59.73'	12'
CI-87-64	29° 58.18'	88° 57.94'	15'
CI-87-65	29° 04.77'	88° 57.81'	26'
CI-87-66	29° 05.77'	89° 03.00'	15'

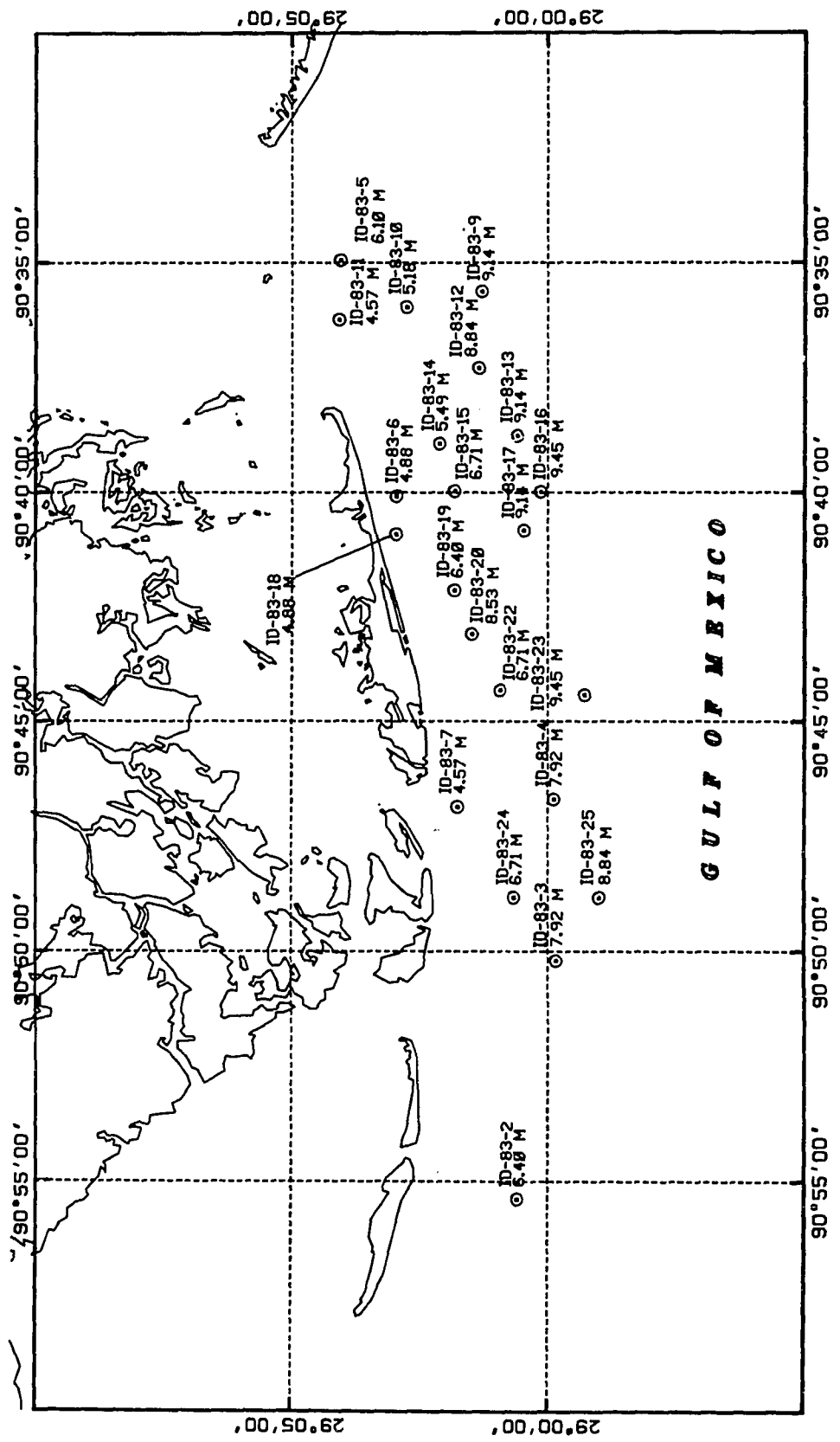

Figure C-1. Vibracores (1983) in the Isles Dernieres area.

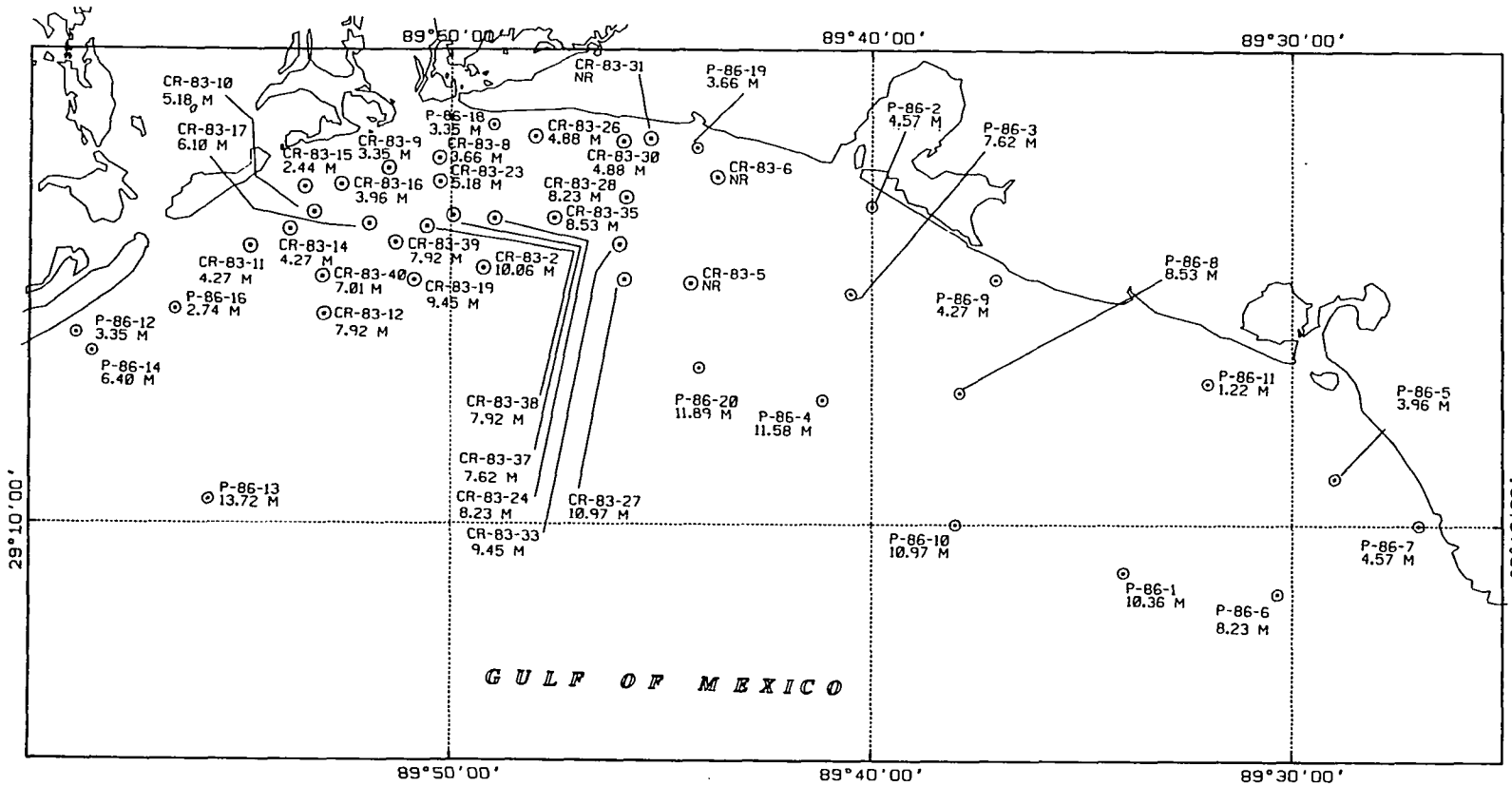

Figure C-2. Vibracores (1983 and 1986) in the Plaquemines shoreline area.

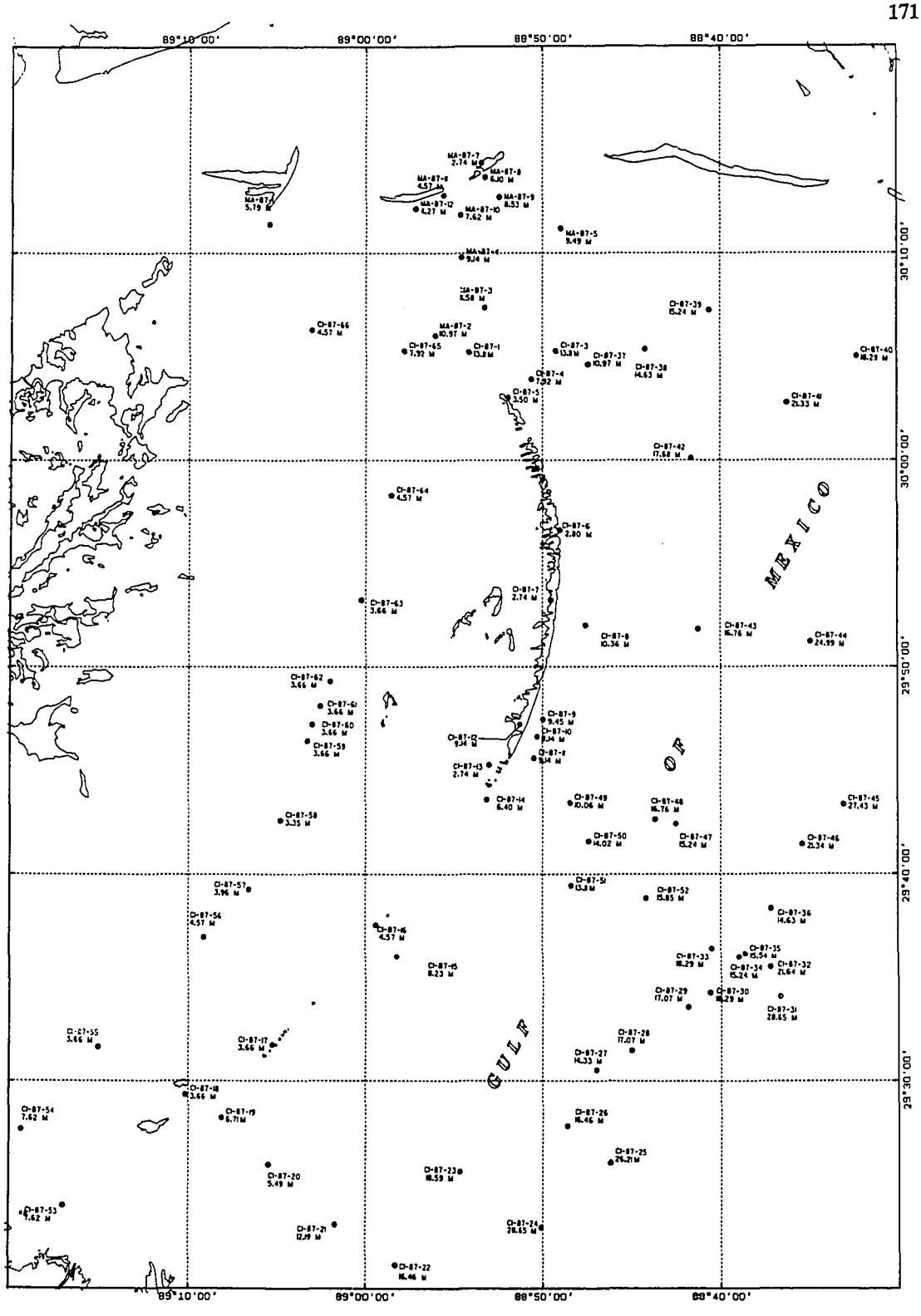

Figure C-3. Vibracores (1987) in the Chandeleur Island area.

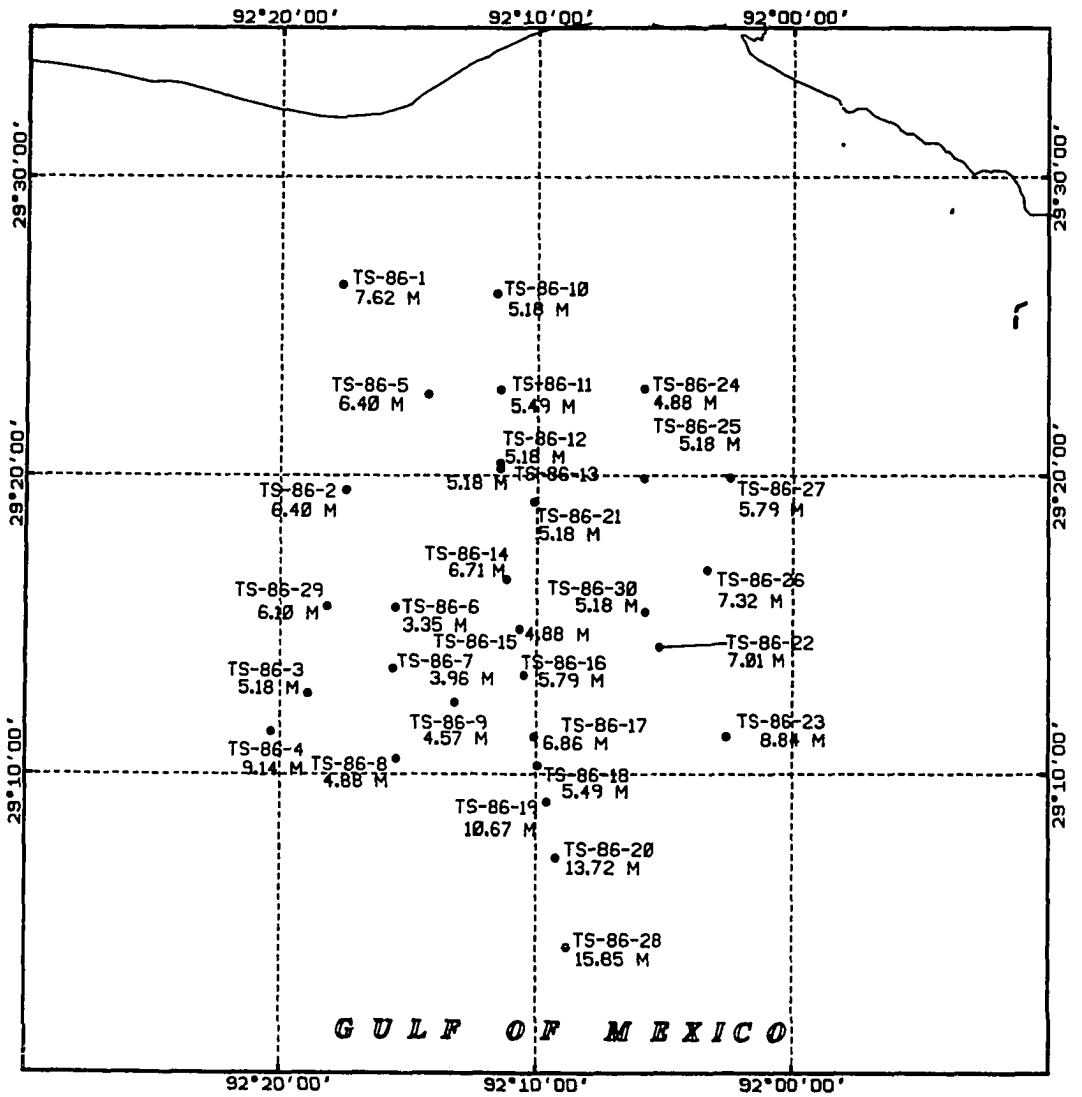

Figure C-4. Vibracore (1986) in the Trinity Shoal area.

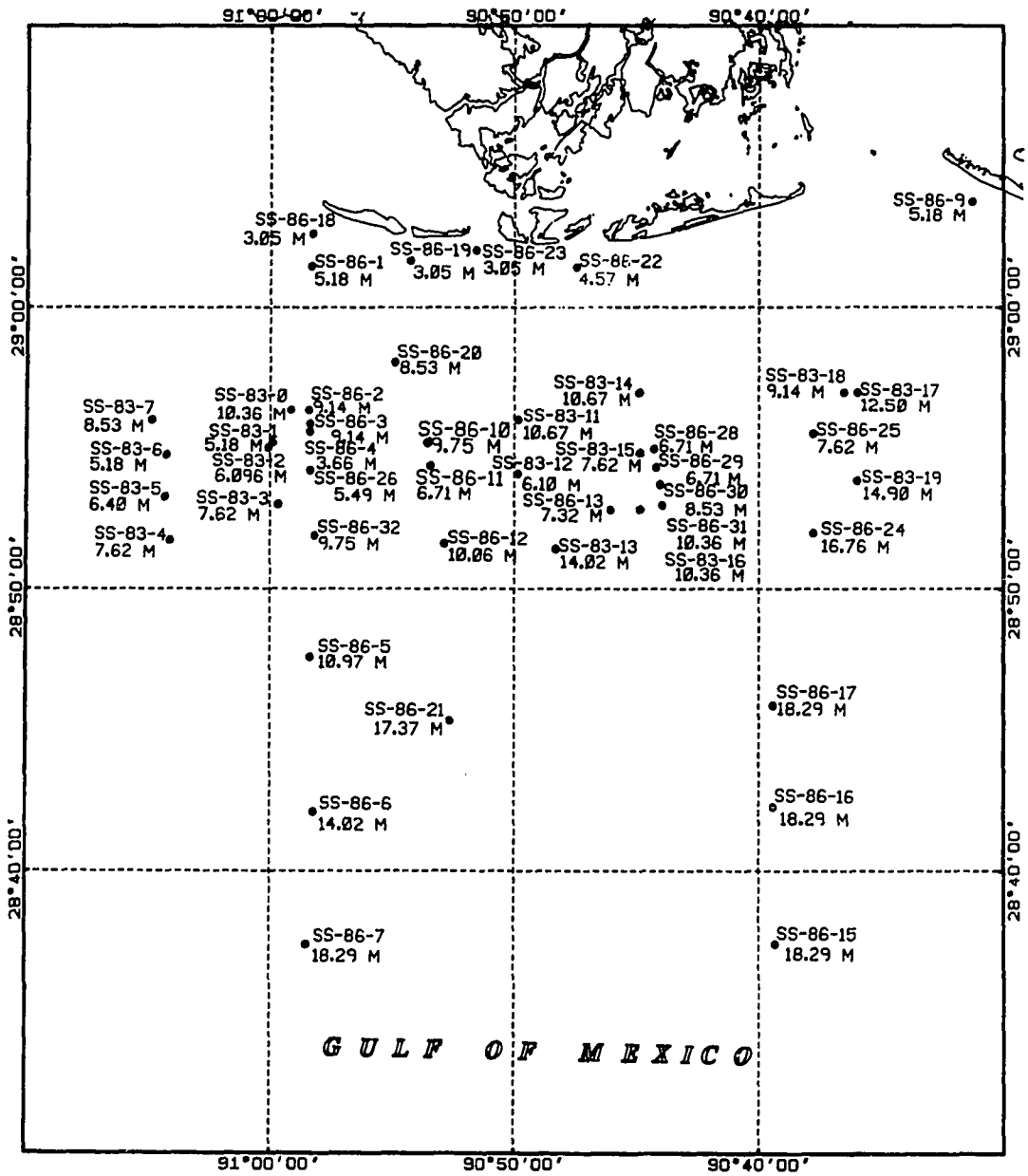

Figure C-5. Vibracores (1983 and 1986) in the Ship Soal area.

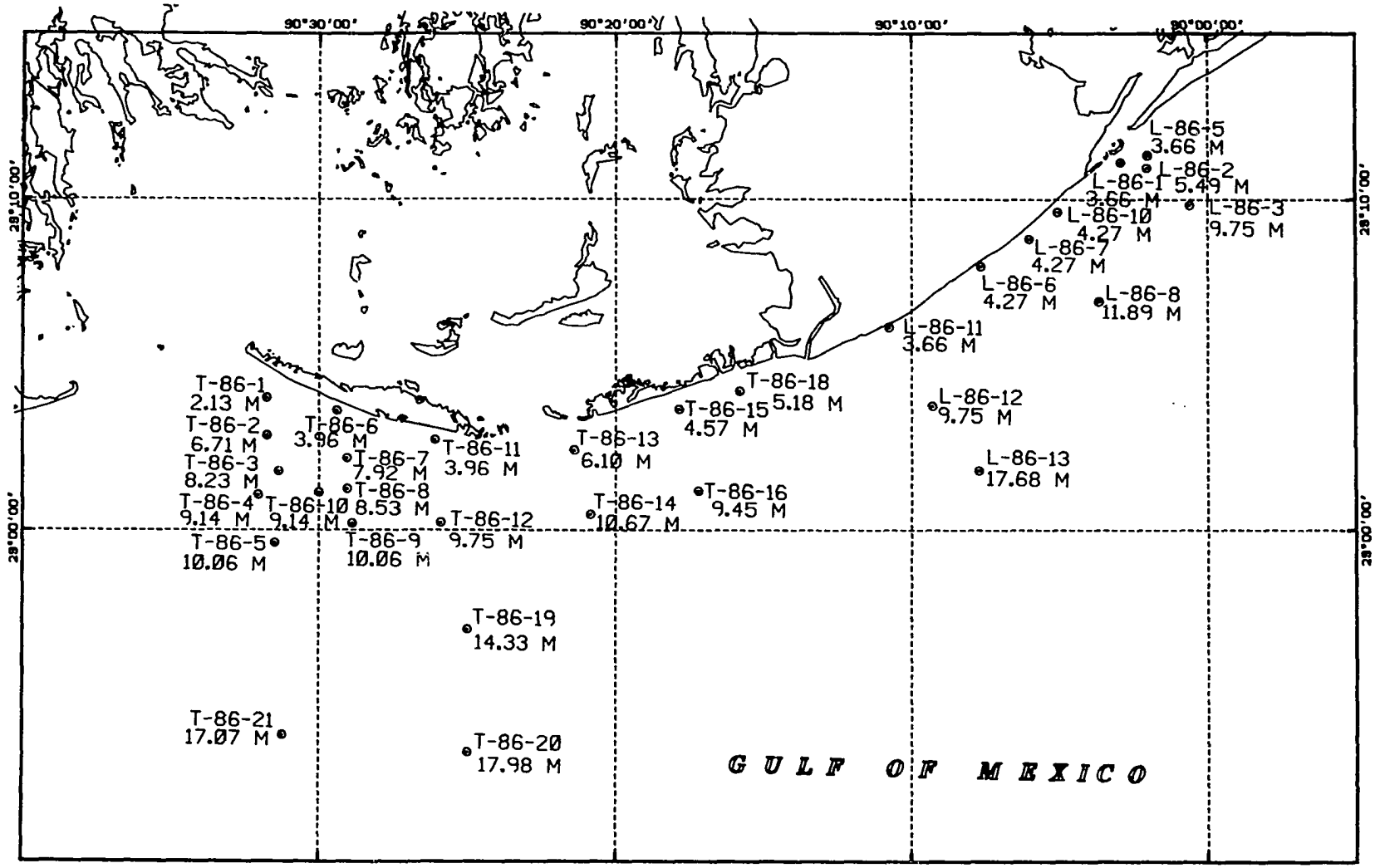

Figure C-6. Vibracore (1986) in the Bayou Lafourche area.

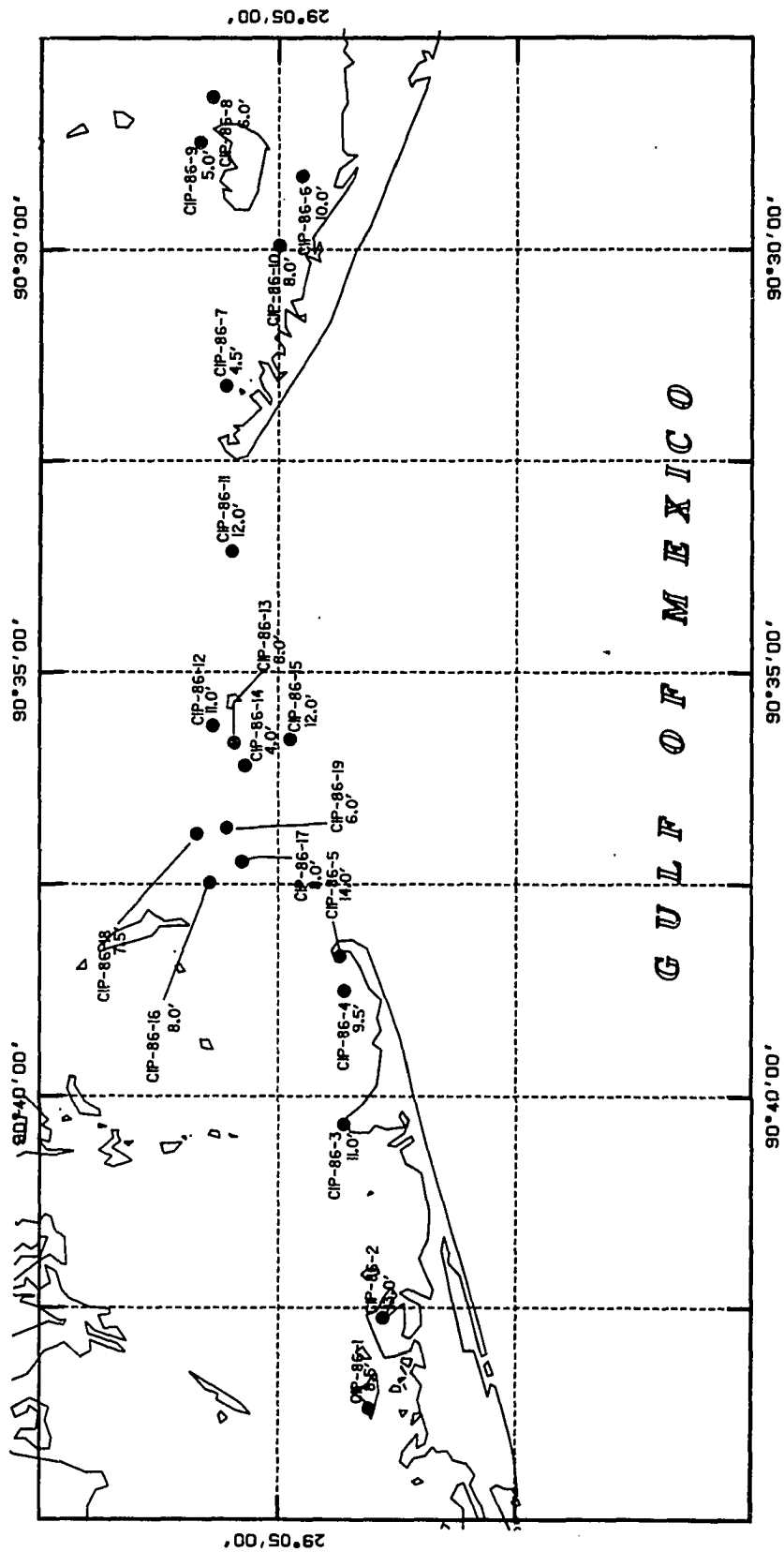

Figure C-7. Vibracore (1986) in the Cat Island Pass area.

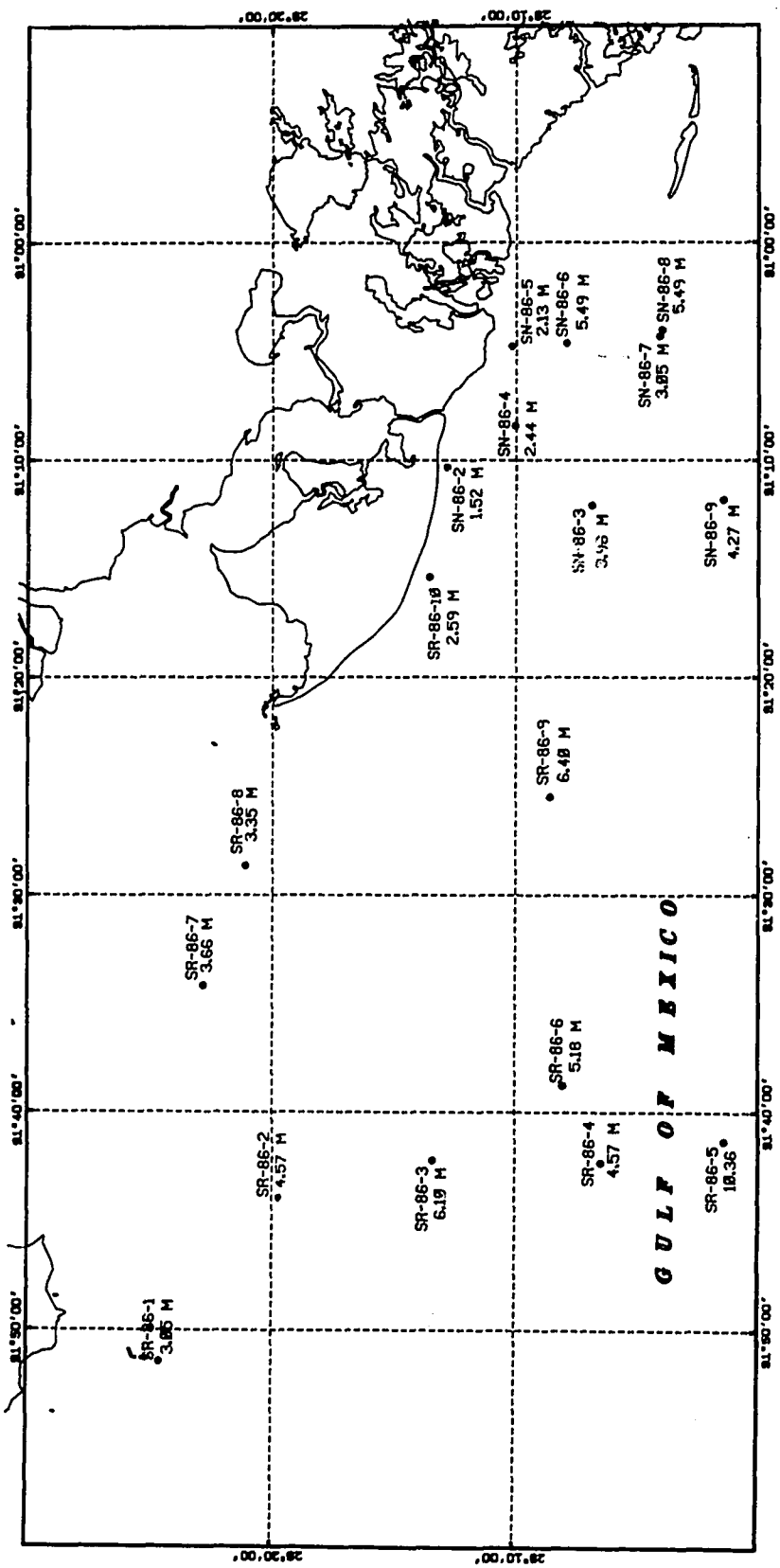

Figure C-8. Vibracore (1986) in the Shell Reef area.

APPENDIX D

Radiocarbon Data

CARBON-14 DATA SUMMARY

Appendix to:

Coastal Geology Technical Report No. 4,

Relative Sea Level Rise and Delta-Plain Development in the Terrebonne Parish Region

by

Shea Penland, Karen E. Ramsey, Randolph A. McBride
John T. Mestayer, and Karen A. Westphal

Open File Series No. 88-05
Louisiana Geological Survey
Baton Rouge, Louisiana
1988

INTRODUCTION

This report presents the following information on vibracore samples subjected to radiometric analysis: sample number, depth, age, subsidence rate, and a description of the sample material. Results based on these data are presented in "Relative Sea Level rise and Delta-Plain Development in the Terrebonne Parish Region," Coastal Geology Technical Report No. 4 of the Louisiana Geological Survey.

Sample Number	Depth (cm)	Age Years before 1950	Subsidence Rate	Material Dated
AB-2b	79.0	150± 70	0.53	hemic peaty muck
AB-8b	90.0	510± 70	0.18	wood
AB-12a	78.0	50 (ultra-modern)	1.56	hemic peaty muck
AB-13	85.0	400± 60	0.21	hemic muck
AB-15	47.15	100 (modern)	0.47	sapric peaty muck
AB-16a	123.12	100 (modern)	1.23	hemic muck
AB-16b	129.20	220± 60	0.59	peaty muck
AB-16c	135.28	400± 60	0.34	peaty muck
AB-17a	47.29	505± 70	0.09	organics
AB-17b	115.37	940± 70	0.12	organics
AB-18a	105.60	100 (modern)	1.06	organics
AB-19c	115.83	520± 70	0.22	organics
AB-20b	49.20	100 (modern)	0.49	organics
AB-20c	90.0	660± 70	0.13	organics
AB-II-1a	74.42	100 (modern)	0.74	peaty muck (silty clay)
AB-II-2b	80.50	300± 70	0.27	organics
AB-II-2c	217.0	950± 75	0.23	sediment and organics
AB-II-3b	147.40	760±100	0.19	hemic muck
AB-II-3c	184.92	880± 60	0.21	hemic silty clayey muck
AB-II-5	73.14	50 (ultra-modern)	1.46	hemic peaty muck
FC-1a	229.0	1210±120	0.19	sapric muck
FC-1b	558.32	1660±190	0.34	sapric peaty muck
FC-3a	709.12	3970± 90	0.18	sapric peaty muck
HC-5a	134.52	865± 80	0.15	fibric peat
HC-5b	148.20	910± 60	0.16	fibric peaty muck
HC-8b	229.40	2520±100	0.09	fibric clayey muck
HC-10-S-1	133.45	100±100 (modern)	1.33	hemic peaty muck (silty clay)
HC-10-S02	133.45	900±130	0.15	hemic peaty muck (loam)
MC-1	77.39	110±145	0.70	organics
MC-2a	232.76	1110±155	0.21	organics
MC-3	12.92	155±140	0.08	organics
MC-4	36.68	326±175	0.12	organics
TB-1	653.00	24201± 80	0.27	Rangia Cuneata
TB-3	222.69	1190± 80	0.19	clayey muck
TB-5	300.08	685± 60	0.44	hemic clayey muck
TB-6a	340.77	3340± 90	0.10	sapric peaty muck
TB-6b	477.30	4690± 70	0.10	muck
TB-7b	167.58	840±160	0.20	hemic clayey muck
TB-1-RC1	18.3	205± 75	0.09	sediment and organics
TB-1-RC2	673.0	3365±195	0.20	sediment and organics
TB-3-RC-1	216.6	1140±115	0.19	sediment and organics
TB-4-RC-1	126.4	1250±145	0.10	sediment and organics
TB-4-RC-2	529.0	5930± 4	0.09	Rangia
SEW-3-RC-1	153.2	320±135	0.47	organics
SEW-4-RC-2	108.0	505± 95	0.21	organics
MC-2-RC-2	288.2	1160±225	0.24	organics
MC-4-RC-2	165.1	1110± 45	0.15	organics
BC-1-RC-2	220	1270± 70	0.17	organics
FC-2-RC-1	56.87	150± 70	0.38	sediment and organics
FC-2-RC-2	94.38	325±120	0.30	sediment and organics
FC-2-RC-4	673.20	6645± 15	0.11	sediment and organics
HC-9-RC-1	33.58	560±120	0.24	sediment and organics

Army Corps of Engineers Carbon-14 Data Summary

Sample Number	Depth (cm)	Age Years before 1950	Subsidence Rate	Material Dated
G-6A-1	457.60	1670±440	0.27	sapric peat
LD-1-3	569.97	3420±380	0.16	sapric peat
BDL-2#18	1076-1101	4660± 80	0.24	peat
BDL-2#18	1040-1050	4050± 90	0.26	peat
BDL-3-1	467.15	2520±470	0.19	peat
BDL-3-2	567.0	3840±150	0.15	black sapric peat
BDL-11-1	173.37	1315±225	0.13	fibric peat
BDL-11-2	421.3	3055±145	0.14	hemic peaty muck
BDL-12-1	386.0	2115±135	0.18	sapric peat
BDL-12-2	551.0	3510±120	0.16	sapric peat
C-11-1	175-187	1840± 80	0.10	brown peat
MC-2-1	333.65	1130±200	0.30	fibric peat
MC-4-1	167.76	1590±110	0.11	hemic peaty muck
MC-6	299.9	1585±200	0.19	sapric peaty muck
G-4#6	413-440	1620± 70	0.27	peat
6-5-1	307.20	2940±720	0.10	hemic peat

APPENDIX E

Terrebonne Coastal Region

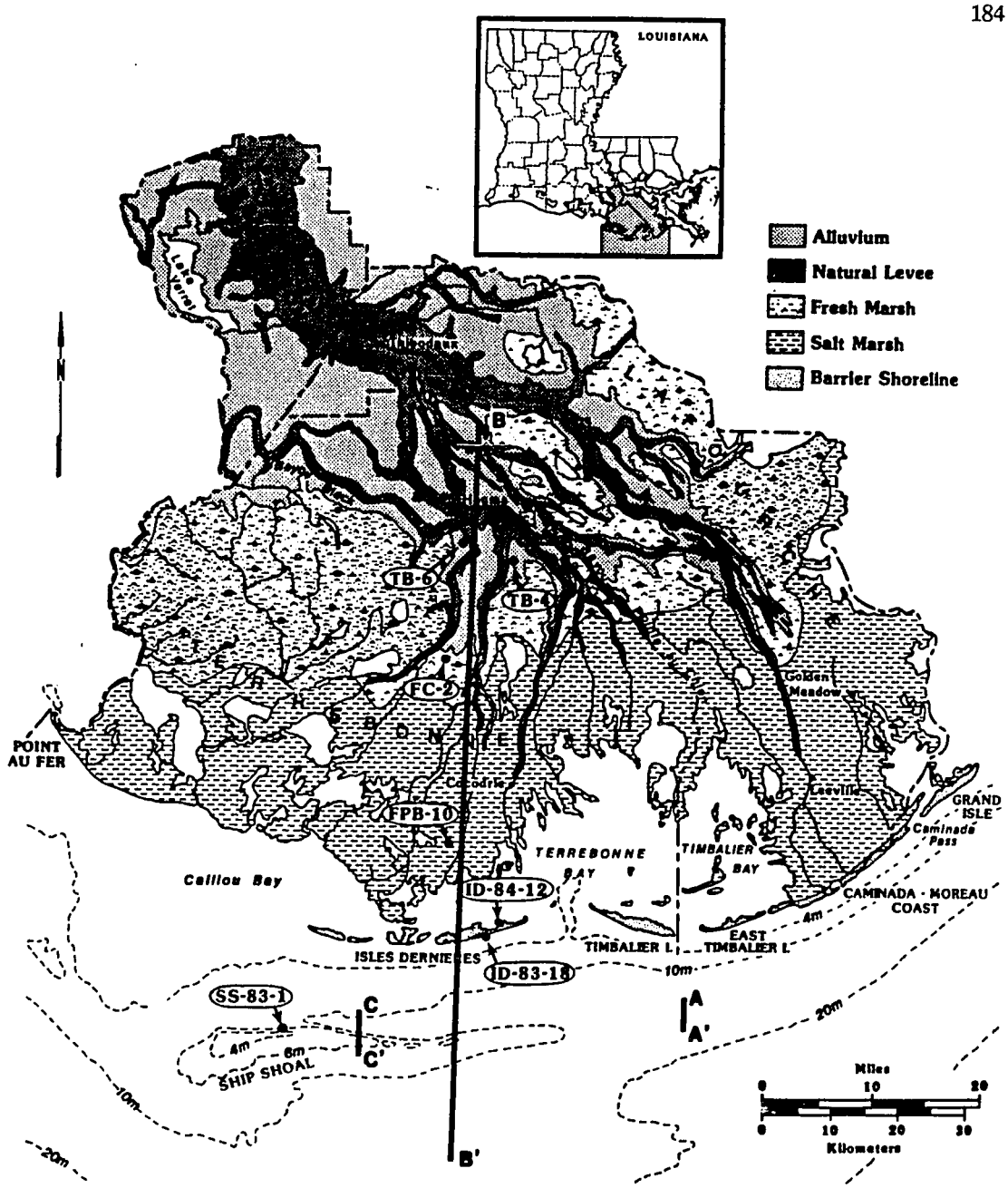

Figure E-1. Locations of vibracores and seismic data in the Terrebonne coastal region (Penland et al. 1987).

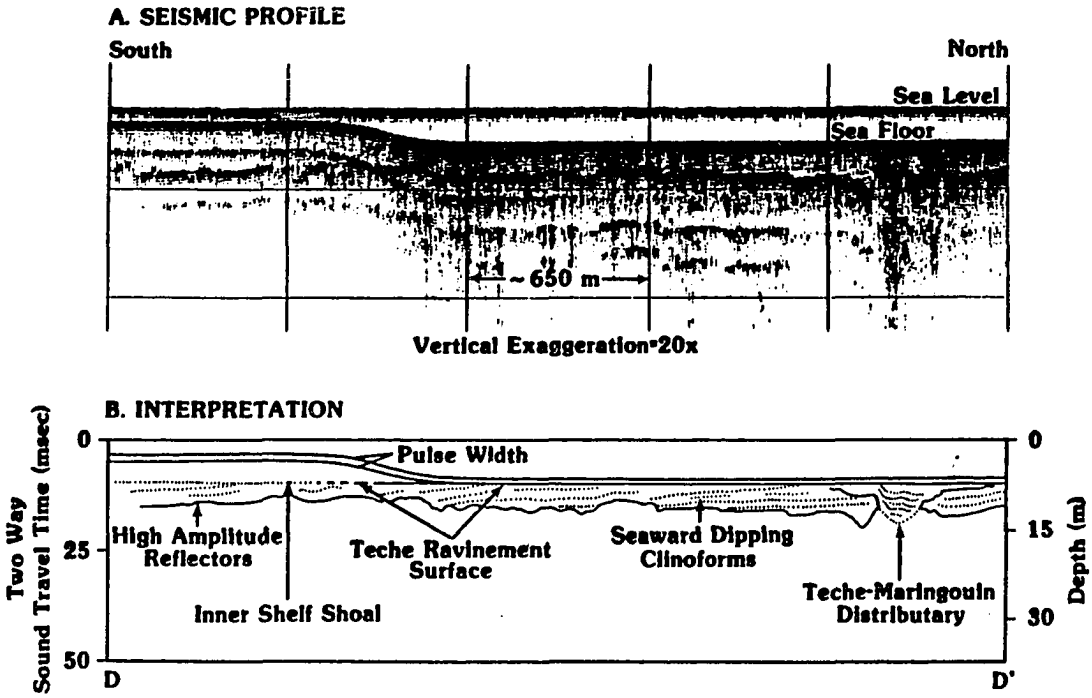

Figure E-2. A high resolution seismic profile (ORE Geopulse) illustrating two ravinement surfaces bounding the Teche delta complex of the late Holocene delta plain (see figure E-1 A-A' for location) (Penland et al. 1987).

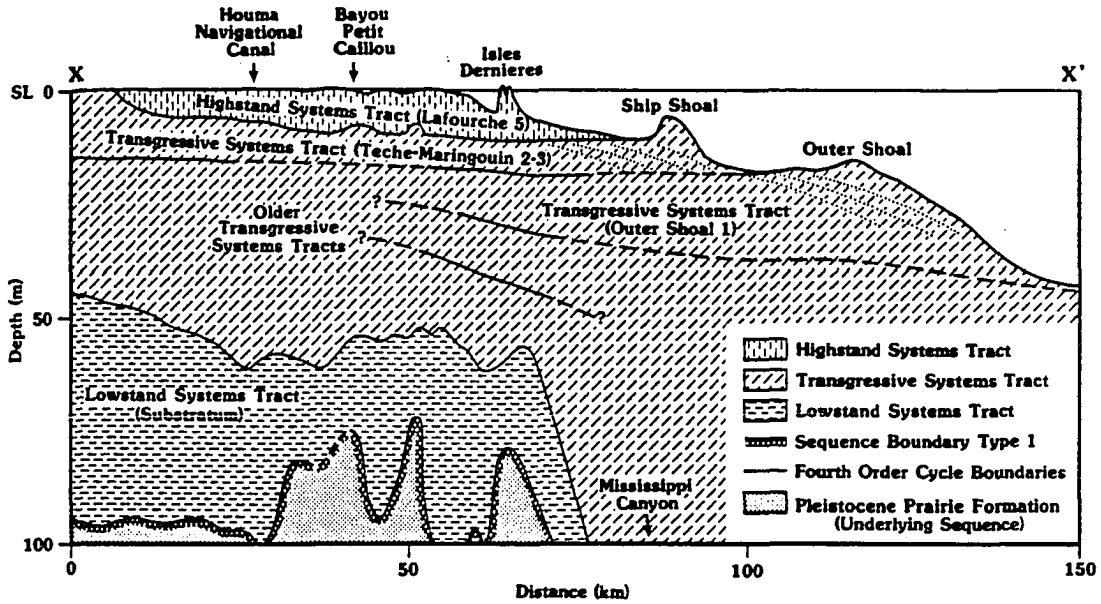

Figure E-3. Generalized dip-oriented cross-section B-B', illustrating the stratigraphic relationship between the Lafourche and Teche delta complex (see Figure E-1 for location) (Boyd et al. 1989).

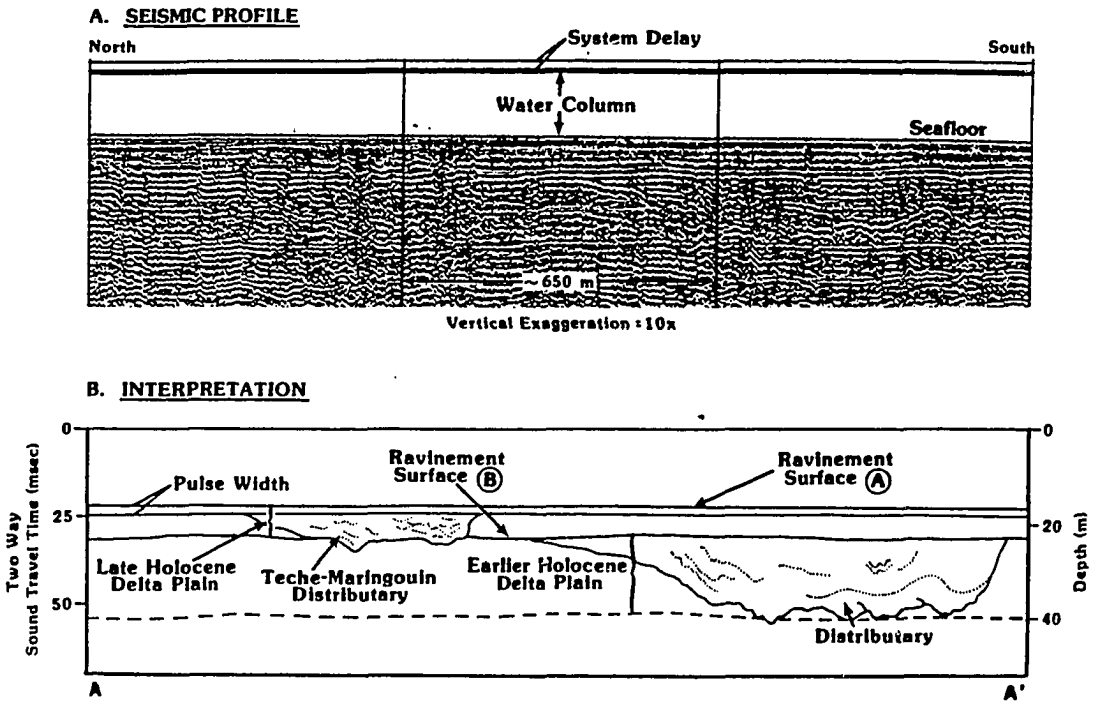

Figure E-4. A high resolution seismic profile C-C' illustrates the Teche ravinement surface upon which Ship Shoal is migrating (see Figure E-1 for location) (Penland et al. 1989).

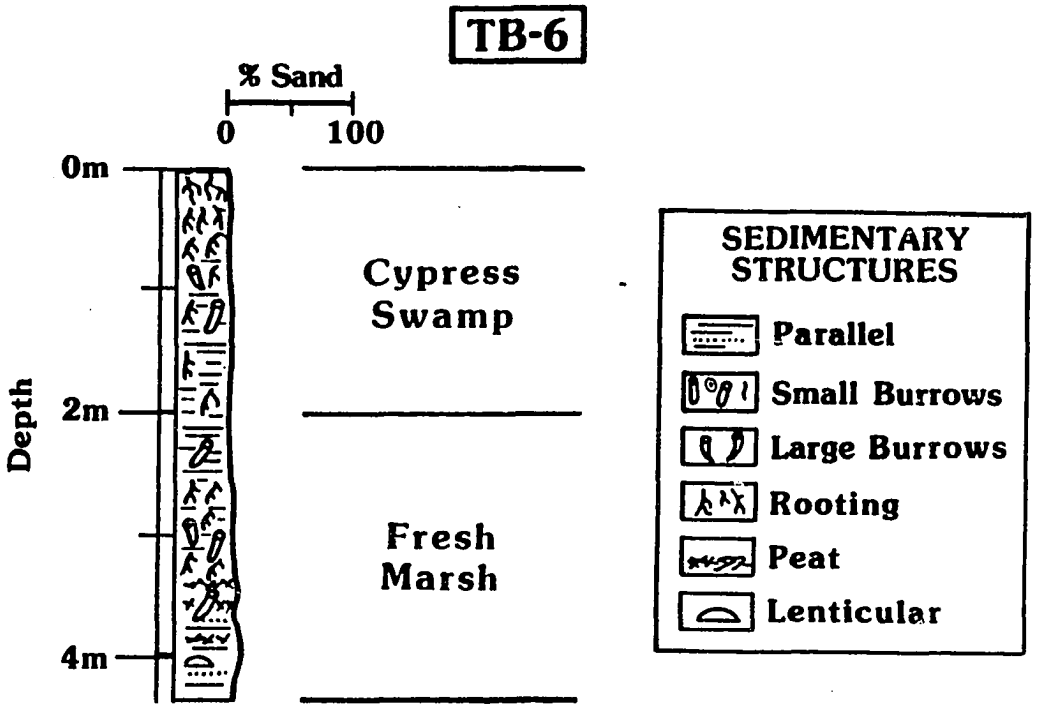

Figure E-5. Log of vibracore TB-6 (see Figure E-1 for location).

Figure E-6. Photograph of vibracore TB-6 (see Figure E-1 for location).

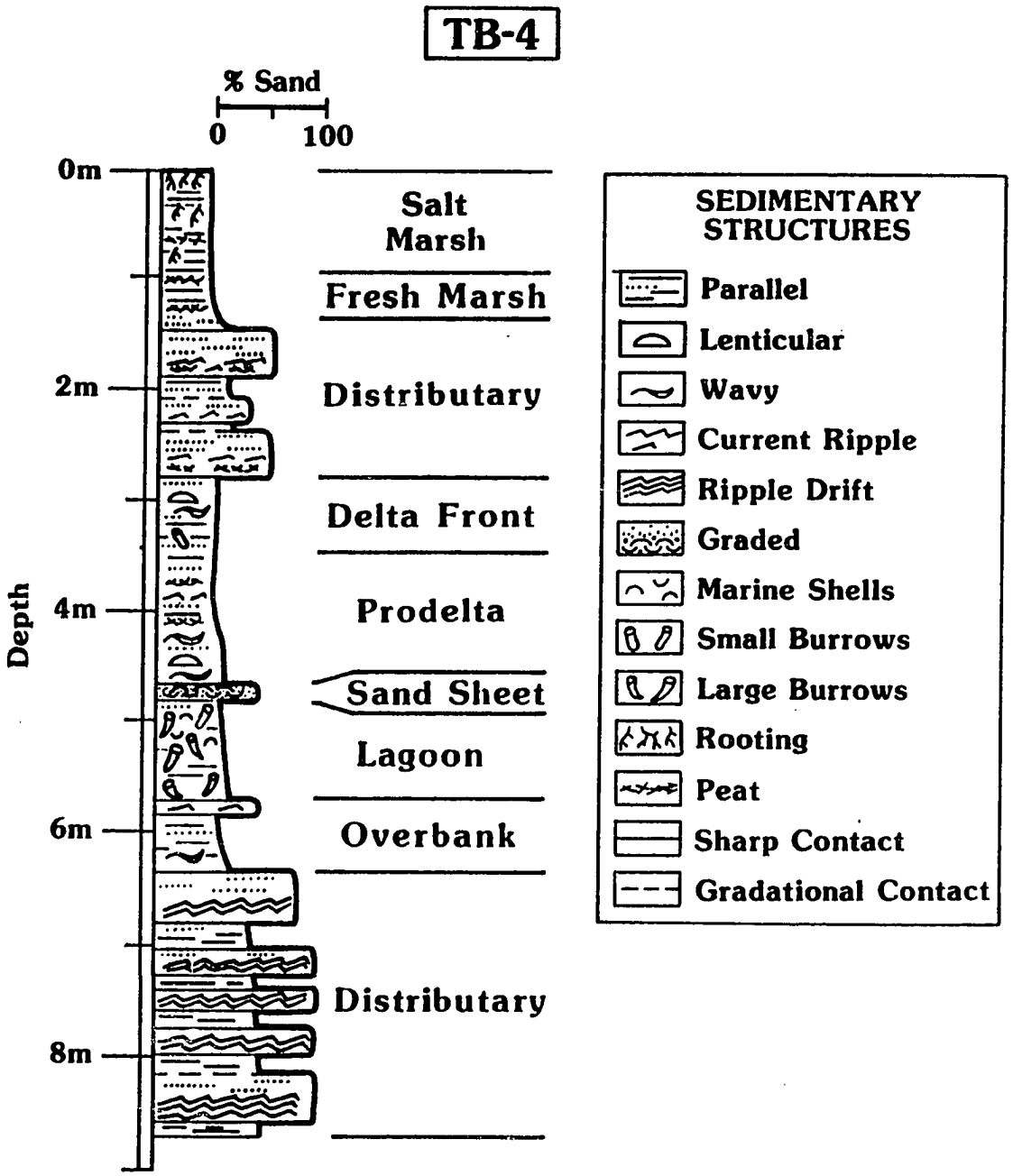

Figure E-7. Log of vibracore TB-4 (see Figure E-1 for location).

Figure E-8. Photograph of vibracore TB-4 (see Figure E-1 for location).

Figure E-9. Photograph of the ravinement surface in TB-4 (see Figure E-1 for location).

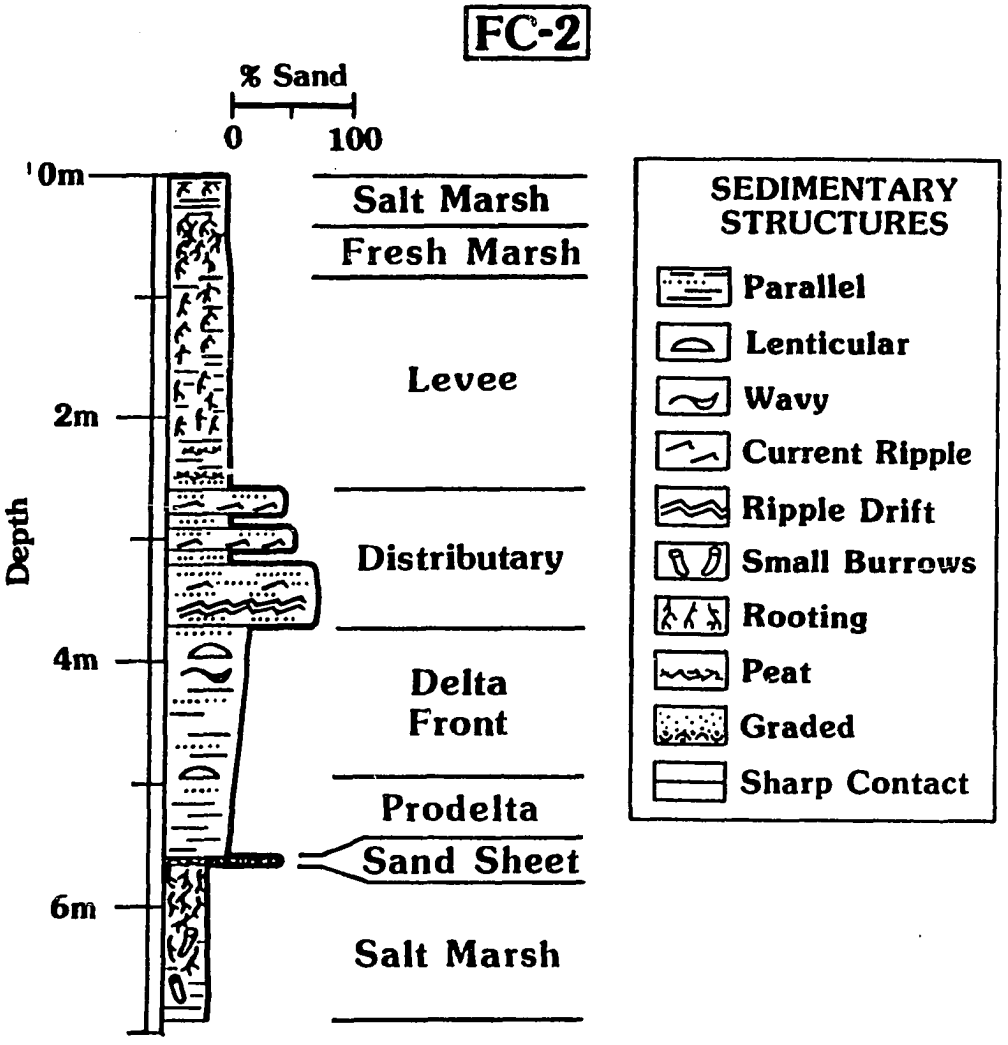

Figure E-10. Log of vibracore FC-2 (see Figure E-1 for location).

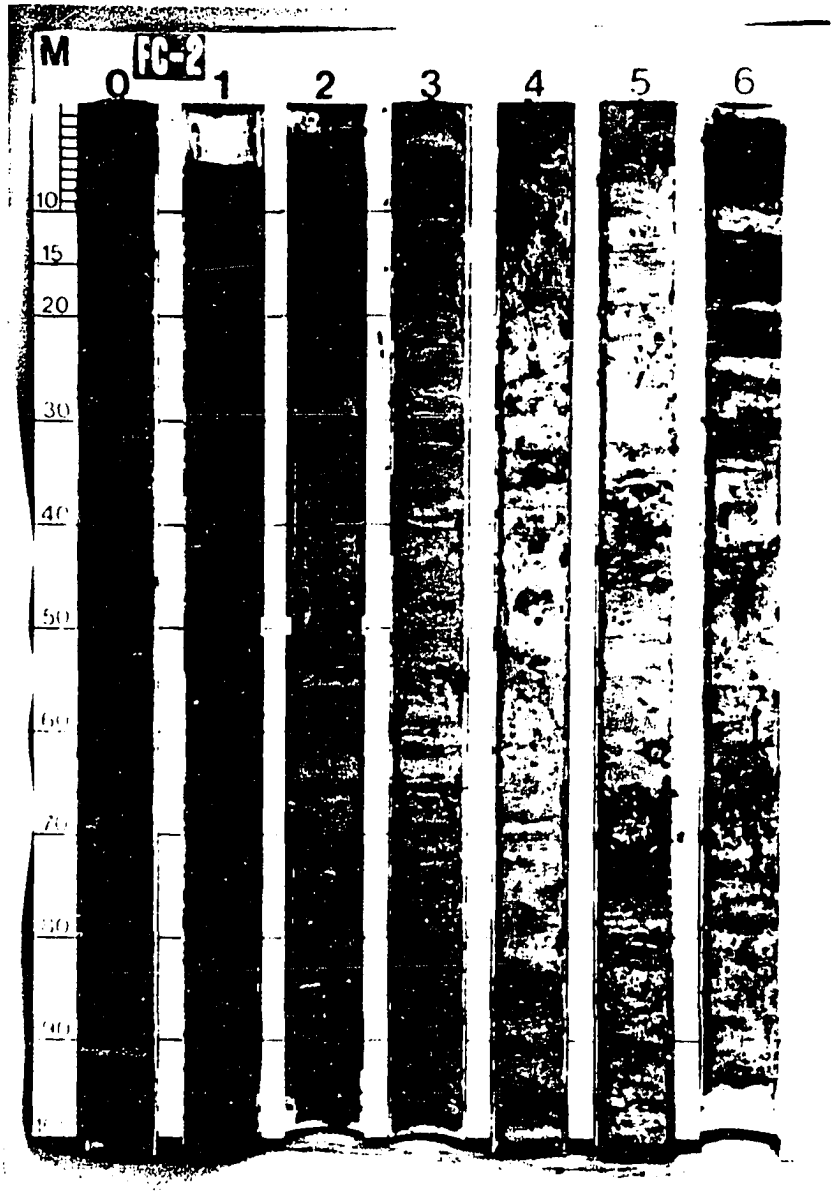

Figure E-11. Photograph of vibracore FC-2 (see Figure E-1 for location).

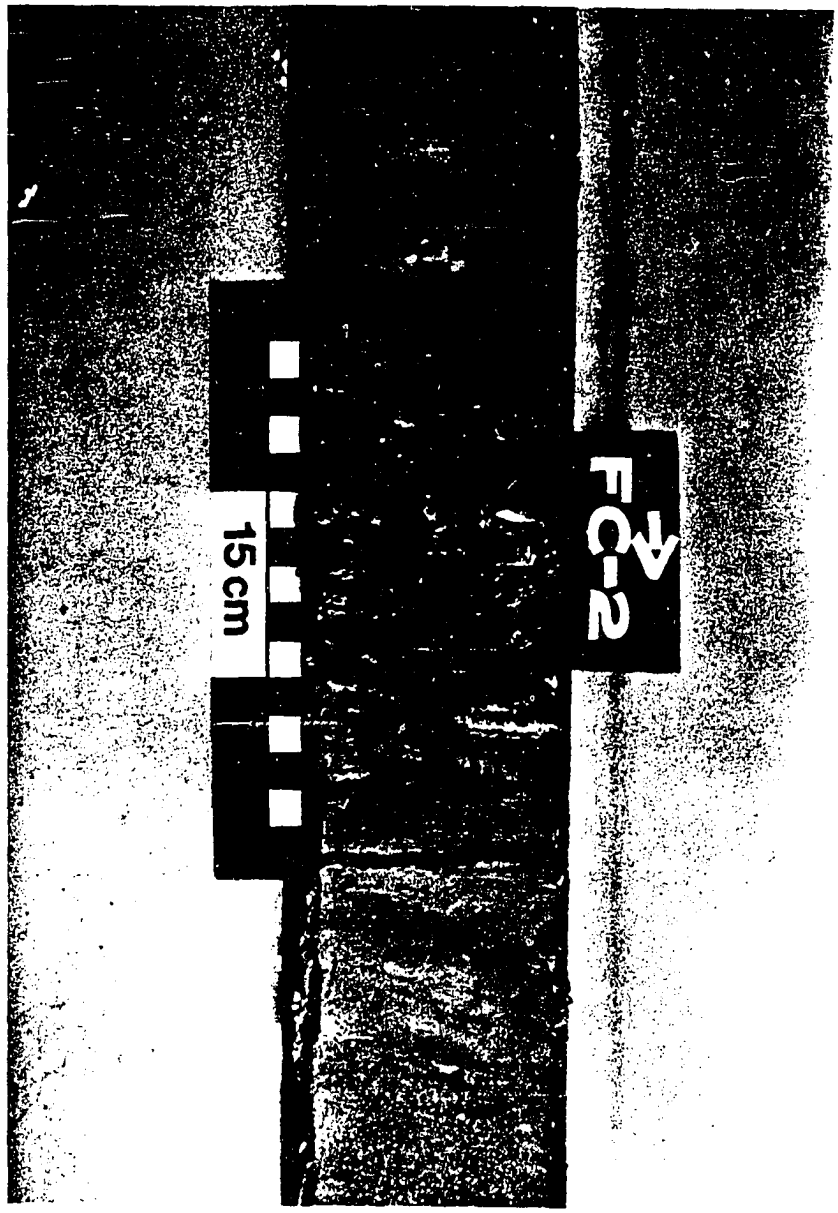

Figure E-12. Photograph of ravinement surface in FC-2 (see Figure E-1 for location).

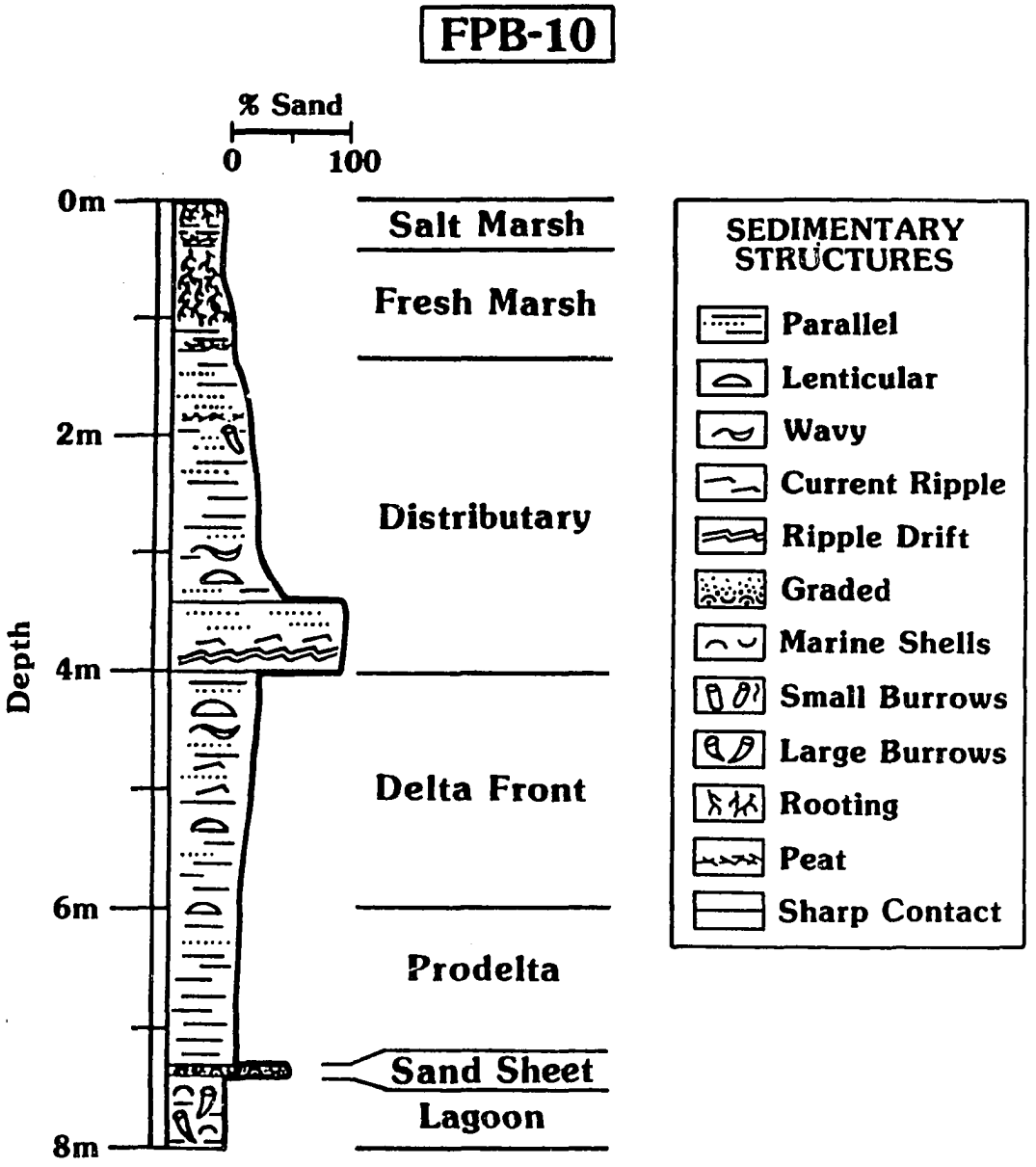

Figure E-13. Log of vibracore FPB-10 (see Figure E-1 for location).

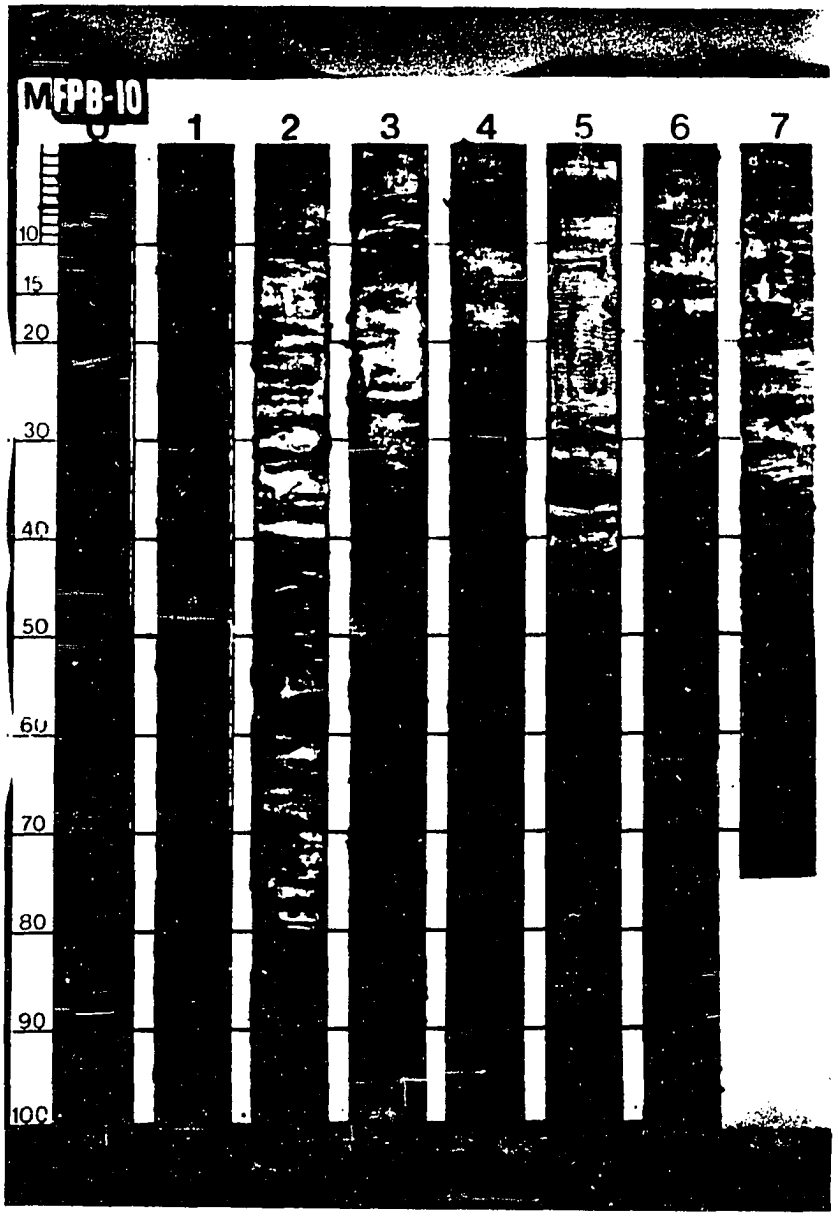

Figure E-14. Photograph of vibracore FPB-10 (see Figure E-1 for location).

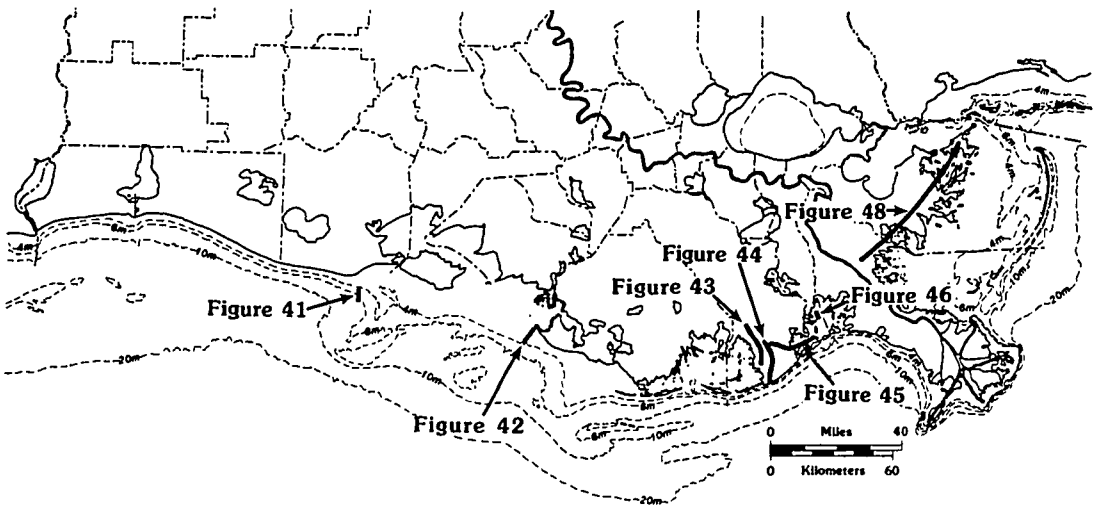

Figure E-15. Location of Figures 41, 42, 43, 44, 45, 46, and 48.

APPENDIX F

Ship Shoal Data

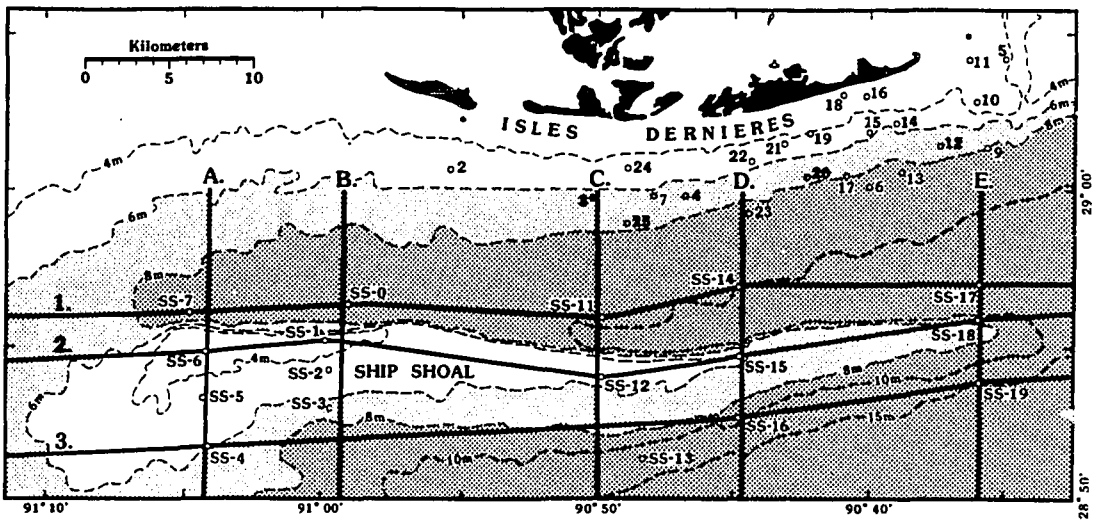

1. Ship Shoal Channel Cross-section
2. Ship Shoal Crest Cross-section
3. Ship Shoal Shelf Cross-section

A. West End Cross-section
B. Western Region Cross-section
C. Central Cross-section
D. Eastern Region Cross-section
E. East End Cross-section

Figure F-1. Location of vibracores and stratigraphic cross-sections in the Ship Shoal region.

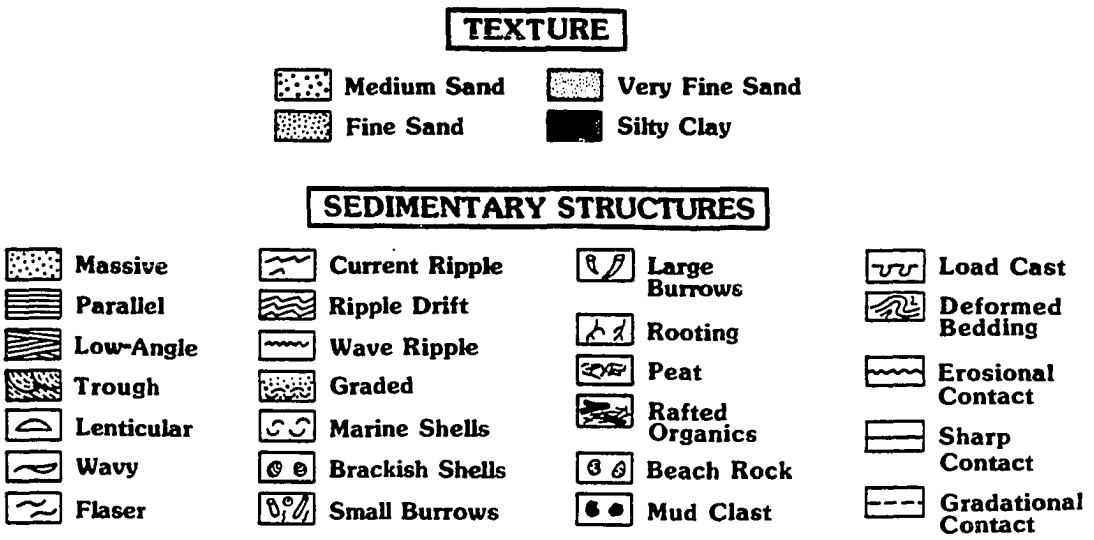

Figure F-2. Sedimentologic symbols used in this investigation.

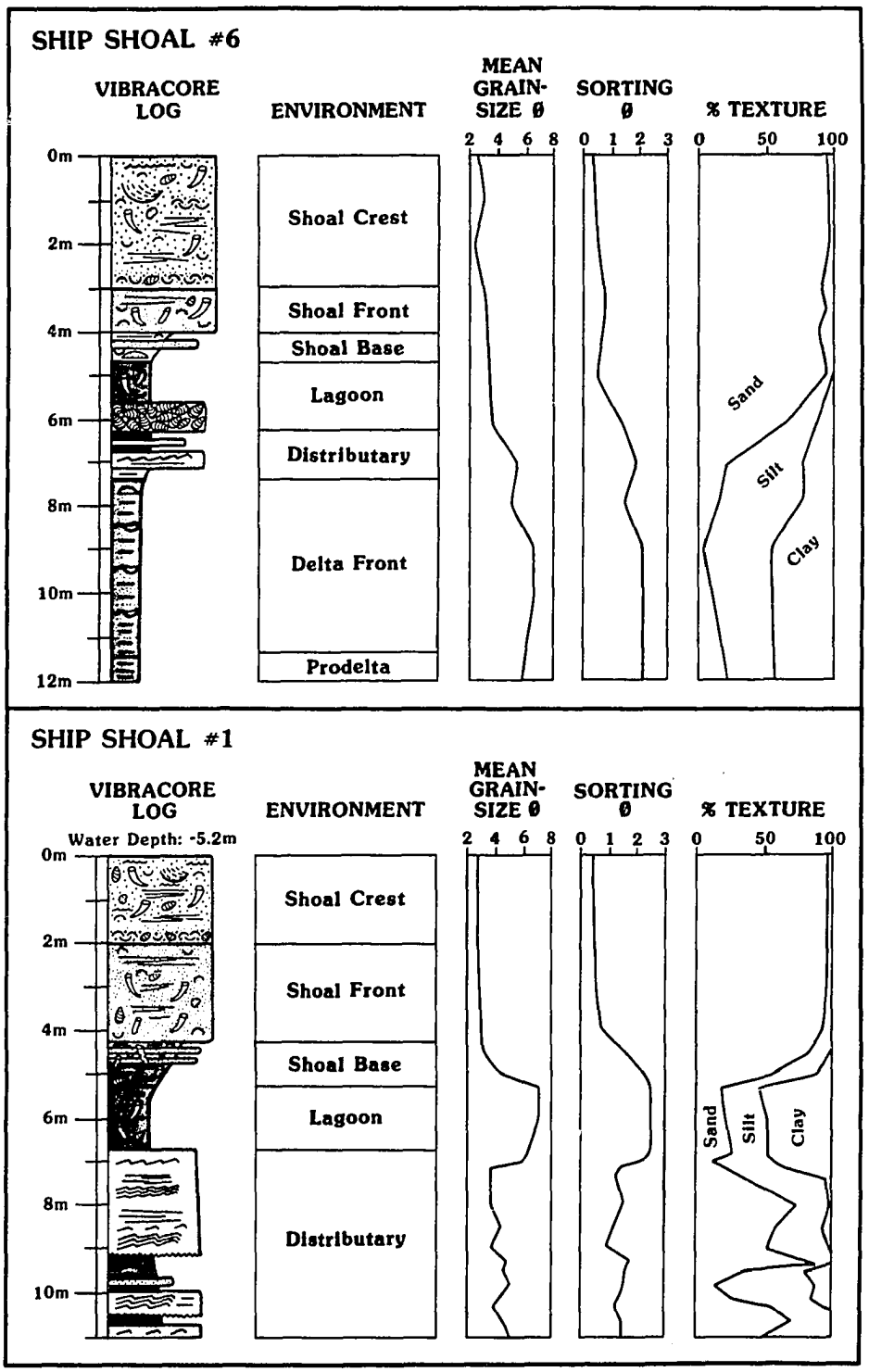

Figure F-3. Representative sedimentary sequences from vibracores SS-1 and SS-6 from the western Ship Shoal region (see figure F-1 for legend).

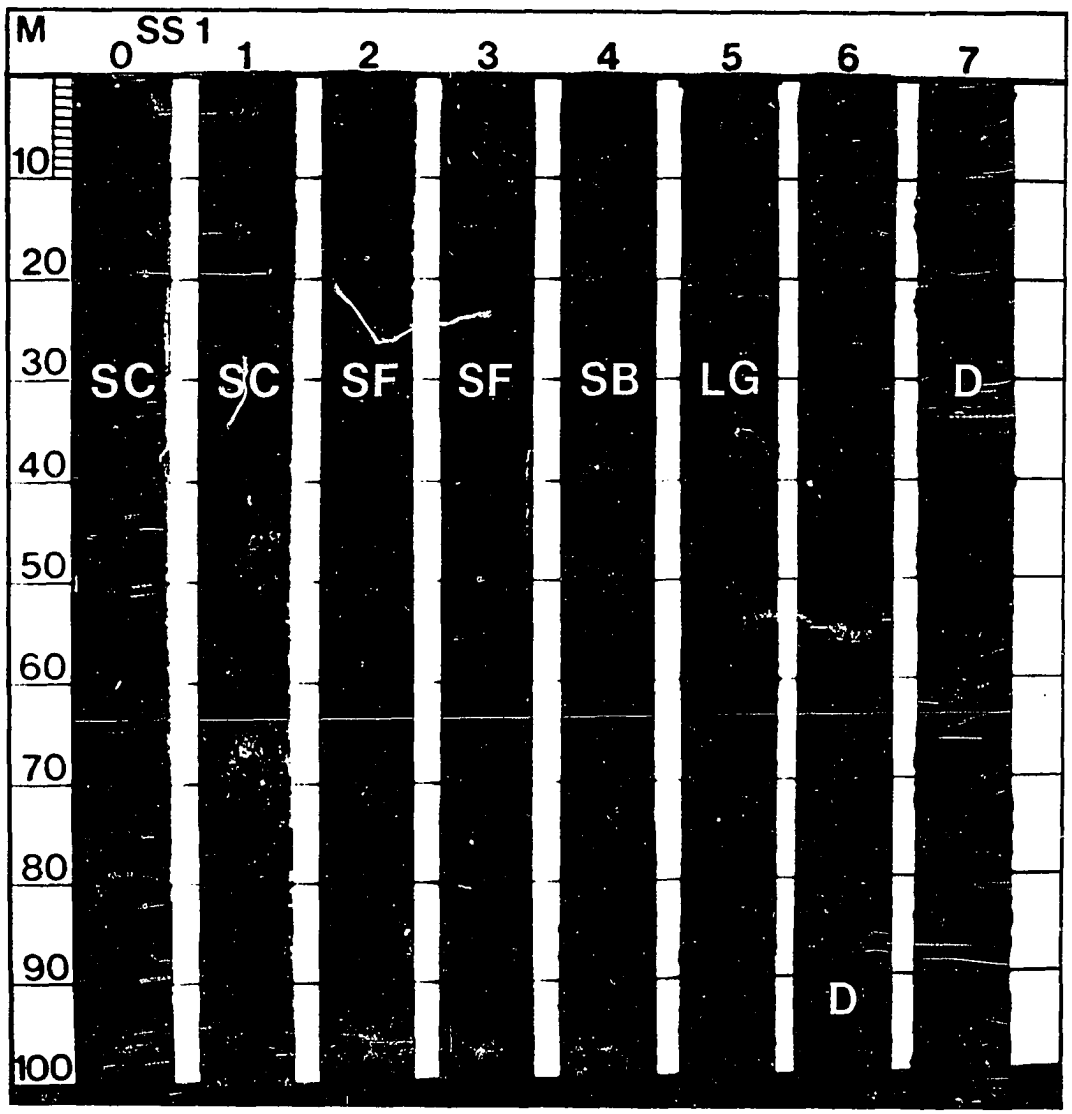

Figure F-4. Photograph of Ship Shoal vibracore SS-1 from the western shoal region. The individual facies illustrated include: SC = shoal crest, SF = shoal front, SB -shoal base, LG = lagoon, and D = distributary (scale on left is in cm).

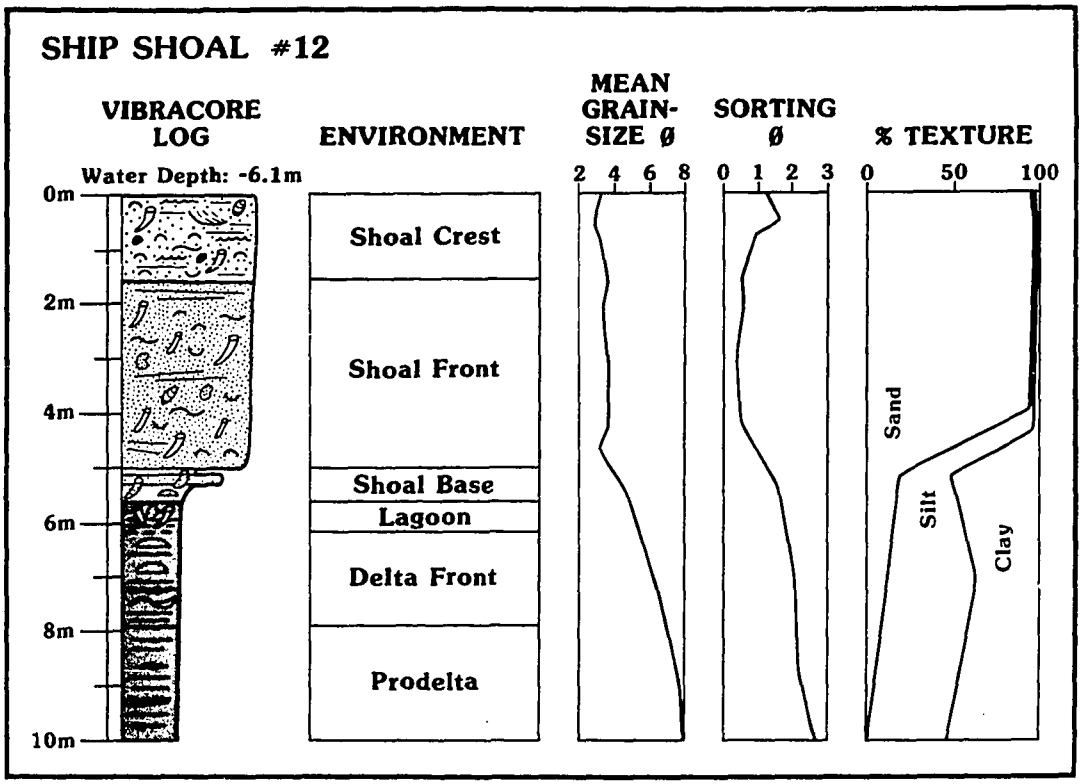

Figure F-5. Representative sedimentary sequences from vibracore SS-12 through the crest of the central Ship Shoal region (see figure F-1 for legend).

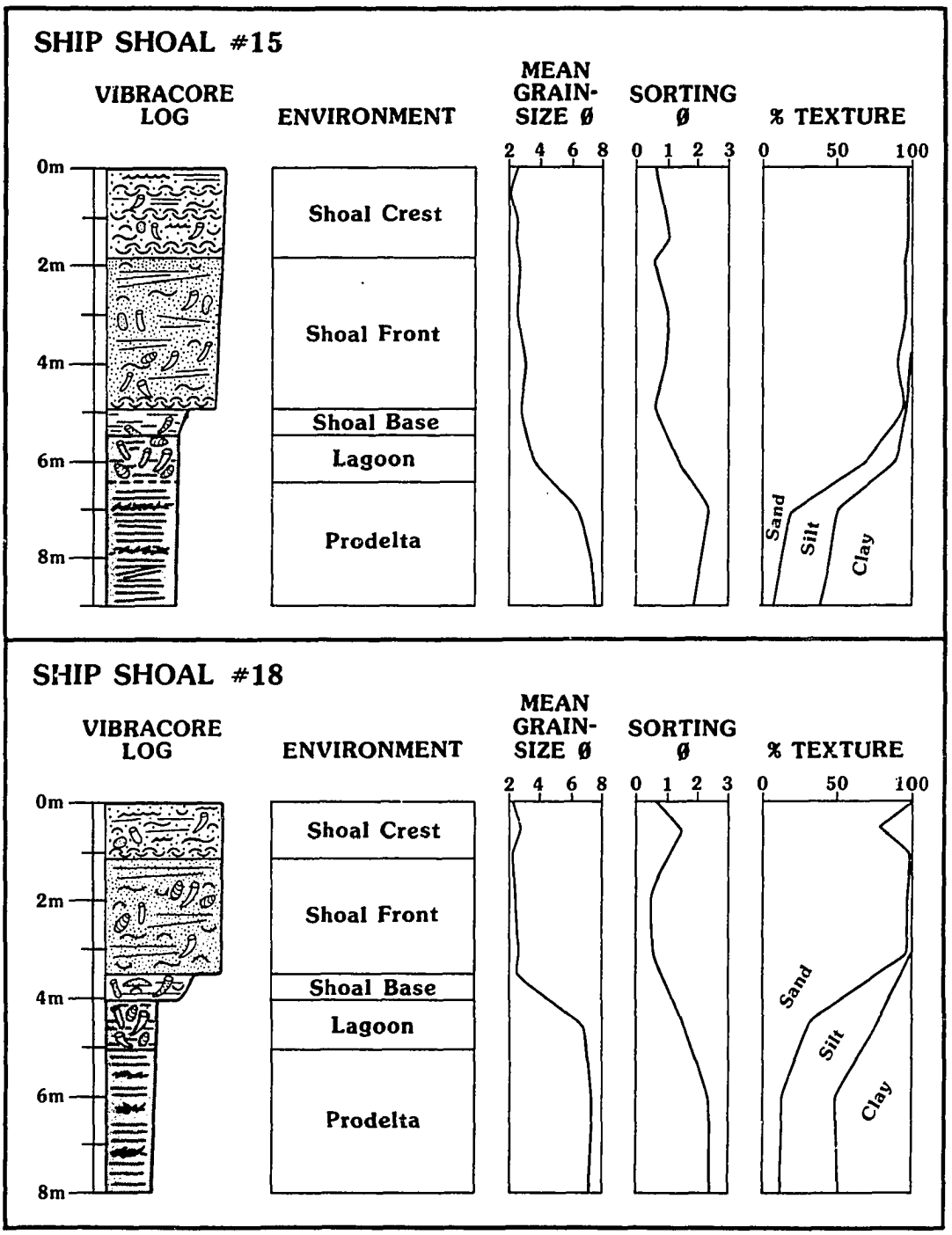

Figure F-6. Representative sedimentary sequences from vibracores SS-15 and SS-18 through the crest of the eastern Ship Shoal region (see figure F-1 for legend).

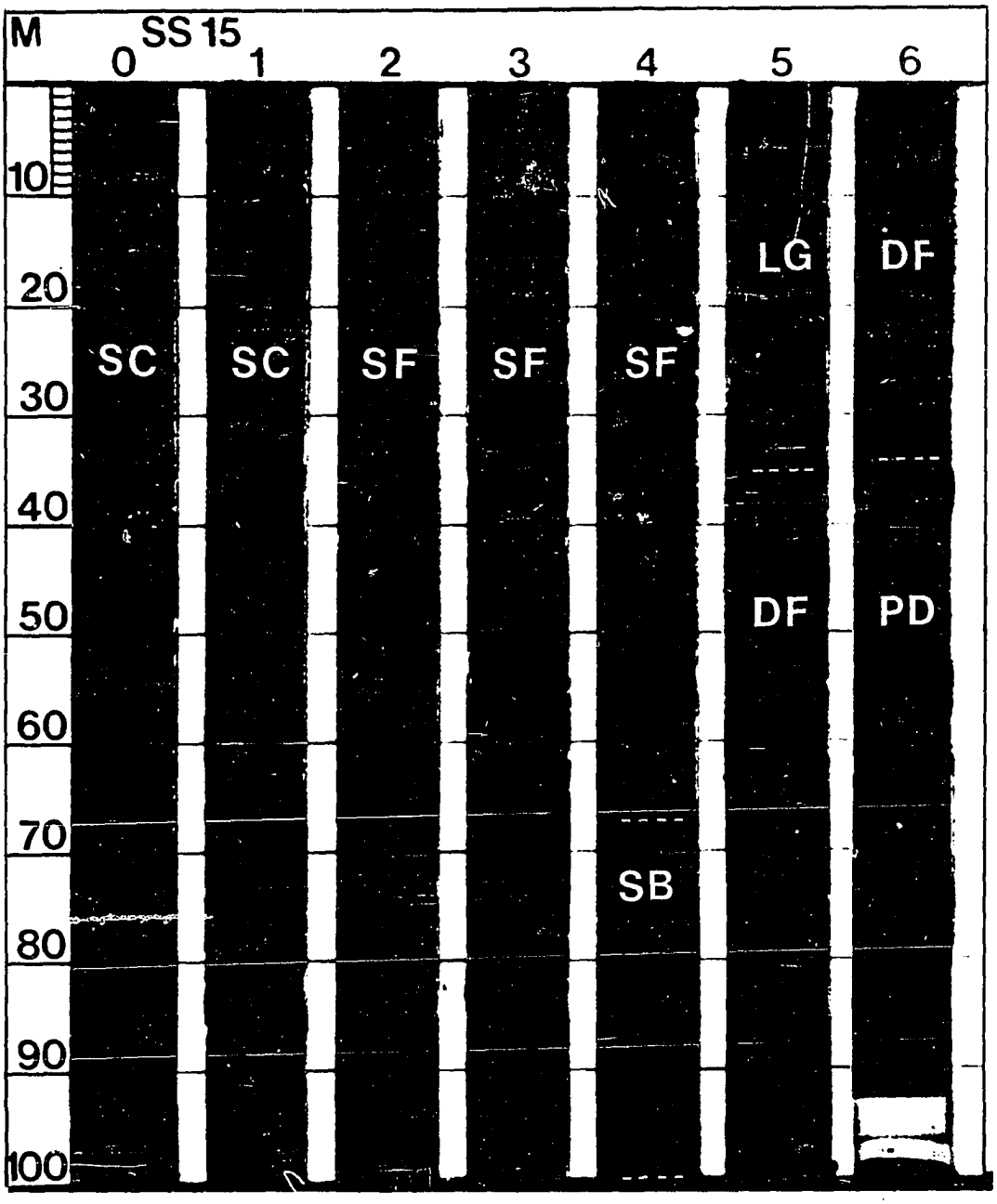

Figure F-7. Photograph of Ship Shoal vibracore SS-15 from the eastern shoal region. The individual facies illustrated include: SC = shoal crest, SF = shoal front, SB = shoal base, LG = Lagoon, and PD - prodelta (scale on left is in cm).

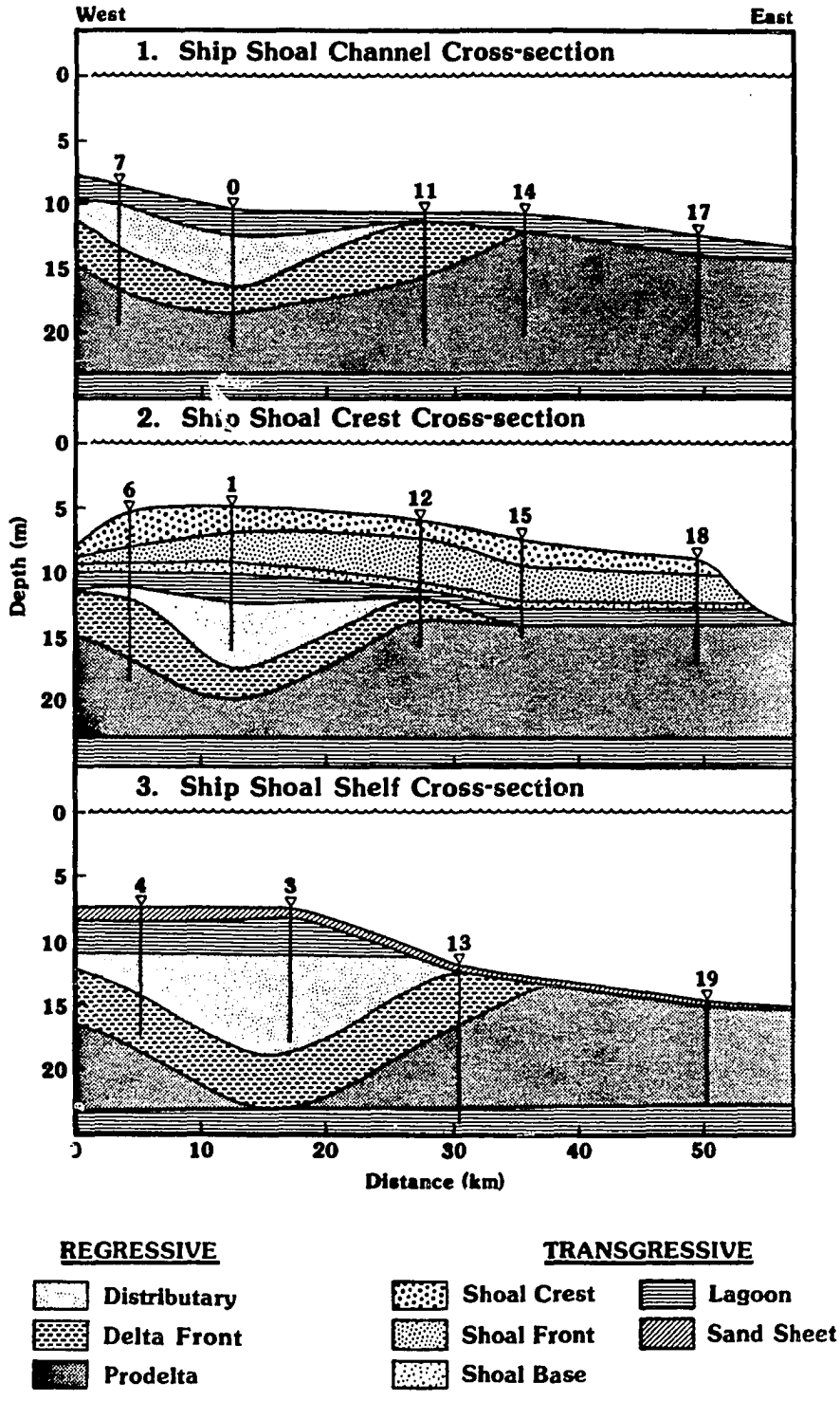

Figure F-8. Depositional strike cross section landward (1), along the crestline (2), and seaward (3) of Ship Shoal (see figure F-1 for locations).

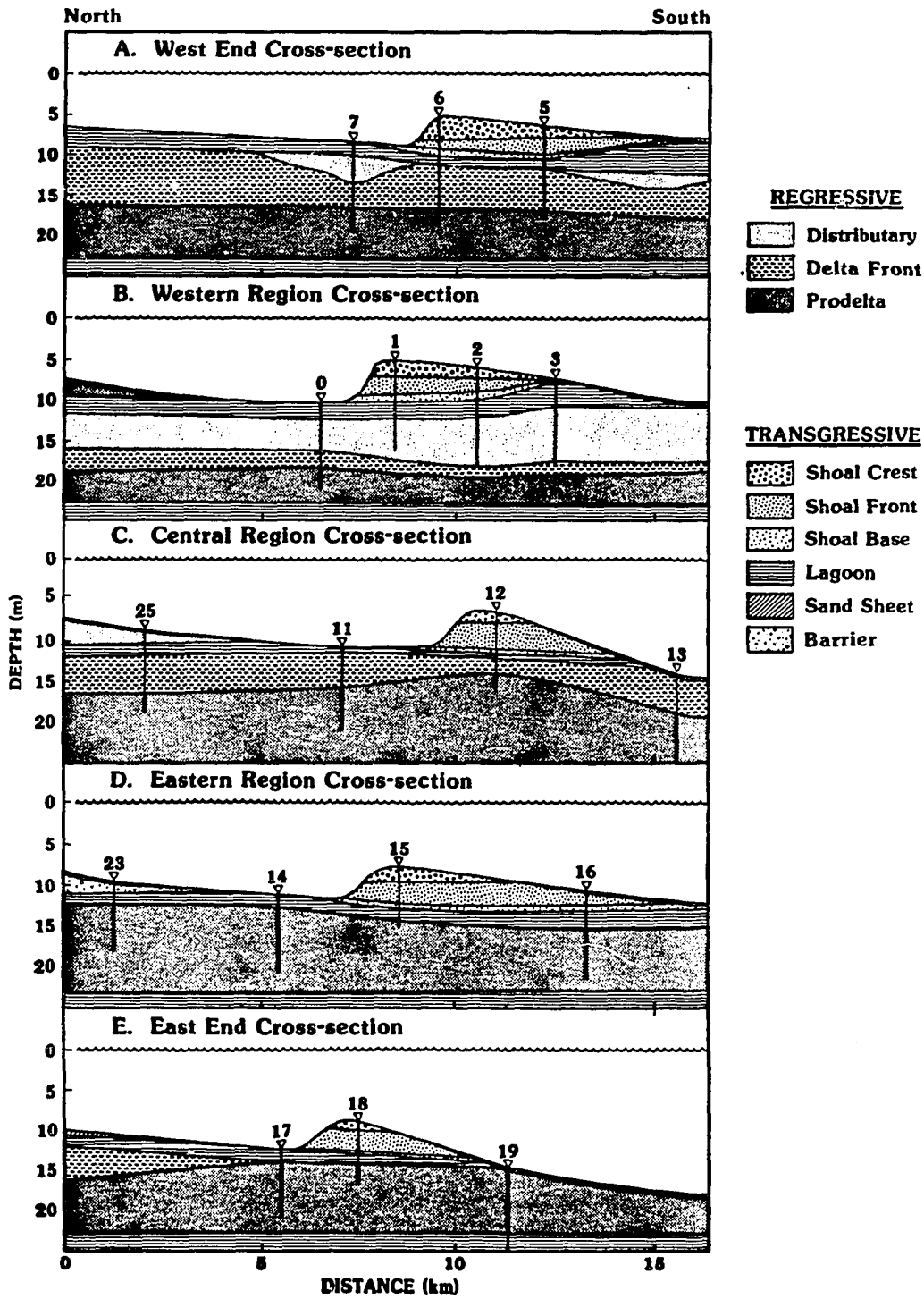

Figure F-9. Stratigraphic dip sections west to east across the crest of Ship Shoal (see figure F-1 for location).

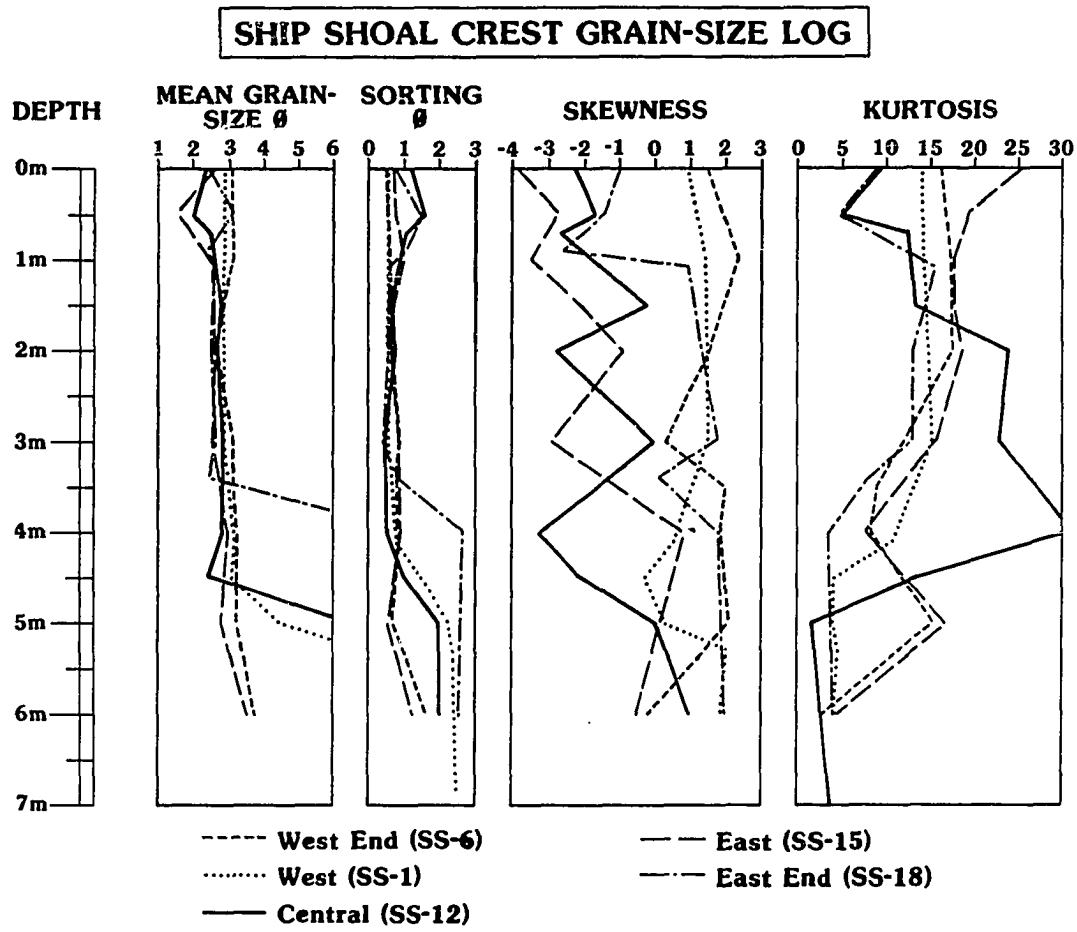

Figure F-10. Grain-size logs from the vibracores acquired along the crestline of Ship Shoal (see figure F-1 for legend).

VITA

Patrick Shea Penland was born on January 6, 1954 in Jacksonville, Florida. Raised along the northeast Florida coast, Penland graduated from The Bolles School in 1972. Following high school graduation, Penland enrolled at Jacksonville University and received a Bachelor of Arts degree (Geography) in 1976. In 1979, Penland received a Master of Science degree from Louisiana State University in physical geography/coastal geomorphology. Between 1979 and 1982, he worked as a research associate at Louisiana State University. In 1982, he worked as a senior staff scientist at Woodward-Clyde Consultants in Victoria, British Columbia. From 1982 to present, Penland works as a research geologist and as the Coastal Geology Section chief at the Louisiana Geological Survey in Louisiana State University. Shea Penland married Carol Ann Van de Burgt on January 24, 1987 and currently have two children, Sasha Terry and Kelsey Penland.

DOCTORAL EXAMINATION AND DISSERTATION REPORT

Candidate: Patrick Shea Penland

Major Field: Geography

Title of Dissertation: Barrier Island Evolution, Delta Plain Development, and Chenier Plain Formation in Louisiana.

Approved:

Richard H. Kuecl
Major Professor and Chairman

Dean of the Graduate School

EXAMINING COMMITTEE:

Harry H. Roberts

Anthony J. Lewis

Dag Nummedal

Mike Richardson

I. Yeaman

Date of Examination:

April 24, 1990